HAL
open science

Identifying and evaluating aging signatures in light emitting diode lighting systems

Sovannarith Leng

To cite this version:

Sovannarith Leng. Identifying and evaluating aging signatures in light emitting diode lighting systems. Electric power. Université Paul Sabatier - Toulouse III, 2017. English. NNT : 2017TOU30035 . tel-01799687

HAL Id: tel-01799687

https://theses.hal.science/tel-01799687v1

Submitted on 25 May 2018

HAL is a multi-disciplinary open access archive for the deposit and dissemination of scientific research documents, whether they are published or not. The documents may come from teaching and research institutions in France or abroad, or from public or private research centers.

L'archive ouverte pluridisciplinaire **HAL**, est destinée au dépôt et à la diffusion de documents scientifiques de niveau recherche, publiés ou non, émanant des établissements d'enseignement et de recherche français ou étrangers, des laboratoires publics ou privés.

THÈSE

En vue de l'obtention du

DOCTORAT DE L'UNIVERSITÉ DE TOULOUSE

Délivré par l'Université Toulouse 3–Paul Sabatier

Présentée et soutenue par

Sovannarith LENG

le 20 Février 2017

Identifying and Evaluating Aging Signatures in Light Emitting Diode Lighting Systems

---

École doctorale et discipline ou spécialité

ED GEET : Génie Electrique

Unité de recherche

Laboratoire PLAsma et Conversion d'Energie (LAPLACE)

Directeurs de Thèse

Dr. Laurent CANALE, CNRS, LAPLACE

Prof. Georges ZISSIS, Université Paul Sabatier, LAPLACE

Jury

Christian GLAIZE, Professeur, Lab. IES, Groupe GEM, Montpellier, Rapporteur

Yannick DESHAYES, Dr/HDR, IMS, Groupe ONDE, EDMINA, Talence, Rapporteur

Geneviève DUCHAMP, Professeur, IMS, Groupe FIABILITE, Bordeaux, Examinateur

Laurent MASSOL, Ingénieur, Directeur Société LED, Montauban, Invité

Laurent CANALE, Dr, Ingénieur de Recherche CNRS, LAPLACE, Directeur de Thèse

Georges ZISSIS, Professeur, Univ. Paul Sabatier, LAPLACE, Directeur de Thèse

Université Toulouse 3–Paul Sabatier
Laboratoire LAPLACE

THÈSE

Pour obtenir le grade de
DOCTEUR DE L'UNIVERSITÉ
Spécialité

Identifying and Evaluating Aging Signatures in Light Emitting Diode Lighting Systems

Sovannarith LENG

Présentée et soutenue publiquement
Le 20 Février 2017

Directeurs
Dr. Laurent CANALE, Ingénieur de Recherche CNRS, LAPLACE
Prof. Georges ZISSIS, Université Paul Sabatier, LAPLACE

JURY

Christian GLAIZE, Professeur, Lab. IES, Groupe GEM, Montpellier, Rapporteur
Yannick DESHAYES, Dr/HDR, IMS, Groupe ONDE, EDMINA, Talence, Rapporteur
Geneviève DUCHAMP, Professeur, IMS, Groupe FIABILITE, Bordeaux, Examinateur
Laurent MASSOL, Ingénieur, Directeur Société LED, Montauban, Invité
Laurent CANALE, Dr, Ingénieur de Recherche CNRS, LAPLACE, Directeur de Thèse
Georges ZISSIS, Professeur, Univ. Paul Sabatier, LAPLACE, Directeur de Thèse

ACKNOWLEDGEMENTS

This thesis was carried out within the PLAsma and Conversion d'Energie (LAPLACE) laboratory in Toulouse. This exciting and rewarding research has led to the contribution of several staff from the laboratory. I would therefore like to express my gratitude to certain individuals who have devoted their efforts and their availabilities to me during this thesis.

First of all, I would like to express my deep gratitude to my supervisor, Georges ZISSIS, Professor at University Paul Sabatier in Toulouse, Head of Light & Matter Research Group at LAPLACE and Director of SH2D Research Federation, for his very important direction in my work and for his encouragement, his advice and his very valuable technical and moral support for the success of my work.

I would also like to express my sincere thanks to my co–supervisor, Dr. Laurent CANALE, CNRS Research Engineer in Light & Matter Research Group and AFE Midi–Pyrénées Region Chairman, for his encouragement, his guidance, including his very useful advice which enabled me to acquire knowledge and skills that are very useful for my research and my career.

I especially wish to thank my thesis committee: Professor Christian GLAIZE, at "Institut d'Electronique et des Systèmes" in Montpellier, Professor Geneviève DUCHAMP, and Dr Yannick DESHAYES, Associate Professor/HDR, both from University of Bordeaux and "Laboratoire de l'Intégration du Matériau au Système", for their valuable advices, thesis supervision, and their positive comment and evaluation on my thesis.

I do not forget to express my gratitude to all staffs, lecturers, professors, PhD students and colleagues of the Laplace with whom I shared very pleasant moments and which allowed me to acquire various technical, social and cultural

knowledges on countless occasions. I would like to specially thank to my best friends, Alaa ALCHADDOUD and Feng TIAN.

I also do not forget to convey my thanks to my Cambodian friends who are / were in Toulouse and France, with whom I shared a lot of pleasant moments and who remain anchored in my memories.

Very special and from bottom of heart thanks and gratitude to my beloved family: **my wife, my son and my parent** for their love, constant moral encouragement, and their invaluable sacrifice of everything for me. They always support and hold me when I am down so I never lost my spirit. No word I can say about their goodness. I am very proud to be their part of family. I also thank to my brothers and sisters for caring and support. It is to all of them that I dedicate this thesis.

The last but not least, I would like to express my deepest appreciation to Erasmus Mundus Techno II project with the support of the Erasmus Mundus Program of the European Union for my financial support, to officers and staffs of the Techno II program for their kindness and help during my study.

Contents

INTRODUCTION 1

1. STATE OF THE ART OF THE GaN LEDS TECHNOLOGY 5

1.1. HISTORY OF LIGHTING SYSTEMS 6
1.1.1. The Sun 6
1.1.2. Incandescent Filament Lamp 7
1.1.3. Mercury and Sodium Vapor Lamps 7
1.1.4. Fluorescent Lamp 9
1.1.5. Light–Emitting Diodes (LEDs) 10

1.2. LED CHIP STRUCTURES 14
1.2.1. Conventional Lateral and Vertical Structure 14
1.2.2. Flip Chip Structure 15
1.2.3. Vertical Thin Film Structure 16
1.2.4. Thin Film Flip Chip Structure 17

1.3. PACKAGING OF LEDS 18
1.3.1. Low Power LED Package 19
1.3.2. High Power LED Package 19
1.3.3. Packaging Process 21
1.3.3.1. Dual in–Line (DIP) Packaging 22
1.3.3.2. SMD LED Packaging 22
1.3.3.2.1. SMD Leadform Packaging 23
1.3.3.2.2. SMD Leadless Package 24
1.3.3.3. LED Array Packaging 26

1.4. MAIN DEGRADATION OF LEDS TECHNOLOGY 29
1.4.1. Degradation and Failure Modes at Chip Level 29
1.4.1.1. Generation and Movement of Defect and Dislocation 29
1.4.1.2. Die Cracking 32
1.4.1.3. Dopant Diffusion 34
1.4.1.4. Electromigration 34
1.4.2. Interconnection Failure Modes 35
1.4.2.1. Bond Wire /Wire Ball Bond Failure 35
1.4.2.2. Electrical Contact Metallurgical Interdiffusion 37
1.4.2.3. Electrostatic Discharge 37
1.4.3. Degradation and Failure Modes at Package Level 40
1.4.3.1. Carbonization of the Encapsulant 40
1.4.3.2. Delamination 41
1.4.3.3. Lens /Encapsulant Failure 43
1.4.3.4. Phosphor Thermal Quenching 44

1.4.3.5. Solder Joint Fatigue 46

1.5. CONCLUSION – CHAPTER 1 47

2. ELECTRICAL AND OPTICAL CHARACTERISTICS OF LEDS 51

2.1. METHODOLOGY FOR JUNCTION TEMPERATURE EVALUATION 52
2.1.1. Temperature Dependence of Forward Voltage (Vf) 53

2.2. OPTICAL PROPERTIES OF LED 60
2.2.1. Internal, Extraction, External, and Power Efficiencies 60
2.2.2. Emission Spectrum 61
2.2.3. Light Escape Cone 64
2.2.4. Radiation Pattern–Lambertian Emission Pattern 66
2.2.5. Epoxy Encapsulant 67
2.2.6. Temperature Dependence of Emission Intensity 68

3. EXPERIMENTAL SETUP FOR LED AGING EVALUATION 69

3.1. A NEW PROTOTYPE OF LED AGING BENCH 70

3.2. TEMPERATURE CONTROLLER (REX–D100) 76
3.2.1. Software Program for REX–D100 Temperature Controller 78
3.2.2. Communication Protocol 80
3.2.2.1. Polling Procedure 80
3.2.2.1. Selection Procedure 81

3.3. SOURCE–METER UNIT (SMU–KEITHLEY 2602A) 81
3.3.1. 2–Wires and 4–Wires Feature 82
3.3.2. Software Program Measurement for SMU–Keithley 2602A 83

3.4. IMPEDANCE ANALYZER (SOLARTRON MODULAB) 87
3.4.1. Instrument Group Modules 87
3.4.2. PC Communication Setup 88
3.4.3. Software Program Control of Solartron ModuLab 89

3.5. SPECTROMETER (SPECBOS 1201) 91
3.5.1. Optical Measurement Hardware Setup 92
3.5.2. Software Program Measurement of Specbos 1201 93

3.6. LED'S DRIVER 94

4. EVALUATION OF FAILURE MECHANISMS FOR LEDS STUDIED 97

4.1. EFFECT OF TEMPERATURE ON LED PERFORMANCE 98

4.2. SELF–HEATING TEST 100

4.3. INITIAL STATE OF ELECTRICAL CHARACTERIZATIONS 101

4.4. ELECTRICAL FAILURE SIGNATURES 110

4.4.1. Electrical Aging Characteristic of Cree's Devices 111
4.4.2. Electrical Aging Characteristic of Osram's Devices 115
4.4.3. Electrical Aging Characteristic of Philips's Devices 118
4.4.4. Electrical Aging Characteristic of Seoul's Devices 122

4.5. OPTICAL FAILURE SIGNATURES 126
4.5.1. Initial State of Photometric Characterization 127
4.5.2. Photometrical Characterizations of LEDs under accelerated aging conditions 136

4.6. CONCLUSION– CHAPTER 4 146

GENERAL CONCLUSION AND PERSPECTIVES 149

REFERENCES 155

ANNEXES I

APPENDIX A: COMMUNICATION IDENTIFIER LIST OF REX–D100 II

APPENDIX B: CONTROLLER SCANNED PARAMETER IV

APPENDIX C: PROGRAM CODE FOR REX–D100 V

APPENDIX D: PROGRAM CODE FOR SMU KEITHLEY 2602A XI

APPENDIX F: DATASHEET OF LEDS XXXI

Liste des tableaux

Table I.1: Discoveries and History of LEDs 13

Table I.2: Comparison of Key Characteristics and Parameter Values for Commercial 14

Table I.3: Factors influent LED packaging 21

Table II.1: Varshni parameters of common semiconductors. 57

Table III.1: Main characteristics of studied LEDs. 71

Table IV.1: dispersion of I–V characteristic of 16 Samples each LED group computed at V=2.9V. 104

Table IV.2: Error of variation of luminance and spectrum of 16 samples each unstressed LED group @350mA. 131

Table des illustrations

Figure I.1: Sun, the first light source. 6

Figure I.2: Artificial Lighting. 6

Figure I.3: Mercury Vapor Lamp. 7

Figure I.4: Low–pressure sodium vapor lamp. 8

Figure I.5: High–pressure sodium vapor lamp. 9

Figure I.6: Fluorescent lamp. 10

Figure I.7: Publication of JH Round in Electrical World. 11

Figure I.8: A replication of H. J. Round's LED experiments. 11

Figure I.9: a) Lateral structure, b) vertical structure. 15

Figure I.10: Flip chip structure. 16

Figure I.11: LED ThinGaN structure by Osram. 16

Figure I.12: TFFC by Philips Lumiled. 17

Figure I.13: SEM images of PSS and GaN grown on PSS 17

Figure I.14: SEM of an N–face GaN surface roughening etched by a KOH–based PEC method 18

Figure I.15: Al–oxide honeycomb nanostructure on thin–GaN LED 18

Figure I.16: a) LED with hemispherical encapsulant, b) LEDs with cylindrical and rectangular encapsulant 19

Figure I.17: High power LED packaging. 20
Figure I.18: Typical package products of high power LED. 20
Figure I.19: Packaging process flows of common LEDs 21
Figure I.20: DIP Packaging 22
Figure I.21: a) Leadform package, b) leadless package. 23
Figure I.22: Main components of the SMT LED package 23
Figure I.23: Packaging of lateral LED chip. 24
Figure I.24: Packaging of vertical LED chip. 24
Figure I.25: Packaging of flipped chip LED structure. 24
Figure I.26: SMD leadless LED packaging 25
Figure I.27: Leadless Wicop2 module (Chip-on-board packaging, Seoul Semiconductor) 25
Figure I.28: QFN LED package (Oslon Black Flat, Osram) 26
Figure I.29: Multichip LED package 26
Figure I.30: Comparison of Rth for each LED chip in 1–, 4–, and 16–chip packages 27
Figure I.31: COB LED package of some leading products. 28
Figure I.32: Dislocations in GaN and discontinuations in Au–metallization 30
Figure I.33: (a) An AFM image and (b) a cross–section TEM image of a pit 30
Figure I.34: Dark–spot defects generation (a), (b), and (c) correspond to initial stage and aging of 67 and 310 h, respectively 31
Figure I.35: a) Good die with proper bonding, b) cracking die with over pressure boding 32
Figure I.36: Large edge defect caused by dicing 32
Figure I.37: Die surface morphology (a) polished, (b) ground, and (c) untreated. 33
Figure I.38: Thermal expansion coefficients of GaN/Si and GaN/Sapphire. 33
Figure I.39: Maximum EL output power as a function of the integrated Mg concentration 34
Figure I.40: Optical microscope photograph of electrode surface before stress and after device failure 35
Figure I.41: Banding pad divorced from banding area 35
Figure I.42: Breaking of wire neck or heat affected zone (HAZ) 36
Figure I.43: Crack in electrode bonding interface 36
Figure I.44: TEM of MHEMT with Pt/Ti/Pt/Au gate before and after stress 37
Figure I.45: Si submount as Zener diode for ESD protection in flip chip structure 38

Figure I.46: GaN LED with an internal Schottky diode and its equivalent circuit model 39

Figure I.47: (a) Bare–chip of LED, (b) Equivalent circuit, (c) an inverse–parallel–connected GaN ESD diode and (d) a GaN LED 39

Figure I.48: Carbonization of phosphor–encapsulating material 40

Figure I.49: a) Optical power b) Output spectra, degradation during stress at 200°C 41

Figure I.50: Possible delamination areas of LEDs. 41

Figure I.51: Delamination between the LED die and encapsulant 42

Figure I.52: SEM photographs of the cross–section of degraded (a) $Au_{80}Sn_{20}$ eutectic sample and (b) silver paste sample 42

Figure I.53: (a) Delamination and (b) curling of phosphor coated LED package 43

Figure I.54: Encapsulant yellowing 43

Figure I.55: Relative light output from 5–mm indicator lamps and high–power illuminator LEDs 44

Figure I.56: Degradation of phosphor (left: untreated sample, right: after stress at 100 A.cm−2, 120°C) 45

Figure I.57: Lifetime result of LED with (a) remote and (b) die–contact phosphor 45

Figure I.58: Creep strain rate vs. tensile stress for different SACxx alloys 46

Figure I.59: Solder fracture due to creep–fatigue under thermal cyclic load 46

Figure I.60: Solder joint cracks (left: SAC305, right: Innolot) 47

Figure II.1: Energy loss of carriers as they are captured into the quantum well. 53

Figure II.2: Current–voltage characteristic of LED showing threshold voltages 2.0 and 1.6 V, at 77°K and 300°K, respectively. 58

Figure II.3: (a) Pulsed calibration and (b) determination of junction temperature for different DC forward currents. 58

Figure II.4: (a) Pulsed calibration measurement (small duty cycle 0.1 %) and (b) junction temperature (T_j) versus DC current of AlGaN UV LED, Schubert, 2006 [17, p. 109]. 59

Figure II.5: Parabolic electron and hole dispersion relations. 61

Figure II.6: Theoretical emission spectrum of an LED. 63

Figure II.7: (a) Definition of the escape cone by the critical angle φ_c. (b) area element dA. (c) area of calotte–shaped section of sphere defined by radius r and angle φ_c. 64

Figure II.8: Light–emitting diodes with (a) planar, (b) hemispherical, and (c) parabolic surfaces, (d) Far–field patterns of the different types of LEDs. 66

Figure II.9: (a) LED without, (b) with dome–shaped epoxy encapsulant, (c) calculated ratio of light extraction efficiency emitted through the top surface of a planar LED with and without an epoxy dome. 67

Figure III.1: Overview of the LED aging Bench. 70

Figure III.2: Overall experimental setup design. 71

Figure III.3: Led types: a) Cree, XLamp® XP–G2 b) Osram, LCW CQ7P.CC c) Philips, LX18–P130–3 and d) Seoul, N42180H–T2. 72

Figure III.4: LEDs mounted on a printed custom–made circuit board. 72

Figure III.5: LED aluminum holder. 73

Figure III.6: stainless steel flexible hose fitting. 74

Figure III.7: Arrangement of the stress condition. 75

Figure III.8: Temperature controller REX–D100. 76

Figure III.9: Control mode of REX–D100. 77

Figure III.10: Electrical wiring of experimental setup. 78

Figure III.11: Application program for REX–D100 controller. 80

Figure III.12: Two–wires connections. 82

Figure III.13: Four–wires connections. 83

Figure III.14: Application program for SMU–Kethley 2602A. 85

Figure III.15: Sweep modes a) linear, b) logarithmic and c) list. 86

Figure III.16: LED measurement configuration. 88

Figure III.17: Networking to PC. 89

Figure III.18: Software control of ModuLab. 89

Figure III.19: C–V Characteristic measurement. 90

Figure III.20: Impedance measurement. 90

Figure III.21: Fitting and equivalent circuit of a measured sample. 91

Figure III.22: Setup measured distance. 92

Figure III.23: Photometrical measurement setup. 93

Figure III.24: Jeti Lival program for Specbos 1201 control and measure. 93

Figure III.25: Drivers of LED samples. 94

Figure III.26: Current regulator circuit. 95

Figure III.27: Switch mode Power supply for LED drivers up to 40A. 96

Figure IV.1: Temperature effect on LED, linear scale. 99
Figure IV.2: Temperature effect on LED, semi–log scale. 99
Figure IV.3: Linearity of forward voltage to temperature. 100
Figure IV.4: Source mode (a) Linear pulse, (b) Linear DC sweep. 101
Figure IV.5: I–V Curve, self–heating test. 101
Figure IV.6: I–V characteristic of Cree@350mA, linear. 102
Figure IV.7: I–V characteristic of Cree@350mA, semi–log. 103
Figure IV.8: I–V characteristic of Cree@1000mA, linear. 103
Figure IV.9: I–V characteristic of Cree@1000mA, semi–log. 103
Figure IV.10: Error bar around average value of 16 samples Cree@350mA, semi–log. 104
Figure IV.11: Error bar around average value of 16 samples Cree@1000mA, semi–log. 105
Figure IV.12: Error bar around average value of 16 samples Cree@350mA, linear. 105
Figure IV.13: Error bar around average value of 16 samples Cree@1000mA, linear. 106
Figure IV.14: I–V characteristic of Philips, linear. 108
Figure IV.15: I–V characteristic of Philips, semi–log scale. 108
Figure IV.16: I–V characteristic of Osram, linear scale. 109
Figure IV.17: I–V characteristic of Osram, semi–log scale. 109
Figure IV.18: I–V characteristic of Seoul, linear scale. 109
Figure IV.19: I–V characteristic of Seoul, semi–log scale. 110
Figure IV.20: Aging I–V characteristic, Cree@stress350mA. 112
Figure IV.21: Aging I–V characteristic, Cree@stres1000mA. 113
Figure IV.22: Effect of series resistance RS after stress (Cree@stress350mA). 113
Figure IV.23: Aging reverse bias I–V characteristic (Cree@stress350mA). 114
Figure IV.24: Aging reverse bias I–V characteristic (Cree@stress1000mA). 114
Figure IV.25: Effect of parallel resistance RP after stress (Cree@stress350mA). 114
Figure IV.26: Aging I–V characteristic (Osram@stress350mA, linear scale). 115
Figure IV.27: Aging I–V characteristic (Osram@stress1000mA, linear scale). 116
Figure IV.28: Effect of series resistance RS after stress (Osram@stress1000mA). 116
Figure IV.29: Aging I–V characteristic (Osram@stress350mA, semi–log scale). 117

Figure IV.30: Aging I–V characteristic (Osram@stress1000mA, semi–log scale). 117
Figure IV.31: Effect of parallel resistance RP after stress (Osram@stress1000mA). 117
Figure IV.32: Aging reverse bias I–V characteristic (Osram@stress350mA). ... 118
Figure IV.33: Aging reverse bias I–V characteristic (Osram@stres1000mA). ... 118
Figure IV.34: Aging I–V characteristic (Philips@stress350mA, linear scale).... 119
Figure IV.35: Aging I–V characteristic (Philips@stress1000mA, linear scale).. 120
Figure IV.36: Effect of resistance RP and RS after stress (Philips@stress1000mA). 120
Figure IV.37: Aging I–V characteristic (Philips@stress350mA, semi–log scale). 121
Figure IV.38: Aging I–V characteristic (Philips@stress1000mA, semi–log scale). 121
Figure IV.39: Aging reverse bias I–V characteristic (Philips@stress350mA).... 121
Figure IV.40: Aging reverse bias I–V characteristic (Philips@stress1000mA).. 122
Figure IV.41: Effect of resistance RP after stress (Philips@stress1000mA). 122
Figure IV.42: Aging I–V characteristic, Seoul@stress350mA, linear scale..... 123
Figure IV.43: Aging I–V characteristic, Seoul@stress1000mA, linear scale..... 124
Figure IV.44: Effect of series resistance RS after stress (Seoul@stress1000mA). 124
Figure IV.45: Aging I–V characteristic, Seoul@stress350mA, semi–log scale... 124
Figure IV.46: Aging reverse bias I–V characteristic, Seoul@stress350mA..... 125
Figure IV.47: Aging I–V characteristic, Seoul@stress1000mA, semi–log scale. 125
Figure IV.48: Aging reverse bias I–V characteristic, Seoul@stress1000mA..... 125
Figure IV.49: Effect of parallel resistance RP after stress (Seoul@stress1000mA). 126
Figure IV.50: Effect of resistance RP after stress (Seoul@stress1000mA)..... 126
Figure IV.51: L–I characteristic (unstressed Cree@350mA). 127
Figure IV.52: L–I characteristic (unstressed Osram@350mA)..... 128
Figure IV.53: L–I characteristic (unstressed Philips@350mA). 128
Figure IV.54: L–I characteristic (unstressed Seoul@350mA)..... 128
Figure IV.55: Spectrum (unstressed Cree@350mA)..... 129
Figure IV.56: Spectrum (unstressed Osram@350mA). 129
Figure IV.57: Spectrum (unstressed Philips@350mA)..... 130
Figure IV.58: Spectrum (unstressed Seoul@350mA). 130

Figure IV.59: Average L–I of 16 samples (unstressed Cree@350mA)..... 131
Figure IV.60: Average L–I of 16 samples (unstressed Osram@350mA). 131
Figure IV.61: Average L–I of 16 samples (unstressed Philips@350mA)..... 132
Figure IV.62: Average L–I of 16 samples (unstressed Seoul@350mA). 132
Figure IV.63: Average spectrum of 16 samples (unstressed Cree@350mA). 132
Figure IV.64: Average spectrum of 16 samples (unstressed Osram@350mA)... 133
Figure IV.65: Average spectrum of 16 samples (unstressed Philips@350mA). . 133
Figure IV.66: Average spectrum of 16 samples (unstressed Seoul@350mA)..... 133
Figure IV.67: L–I characteristic (unstressed COPS LEDs@350mA). 134
Figure IV.68: Spectrum (unstressed COPS LEDs@350mA)..... 135
Figure IV.69: Chromaticity (unstressed COPS LEDs). 135
Figure IV.70: Color rendering index a) Cree, b) Osram, c) Philips and d) Seoul. 136
Figure IV.71: Aging luminance (350mA–stressed Cree). 137
Figure IV.72: Aging luminance (1000mA–stressed Cree). 138
Figure IV.73: Aging spectrum (350mA–stressed Cree). 138
Figure IV.74: Aging spectrum (1000mA–stressed Cree). 138
Figure IV.75: Aging luminance (1000mA–stressed Philips). 139
Figure IV.76: Aging spectrum (1000mA–stressed Philips). 139
Figure IV.77: Aging luminance (1000mA–stressed Philips). 139
Figure IV.78: Aging spectrum (1000mA–stressed Philips). 140
Figure IV.79: Aging luminance (350mA–stressed Osram)..... 141
Figure IV.80: Aging spectrum (350mA–stressed Osram)..... 141
Figure IV.81: Aging chromaticity to blueish light (350mA–stressed Osram).... 142
Figure IV.82: Aging luminance (1000mA–stressed Osram)..... 142
Figure IV.83: Aging spectrum (1000mA–stressed Osram)..... 143
Figure IV.84: Aging luminance (350mA–stressed Seoul)..... 144
Figure IV.85: Aging spectrum (350mA–stressed Seoul)..... 144
Figure IV.86: Aging luminance (1000mA–stressed Seoul)..... 144
Figure IV.87: Aging spectrum (1000mA–stressed Seoul)..... 145
Figure IV.88: Aging optical power (COPS LEDs). 145

INTRODUCTION

Since less than a decade, we can find a new light source technology in our daily lives. The first building blocks of this revolution were born in the early 90s with a breakthrough: the invention of the blue light LED. Since then, electroluminescence is not only used as an indicator lights but also used to enlighten everything around us.

These new light sources are low–power consumption, robust, long lifetime… they show many advantages but they are not yet recyclable and with an important investment cost. That is why reliability is a crucial point and a well–understanding of degradation mechanisms is the spearheading to improve products.

In this thesis, we present an innovative study of four kinds of High Power LED used for lighting, from four different manufacturers, with different technologies and manufacturing processes but with closed the same characteristics as monochip, same luminous flux, same color temperature, same nominal DC current and same power… To achieve these objectives, we have needed to build a new prototype of aging test bench to allow us to apply electrical and thermal stresses.

The first chapter will remind a brief history of the light sources from the natural one to the most current usual artificial light sources such as incandescent filament lamps, mercury and sodium vapor lamps, fluorescent lamps. It gives the chronological revolution of those light sources and the motivated challenge to research and develop them. The discovery of the electroluminescence and, finally, the LEDs will take a great place in this chapter. From a technical point of view, this chapter will present also the state of the art of technologies of LED (chip structures, assembling and packaging). We will close this chapter with an overview of the main encountered degradations from the chip and interconnection failures modes to the package level degradation linked, as an exemple, to the phosphor or the encapsulant.

The second chapter will present all theoritical aspects needed to explain and understand the electrical and optical characteristics of LEDs. Firstly, we

present the electrical effects due to the temperature; indeed, the increase of this parameter can leads to deprivation of light emitted intensity due to several mechanisms. Secondly, with some notions about radiation pattern, the optical characteristics are described and the link between temperature and emission intensity is also explained.

The innovative prototype of aging bench used in this study will be described in the third chapter. This one allows us to introduce also all measurements tools, like the sourcemeter unit or the impedance analyser for the electrical characterizations but also the spectrum meter for photometrical characterizations. We present also the software that has been developed specially for this thesis.

The Chapter IV will report the electrical and photometrical characterizations of the 128 LEDs, focused on an electrical point of view with the evolution of the electrical parameters from the equivalent model and I–V curves evolutions, and the effects of stresses on the spectrum, the luminance and the color temperature will end this chapter.

A general conclusion presenting the most important results and perspectives to enhance this study will close this work.

1.

STATE OF THE ART OF THE GaN LEDS TECHNOLOGY

1.1. HISTORY OF LIGHTING SYSTEMS

1.1.1. The Sun

The sun, Figure I.1, is well known as the first natural light source for all the people. It allows them to perceive every object due to its generated light in the range of visible spectrum. Human eye perfectly got used to this light source, this is why the sun still remains an absolute reference like, as an example, the color rendering index. However, because of the absence of that natural light source during night time, it becomes as a challenge to mankind to generate a similar spectral power distribution light source to replace the sun during the darkness which leads to innovation and invention of various light sources along our evolution.

Figure I.1: Sun, the first light source.

Figure I.2: Artificial Lighting.

Approximately $5x10^5$ years ago, man started to use fire burning wood, fiber immersed in molten fat, sesame oil, nut oil, castor oil, fish oil and so on (Figure I.2). Following paragraphs will briefly present the main artificial light sources but mankind's story is paved with many great inventors like Sir Humphry Davy,

Foucault, Yablochkov who have built new light sources. We have chosen to present only the most significant artificial light sources.

1.1.2. Incandescent Filament Lamp

Francis Hauksbee, in 1705, builds a gas discharge lamp and this could be considered as the first light source ever built. But the most well–known revolution in artificial light source still remains the incandescent lamp. In 1860, it is the first time of success in producing a light source without combustion, odor and smoke – incandescent filament lamp – by Joseph Wilson Swan and the technology was enhanced thereafter by Thomas Alva Edison (1879). The first filament to be used is carbonized–paper filament followed by cerium oxide–based solid electrolyte and thereafter filaments of metals such as osmium, tantalum, and tungsten. It is an electric light which produces light with a wire filament heated to a high temperature by an electric current passing through it, until it glows (with 12 to 14 lm/W and a lifetime of ~1500 hours).

1.1.3. Mercury and Sodium Vapor Lamps

Mercury vapor lamp (Figure I.3) was patented by Peter Cooper Hewitt in 1901. The lamp produces a bluish–green. It is a gas discharge lamp that uses an electric arc through vaporized mercury to produce light. Mercury vapor lamps are more energy efficient than incandescent and most fluorescent lights, with luminous efficacies of 35 to 65 lm/W. Their other advantages are a long bulb lifetime in the range of 24,000 hours and a high intensity, clear white light output. For these reasons, they are used for large area overhead lighting, such as in factories, warehouses, and sports arenas as well as for streetlights. Clear mercury lamps produce white light with a bluish–green tint due to mercury's combination of spectral lines.

Figure I.3: Mercury Vapor Lamp.

Color corrected mercury bulbs overcome this problem with a phosphor on the inside of the outer bulb that emits white light. They offer better color rendition than the more efficient high or low–pressure sodium vapor lamps. They operate at an internal pressure of around one atmosphere and require special fixtures, as well as an electrical ballast. They also require a warm–up period of 4 to 7 minutes to reach full light output. Mercury vapor lamps are becoming obsolete due to the higher efficiency and better color balance of metal halide lamps.

Sodium Vapor Lamp is a gas–discharge lamp that uses sodium in an excited state to produce light. There are two varieties of such lamps: low pressure and high pressure. Low–pressure sodium vapor lamp (

Figure I.4) was invented in 1919 by Arthur Holly Compton (1892–1962) of Westinghouse Electric in the United States. It is highly efficient electrical light sources, but their yellow light restricts applications to outdoor lighting such as street lamps. It only gives monochromatic yellow light and so inhibits color vision at night. High–pressure sodium lamp (Figure I.5) was first developed by General Electric (GE) and has a broader spectrum of light than the low–pressure lamps, but still poorer color rendering than other types of lamps.

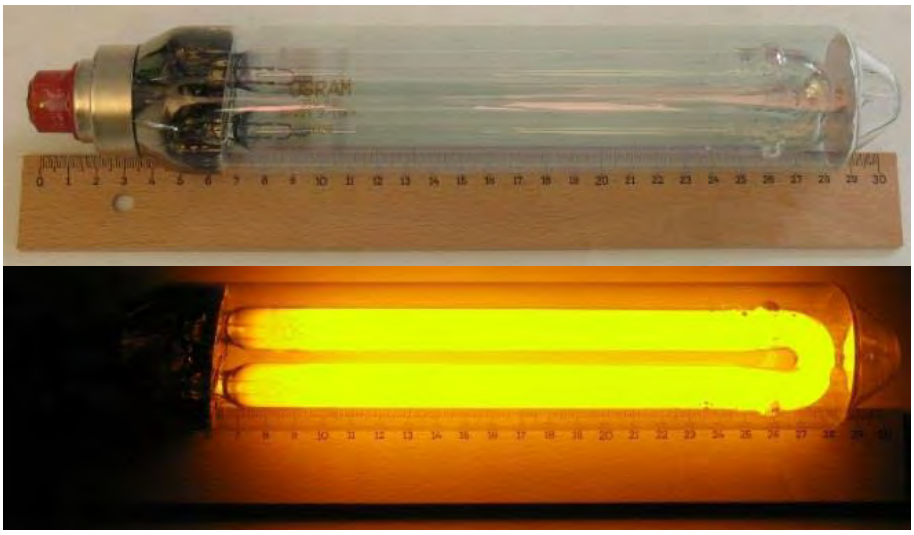

Figure I.4: Low–pressure sodium vapor lamp.

Figure I.5: High–pressure sodium vapor lamp.

1.1.4. Fluorescent Lamp

In 1938, the Westinghouse Electric Corporation began marketing the fluorescent lamps (Figure I.6). It is a low pressure mercury–vapor gas–discharge lamp that uses fluorescence to produce visible light. An electric current in the gas excites mercury vapor which produces short–wave ultraviolet light that then causes a phosphor coating on the inside of the bulb to glow. A fluorescent lamp converts electrical energy into useful light much more efficiently than incandescent lamps. The typical luminous efficacy of fluorescent lighting systems is 50–100 lumens per watt, several times the efficacy of incandescent bulbs with comparable light output.

Figure I.6: Fluorescent lamp.

1.1.5. Light–Emitting Diodes (LEDs)

In 1907, the British electrical engineer and experimenter Captain Henry Joseph Round was investigating the possibility of using Carborundum or silicon carbide (SiC) crystals as rectifying solid–state detectors, then called "crystal detectors." During his experiments on the flow of electric current through SiC, Round observed a curious phenomenon: when a potential difference of ~10 V was applied across a SiC crystallite, a first visible shaft of light was emitted (Figure I.8). This marked the birth of the first LED. Interestingly, it was a metal–semiconductor or Schottky diode, not a PN junction diode. Round further observed that only one or two crystallites glowed at such a low voltage while a larger number of crystallites emitted light at a much higher voltage, ~110 V. Although at that time, the material properties were inadequately controlled, and the emission process was improperly understood, Round reported his findings to the journal Electrical World.

A Note on Carborundum.

To the Editors of Electrical World:

SIRS:—During an investigation of the unsymmetrical passage of current through a contact of carborundum and other substances a curious phenomenon was noted. On applying a potential of 10 volts between two points on a crystal of carborundum, the crystal gave out a yellowish light. Only one or two specimens could be found which gave a bright glow on such a low voltage, but with 110 volts a large number could be found to glow. In some crystals only edges gave the light and others gave instead of a yellow light green, orange or blue. In all cases tested the glow appears to come from the negative pole, a bright blue-green spark appearing at the positive pole. In a single crystal, if contact is made near the center with the negative pole, and the positive pole is put in contact at any other place, only one section of the crystal will glow and that the same section wherever the positive pole is placed.

There seems to be some connection between the above effect and the e.m.f. produced by a junction of carborundum and another conductor when heated by a direct or alternating current; but the connection may be only secondary as an obvious explanation of the e.m.f. effect is the thermoelectric one. The writer would be glad of references to any published account of an investigation of this or any allied phenomena.

NEW YORK, N. Y. H. J. ROUND.

Figure I.7: Publication of JH Round in Electrical World.

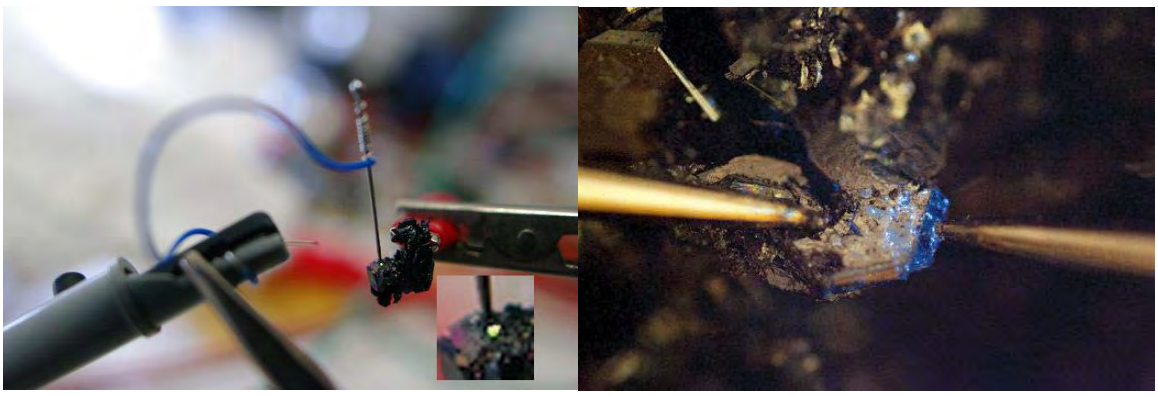

Figure I.8: A replication of H. J. Round's LED experiments.

It was until 1929, the Russian scientist and inventor Oleg Vladimirovich Losev reported detailed investigations of the luminescence phenomenon observed with SiC metal–semiconductor rectifiers. He noticed that (i) in some diodes, luminescence occurred when they were biased in the reverse direction and (ii) in other diodes when they were biased in the forward and reverse directions. He hypothesized that this light emission was quite akin to cold electronic discharge. He

also noted that the light could be switched ON and OFF at tremendous speed, such that the device was usable as a light relay.

Before 1950s, SiC and II–VI semiconductors were well known. Many II– VI semiconductors, for example, ZnS and CdS, occur in nature. The very first LEDs had been made using SiC and there had been one testimony of LEDs made from zinc blende (ZnS). The era of III–V compound semiconductor materials was ushered in the 1950s. These semiconductors do not occur naturally but are made by man. In the 1950s, large single–crystal boules of gallium arsenide (GaAs) wafers were made. Infra–red (IR) region LEDs and lasers based on GaAs were first reported in 1962. GaAs has a direct bandgap of 1.424 eV (300 K), and emits light of wavelength 870 nm.

The phenomenon of light emission would have been forgotten but for the efforts of Nick Holonyak Jr., who in 1962, working at GEC, developed the first practical visible spectrum red LED (Holonyak and Bevacqua 1962). He is aptly called the father of the LED. These gallium arsenide phosphide (GaAsP) LEDs are used as indicator lights, seven–segment numeric displays, and alphanumeric displays.

From 1962 onward, laser and LEDs based on III–V compound semiconductormaterials took their place. In 1968, the first commercialized LED produced 10^{-3} lm.

Being an indirect–gap semiconductor, it does not emit significant amounts of light due to the requirement of momentum conservation in optical transition. In the pure state, GaP is out of place for LED fabrication. But doping it with active impurities, such as N or ZnO, improves its characteristics. In the 1970s, green LEDs were fabricated with an efficiency of 0.6% by doping N.

The phase of development consisted of aluminum gallium arsenide (AlGaAs) LEDs grown on GaAs substrates, employing fully lattice–matched direct bandgap systems and heterostructure active regions. By this improvement, the luminous efficiency of the early red LEDs surpassed that of a red filtered incandescent bulb.

In the 1990s, new materials such as InGaP/GaAs, GaInAlN/gallium nitride (GaN), and so on developed in the search for red and blue lasers. The introduction of a new material system, AlGaInP on GaAs was enabled through the maturity of

organometallic vapor–phase epitaxy (OMVPE) crystal growth techniques. AlInGaP facilitated the fabrication of high–brightness materials from yellow to red.

Table I.1: Discoveries and History of LEDs [1]

Year	Event
1907	The British scientist Captain Henry Joseph Round (June 2, 1881 to August 17, 1966), Marconi Labs, discovered electroluminescence using SiC crystal and a cat's whisker detector.
1927	The Russian Oleg Vladimirovich Losev (May 10, 1903 to January 22, 1942) independently reported the creation of LED in Russian, German, and British scientific journals but his research was ignored at that time.
1955	Rubin Brunstein, Radio Corporation of America (RCA), USA, reported IR emission from GaAs and other semiconductor alloys such as GaSb, InP, and so on.
1961	Robert Biard and Gary Pittman, Texas Instruments, USA, found that GaAs emitted IR on passing current and received patent for IR LED. Although the first LED, its emission was outside the spectrum of visible light.
1962	First practical red LED developed by Nick Holonyak, Jr., General Electric Company; he is seen as the "father of the light–emitting diode."
1968	Monsanto Company started mass–producing visible red LEDs using GaAsP.
1972	M. George Crawford, former graduate student of Holonyak, invented yellow LED and raised the brightness of red and orange–red LEDs by a factor of 10.
1976	Thomas P. Pearsall produced high–brightness, high–efficiency LEDs.
1994	Replacement of GaAs substrate in AlGaInP red LED with transparent GaP.
1994	First WLED. S. Nakamura, demonstrated the first high–brightness blue LED based on InGaN; he is regarded as the inventor of the blue LED.
1998	First commercial high–power LED.
2014	The Nobel Prize in Physics for 2014 was awarded to Professor. S. Nakamura, University of California, Santa Barbara, CA, USA, for the invention of efficient blue light–emitting diodes which has enabled bright and energy–saving white light sources.

Table I.2: Comparison of Key Characteristics and Parameter Values for Commercial Lamps [2]

	Halogen (HA)	Fluorescent (FL)	Low-pressure sodium (LPS)	High-pressure sodium (HPS)	Metal halide (MH)	Ceramic metal halide (CMH)	Light-emitting diode (LED)
Efficacy lm/W	30	<120	200	50−150	100	<95	<80
Power/W	<2000	5−165	<180	35−1000	<2000	20−250	0.1−7
Color temperature/K	<3500	Wide	1700	<3500	Wide	3000-4200	Wide
Color rendering index (CRI)	100	>90	0	20−85	>90	>90	>90
Lifetime/kHrs	2−5	10−30*	20	10−30	10−20	10−20	>50

* Inductive mercury fluorescent lamps offer more than a 60,000-hour lifetime.

In 1996, the first white LED (WLED) was developed and it was pioneered by Shuji Nakamura and Gerhard Fasol by whom a blue AlInGaN LED has been successfully developed to complete the full color missing of white light illumination.

Table I.2 presents comparison of key characteristics and parameter values for various light sources.

1.2. LED CHIP STRUCTURES

1.2.1. Conventional Lateral and Vertical Structure

In November 1993, Nichia Chemical Industries, Ltd has shown their first nitride–based high–brightness light emitting diodes by using a conventional lateral or horizontal chip, Figure I.9a, [3]–[5]. The drawback of this LED structure causes by the low electrical conductivity of Mg–doped p–type. The semi–transparent material has been spread to the top contact to get better current injection uniformity, however, the result leads to the lowering of light extraction due to the absorption of semi–transparent material.

Afterward, a better light extraction and thermal dissipation LED's structure has been developed by Cree Inc. by using vertical injection structure with SiC substrate material, Figure I.9b. The vertical LED structure has gained the advantage of using smaller top area of the chip as electrodes which leads to higher

light extraction comparing to the conventional lateral LED structure. In addition, SiC substrate material as described in previous section has better thermal conductivity comparing to sapphire material used in lateral structure that results in better thermal evacuation.

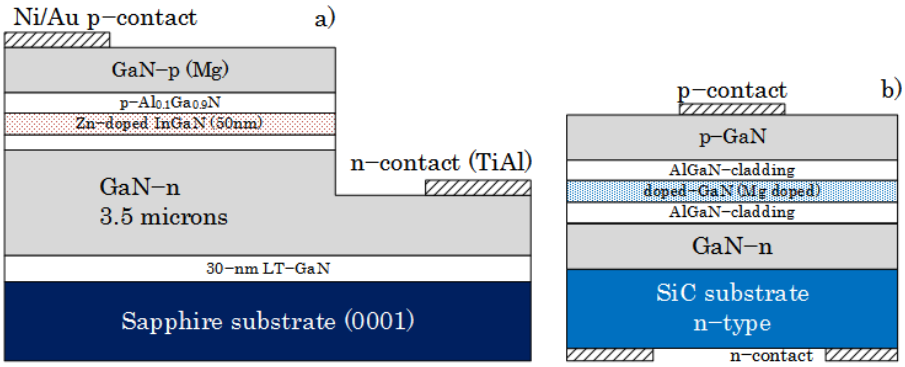

Figure I.9: a) Lateral structure, b) vertical structure.

1.2.2. Flip Chip Structure

Another leading firm for high–power LED development, Philips Lumileds, has developed an alternate LED structure by inventing Luxeon devices based on flip chip technology, Figure I.10. Flip chip structure is confirmed to present higher light extraction comparing to the two previous chip configurations. The advantages of this LED structure are indeed due to the possibility of a larger light escaping cone when a low refractive index sapphire is flipped along the path of emitting light output. By flipping the chip, sapphire which is a low thermal conductivity material can also be removed from heat dissipation path. In addition, the configuration also allows heat–sink can be placed close to the junction as the result heat dissipation is improved [6]. Moreover, the structure get rids of light–absorbing semitransparent material from the light emitting path this leads to the increase of light extraction. However, the structure is still prone to the light absorber caused by sapphire material and also the cost and the technical difficulty of mounting.

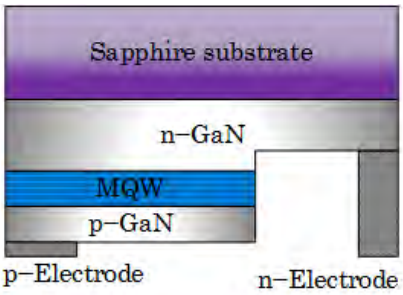

Figure I.10: Flip chip structure.

1.2.3. Vertical Thin Film Structure

There is a trade–off between advantages and disadvantages of sapphire substrate material that is commonly used for GaN–based LED epitaxial structure. So, in order to keep using this substrate material, there are some research developments [7]–[10] that have proposed a new laser lift–off (LLO) technic. LLO is the process of separation GaN from sapphire substrate by laser heating. The technic allows removing of poor thermal conductivity of sapphire material and instead the high electrical resistivity n–type GaN (GaN: Si ~ 0.005 Ω.cm) material takes place providing a good current spreading on the whole diode surface so that the light output obstacle caused by current spread layer material in conventional LED structure is eliminated [6]. The technology is patented to Osram jointly developed in cooperation with the Schottky Institut in Munich as ThinGaN or vertical thin–film (VTF) structure and the extraction efficiency was reported to reach up to 75% [11]. The structure also accomplishes a better thermal management due to the fact that in VFT structure, p–type side can be bonded to an alternate material such as high thermal conductivity and low cost material silicon (Si) [9], [12] and high thermal conductivity gold plated layer on a highly reflective platinum [7].

Figure I.11: LED ThinGaN structure by Osram.

1.2.4. Thin Film Flip Chip Structure

N–type contact is deposited in the center of the top surface leading to electrode shading in VTF structure which leads to obstacle of some light extraction. Philips Lumiled has taken advantages of combination between vertical and flip chip structure developing its Luxeon Rebel and Flash products based on thin film flip chip (TFFC) technology. The structure allows minimizing of absorption caused by electrodes in vertical configuration [13].

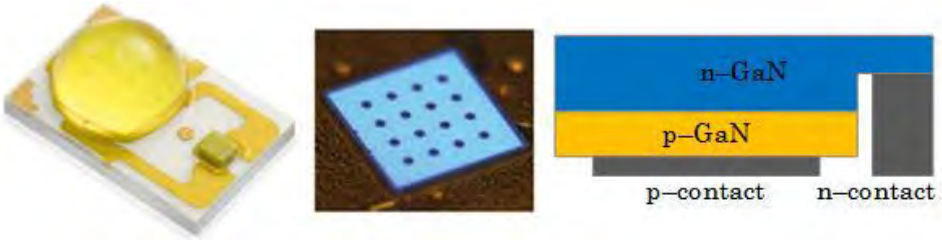

Figure I.12: TFFC by Philips Lumiled.

Following the above fundamental LED structures, LED chip technologies have been in a long path of research development to improve more internal quantum and external light extraction efficiency, heat dissipation and effective cost consideration in term of epitaxial growth method, electrode geometry and surface texturing design in order to accomplish high–brightness LED application. As example, internal quantum efficiency (IQE) can be improved by growing GaN on micro–patterned sapphire substrate (PSS) where the cone–shape patterned sapphire is obtained by dry etching technic [14]. PSS growth shows a lowering of density of edge dislocation that leads to the increase in the IQE comparing to the conventional sapphire substrate structure.

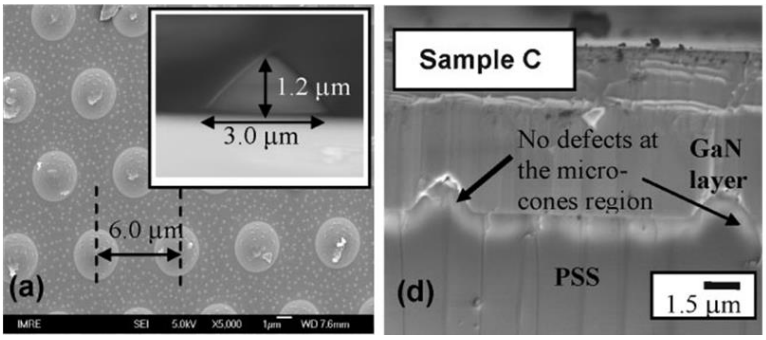

Figure I.13: SEM images of PSS and GaN grown on PSS [14].

In [15], roughening the surface of an n–side–up GaN–based LED with a hexagonal "conelike", Figure I.14, after LLO process, has been proposed showing twofold to threefold increase of power output comparing to that of an LED before surface roughening. Reported in [16], there is 35% of light output enhancement by texturing Al oxide honeycomb nanostructure on the n–GaN top layer of a thin–GaN LED structure, Figure I.15.

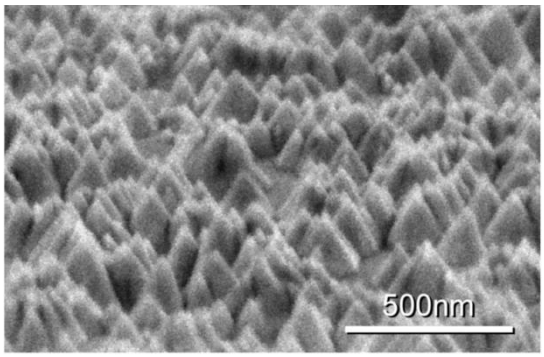

Figure I.14: SEM of an N–face GaN surface roughening etched by a KOH–based PEC method [15].

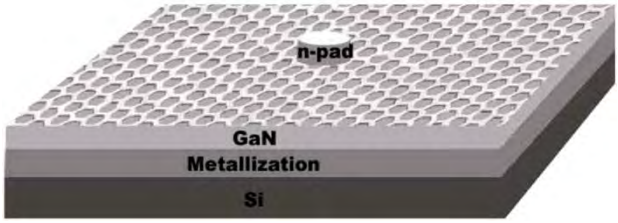

Figure I.15: Al–oxide honeycomb nanostructure on thin–GaN LED [16].

1.3. PACKAGING OF LEDS

As described in previous section, LED–generated heat has become a main concern after emerging of high–brightness LEDs since the 1980s, especially the high power LEDs that are used for general lighting application. So, LEDs have to be housed in a good package that can provide good thermal path for heat dissipation and also good emission path for light output to the outside world. The following section will briefly describe about packaging technologies that have been apply for LED.

1.3.1. Low Power LED Package

In the past, light emitting diodes were mainly served in the purpose of indicators because of its low luminance and its electrical power input is lower than 0.1 watt. LEDs are packaged in two–lead devices. The package also known as dual in–line package (DIP) and mostly comes with diameter size of 5mm or is called "T1–3/4" package. The plastic epoxy resin is used as an encapsulant of the package to provide mechanical and humidity protection and also to shape the beam of light output. The epoxy resin material of the encapsulant is easily susceptible to short wave length of light emission and high temperature which leads to optical attenuation. Under high temperature and moisture operation, the high elastic modulus of such encapsulant can cause the bond wire to fracture.

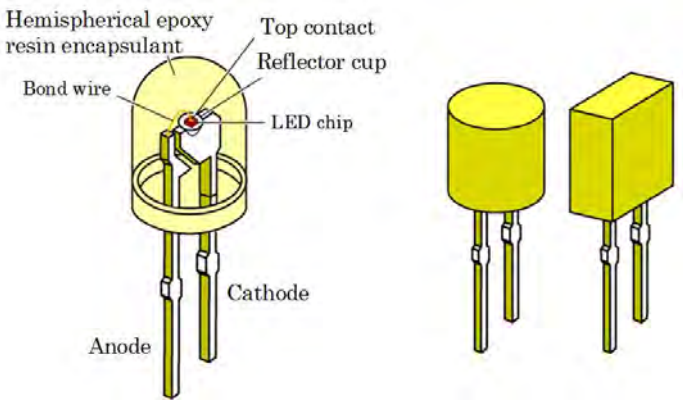

Figure I.16: a) LED with hemispherical encapsulant, b) LEDs with cylindrical and rectangular encapsulant [17].

At the first stage of high–brightness LEDs appearance, the adaptation of LEDs package continued to follow this package style until it was notified about the issue of the package related to its thermal limitation because a small size of metal leadframe served as a thermal evacuation path in the package. Such problem has initiated a new challenge to the development of high power LED's package in order to accommodate the high injected current drive devices that provides a gateway to general lighting application.

1.3.2. High Power LED Package

In 1998, migration of low power LED package has been begun by Lumileds Luxeon™ to be able to support devices current injection up to 350 mA with a power approximate to 1W. Luxeon's package is a plastic leadframe packaging structure

Figure I.17. The package has notably solved the problem of heat dissipation that encounter in low power package due to a significant reduction of thermal resistance of the package. However, there is a main drawback of the package design during that time, it is the large size of the metal slug leads that causes large volume and weight unfavorable to some applications.

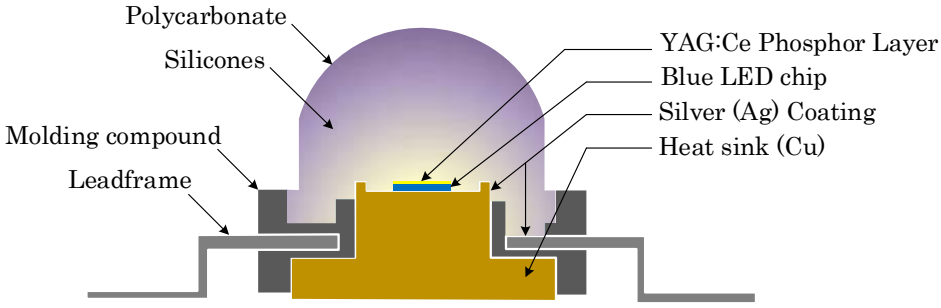

Figure I.17: High power LED packaging.

Following Luxeon's packaging, Osram thereby starting invention their Golden Dragon product patterning leadframe technology. Thereafter, package design based on chip on ceramic board has been proposed by Cree Inc. and then Lumileds also has released their new version of Rebel product. Figure I.18 illustrates the package technology used by these leading LED manufacturers. There are three main factors that influent on the package design consideration including heat dissipation, light extraction and size of the chip that becomes larger in order to adapt the new application field such as general illumination or general lighting usage.

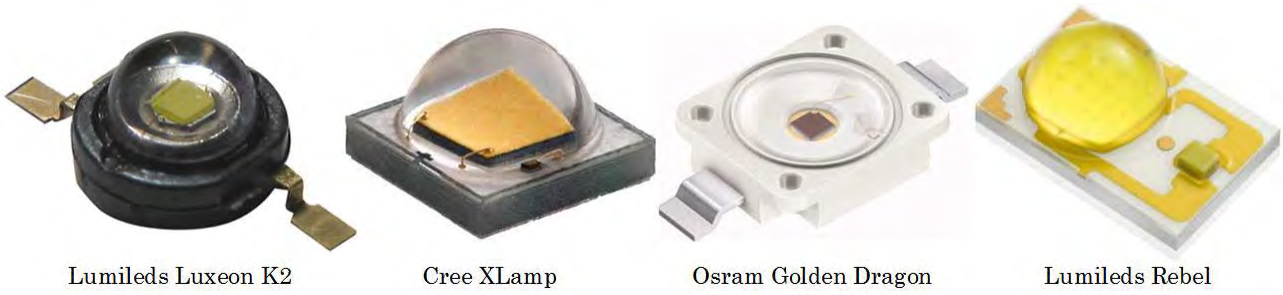

Figure I.18: Typical package products of high power LED.

Table I.3: Factors influent LED packaging *[6]*

	Standard LED	High–Brightness LED	Ultra–High–Brightness LED
Size (µm)	350x350	~ 1,000x1,000	Up to 2,000x2,000
Input	30 mA, 3.5 V	350 mA, 3.5 V	1 to 1.5 A, 3.5 V
Electrical power (W)	< 0.2	Up to 1	Up to 5 or 10
Luminous flux (lumen) @ $I_{nominal}$	1 to 3	5 to 50	100 to 500
Efficiency (lm/W)	20	> 50	> 100

1.3.3. Packaging Process

Figure I.19 adapted from [18], illustrates the most common "single chip" LED packaging process starting from wafer level up to the completely testing stage. The following section briefly illustrates the process of packaging of the aforementioned low and high power package technology.

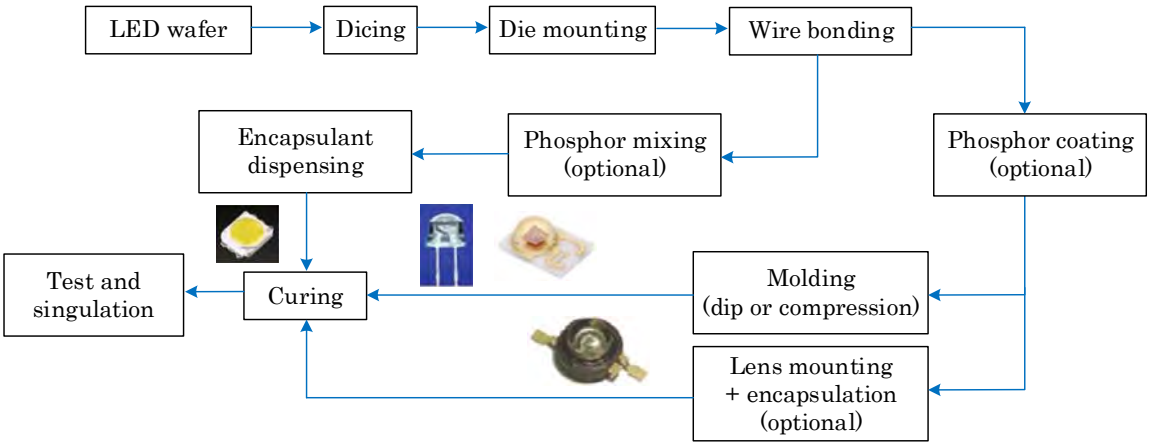

Figure I.19: Packaging process flows of common LEDs [18].

1.3.3.1. Dual in–Line (DIP) Packaging

DIP, Figure I.20, is low power package in which chip (5) is firstly bonded to the leadframe (1c) served as electrical and thermal path, and situated in a metallic cap (6). Then a gold or aluminum wire (4) is connected between the top side of chip to another leadframe(1a). Next step, it is molded with epoxy resin. And after demolding, a hemispherical lens is formed. This lens serves as mechanical protection to the LED's chip and also to converge the emitting light close to the lens axes that is mostly applied for indication field.

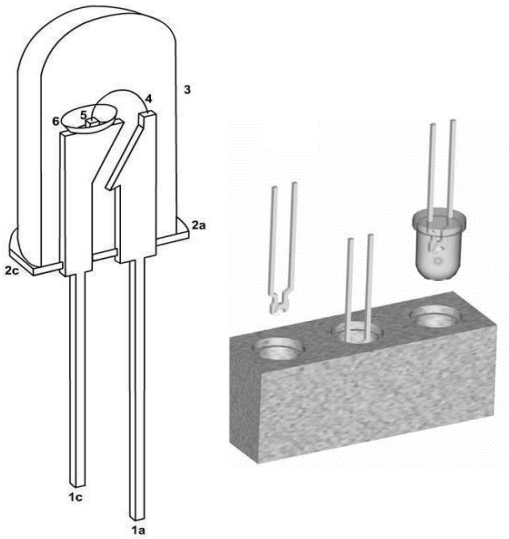

Figure I.20: DIP Packaging [19].

1.3.3.2. SMD LED Packaging

Beside the thermal problem of the DIP package, there're also some other disadvantages associated to such LED package including the supplementary cost needed for making board drilling. The drilled holds also put some constrains on electronics components integration on the PCB (unlike CMS components that allows using both side of a PCB). The surface–mount device (SMD) or surface–mount technology (SMT) package of high power LED, Figure I.21, has been designed adopting the electronic package technology to minimize the space and reduce the PCB size. There are two types of SMT package commonly used in high power LED package. They are leadform package and leadless package.

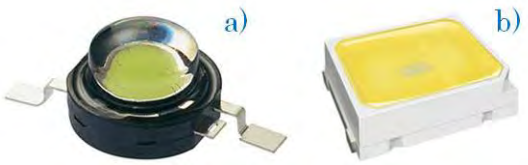

Figure I.21: a) Leadform package, b) leadless package.

1.3.3.2.1. SMD Leadform Packaging

Figure I.22 is the cross section of high–power LED to show the main component of the SMT lead form package. The packaging process is starting from the chip bonding. The chip is first attached to the heatsink acting as mechanical supporter and also as heat dissipation. Sometime the chip is mounted on silicone sub–mount as an electrostatic discharge (EDS) protection. Silver or silver paste is commonly use as adhesive material for chip attachment. After chip is attached, the wire bonding process is performed. The wires are connected from chip electrodes to leadframe of the package.

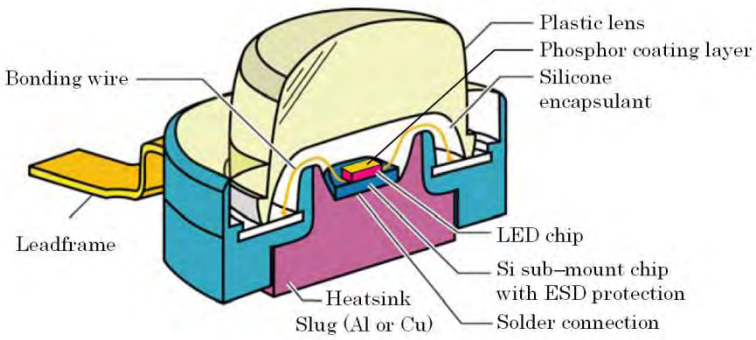

Figure I.22: Main components of the SMT LED package [17].

Figure I.23 to Figure I.25 show bonding process the lateral, vertical and flip–chip technologies described in previous section during packaging. Then the phosphor coating layer is integrated direct to the chip called chip level conversion (CLC) or phosphor is dispersed in casting or molding encapsulant material called volume conversion to convert light output to a desired wavelength. Next step encapsulant material is molded to form a protection layer of chip and bonding wire. Last step is the incorporation of lens to realize the various optical requirements of applications. All parts of the packaging process have been performed carefully in order to obtain a good reliability of product, however, they inevitably degrade

during operation and its degradation mechanisms will be demonstrated more detail in the next chapter of this work.

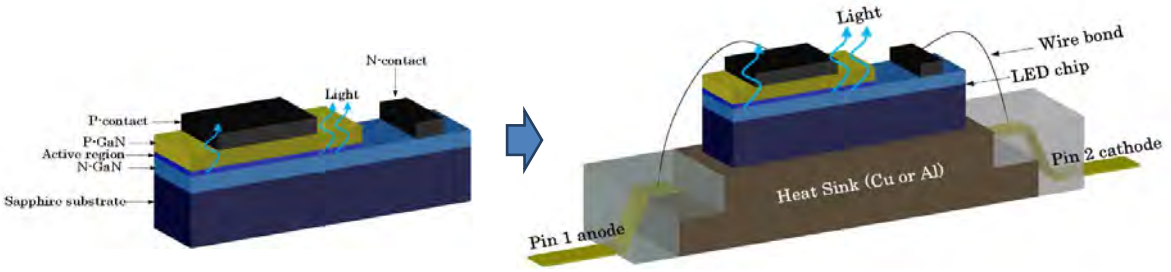

Figure I.23: Packaging of lateral LED chip.

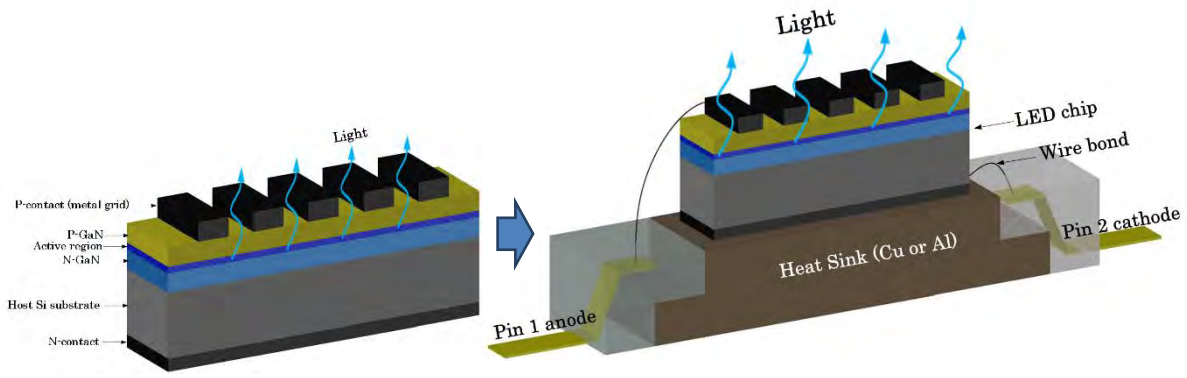

Figure I.24: Packaging of vertical LED chip.

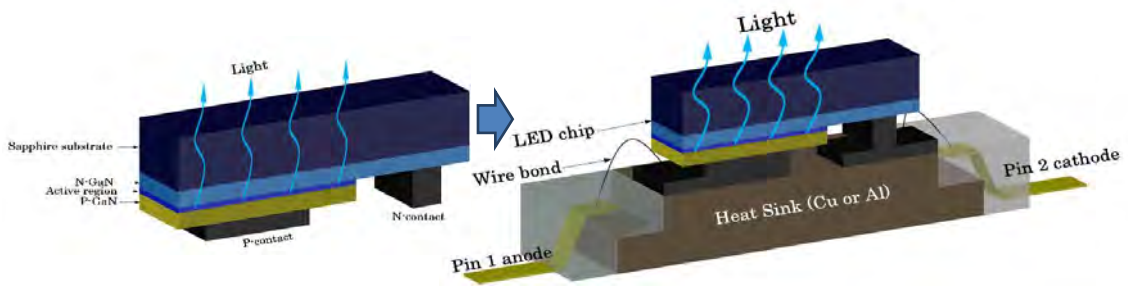

Figure I.25: Packaging of flipped chip LED structure.

1.3.3.2.2. SMD Leadless Package

As applied by its name, leadless or no–lead package is the SMT package type that comes without leadframe, Figure I.26. It has been designed to minimize more space used and also to be able to reduce additional thermal resistance because there is no need leadframe and substrate in the package. In addition, the absence of some parts of packaging process such as chip bonding, wire bonding, dispensing etc. contributes

to the lowering of total packaging cost. In 2012, Seoul Semiconductor was claimed to be the first company which is commercially success in the Wicop LED package products, Figure I.27. Instead of ceramic base, in 2013, Osram, release their Oslon Black Plate package product based on another SMD technology by using Quad Flat No lead (QFN) as based substrate, Figure I.28.

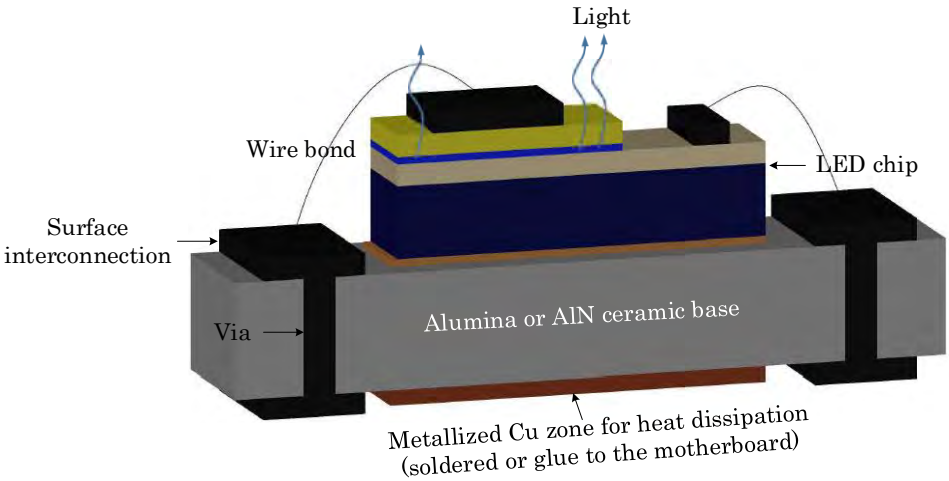

Figure I.26: SMD leadless LED packaging.

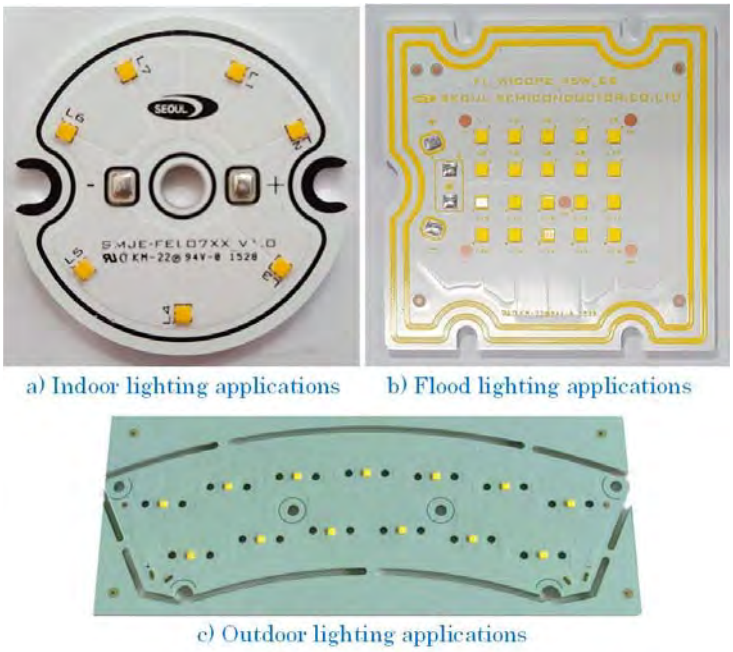

Figure I.27: Leadless Wicop2 module (Chip-on-board packaging, Seoul Semiconductor) [20].

Figure I.28: QFN LED package (Oslon Black Flat, Osram) [21].

1.3.3.3. LED Array Packaging

Although there is a great breakthrough of semiconductor materials that allows developing the high–brightness LEDs, there're still constrains on substrate materials and growth technic that limit a larger size of LED chip to produce required luminous flux from just a single chip. So a single LED in one housing with hundreds of luminous outputs cannot provide enough high luminous flux for some applications such as retrofit lamp for household lighting application, street light and automobile which require from thousands of luminous fluxes. To achieve high luminous flux, there's effort to build a multichip LED package by integration the array of single chip packages into a single package. Figure I.29 shows the arrangement of both leadless led package and leadframe led package in an array to form as a single housing package.

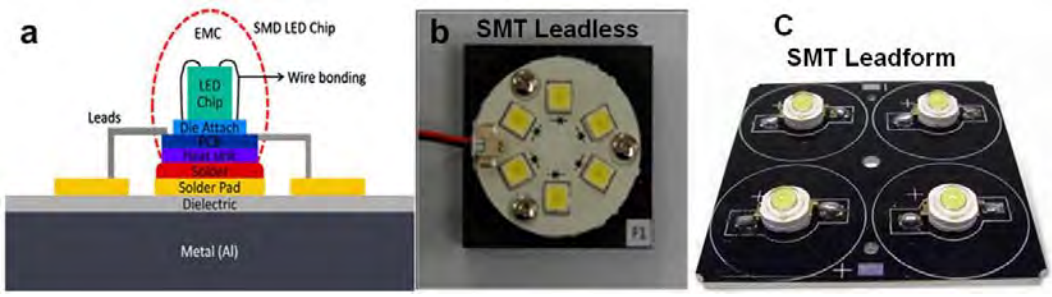

Figure I.29: Multichip LED package [22].

However, in the case where higher luminous flux is required for some application such as large commercial building or industrial space illumination, the solution of single chip array arrangement is not a good choice in such circumstance. The array may need a large amount of single led packages, 50 to hundreds, in order to accomplish the required luminous flux. Implementation of chips in large quantities

can be difficult in a dense integration board. Then, thermal effects become a critical problem because they are reinforced by mutual thermal interactions. Thermal effect is the main problem that limit application of multichip arrangement because when the single chip packages are densely integrated in an array package, thermal resistance of led chip significantly increase and is strongly related to the number of chips as depicted in Figure I.30. The increase of thermal resistance is mainly caused by the thermal overlap when the devices are arranged closely to each other [23].

Therefore, LED array packaging has been shifted to alternative technology in order to solve better thermal effect problem of the high luminous led package. One technology known as Chip–on–Board (COB) LED package have been developed. In COB technology, LED chips are directly bonded to heat dissipation substrate and there is no insulation layer between substrate and LED chips which results in shortening of heat dissipation path enabling better heat removal. It also reduces the overall packaging cost due to none existing of some assembly parts [24]. As a consequence of thermal dissipation improvement, better lifetime, reliability and stability are achieved and it also allows high density of chip integration leading to better light uniformity. Figure I.31 shows COB package products of some leading LED manufactures.

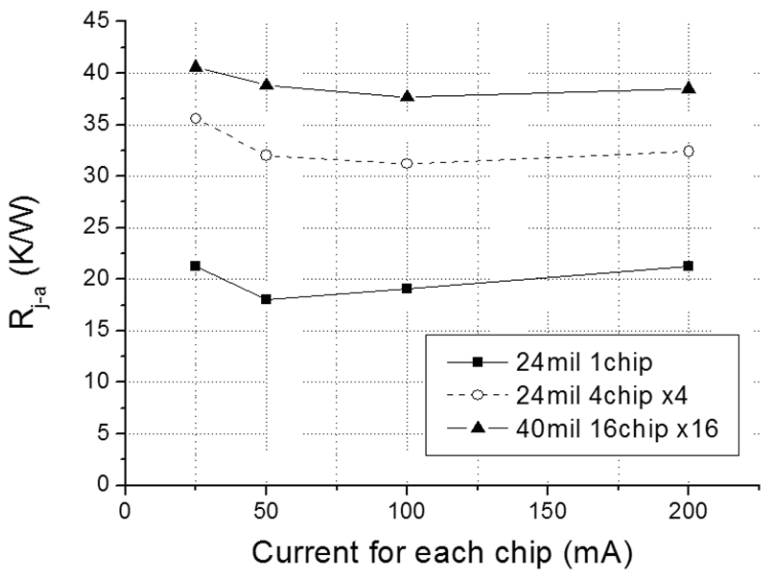

Figure I.30: Comparison of Rth for each LED chip in 1–, 4–, and 16–chip packages [23].

Figure I.31: COB LED package of some leading products.

1.4. MAIN DEGRADATION OF LEDS TECHNOLOGY

The aim of this work is to study the degradation and failure mechanisms of different chip technologies of LED products. This section presents the main LED's degradation and failure modes that are mostly encountered. Degradations and failure modes are described for each level from the chip to the silicone packaging including connections with their respective origin: electronic (as electro–migration), thermal (encapsulation failures…), or mechanical effects (i.e. lattice mismatch between layers, cracks…).

As mentioned in previous section, LEDs are composed of different parts during fabrication process including semiconductor chip formation, wire bonding and contact formation, and optical packaging. In every process and parts of manufacturing devices, it matches one specific degradation and failure mechanisms or more. These effects can be divided into sub–locations and are described in the following paragraphs.

1.4.1. Degradation and Failure Modes at Chip Level

There are various mechanisms of defects or other mechanisms such as die/chip cracking, dopant diffusion and electromigration that possibly and randomly occur in semiconductor chip level leading to the degradation or failure to LEDs as historically reported by many research work such as [25]–[29].

1.4.1.1. Generation and Movement of Defect and Dislocation

During epitaxial growth, due to lattice mismatch threading dislocation defects can be formed at the interface of GaN layer and substrate materials and then thread through the entire crystal and active region. Figure I.32 shows threading dislocation generated in bulk GaN layer.

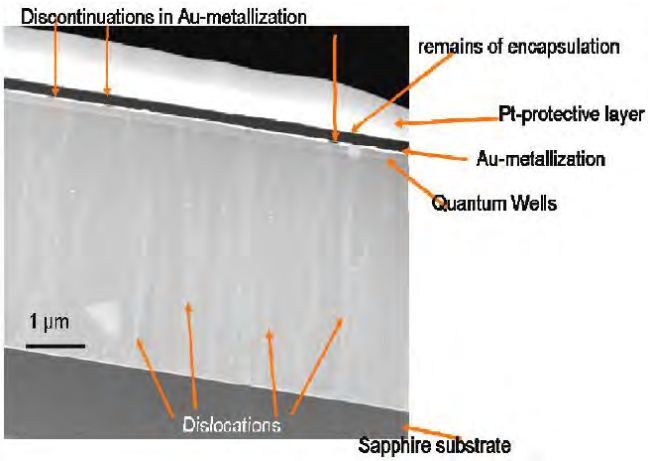

Figure I.32: Dislocations in GaN and discontinuations in Au–metallization [26].

Threading dislocations along the bulk crystal also associate to the pits formation on the chip surface. Report from Chen et al. , [30] has shown clearly the pits formation and threading dislocation along its vertex by using atomic force microscopy (AFM) to analyze the surface morphology of their LED–like conventional vertical structure in conjunction with transmission electron microscopy (TEM) to verify their results in cross–section view.

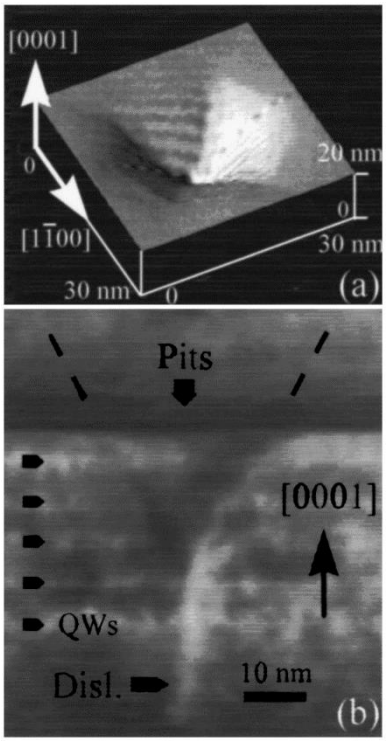

Figure I.33: (a) An AFM image and (b) a cross–section TEM image of a pit [30].

From Figure I.33a, it shows that as viewed from [0001] plan the pit has hexagon shape and in Figure I.33b, it shows the V–shape form of the pit and its interrelated threading dislocation in cross–section plan view.

In this study, the formation of these defects was investigated in the case where the chip was grown on a large lattice mismatch sapphire substrate. However it was also reported by [31], [32] that there is the same defects growing on SiC substrate material and patterned sapphire substrate (PSS). The mechanism of these defect formations also have been highlighted in some literatures [33]–[35]. The mechanism of threading dislocation formation was agreed to follow the theoretical demonstration proposed by [33] confirming that dislocation is caused by the higher strain of high energy materials existing around the defect core. However, the pits formation that mostly related to threading dislocation were ascribed to be the result of appearance of impurity of foreign atoms like oxygen or other dopants such as Al, In, Si, or Mg during growing process [34]. Dark–spot defects (DSDs) are also confirmed to be a mechanism that causes the degradation of LED characteristic. The investigation of DSDs were observed on InGaN/AlGaN LED [35]. Figure I.34a shows slight pre–existing of dark–sport defects at initial stage of sample, then dark spots become to increase in size after first stage of aging at 67 hours Figure I.34b and finally, at 310 hours of aging state the defects more enlarge and the whole region also become dark (Figure I.34c). The dark sports and region are observed to occur close to left electrode due to the concentration of injected current in this area.

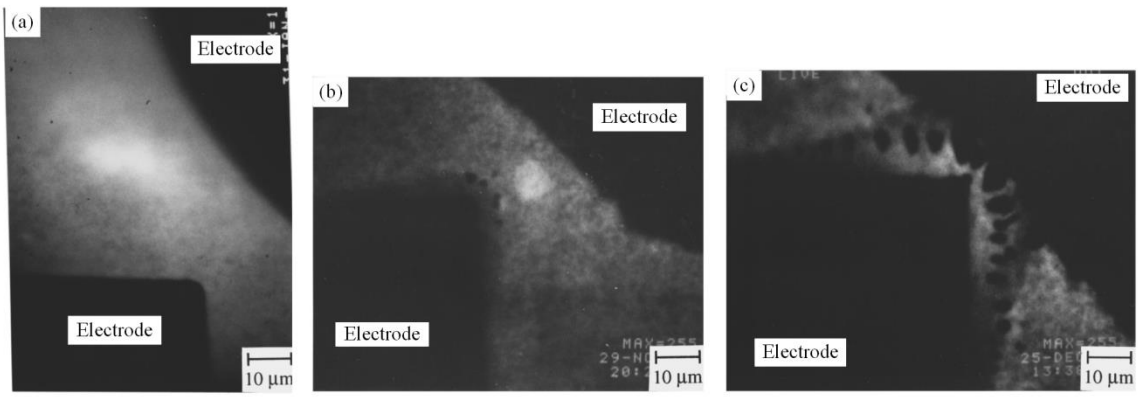

Figure I.34: Dark–spot defects generation (a), (b), and (c) correspond to initial stage and aging of 67 and 310 h, respectively [35].

1.4.1.2. Die Cracking

Die cracking is one of the main degradation mechanisms of LED by which it can leads to the increase of the operation threshold voltage of the device because the cracking can cause the increase of series and thermal resistance [25]. The failure mode of die cracking can be caused during wire bonding process when the over bonding pressure is applied to the chip. In Figure I.35b, it shows the internal inspection of a large area crack of the chip produced by over bonding stress during bonding process.

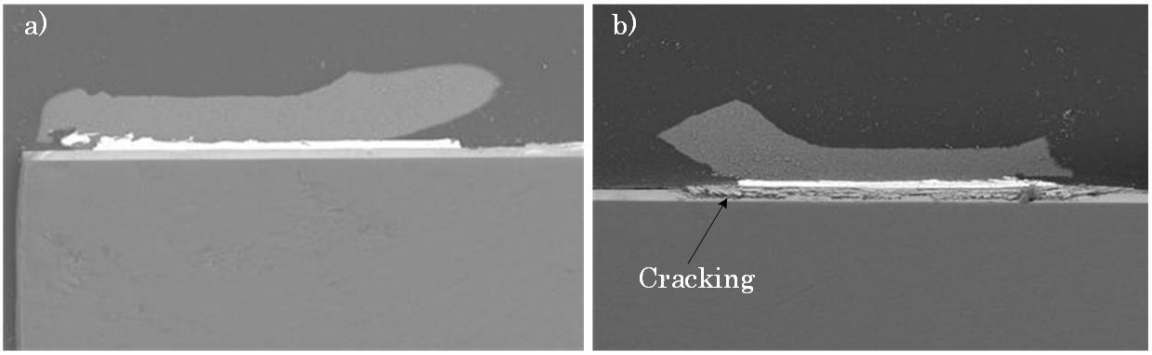

Figure I.35: a) Good die with proper bonding, b) cracking die with over pressure boding [25].

The quality of the chip can also be affected by the process of chip dicing. The poor quality of dicing can produce the edge defects that can lead to the fracture of LED die [36], [37]. Figure I.36 shows a large edge defect caused by poor dicing process.

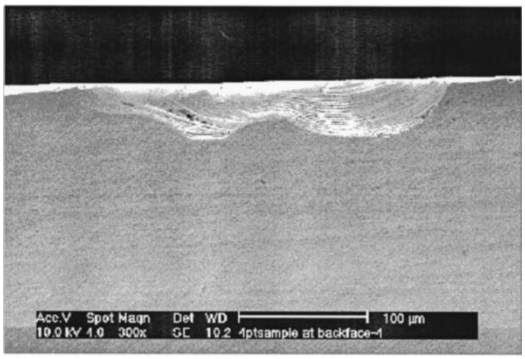

Figure I.36: Large edge defect caused by dicing [36].

In addition, different conditions of die wafer surface such as untreated surface, grinding surface or polished surface can influence to the strength of the die leading to the crack when it is subjected to the stressed load such as thermal, mechanical and environmental loading during fabrication or operation. As shown in

Figure I.37, surface morphology of die was further studied using scanning electron microscopy (SEM) by Wu et al., [38] and it was revealed that the grinding or sawing can cause defect to the surfaces with the presence of tiny notches or micro–cracks. These defected surfaces are susceptible to applied strength and easily lead to die fracture.

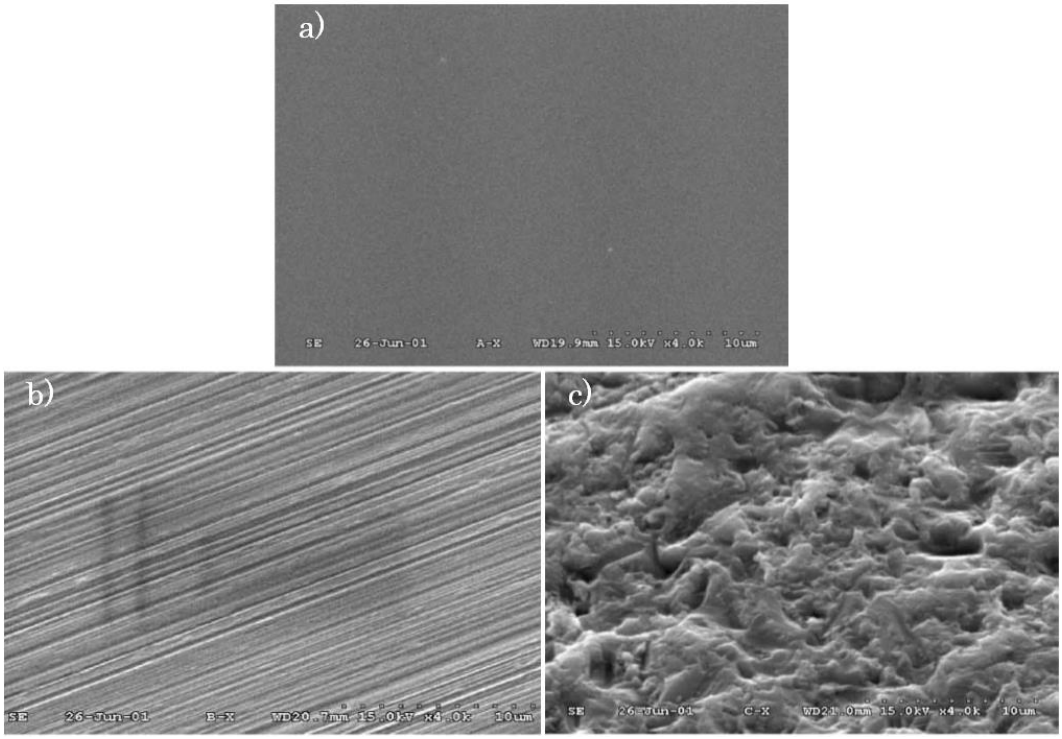

Figure I.37: Die surface morphology (a) polished, (b) ground, and (c) untreated [38].

Thermal effect, whether it is generated by joule heating when the high current drive is applied or by high ambient temperature, is the main cause involving to the failure mode of die cracking. Differences in thermal coefficient expansion between the substrate materials and epitaxial layer can cause expansion or contraction force exerting to the chip during high and fast–rate thermal heating is applied to LED. The force will eventually lead to the break of LED die and as a consequence leading to the degradation of LED performance. Figure I.38 shows different thermal expention of GaN/Si and GaN/Sapphire.

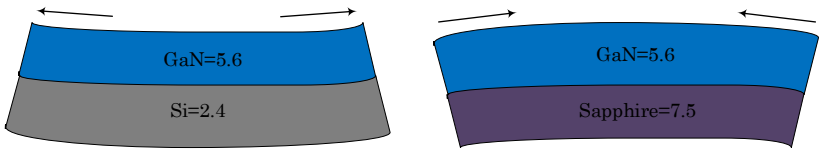

Figure I.38: Thermal expansion coefficients of GaN/Si and GaN/Sapphire.

1.4.1.3. Dopant Diffusion

Dopant diffusion is defined as the event when the distribution of Mg dopants diffuses into the quantum well of LED active region. Mg is a commonly used material as a p–type dopant material to provide number of hole for nitride–based LED fabrication and it was shown that when the concentration of Mg was optimized by accurate controlling of its doping profile along the path from p–contact to the top layer of active region during the growth, it can provide the maximized electroluminous efficiency of LED. The result studied by Köhler et al. , [39] as illustrated in Figure I.39 has been revealed that the efficiency of optical output power tends to increase when the amount of Mg dopants is increased. However, the optical output power starts to reduce when the concentration of Mg dopants continues to increase beyond the maximized value. The decrease of optical output power is due to the high possibility of diffusion of excessive dopant into the active region and acts as defects of non–radiative recombination center.

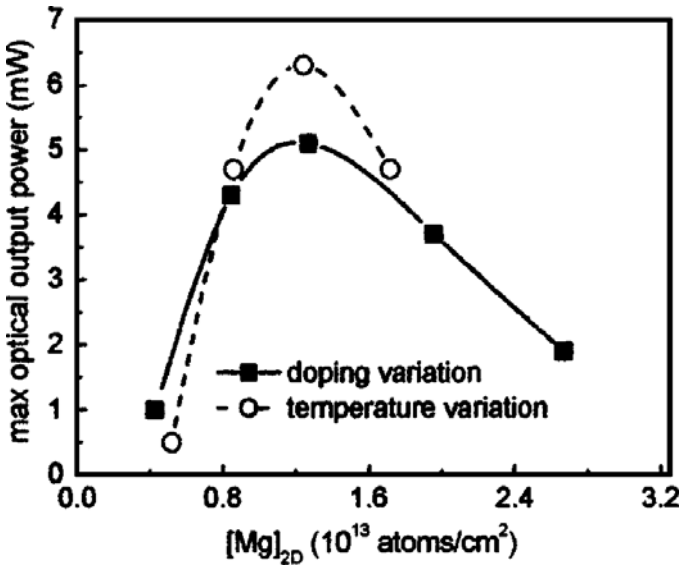

Figure I.39: Maximum EL output power as a function of the integrated Mg concentration [39].

1.4.1.4. Electromigration

Electromigration to be one of LED failure mechanisms is a process that metal atoms of electrical contact migrate to the p–n junction of LED through threading dislocation defects or defect tubes [29], [40], [41]. The movement of this metal contact is caused by the excessive current density of high electrical current drive.

The electromigration of metal atoms between P and N region of die along the defect path, produces the spikes along the flowing path and possibly causes short circuit to the device. As illustrated by Kim et al. , [41], Figure I.40 indicates the increase of dot spot on the electrode surface and is extrapolated to be caused by electromigration.

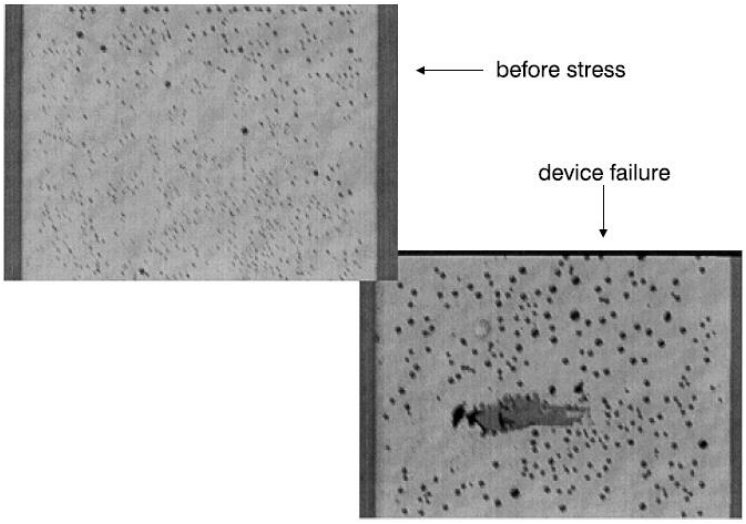

Figure I.40: Optical microscope photograph of electrode surface before stress and after device failure [41].

1.4.2. Interconnection Failure Modes

1.4.2.1. Bond Wire /Wire Ball Bond Failure

The wire and the ball bonding are part of electrode connection and can be failure during operation due to thermal heating. The wire bonding can be divorced from bonding area due to the thermal stress. The thermal expanding coefficient's mismatch can cause the bonding wire to be pulled off as shown in Figure I.41.

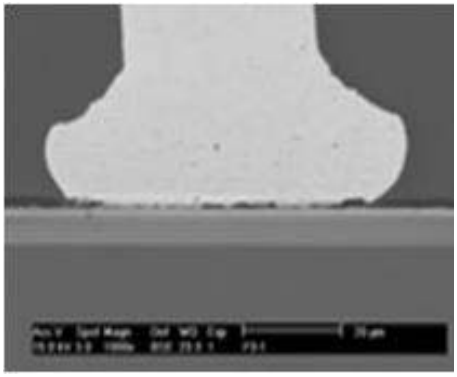

Figure I.41: Banding pad divorced from banding area [25].

Thermal expansion mismatch also can result in wire bonding to be broken, chipping or wire ball bonding fatigue when the bonding process is formed by a ball bonding. As indicated in Figure I.42, the wire neck is the weakness part of the wire and it is the most easily broken zone after thermal stress is applied.

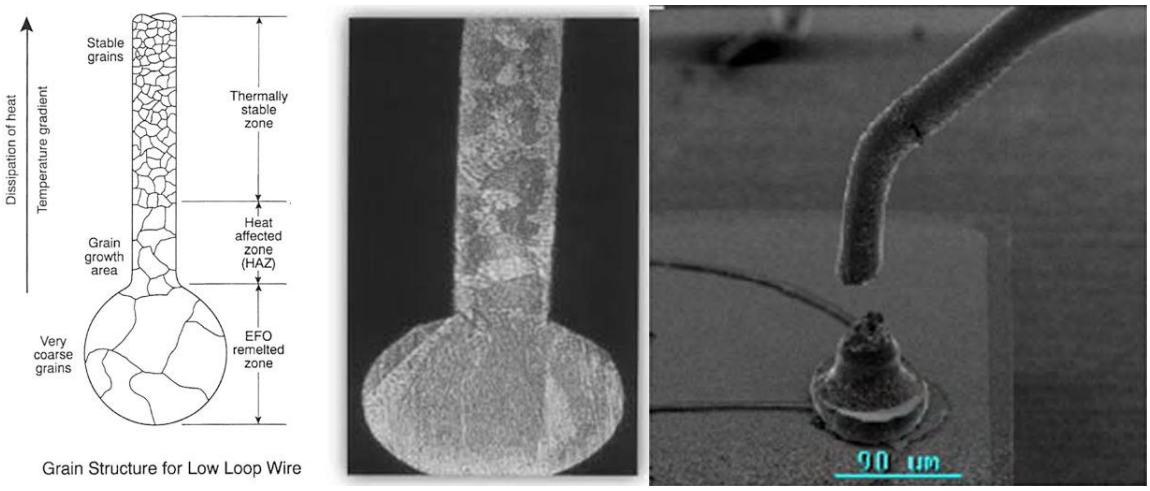

Figure I.42: Breaking of wire neck or heat affected zone (HAZ) [42].

As published by Wu et al., [43], the connection interface of bonding wire also can be cracked resulting of significant drop of luminous efficiency and accelerate contact degradation and catastrophic failure.

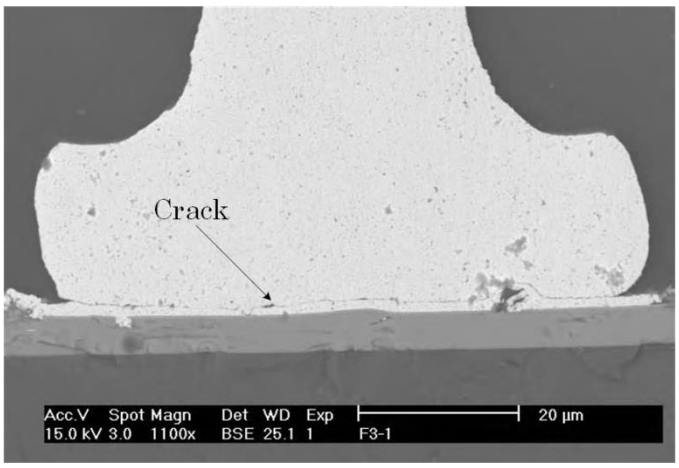

Figure I.43: Crack in electrode bonding interface [43].

1.4.2.2. Electrical Contact Metallurgical Interdiffusion

Unlike electromigration that the electrical contact degradation is caused by crystalline defects or defect tubes, in case of electrical contact metallurgical interdiffusion, the degradation is caused by thermally activated metal–metal and metal–semiconductor interdiffusion. Although it cannot find specific topic on direct effect of electrical contact metallurgical interdiffusion to LED electrical contact degradation, there are many researches working on failure modes and mechanisms of LED have linked the electrical contact degradation to the out–diffusion and in–diffusion of electrical contact [42, p. 77], [44], [45, p. 20]. These researches are based on studies about metal contact degradation of high electron mobility transistors (HEMTs) caused by thermally–activated metal interdiffusion such as in [46]–[48]. Figure I.44 illustrates a TEM cross–section analysis of metal diffusion mechanism of Pt into semiconductor after the stress is applied across the device. The Pt layer becomes thicker and the interface is rough after the stress period. Metallurgical interdiffusion results in alloying and intermixing of the contact metals. This can lead to an increase of the parasitic series resistance, a short circuit of LED and eventually, to cause degradation of light output or permanent catastrophic failure when the high temperature is reached during operation or stress conditions.

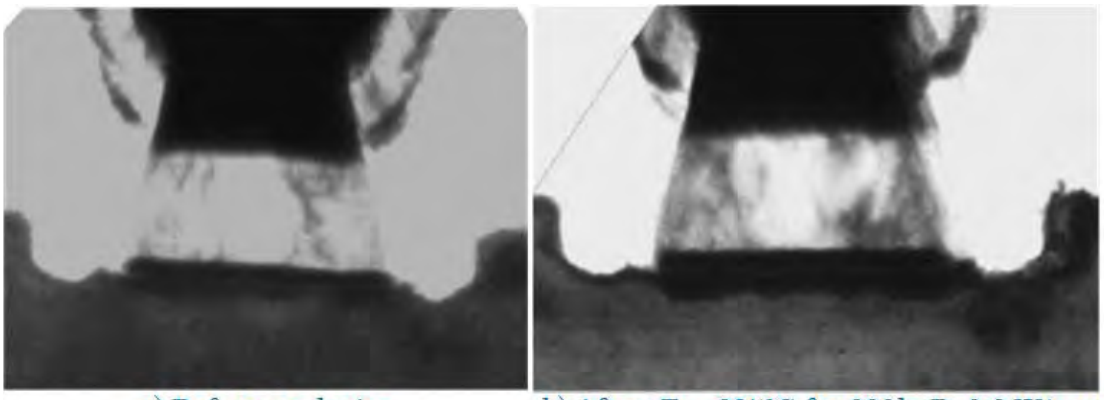

a) Reference device b) After: T_{ch}=235°C for 200h, P=0.2 W/mm

Figure I.44: TEM of MHEMT with Pt/Ti/Pt/Au gate before and after stress [47].

1.4.2.3. Electrostatic Discharge

Electrostatic discharge (ESD) is an inevitable phenomenon that can happens randomly during manufacture, selection, testing, packaging, storage, transportation

and installation process [25]. It is a type of catastrophic failure mechanism of LED resulting in rapid open circuit. Different solutions have been proposed to various LED structure based on their pros and cons in order enhance the reliability performance involving ESD such as incorporation of Zener diode in parallel to the LED chip, integration of an internal GaN Schottky diode into the LED chip, or inverse–parallel shunt GaN ESD diodes etc.

Jian-Ming et al., [48] has proposed a flip chip mounted on Si submount acting as Zener diode. This one is connected in parallel with LED die to protect LED from ESD as indicated in Figure I.45. The study shows that the integration of Zener diode protection in flip chip LED structure can increase the capability of ESD up to 10kV comparing to the conventional device's structure.

As shown in Figure I.46, Chang et al. have developed the concept of ESD protection by integration of GaN Schottky diodes internally inside GaN LED with vertical structure [50]. From this structure, under normal forward bias operation, current could flow across the GaN LED from P_L to N_L. On the other hand, if a reverse biased ESD induced electrical pulse originated from the skin of human body occurs, ESD current could flow across the GaN Schottky diode from P_S to P_N. Thus, such a design could effectively protect the GaN LEDs from electrical stress damage [50].

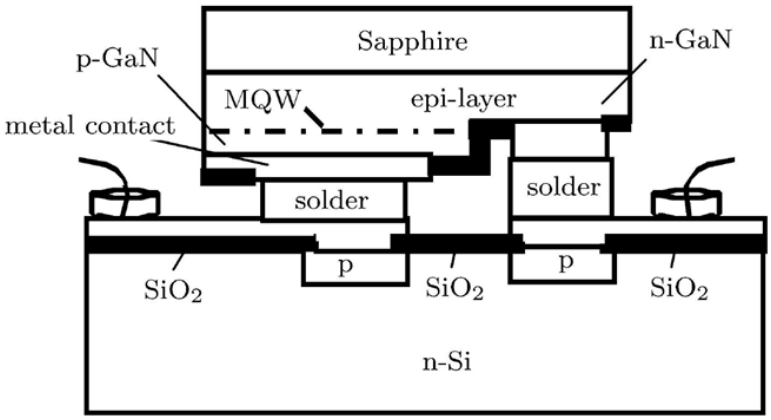

Figure I.45: Si submount as Zener diode for ESD protection in flip chip structure [49].

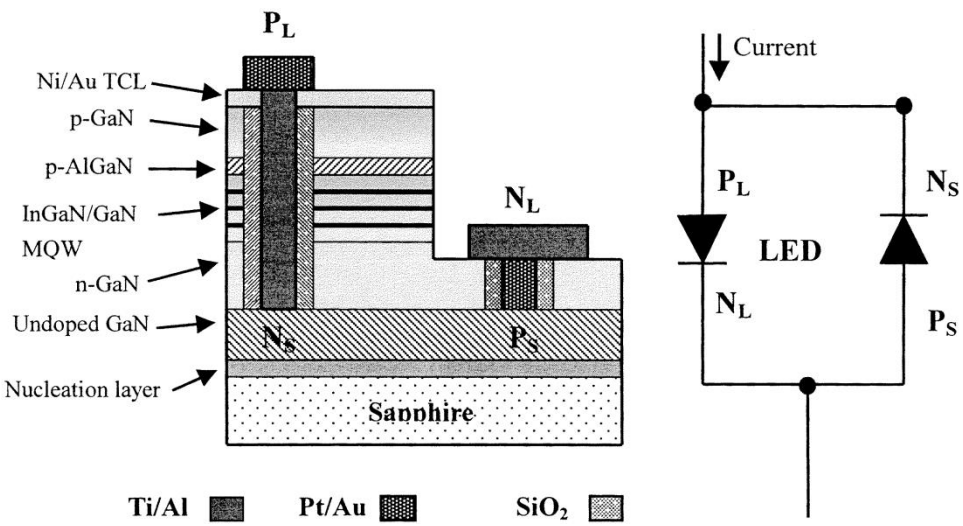

Figure I.46: GaN LED with an internal Schottky diode and its equivalent circuit model [50].

Another proposal of ESD protection has been developed by Shei et al. , [51]. In this research, the electrostatic discharge performance has been improved through the use of a shunt GaN ESD diode connected in inverse–parallel to the GaN LED. The proposed structure is shown in Figure I.47. LED can be protected from ESD or abnormally high reverse voltage by incorporating inverse–parallel shunt GaN ESD diode to GaN LED diode.

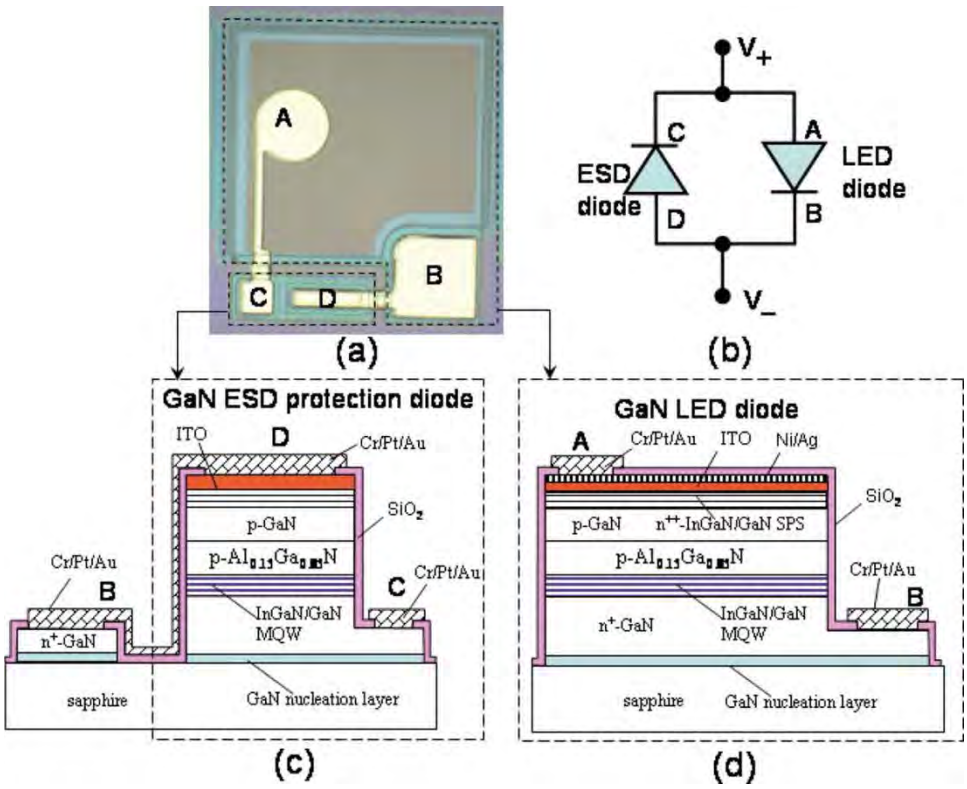

Figure I.47: (a) Bare–chip of LED, (b) Equivalent circuit, (c) an inverse–parallel–connected GaN ESD diode and (d) a GaN LED [51].

1.4.3. Degradation and Failure Modes at Package Level

1.4.3.1. Carbonization of the Encapsulant

Joule heating of electrical overstress current and/or high ambient temperature are the main causes of carbonization of the encapsulant material on the diode surface. Figure I.48b shows the carbonization of a phosphor–encapsulating material under electrical overstress current comparing to the virgin state of device, Figure I.48a, and the carbonization of LED when it's submitted to a high–temperature stress, Figure I.48c. Carbonization leads to the formation of conductive path across the LED and can leaves a conductive carbon film on the LED die that results in forming of short circuit across the LED die [42, p. 79]. Carbonization also can cause the degradation of LED by decrease the electroluminescence of light output due to the cancelation of light reflection from the plastic cover as reported by Meneghini et al. [52]. As adapted from the report, Figure I.49 illustrates the study result of optical power output and the optical spectrum of LED under high thermal stress and it shows that after stress period there is large reduction of optical power and decrease in yellow emission due to reduction of phosphor–converted volume. The modification of these parameters are ascribed to package carbonization that is one of the major failure mechanisms of LED.

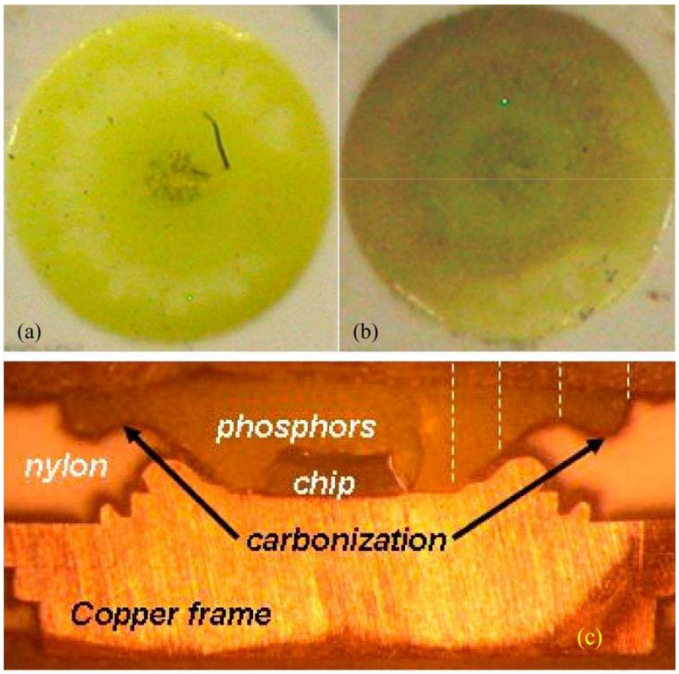

Figure I.48: Carbonization of phosphor–encapsulating material [53].

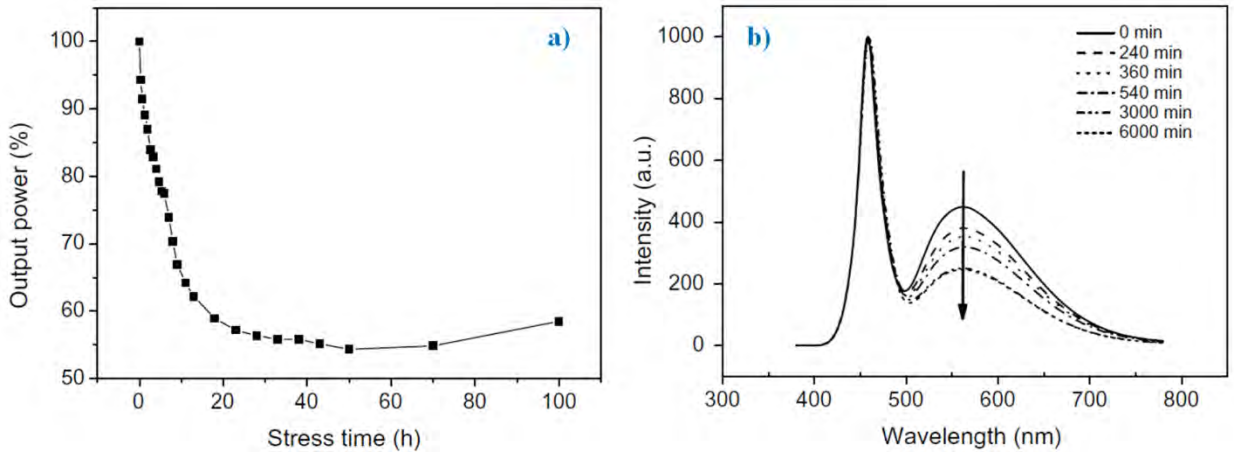

Figure I.49: a) Optical power b) Output spectra, degradation during stress at 200°C [52].

1.4.3.2. Delamination

Thermomechanical stresses, moisture absorption, and/or interface contamination are the main failure mechanisms of delamination and can be found in many separated studies such as [54]–[57]. Delamination can happen at different locations throughout the LED die as shown in Figure I.50. In Luxeon reliability datasheet RD25 [58], It was reported that the delamination occurs between LED die and encapsulant, which causes a thin *chip–air–silicone interface* within the package, Figure I.51. However, it does not cause a catastrophic failure, but this lead to a permanent degradation of the light output because a large amount of light portion generated from the LED chip cannot escape to the surrounding due to the reflection of light output between the interface surfaces of the gap.

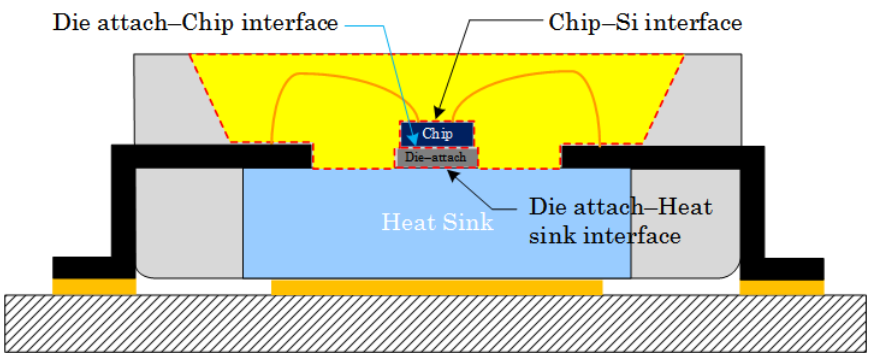

Figure I.50: Possible delamination areas of LEDs.

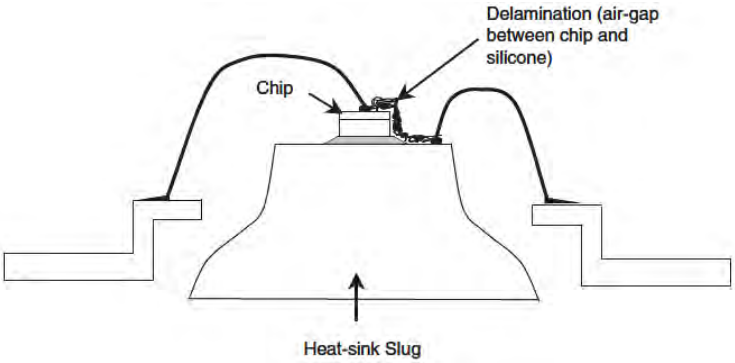

Figure I.51: Delamination between the LED die and encapsulant [58].

It was also reported in [59] that delamination can also come along with either delamination of the *chip–to–die attach interface* or the *die attach–to–heat sink interface* and these will reduce the contact area between the die attach material and its adjacent component, resulting in an increase of the corresponding thermal resistance at chip or die attach level that can lead to the increase of junction temperature, which also affects many other failure mechanisms and ultimately reduces the life of LED packages. Figure I.52 shows the SEM photographs of the cross–section of degraded LED that used two different materials of die attach Figure I.52a Au80Sn20 eutectic and Figure I.52b silver paste under power stress cycle with the high injection current of 700 mA that produces the junction temperature up to 145°C. It was also reported that the mechanism of delamination of die attach layer happen at the interface between chip and die attach and is in the form of void defects for the sample packaging with die attach of $Au_{80}Sn_{20}$ eutectic. On the other hand, the sample packaging with silver paste shows the delamination at the interface between die attach and heat sink by die attach cracking formation.

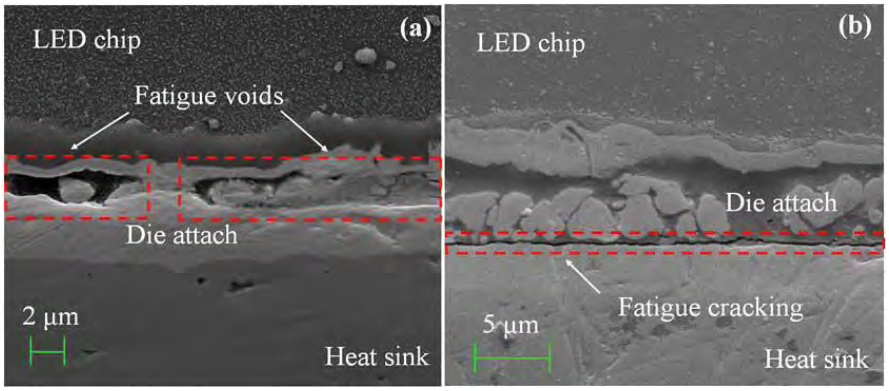

Figure I.52: SEM photographs of the cross–section of degraded (a) $Au_{80}Sn_{20}$ eutectic sample and (b) silver paste sample [59].

It was also reported in [60], the delamination can occur during high temperature operation at the interface of die and phosphor layer in the case of phosphor chip level conversion packaging structure as indicated in Figure I.53. In this case, the failure mode of LED is the color shift characteristic as the result of increasing of the angle at which the blue photons pass through phosphor.

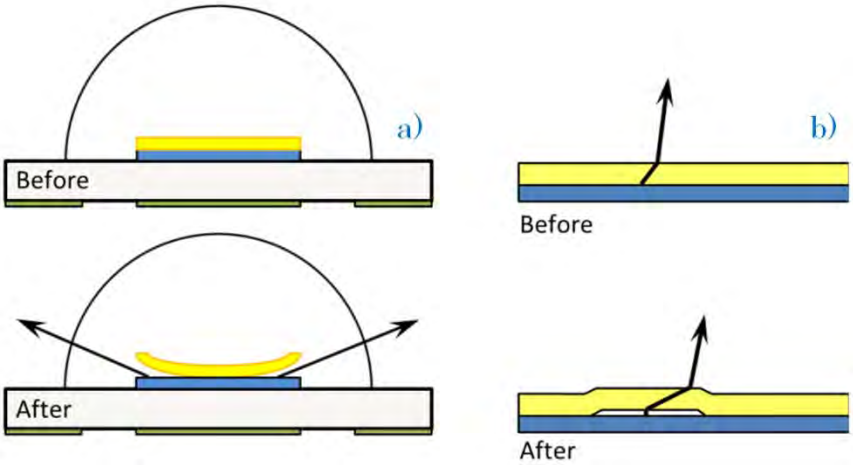

Figure I.53: (a) Delamination and (b) curling of phosphor coated LED package [60].

1.4.3.3. Lens /Encapsulant Failure

Even silicone encapsulant is used instead of optical–grade epoxy encapsulant in order to enhance the quality of LED package, it still exhibits to the degradation becoming to yellowing, Figure I.54 when it is prolonged exposure to the short wavelength UV or high levels of blue light that inevitable emitted from GaN–base LED its self [58]. There are many mechanisms that can lead to lens/encapsulant yellowing such as (1) prolonged exposure to blue/UV radiation, (2) excessive LED junction temperature, (3) presence of phosphor, or (4) contact with metal silver with Cu impurities.

Figure I.54: Encapsulant yellowing [42].

The degradation of light output due to the decrease of encapsulant transparency and discoloration of the encapsulant is extrapolated from the encapsulant yellowing. Figure I.55 shows light out depreciation of a conventional epoxy–encapsulant small signal 5mm white LED and silicone–encapsulate high power LED. Even silicone–encapsulate LED has better performance than epoxy case but the both exhibits the degradation during the operated time.

In addition, to the yellowing process, lens can also present the failure mode of degradation by a number of small hairline cracks that decrease light output due to increased internal reflection of LEDs. The degradation appears due to thermomechanical stresses, hygromechanical stresses, and poor board assembly processing [42, p. 86].

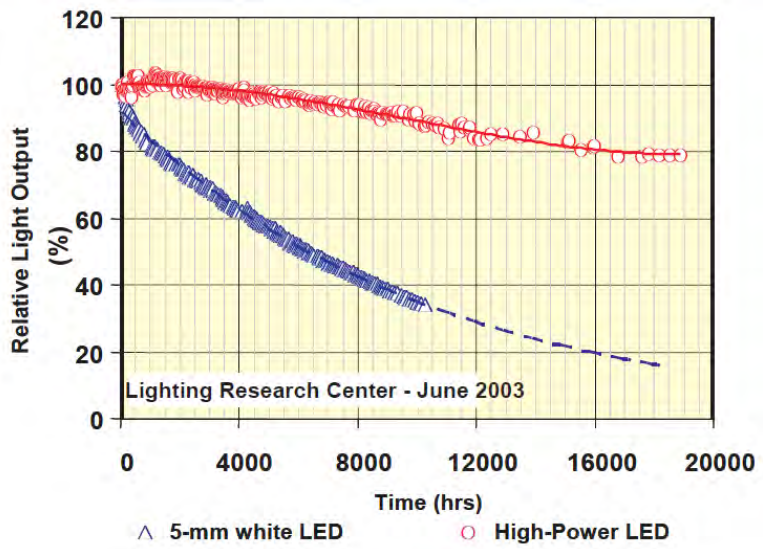

Figure I.55: Relative light output from 5–mm indicator lamps and high–power illuminator LEDs [58].

1.4.3.4. Phosphor Thermal Quenching

The lowering efficiency of yellow light–converted phosphor in the application of white light LED caused by the rise of temperature level, is assigned as phosphor thermal quenching process and it leads to the failure mode LEDs package like color shift or reduce in light output. Similar to most of other LED failure mechanisms, the driving forces phosphor degradation are high driving current and excessive temperature of LED junction. Figure I.56 indicates the quenching process of phosphor layer after a consequence of high temperature stress. The browning of

phosphor layer leads to the modification of optical spectrum and reduces the light output efficiency of the devices [61].

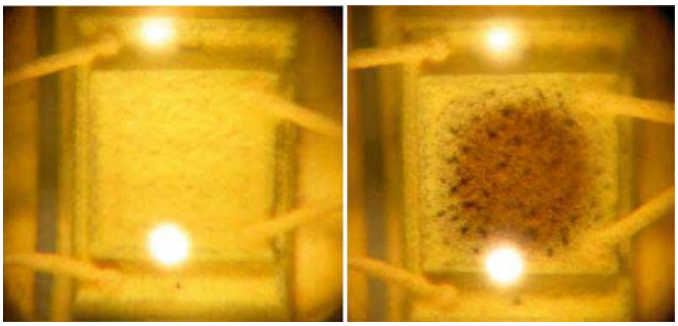

Figure I.56: Degradation of phosphor (left: untreated sample, right: after stress at 100 A.cm−2, 120°C) [61].

In addition, the study that has been done by Hwang et al. [62] reveals that phosphor layer of die–contact or chip level conversion (CHC) exhibits lower degradation rate comparing to that of remote phosphor layer. It was shown that the rapid degradation of remote phosphor layer is due to the higher temperature caused by heat generation by phosphor (conversion loss of phosphor) when dealing with high input power LED. When LEDs operate at high input power, both junction temperature and temperature of phosphor are increase, however their result confirms that the increasing rate temperature of phosphor is higher than the junction temperature. The result contradicts other research works such as [63], [64]. The position of phosphor layer in package LEDs shows that the lifetime of LEDs with die–contact phosphor layer is better then the remote case as indicated in Figure I.57.

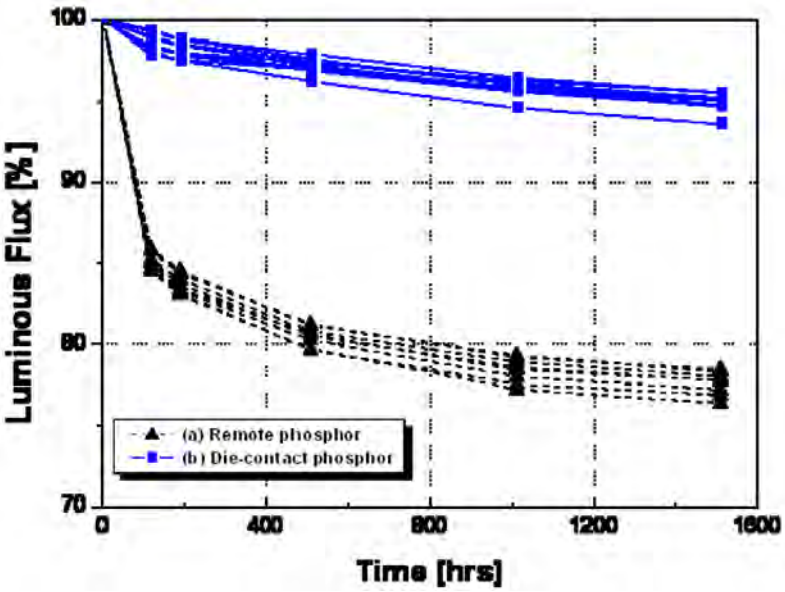

Figure I.57: Lifetime result of LED with (a) remote and (b) die–contact phosphor [62].

1.4.3.5. Solder Joint Fatigue

From time to time, there are many efforts that have been done to increased reliability of LED. In this context, solder interconnect process of LED package has shown its revolution to achieve this objective as an example SMT assemblies using lead–free solder SAC (Sn–Ag–Cu) solder alloy is applied for LED package solder technic to improve the creep strain rate of the solder. As frequently mentioned in in the references of this thesis [42], it demonstrates a various improvement of different SAC alloys on the creep rate of LED solder material and Figure I.58 reveals the result that has been reported.

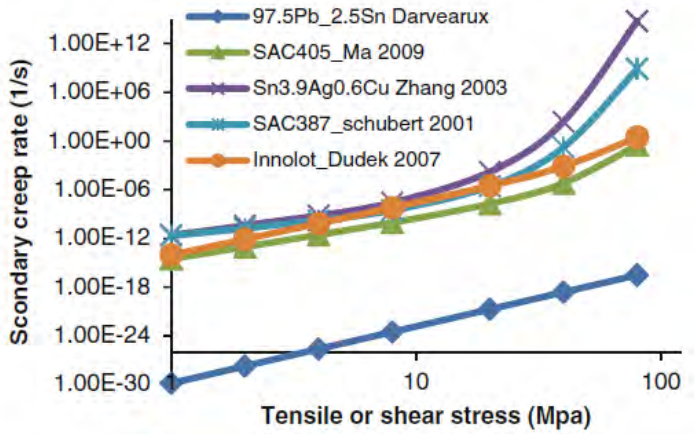

Figure I.58: Creep strain rate vs. tensile stress for different SACxx alloys [42].

However, many research groups such as [65]–[68] have revealed that solder interconnect fatigue is still one of the failure mechanisms in LED applications when it was exposed to the high temperature application or test which would drive the solder creep specially when there is a mismatch CTE between LED sub–mount and heat slug. Figure I.59 illustrates the case of solder fracture due to creep fatigue when it is applied to thermal cycle test.

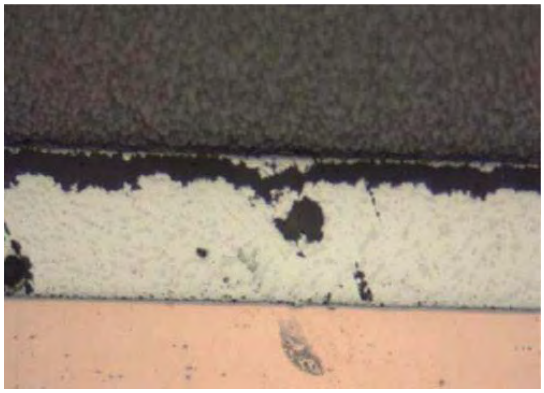

Figure I.59: Solder fracture due to creep–fatigue under thermal cyclic load [42].

Elger et al., [66] have investigated on the solder joint of ceramic LED Packages soldered on Al–IMS (Aluminum Insulated Metal Substrates) boards. In this study, it was demonstrated that the solder joint exhibits the cracks under temperature cyclic stress. In addition, their study has performed on two different solder joints: tin–silver–copper (SAC305: Sn96.5/Ag3/Cu0.5) and Innolot (FL–640: Sn91,175/Ag3,5/ Cu0,7/Ni0,125/Sb1,5/Bi3) and it was confirmed that Innolot has a better creep resistance under the same stress condition as indicated in Figure I.60.

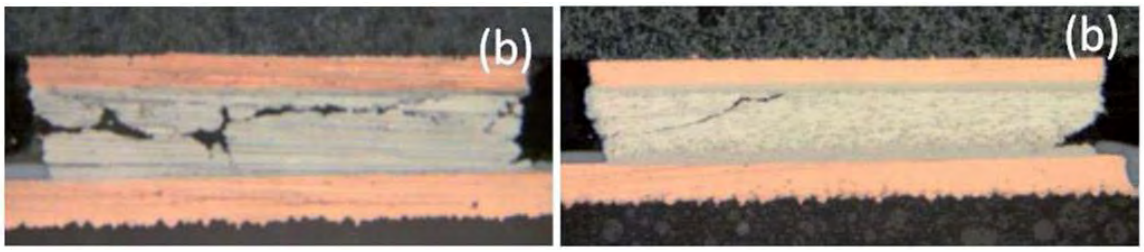

Figure I.60: Solder joint cracks (left: SAC305, right: Innolot) [67].

The cracks of solder joint lead to the increase of thermal resistance and then can cause the increase of junction temperature and eventually it can result in many other failure modes of LED such as light output degradation, acceleration of chip degradation, modification of emission spectrum and color, and also alteration of forward voltage.

1.5. Conclusion – Chapter 1

Many different LED technologies have been developed by many leading LED manufacturers. The revolution of these various technologies is due to the reason of improving the device's performance such as enhancement of thermal path of heat generation as a result it can increase lifespan of the device and specially improvement of light extraction leading to increase of device's efficiency. However, there is trade–off between device's performance of technology design and cost and ease of device's fabrication.

Package engineering also contribute a remarkable impact on device's performance. Migration from conventional low power LED package into high power package design allow better heat dissipation leading to realization of high power

LED application specially for lighting illumination domain. Two package technologies are commonly seen in high power LED package design including leadframe and leadless package. The latter, however, more desire than the former due to some features such as space minimizing and reduction of thermal resistance and also cost effective during package process.

Array package of multiple LED chip integrated into a single package has been designed to solve the problem of high luminous flux required for some specific applications such as retrofit lamp for household lighting application, street light and automobile which require from thousands of luminous fluxes. Concurrence of high luminous flux requirement, the thermal issue of heat generation becomes another challenge to package technology. Based on the challenge of heat dissipation of multiple single–LED chip array, chip–on–board (COB) LED package has been developed. Such LED package allows better heat removal due to less heat dissipation structure (directly bonded to heat dissipation substrate and there is no insulation layer between substrate and LED chips) leading to better lifetime, reliability and stability. COB structure also allows high density of chip integration leading to better light uniformity.

There are many failure modes that LED can encounter after they are operated for a period of time. The failure modes or degradation process of LED are also caused by many types of mechanism. The relevant issues have been described detail in this chapter. It shows that the failure modes of LED can exist at various locations that can be classified into failure sites such as chip level failure, interconnection failure and package level failure. Among these failure modes, each can interface to many failure mechanisms for instant:

i) the degradation or failure at chip level can be caused by the generation and movement of defect and dislocation, die cracking, dopant diffusion and electromigration;

ii) interconnection failure modes can be a result of bond wire or wire ball bond failure and electrical contact metallurgical interdiffusion etc. and

iii) the degradation and failure of LED package can be observed due to carbonization of the encapsulant, delamination mechanism, failure of lens or

encapsulant, the degradation of phosphor materials, or it can be due to fatigue of solder joint. All these failure mechanisms are the main causes that can have effect to the LED degradation or LED catastrophic failure

.

2.

ELECTRICAL AND OPTICAL CHARACTERISTICS OF LEDS

2.1. METHODOLOGY FOR JUNCTION TEMPERATURE EVALUATION

The energy of an injected electron (eV) is converted into optical energy ($h\nu$) upon electron–hole recombination. Thus, the diode voltage is given by Eq. II.1.

$$V = \frac{h\nu}{e} \approx \frac{E_g}{e} \qquad \text{(Eq. II.1)}$$

However, there are several mechanisms can cause the diode voltage slightly different from Eq. II.1 such as additional voltage drops of inevitable series resistances or additional energy loss of carriers upon injection to quantum well.

Firstly, drive voltage can be increased due to the additional drop along series resistance that can be caused by *(i) contact resistance*, *(ii) resistances caused by abrupt heterostructures*, and *(iii) bulk resistance occurring particularly in materials with low carrier concentrations or low carrier mobility*.

Secondly, carrier energy may be lost upon injection into a quantum well structure or double heterostructure, Figure II.1. Eq. II.2 and Eq. II.3 are the energy losses of electron and hole non–adiabatically injected into quantum well, respectively.

$$\Delta E_C - E^e_0 \qquad \text{(Eq. II.2)}$$

$$\Delta E_V - E^{hh}_0 \qquad \text{(Eq. II.3)}$$

Where ΔE_C is the band discontinuity and E^e_0 and E^{hh}_0 are the energy of the lowest quantized state in the conduction–band and valent–band quantum well, respectively.

The energy loss due to carrier injection is dissipated by phonon emission that is converted into heat and strongly effected by large band discontinuities semiconductor such as GaN and other group–III nitride materials.

Thus, the total voltage drops across a forward–biased LED is given by Eq. II.4.

$$V = \underbrace{\frac{E_g}{e}}_{\text{Theoretical voltage minimum}} + \underbrace{IRs}_{\text{Series resistance voltage}} + \underbrace{\frac{\Delta E_C - E_0}{e} + \frac{\Delta E_V - E_0}{e}}_{\text{non-adiabatic injection of carriers into the active region}} \qquad \text{(Eq. II.4)}$$

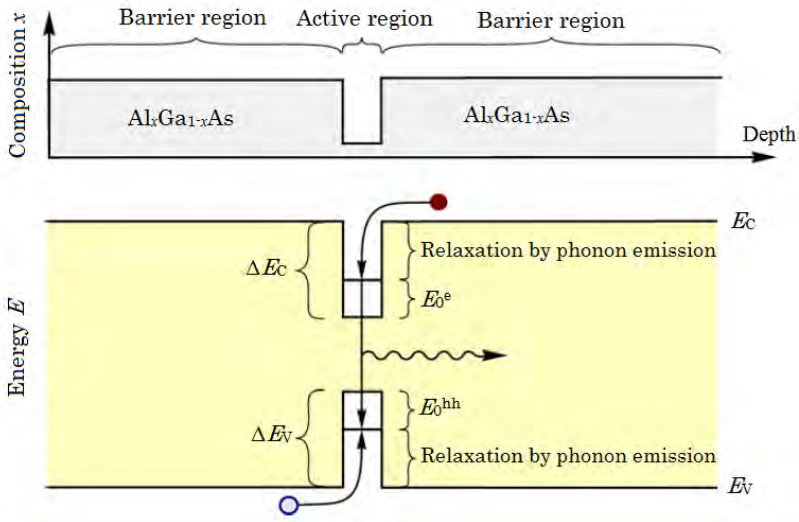

Figure II.1: Energy loss of carriers as they are captured into the quantum well.

However, there is the case where the diode voltage can be experimentally observed slightly lower than the minimum value predicted by Eq. II.4 (slightly lower than $E_g/e \approx hv/e$), This is due to the fact that both electrons and holes can carry additional thermal energy multiple of kT value.

2.1.1. Temperature Dependence of Forward Voltage (Vf)

This section provides the expression of temperature dependence of the forward voltage. With a closer observation of the Shockley equation of an ideal p–n junction diode, the total current density in p–n junction diode is given by Eq. II.5.

$$J_f = J_S\left[\exp\left(\frac{eV_f}{kT}\right) - 1\right] \qquad \text{(Eq. II.5)}$$

Where J_S is the saturation current density and given by Eq. II.6.

$$J_S = e\left[\frac{1}{N_D}\sqrt{\frac{D_n}{\tau_n}} + \frac{1}{N_A}\sqrt{\frac{D_p}{\tau_p}}\right]n_i^2 \qquad \text{(Eq. II.6)}$$

In the case where it's fully ionized, dopants with concentration N_D and N_A have no temperature dependence. While the other terms are temperature dependence: diffusion constant of electrons (D_n) and diffusion constant of holes (D_p) are a $T^{-1/2}$ dependence, the carrier lifetime of electrons (τ_n) and the carrier lifetime of holes (τ_p) can decrease (non–radiative recombination) or increase (radiative recombination) with temperature, and the intrinsic carrier concentration (n_i) is strongly temperature dependent Eq. II.7.

$$n_i = \sqrt{N_C N_V} \exp\left(\frac{-E_g}{2kT}\right) \qquad \text{(Eq. II.7)}$$

Where N_C and N_V are effective densities of states at the conduction–band and valence–band edges given by Eq. II.8 and Eq. II.9, respectively.

$$N_C = 2\left(\frac{2\pi m_{de} kT}{h^2}\right)^{3/2} \propto T^{3/2} \qquad \text{(Eq. II.8)}$$

$$N_V = 2\left(\frac{2\pi m_{dh} kT}{h^2}\right)^{3/2} \propto T^{3/2} \qquad \text{(Eq. II.9)}$$

Where m_{de} and m_{dh} are the density–of–state effective mass for electrons and holes, respectively.

For non–degenerate semiconductors and under forward bias conditions, $V_f >> kT/e$, Eq. II.5 can be rewritten into Eq. II.10.

$$J_f = J_S \exp\left(\frac{eV_f}{kT}\right) \qquad \text{(Eq. II.10)}$$

Solving Eq. II.10 for the junction voltage yields Eq. II.11.

$$V_f = \frac{kT}{e} \ln\left(\frac{J_f}{J_S}\right) \qquad \text{(Eq. II.11)}$$

Derivative of the junction voltage with respect to the junction temperature can be written as Eq. II.12.

$$\frac{dV_f}{dT} = \frac{d}{dT}\left[\frac{kT}{e}\ln\left(\frac{J_f}{J_S}\right)\right] \qquad \text{(Eq. II.12)}$$

From Eq. II.10, the following expression can be derived

$$\frac{dV_f}{dT} = \frac{k}{e}\frac{d}{dT}\left[T\ln\left(\frac{J_f}{J_S}\right)\right] = \frac{k}{e}\left[\ln\left(\frac{J_f}{J_S}\right) + T\frac{d}{dT}\ln\left(\frac{J_f}{J_S}\right)\right]$$

$$\frac{dV_f}{dT} = \frac{k}{e}\left[\ln\left(\frac{J_f}{J_S}\right) + T\frac{d}{dT}\left(\ln J_f - \ln J_S\right)\right] \qquad \text{(Eq. II.13)}$$

For a constant current density $d(\ln J_S)/dT = 0$, Eq. II.13 becomes

$$\frac{dV_f}{dT} = \frac{k}{e}\left[\ln\left(\frac{J_f}{J_S}\right) - T\frac{d(\ln J_S)}{dT}\right] \qquad \text{(Eq. II.14)}$$

From Eq. II.6, once obtains

$$J_S = e\left[\frac{1}{N_D}\sqrt{\frac{D_n}{\tau_n}} + \frac{1}{N_A}\sqrt{\frac{D_p}{\tau_p}}\right]n_i^2 = C_1 n_i^2 \qquad \text{(Eq. II.15)}$$

Where $C_1 = e\left[\frac{1}{N_D}\sqrt{\frac{D_n}{\tau_n}} + \frac{1}{N_A}\sqrt{\frac{D_p}{\tau_p}}\right]$ is a constant.

Substitute Eq. II.15 into Eq. II.14 yields

$$\frac{dV_f}{dT} = \frac{k}{e}\left[\ln\left(\frac{J_f}{J_S}\right) - T\frac{d}{dT}\ln\left(C_1 n_i^2\right)\right] \qquad \text{(Eq. II.16)}$$

And by substituting Eq. II.8 and Eq. II.9 into Eq. II.7 and raise the square power gives

$$n_i^2 = C_2 T^3 \exp\left(\frac{-E_g}{kT}\right) \qquad \text{(Eq. II.17)}$$

Where $C_2 = 2\left(\frac{2\pi m_{de}k}{h^2}\right)^{3/2} 2\left(\frac{2\pi m_{dh}kT}{h^2}\right)^{3/2}$ is a constant

Again substitute Eq. II.17 into Eq. II.16, Eq. II.18 is derived.

$$\frac{dV_f}{dT} = \frac{k}{e}\left[\ln\left(\frac{J_f}{J_S}\right) - T\frac{d}{dT}\ln\left(C_1 C_2 T^3 \exp\left(\frac{-E_g}{kT}\right)\right)\right] \qquad \text{(Eq. II.18)}$$

$$\frac{dV_f}{dT} = \frac{k}{e}\left[\ln\left(\frac{J_f}{J_S}\right) - T\frac{d}{dT}\left(\ln(C_1C_2) + 3\ln(T) + \frac{-E_g}{kT}\right)\right]$$

$$\frac{dV_f}{dT} = \frac{k}{e}\left[\ln\left(\frac{J_f}{J_S}\right) - T\left(\frac{3}{T} - \frac{1}{kT}\frac{dE_g}{dT} + \frac{E_g}{kT^2}\right)\right]$$

$$\frac{dV_f}{dT} = \frac{k}{e}\ln\left(\frac{J_f}{J_S}\right) - 3\frac{k}{e} + \frac{1}{e}\frac{dE_g}{dT} - \frac{E_g}{eT} \qquad \text{(Eq. II.19)}$$

From Eq. II.11, the expression $\frac{k}{e}\ln\left(\frac{J_f}{J_S}\right) = \frac{V_f}{T}$ is obtained then substitute to Eq. II.19 gives

$$\frac{dV_f}{dT} = \frac{V_f}{T} - 3\frac{k}{e} + \frac{1}{e}\frac{dE_g}{dT} - \frac{E_g}{eT} \qquad \text{(Eq. II.20)}$$

Therefore, the fundamental expression of forward voltage dependent to the temperature is given as Eq. II.21.

$$\frac{dV_f}{dT} = \underbrace{\frac{eV_f - E_g}{eT}}_{\substack{\text{T dependence of} \\ n_i}} + \underbrace{\frac{1}{e}\frac{dE_g}{dT}}_{\substack{\text{T dependence of} \\ \text{bandgap energy}}} - \underbrace{\frac{3k}{e}}_{\substack{\text{T dependence of} \\ \text{effective densities of state}}} \qquad \text{(Eq. II.21)}$$

As stated by Xi and Schubert , [69], the temperature dependences of diffusion constants and lifetimes are neglected due to the small contribution in the calculation (≤5%).

LEDs are typically operated with their forward voltage close to the built–in voltage, ($V_f < V_{bi}$) so in the case of non–degenerate doping concentrations, Eq. II.22 can be derived.

$$eV_f - E_g \approx kT\ln\left(\frac{N_D N_A}{n_i^2}\right) - kT\ln\left(\frac{N_C N_V}{n_i^2}\right) = kT\ln\left(\frac{N_D N_A}{N_C N_V}\right) \qquad \text{(Eq. II.22)}$$

From Varshni , [70], the temperature dependence of bandgap energy can be written as

$$E_g = E_0 - \frac{\alpha T^2}{T+\beta} \qquad \text{(Eq. II.23)}$$

Where E_g, is the energy gap which may be direct (E_{gd}) or indirect (E_{gi}), E_0 is its value at 0°K, and α and β are constants (***Varshni parameters***), Table *II.1* shows these parameters for several semiconductors.

Most of the variation in the energy gap with temperature is believed to arise from the following two mechanisms:

Firstly, A shift in the relative position of the conduction and valence bands due to the temperature–dependent dilatation of the lattice.

Secondly, a shift in the relative position of the conduction and valence bands due to a temperature–dependent electron lattice interaction.

Substituting Eq. II.22 and Eq. II.23 into Eq. II.21, the final expression of temperature dependence of forward voltage can be obtained Eq. II.24.

$$\boxed{\frac{dV_f}{dT} = \underbrace{\frac{k}{e}\ln\left(\frac{N_D N_A}{N_C N_V}\right)}_{\text{T dependence of } n_i} - \underbrace{\frac{\alpha T(T+2\beta)}{e(T+\beta)^2}}_{\text{T dependence of bandgap energy}} - \underbrace{\frac{3k}{e}}_{\text{T dependence of effective densities of state}}} \qquad \text{(Eq. II.24)}$$

Table II.1: Varshni parameters of common semiconductors *[17]*.

Semiconductor	E_g at 0°K (eV)	α(10–4eV/°K)	β(°K)	Validity range
AlN (wurtzite)	6.026	18.0	1462	T ≤300 K
GaN (wurtzite)	3.47	7.7	600	T ≤600 K
GaP	2.34	6.2	460	T ≤1 200 K
GaAs	1.519	5.41	204	T ≤1 000 K
GaSb	0.813	3.78	94	T ≤300 K
InN (wurtzite)	1.994	2.45	624	T ≤300 K
InP	1.425	4.50	327	T ≤800 K
InAs	0.415	2.76	83	T ≤300 K
InSb	0.24	6.0	500	T ≤300 K
Si	1.170	4.73	636	T ≤1 000 K
Ge	0.744	4.77	235	T ≤700 K

Eq. II.24 is a very useful expression for temperature coefficient of forward voltage. It also clarifies the linearity dependence (results are obtained from empirical measurements) of the forward voltage with respect to the temperature.

Figure II.2 illustrates the temperature dependence of I–V characteristic at 77°K and at room temperature. It reveals that the threshold voltage as well as the series resistance of the diode increases as the diode is cooled so in the case when device is driven at a constant voltage a large current change would result from the change in temperature.

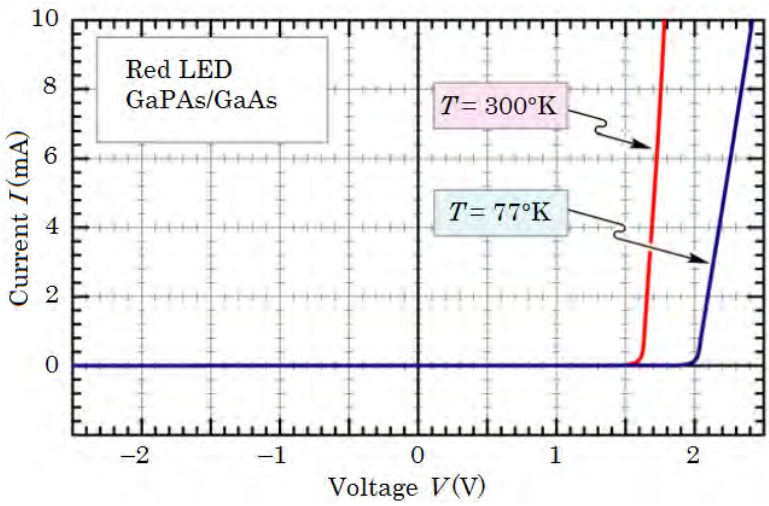

Figure II.2: Current–voltage characteristic of LED showing threshold voltages 2.0 and 1.6 V, at 77°K and 300°K, respectively.

Depending on the linearity forward voltage–temperature dependence characteristic of the LED, the junction temperature can be interfered by using method of V_f calibration measurement under pulsed–current injection (I_f), and a V_f measurement under DC–current injection as indicated in Figure II.3.

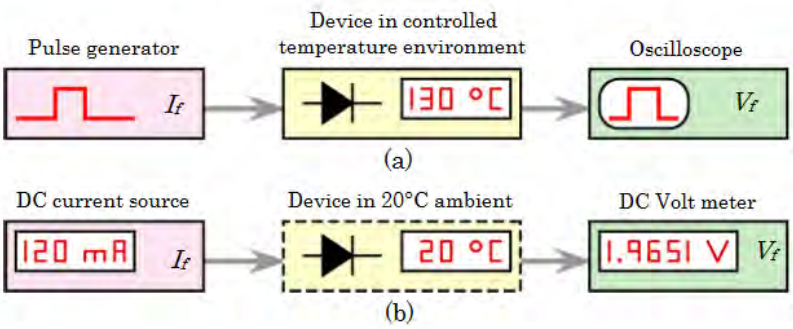

Figure II.3: (a) Pulsed calibration and (b) determination of junction temperature for different DC forward currents.

In the process, temperature of the device and junction (T_0) is predefined by various environment controlled temperature, then a pulsed mode with a very small duty cycle (avoiding self–heating effect) is applied at each temperature level and the forward voltage is measured and the relation between forward voltages (V_f) and junction temperatures (T_0) are derived for the forward currents (I_f), Figure II.4.

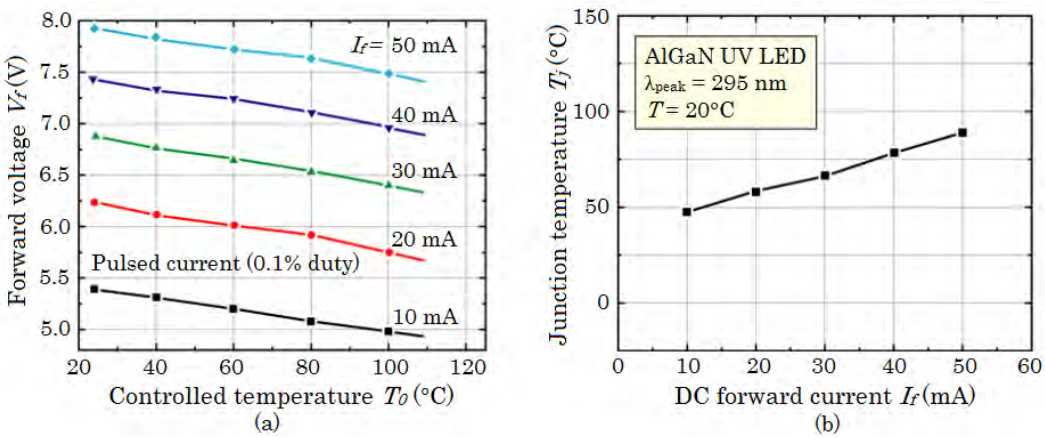

Figure II.4: (a) Pulsed calibration measurement (small duty cycle 0.1 %) and (b) junction temperature (T_j) versus DC current of AlGaN UV LED, Schubert, 2006 [17, p. 109].

Finally, the junction temperature (T_j) under test or operation can be interfered by using the expression in Eq. II.25.

$$T_j = T_0 + \frac{V_t - V_0}{K} \qquad \text{(Eq. II.25)}$$

Where T_0 is reference ambient temperature; V_t and V_0 are the forward voltages at the test condition temperature and the reference ambient temperature, respectively; and K is the temperature coefficient of the forward voltage and can be defined from the data of previous step of V_f calibration measurement method, Eq. II.26.

$$K = \frac{V_0 - V_1}{T_0 - T_1} \qquad \text{(Eq. II.26)}$$

Where V_0 and V_1 are forward potentials at two known ambient temperatures, T_0 and T_1, respectively. Therefore, the constant K can be determined by measuring

the voltage drop across the LED junction at two known ambient or controlled temperatures. *Using* Eq. II.26, *the junction temperature of the LED can be estimated by measuring the change in forward voltage*.

2.2. OPTICAL PROPERTIES OF LED

2.2.1. Internal, Extraction, External, and Power Efficiencies

The active region of an ideal LED emits one photon for every electron injected. Each charge quantum–particle (electron) produces one light quantum–particle (photon). Thus, the ideal active region of an LED has a quantum efficiency of unity. However not all electrical injected carriers can be converted into light due to some reasons such as defect formation or phonon emission leading to the *internal quantum efficiency* as defined in Eq. II.27.

$$\eta_{int} = \frac{number\ of\ photons\ emitted\ from\ active\ region\ per\ second}{number\ of\ electrons\ injected\ into\ LED\ per\ second} = \frac{P_{int}/(h\nu)}{I/e} \quad \text{(Eq. II.27)}$$

Where P_{int} is the optical power emitted from the active region and I is the injection current.

Likewise, all generated light cannot 100% escape into free space as a result of some consequences including reabsorption of light in the substrate of the LED, absorption of light by metallic contact when the light incidents to that contact, and total internal reflection (trapped light) issue. The light *extraction efficiency* is defined by Eq. II.28.

$$\eta_{extraction} = \frac{number\ of\ photons\ emitted\ into\ free\ space\ per\ second}{number\ of\ photons\ emitted\ from\ active\ region\ per\ second} = \frac{P/(h\nu)}{P_{int}/(h\nu)} \quad \text{(Eq. II.28)}$$

Where P is the optical power emitted into free space. Finally, the *external quantum efficiency* of LED is defined as Eq. II.29.

$$\eta_{ext} = \frac{number\ of\ photons\ emitted\ into\ free\ space\ per\ second}{number\ of\ electrons\ injected\ into\ LED\ per\ second} = \frac{P/(h\nu)}{I/e} = \eta_{int}\eta_{extraction} \quad \text{(Eq. II.29)}$$

The external quantum efficiency gives the ratio of the number of useful light particles to the number of injected charge particles so power efficiency is derived, Eq. II.30.

$$\boxed{\eta_{power} = \frac{P}{IV}} \qquad \text{(Eq. II.30)}$$

Where IV is the electrical power provided to the LED.

2.2.2. Emission Spectrum

Figure II.5 shows the electron–hole recombination process. Both electrons and holes have parabolic dispersion relation in the conduction band (Eq. II.31) and valent band (Eq. II.32), respectively.

$$E = E_C + \frac{\hbar^2 k^2}{2m_e^*} \qquad \text{(for electrons)} \qquad \text{(Eq. II.31)}$$

$$E = E_V - \frac{\hbar^2 k^2}{2m_h^*} \qquad \text{(for holes)} \qquad \text{(Eq. II.32)}$$

Where m_e^* and m_h^* are the electron and hole effective masses, $\hbar$ is Planck's constant divided by 2π, k is the carrier wave number, and E_V and E_C are the valence and conduction band edges, respectively.

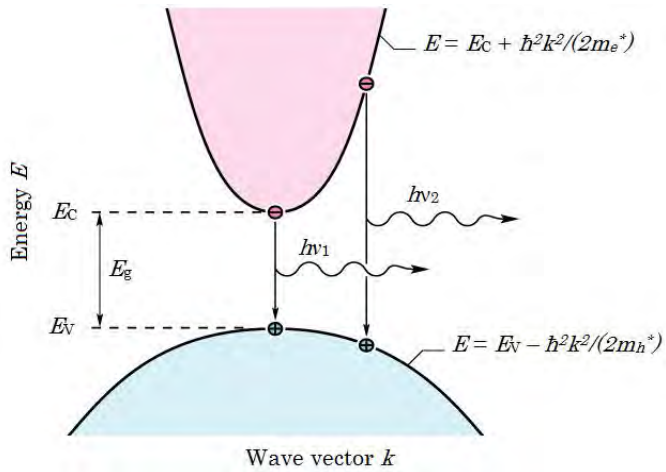

Figure II.5: Parabolic electron and hole dispersion relations.

Photon energy is given by equation Eq. II.33. Based on Boltzmann distribution, most of electrons and holes possess an average kinetic energy of kT, so

photon energy can be approximated to the bandgap energy (E_g,) if the thermal energy is small compared with the bandgap energy ($kT << E_g$). Thus, by appropriate choosing of semiconductor material, the LED of a desired emission wavelength can be developed. As in the case of GaAs, LED can emit light at infrared of 870 nm wavelength with bandgap energy of the material 1.42 eV.

$$h\nu = E_e - E_h \approx E_g \qquad \text{(Eq. II.33)}$$

Figure II.5 also reveals that the transitions of carriers are vertical due to the fact that the momentum of carriers cannot change significantly during the transition from conduction band to valent band and it can be explained by the lager magnitude of momentum of the carriers (Eq. II.34) comparing to the momentum of photon (Eq. II.35). This means that electrons only recombine with holes that have the same momentum or k value.

$$p = m^* v = \sqrt{2m^* \frac{1}{2} m^* v^2} = \sqrt{2m^* kT} \qquad \text{(Eq. II.34)}$$

$$p = \hbar k = \frac{h\nu}{c} = \frac{E_g}{c} \qquad \text{(Eq. II.35)}$$

Due to the equality of electron and hole momenta, photon energy of joint dispersion relation can be derived as in Eq. II.36.

$$h\nu = \underbrace{E_C + \frac{\hbar^2 k^2}{2m_e^*}}_{E_e} - \underbrace{E_V + \frac{\hbar^2 k^2}{2m_h^*}}_{E_h} = E_g + \frac{\hbar^2 k^2}{2m_r^*} \qquad \text{(Eq. II.36)}$$

Where m_r* is the reduced mass given by $\frac{1}{m_r^*} = \frac{1}{m_e^*} + \frac{1}{m_h^*}$

By using the joint dispersion relation, the joint density of states can be calculated as in Eq. II.37.

$$\rho(E) = \frac{1}{2\pi^2}\left(\frac{2m_r^*}{\hbar^2}\right)^{3/2}\sqrt{E - E_g} \qquad \text{(Eq. II.37)}$$

Then the distribution of carriers in the allowed bands is given by the Boltzmann distribution (Eq. II.38).

$$f_B(E) = \exp\left(-\frac{E}{kT}\right) \qquad \text{(Eq. II.38)}$$

Lastly, the *emission intensity* as a function of energy is proportional to the product of Eq. II.37 and Eq. II.38 and can be derived as in Eq. II.39.

$$\boxed{I(E) \propto \sqrt{E - E_g}\,\exp\left(-\frac{E}{kT}\right)} \qquad \text{(Eq. II.39)}$$

The line shape of Eq. II.39 shown in Figure II.6 is a spectrum of LED with the maximum of emission intensity occurs at E_{max} (Eq. II.40).

$$\boxed{E_{\max} = E_g + \frac{1}{2}kT} \qquad \text{(Eq. II.40)}$$

and the full–width at half–maximum of the emission is found from the condition $\sqrt{E - E_g}\,\exp\left(-\frac{E}{kT}\right) = \frac{1}{2}\left(E_{\max} - E_g\right)\exp\left(-\frac{E_{\max}}{kT}\right)$, numerical solution gives

$$\boxed{\Delta E = 1.8kT \quad \text{or} \quad \Delta\lambda = \frac{1.8kT\lambda^2}{hc}} \qquad \text{(Eq. II.41)}$$

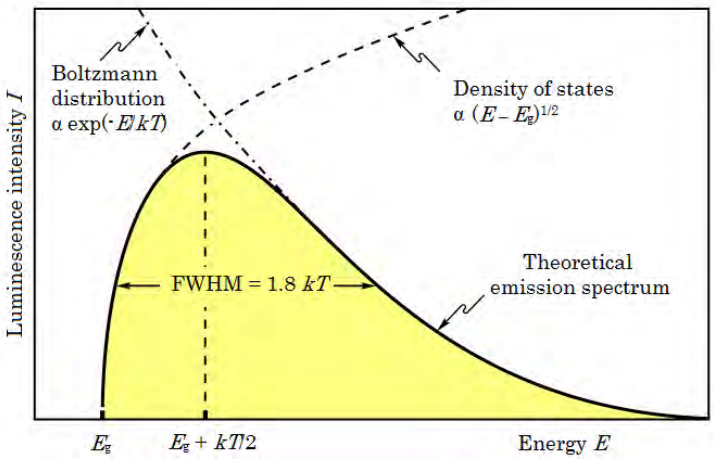

Figure II.6: Theoretical emission spectrum of an LED.

2.2.3. Light Escape Cone

Due to the optical property, light propagates from one material (with high–refractive index material) to another material (with a lower refractive index). Different materials can face the condition where total reflection occurs. In the case of LED, a portion of light emitted with the incidental angle at the interface of LED's material and air greater than the critical incident angle (φ_c) can also encounter the *total internal reflection* that leads to a significant decrease in external efficiency.

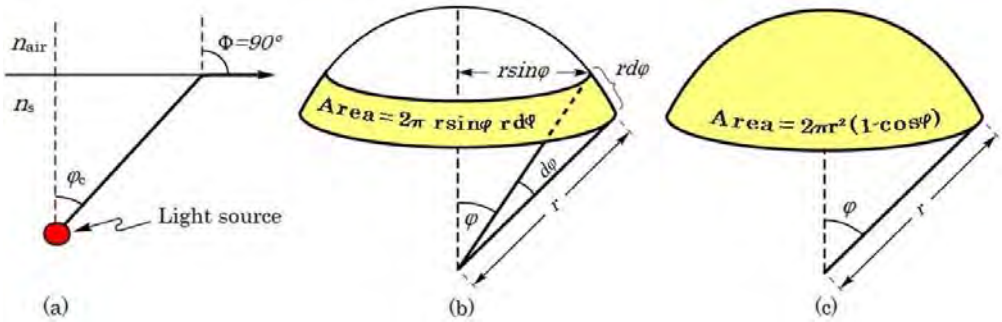

Figure II.7: (a) Definition of the escape cone by the critical angle φ_c. (b) area element dA. (c) area of calotte–shaped section of sphere defined by radius r and angle φ_c.

From Figure II.7 by using Snell's law (Eq. II.42), the *critical angle* for total internal reflection is obtained using refraction angle ($\Phi = 90°$) can be obtained as in Eq. II.43.

$$n_s \sin\varphi = n_{air} \sin\Phi \qquad \text{(Eq. II.42)}$$

$$\sin\varphi_c = \frac{n_{air}}{n_s}\sin 90^\circ = \frac{n_{air}}{n_s} \text{ and } \varphi_c = \arcsin\frac{n_{air}}{n_s} \qquad \text{(Eq. II.43)}$$

With quite high of refractive indices of LED's material (n_s) comparing to air (n_{air}), the critical angle for total internal reflection (φ_c) can be approximately given by Eq. II.44.

$$\boxed{\varphi_c \approx \frac{n_{air}}{n_s}} \qquad \text{(Eq. II.44)}$$

The angle of total internal reflection defines the light *escape cone,* where the light emitted into this cone can escape into surrounding air and light emitted outside the cone is subject to total internal reflection.

From Figure II.7, the surface area of the calotte–shaped is given by Eq. II.45.

$$A = \int dA = \int_{\varphi=0}^{\varphi_c} 2\pi r \sin\varphi r d\varphi = 2\pi r^2 (1 - \cos\varphi_c) \qquad \text{(Eq. II.45)}$$

If P_{source} is the total power of light generated, then the power of portion light escaped from the LED (P_{escape}) is given by Eq. II.46.

$$P_{escape} = P_{source} \frac{2\pi r^2 (1 - \cos\varphi_c)}{4\pi r^2} \qquad \text{(Eq. II.46)}$$

Only a fraction of the light generated inside a LED can escape from the semiconductor is given by Eq. II.47.

$$\boxed{\frac{P_{escape}}{P_{source}} = \frac{1}{2}(1 - \cos\varphi_c)} \qquad \text{(Eq. II.47)}$$

Due to the high–refractive index materials of LED, it leads to small critical angle of total internal reflection. So, cosine term in Eq. II.47 can be expanded into a power series and by neglecting higher than second order terms yields Eq. II.48.

$$\frac{P_{escape}}{P_{source}} \approx \frac{1}{2}\left[1 - \left(1 - \frac{\varphi_c^2}{2}\right)\right] = \frac{1}{4}\varphi_c^2 \qquad \text{(Eq. II.48)}$$

Comparing Eq. II.47 to Eq. II.44, one obtains

$$\boxed{\frac{P_{escape}}{P_{source}} \approx \frac{1}{4}\frac{n_{air}^2}{n_s^2}} \qquad \text{(Eq. II.49)}$$

In conclusion, with a quite high refractive index of LED semiconductor material it can cause a serious problem for high–efficiency LED. So, there are more considerations for LED design to be considered in order to improve better light extraction.

2.2.4. Radiation Pattern–Lambertian Emission Pattern

Light emitted from the LED follows a certain pattern of emission and the term *Lambertian emission pattern* is derived from the *cosine pattern* (*cosΦ*) of light intensity in the air as indicated in Eq. II.50.

$$I_{air} = \frac{P_{source}}{4\pi r^2}\frac{n_{air}^2}{n_s^2}\cos\Phi \qquad \text{(Eq. II.50)}$$

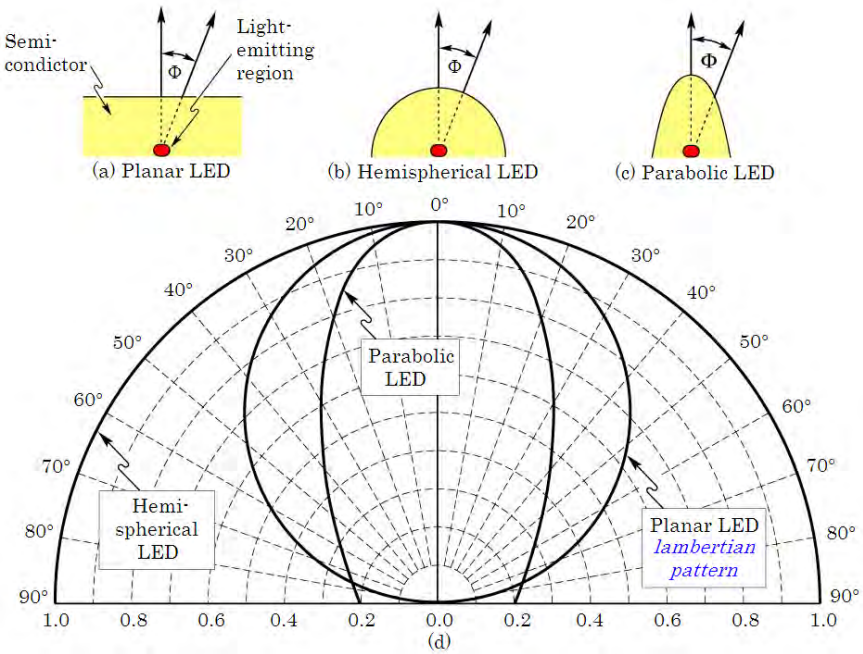

Figure II.8: Light–emitting diodes with (a) planar, (b) hemispherical, and (c) parabolic surfaces, (d) Far–field patterns of the different types of LEDs.

Figure II.8 shows three different shapes of LED: plan, hemisphere and parabola and their emission patterns. Hemispherical shaped LEDs, which have the light–emitting region in the center of the sphere has an isotropic emission pattern while a LEDs with parabolic shaped surfaces shows a strongly directed emission pattern. However, there is difficulty to reach the hemispherical as well as parabolic surfaces of semiconductor during fabrication.

2.2.5. Epoxy Encapsulant

The purpose of using encapsulation is to be able to enhance the efficiency of light extraction and also to serve as spherical lens for applications requiring a directed emission pattern. Dome–shaped encapsulant with a large refractive index is commonly used to increase the angle of total internal reflection through the top surface of the semiconductor. As adapted from Eq. II.47, the ratio of extraction efficiency with and without epoxy encapsulant is given by Eq. II.51.

$$\frac{\eta_{epoxy}}{\eta_{air}} = \frac{1-\cos\varphi_{c,epoxy}}{1-\cos\varphi_{c,air}} \qquad \text{(Eq. II.51)}$$

Where $\varphi_{c,epoxy}$ and $\varphi_{c,air}$ are the critical angles for total internal reflection at the semiconductor–epoxy and semiconductor–air interface, respectively.

Figure II.9 shows the calculated ratio of the extraction efficiency with and without an epoxy dome. Inspection of the figure yields that the efficiency of a typical semiconductor LED increases by a factor of 2–3 upon encapsulation with an epoxy having a refractive index of 1.5. The refractive indices of typical epoxies range between 1.4 and 1.8.

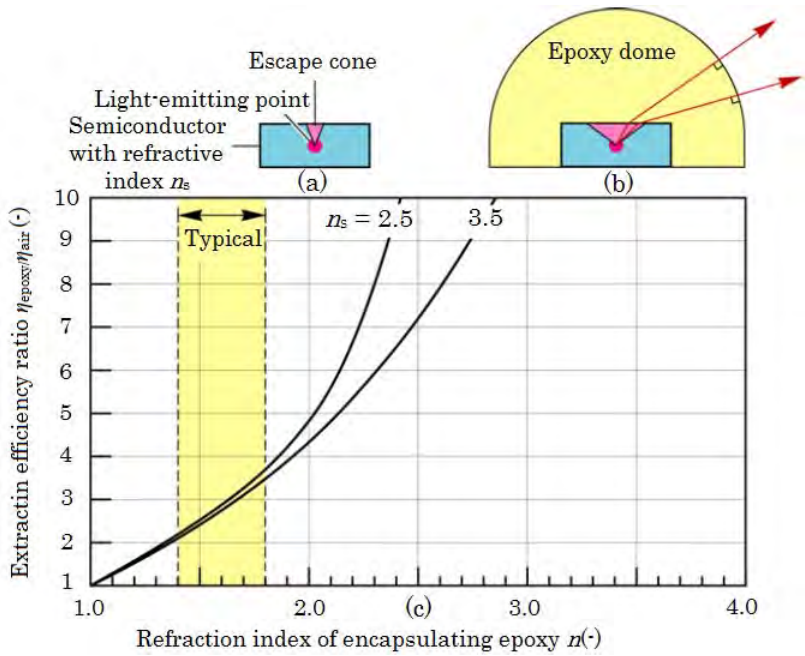

Figure II.9: (a) LED without, (b) with dome–shaped epoxy encapsulant, (c) calculated ratio of light extraction efficiency emitted through the top surface of a planar LED with and without an epoxy dome.

2.2.6. Temperature Dependence of Emission Intensity

Temperature can cause strong effect to the emission intensity of LED. Increasing of temperature operation can leads to deprivation of light emitted intensity due to several mechanisms such as *(i) non–radiative recombination via deep levels*, *(ii) surface recombination*, and *(iii) carrier loss over heterostructure barriers*.

Eq. II.52 is the expression of temperature dependence of the LED emission intensity.

$$I = I\big|_{300K} \exp\left(-\frac{T-300K}{T_1}\right) \qquad \text{(Eq. II.52)}$$

Where T_1 is the characteristic temperature. A high characteristic temperature T_1 is desirable because it implies weak temperature dependence.

3.
EXPERIMENTAL SETUP FOR LED AGING EVALUATION

3.1. A NEW PROTOTYPE OF LED AGING BENCH

In order to study the degradation of LEDs, this prototype has been developed and built in Laplace laboratory including many assembly parts as shown in Figure III.2. Figure III.1 shows the implementation of the complete experimental bench. This aging bench is designed to be able to apply the two stress modes of LEDs degradation of the two different driving forces including electrical and thermal stress. In electrical stress mode, it consists of two different current sources LED drivers, 350 mA and 1000 mA, including a thermal stress mode. It provides also the possibility of various heating/cooling source temperature controls.

Figure III.1: Overview of the LED aging Bench.

The experimental setup encompasses four different commercial LED types including the group LEDs of Cree (C), Osram (O), Philips (P) and Seoul (S), Figure III.3, hereafter referring to "*COPS*" with the main characteristic of these studied LEDs is presented in Table III.1 and its full datasheet is provided in

Appendix F: Datasheet of LEDs. Each group contains 32 LED samples and they are divided into two another groups for applying two different electrical stress conditions with a high stability and accuracy. Thus, our results are averaged with 16 LED samples under the same stress conditions.

Table III.1: Main characteristics of studied LEDs.

Manufacturer	reference	Color temp. (K)	Lum. Efficiency @350mA (lm/W)	If (mA)	Vf (V)	Power (W)	Chip
Cree	XPGBWT-L1-R250-CE7	3000	115	350	2,8	0,98	monochip
Osram	LCW CQ7P.CC -KPKR-5R8T-1-K	3000	72	350	3,2	1,12	monochip
Philips	LX18-P130-3	3000	98	350	2,76	0,97	monochip
Seoul Semicond.	N42180H-T2	3000	63	350	3,25	1,14	monochip

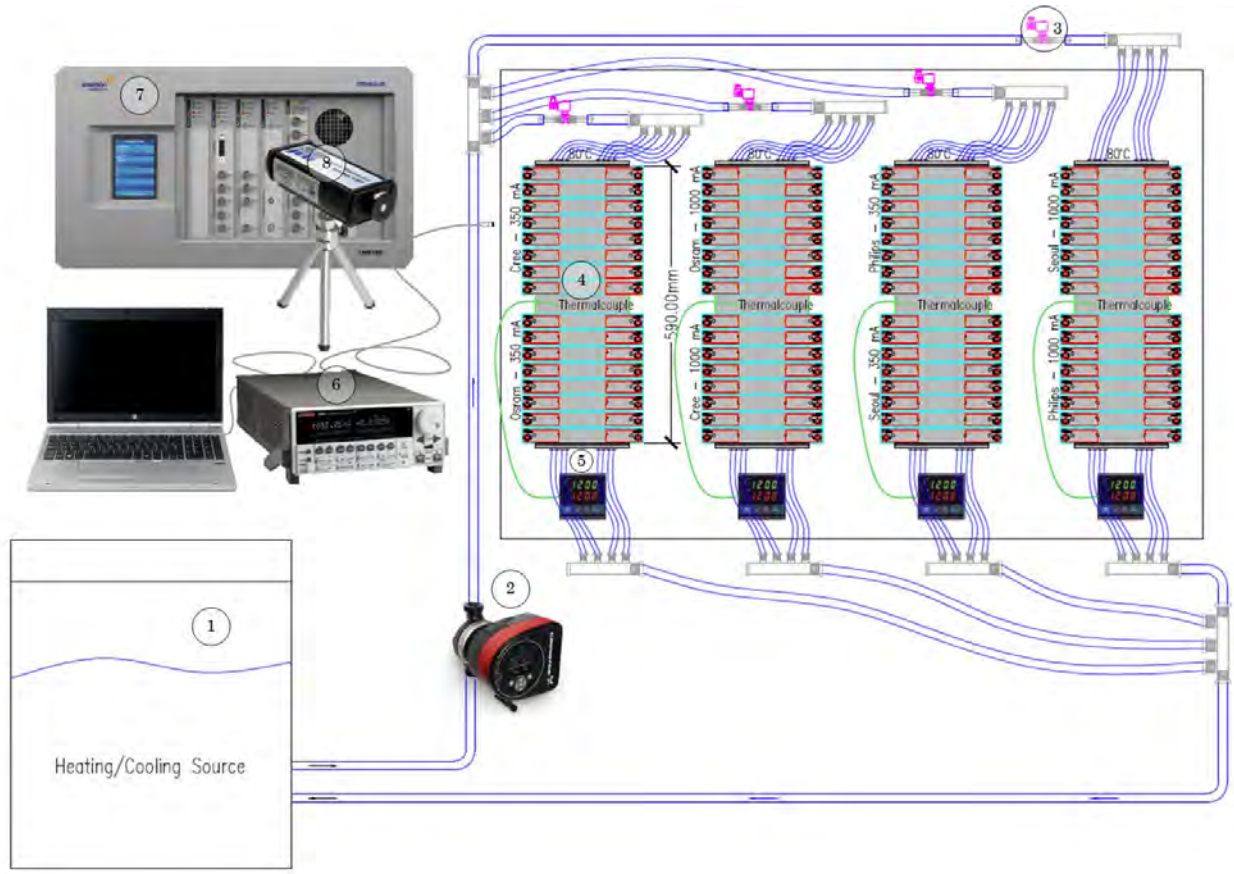

Figure III.2: Overall experimental setup design.

In total, there are 128 LED samples to be characterized its performance. The data obtained by this large number of samples will be implemented as a statistical

data to judge the better accuracy of a subsequent aged–LED behaviour modification. The four types of COPS LED group from different manufacturers are the GaN–based high power LED used for solid state lighting application with 1 W power and a warm white color temperature and all monochip.

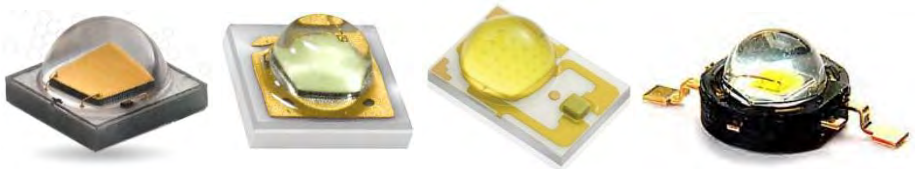

(a) (b) (c) (d)

Figure III.3: Led types: a) Cree, XLamp® XP–G2 b) Osram, LCW CQ7P.CC c) Philips, LX18–P130–3 and d) Seoul, N42180H–T2.

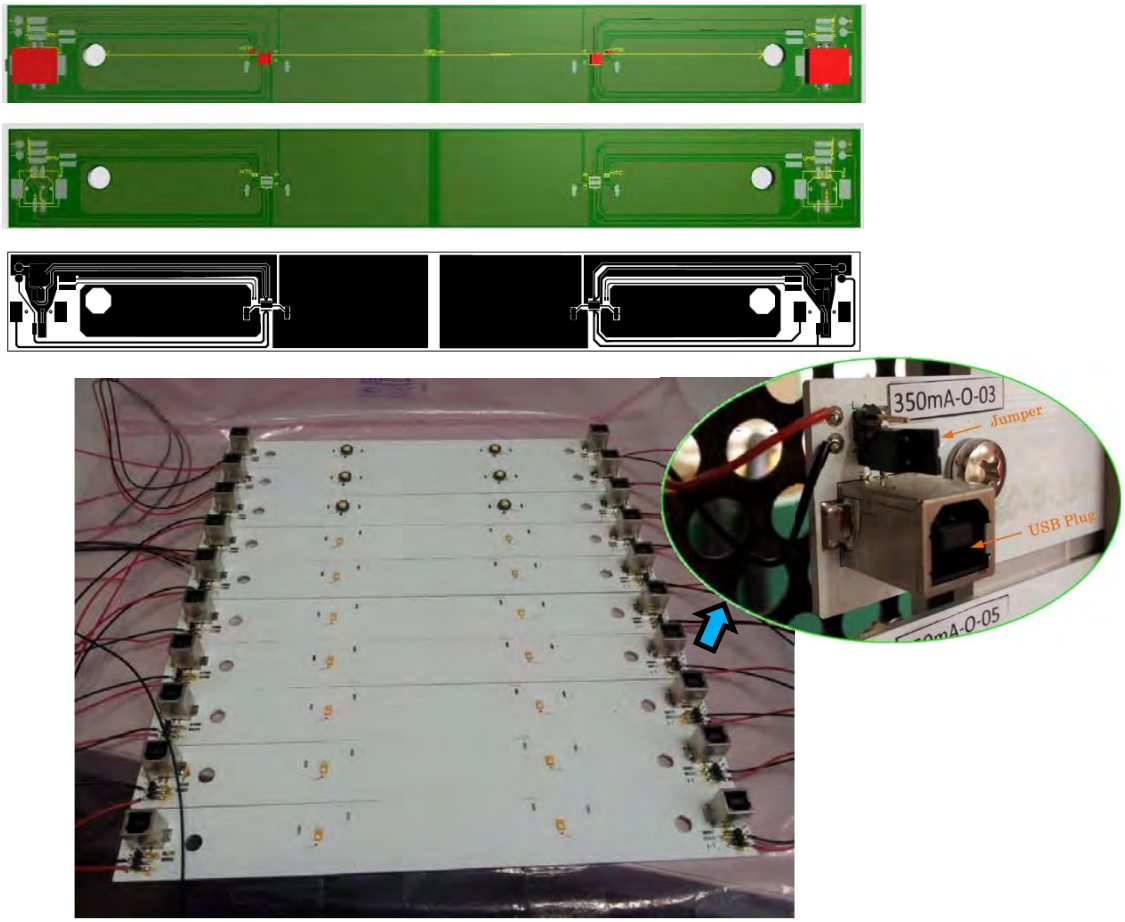

Figure III.4: LEDs mounted on a printed custom–made circuit board.

In order to make an easier thermal exchange between the LED and the heated holder (that allows controlling the junction temperature of LED chip for various predefined thermal stress conditions), LED samples are mounted on an aluminum printed circuit board (MPCB), Figure III.4. This one is custom–made to facilitate

the measurements while protecting against EMI. USB shielded plugs are also integrated on the MPCB in order to provide the ease and the fast measurement process with the Source–Meter Unit "Keithey–2602A" and the impedance analyser "Solatron ModuLab" to measure electrical characteristic of the large number of samples. In addition, jumper terminal connection is incorporated in order to be able to switch easily between the position of measure mode when using with the measurement equipment such as the sourcemeter unit or the impedance analyser and the position of stress operation mode when driving on LED drivers.

Then, the PCBs are tight–fitted against the aluminum holders (Figure III.5). There are four aluminum holders that are used to hold the four different LEDs COPS, which serves as thermal conducting material between LED packages and flowing fluid. Silicon oil is used instead of water or coolant fluid as a medium for convection heat transfer circulating around the system. This one was chosen to avoid evaporation, gas in the top parts of pipes and corrosion with some metallic parts.

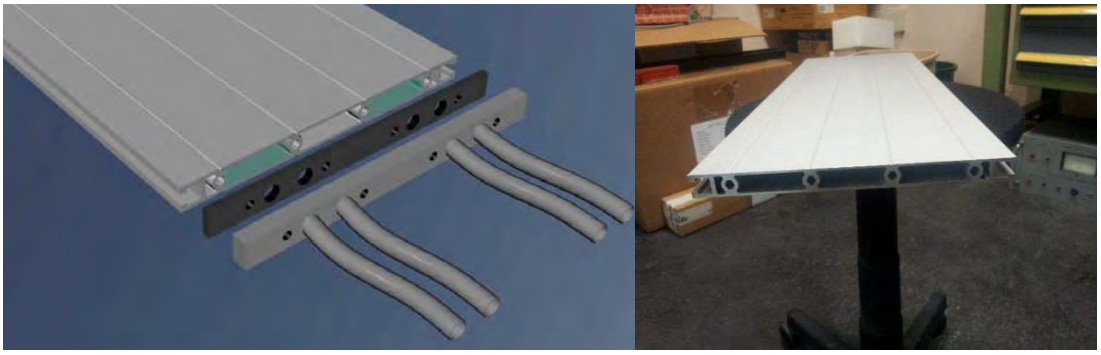

Figure III.5: LED aluminum holder.

The fluid is injected to aluminum panel by stainless steel flexible hoses fitting Figure III.6. Referring to Figure III.2, the flowing fluid circulates around the system from heating and cooling source – MPC TR40 chiller, part (1), by the intervention of pumping motor, part (2), then passes through an adjustable proportional valve (driven with a 0–10V output voltage by the controller through the average temperature of the aluminum support), part (3), that can control the valve position to adjust the flow rate of the fluid in order to regulate the amount of heat exchange by conduction. The fluid that leaves from the valve is injected to an

aluminum container where the heat exchange occurs. Thermocouples are glued onto the middle of the support to return an average temperature, part (4). Temperature controllers, part (5), are used to sense the temperature of thermocouples and provide the control voltage to drive the aperture of the proportional valves.

Figure III.6: stainless steel flexible hose fitting.

The measurements are done by using Keithley 2602A source meter unit, part (6), to obtain I–V characteristic, Solartron ModuLab impedance analyzer, part (7), to extract C–V characteristic, and Specbos 1201 spectrometer, part (8), to get L–I characteristic and its spectrum.

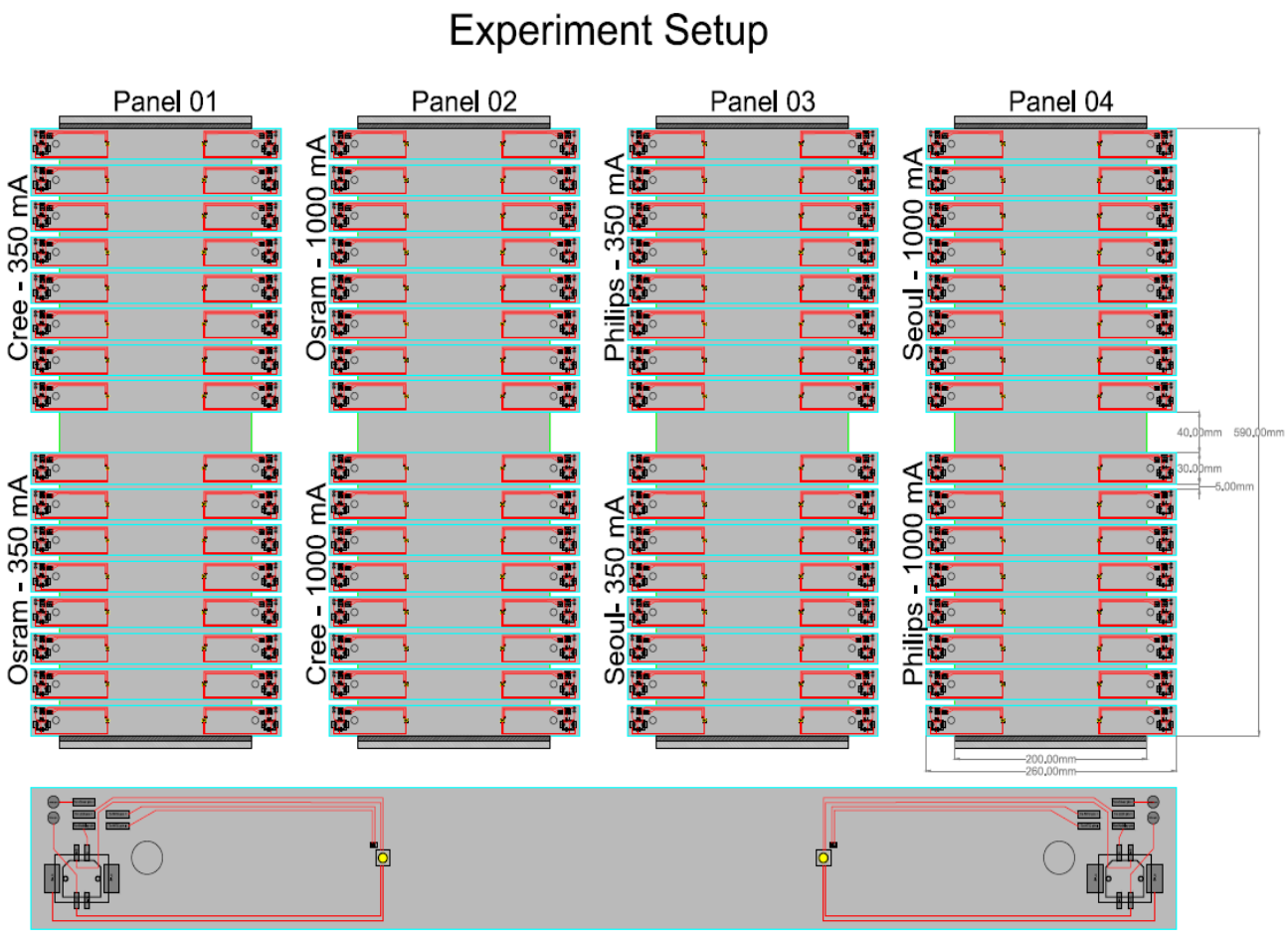

Figure III.7: Arrangement of the stress condition.

Figure III.7 shows the arrangement of the stress system which is performed by 16 LED samples of Cree and 16 LED samples of Osram are fixed on one aluminum panel for conducting a 350 mA stress current – panel 01. Likewise, 16 LED samples of Philips and 16 LED samples of Seoul are maintained on another aluminum panel for the same test condition 350 mA – panel 03. The same number of samples and the same arrangement of experiment were done with the test condition 1000 mA. 16 LED samples of Cree and 16 LED samples of Osram are hold on one aluminum panel for conducting a 1000 mA stress (on the panel 02) and 16 LED samples of Philips and 16 LED samples of Seoul are screwed on another aluminum panel for the same test condition 1000 mA – panel 04.

3.2. Temperature Controller (REX–D100)

Temperature is one of the main driving forces that can affect to the operation of light–emitting diode. LEDs are very long–life light sources, thus, in order to accelerate aging effect, all panels are heated in the same conditions. The temperature must be well controlled and this was done by the aid of a temperature controller. REX–D100 temperature controller, Figure III.8, is used to provide a controlled signal (0 to 10V) to the proportional valve according to the temperature.

Figure III.8: Temperature controller REX–D100.

Figure III.9 shows the control mode performing by the controller. The fuzzy logic algorithm automatically starts during operation or set point change to eliminate overshoot and undershoot. The controller performs conventional PID control and can be easily operated with automatic auto tuning which calculates optimum PID constants.

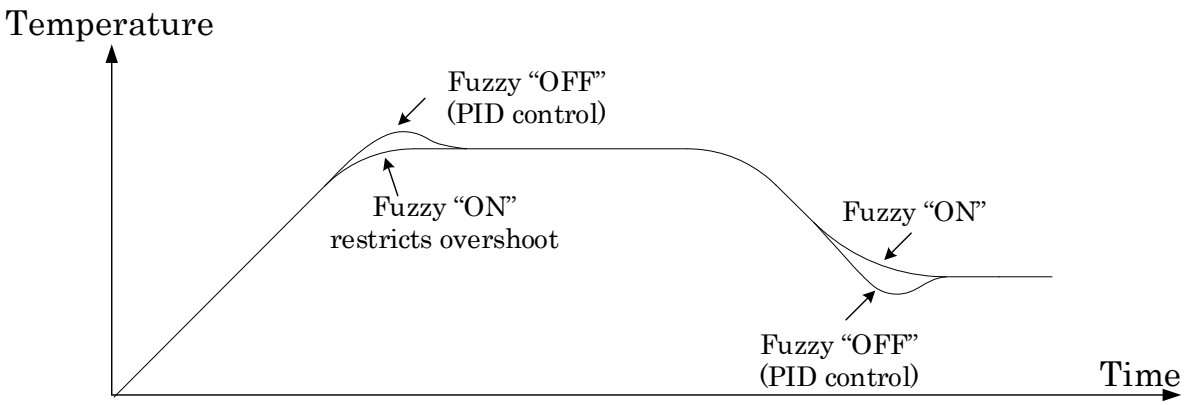

Figure III.9: Control mode of REX–D100.

Up to 31 controllers can be connected to one host computer by the RS–485 or RS–422A communication function. In this work, there are 4 controllers that were used to control the temperature of the four LED aluminum holders. These four controllers were connected to the host computer by using USB to RS485 Serial Converter Cable from FTDI Chip, and they are connected to a common bus and each node can work as either a sender or receiver of information from the bus as seen in electrical wiring diagram of the experiment setup, Figure III.10. Each terminal connected to the bus has a tri–state and a unique address (ID), and the communication between sender and receiver is performed based on this ID.

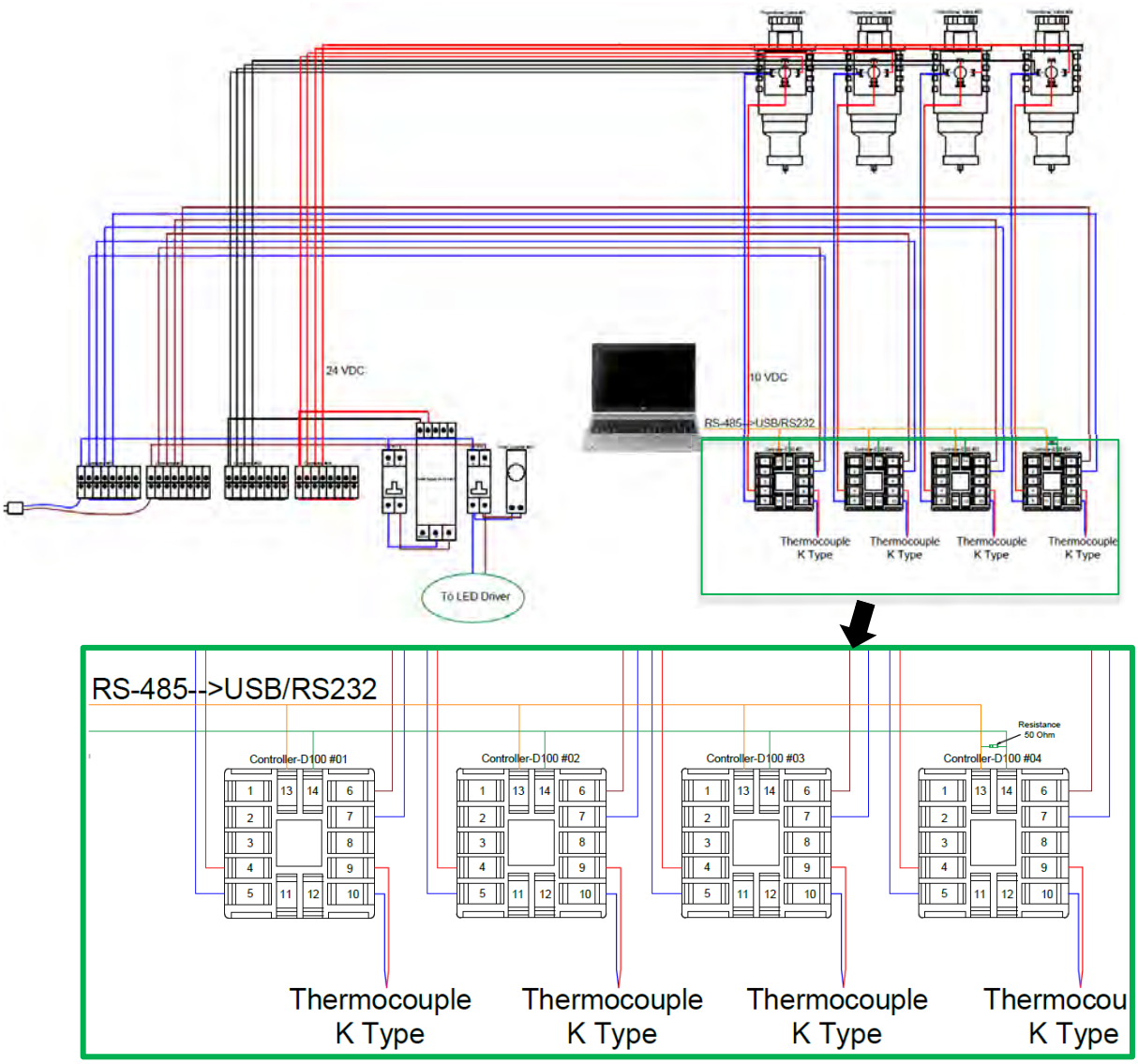

Figure III.10: Electrical wiring of experimental setup.

The ID of each REX–D100 controller is manually set as predefine 01, 02, 03 and 04 respectively and will be used as an address to communicate with PC base on a developed application program called REX–D100 that will be descript in the following section.

3.2.1. Software Program for REX–D100 Temperature Controller

In order to quickly and easily access a large number of internal parameters to check their operating status and also to set all the referent parameter's value, a program called "**REX D100**", Figure III.11, was developed to accomplish this task.

The program was developed in Visual Basic platform that is a third–generation event–driven programming language and integrated development environment (IDE) from Microsoft. From this developed program, it provides a user interface and is divided into two group panels including *"Setup parameters"* and *"Get parameters status"*.

Setup parameters panel allows to set all the parameters of REX–D100 of a specific device. The specific device is accessible by providing device's address in the *"Device Address"* textbox field of the interface. This setup value can be effectuated by *"Identifier"* textbox field following by user setup value in *"Value to Set"* textbox field. All the identifiers of and its meaning can be found in Appendix A. Then the setup was done by *"Set Value"* push button.

Get parameters status panel allows to inspect all status of each operating parameter such as the referent setting temperature (identifier "S1"), actual temperature of the measuring LED (identifier "M1"), the position of operating valve (identifier "O1"), and so on. Likewise, to get all controller's parameters of a specific device, the device's address in the *"Device Address"* textbox field and *"Identifier"* textbox field have to be provided. The value or the status of the inquired parameter is shown in *"Respond"* textbox field by activate *"Get Value"* push button. The communication between the host computer and controller to request and respond of an inquired parameter is triggered every minutes to see the change of operating value or status of that parameter until *"Stop Get Value"* is pressed. This application allows also to scan quickly all internal parameter's status and value of each controller by clicking the *"Scan Setting"* push button. The requested data are saved in a spreadsheet file that can allow an easy access to all these parameters. The full scanned parameter values of each controller can be obtained as shown in Appendix B. Before launching all specific operations, the communication between the host computer and each controller must be established by selecting a communication port provided by the "*Select Port"* textbox field in the program. The complete source code of the "REX–D100" program is provided in Appendix C.

3.2.2. Communication Protocol

The developed program is able to communicated to the controller by using polling/selection type for the method of establish data link. The polling/selection method is such that all controllers are supervised by the host computer and controller is permitted. In order to force controller to send and receive data messages, send the message from the host computer according to the polling or selection procedure. The code use in communication is 7– bit JIS/ ASCII code including transmission control character. The transmission control characters are [EOT] (04H), [ENQ] (05H), [ACK] (06H), [NAK] (15H), [STX] (02H), [ETX] (03H).

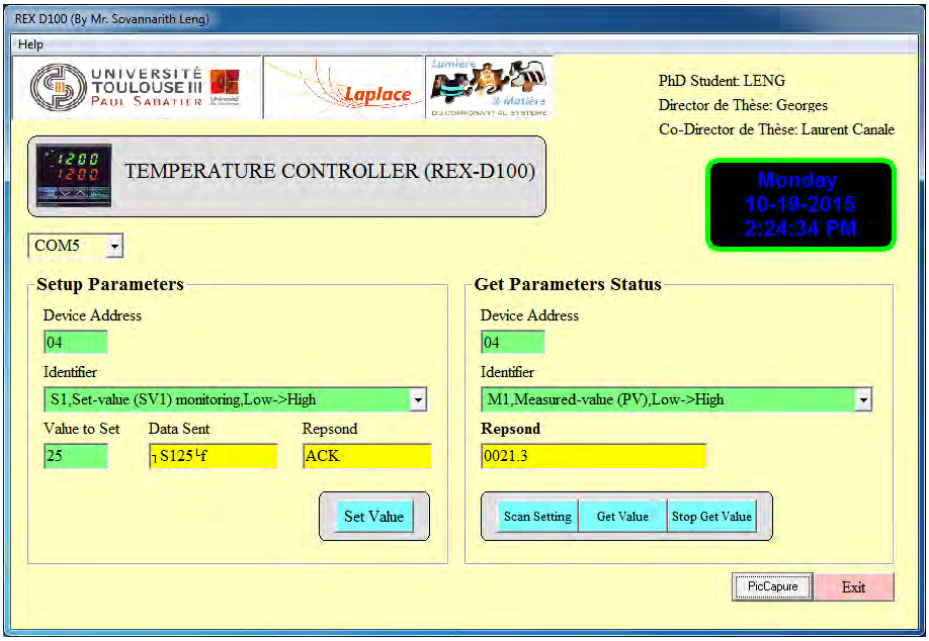

Figure III.11: Application program for REX–D100 controller.

3.2.2.1. Polling Procedure

Polling and Selection are the communication protocol that is used by the controller. Polling is the action that allows sending data from a host computer to one specific controller among all connected devices. The sequence of polling process is illustrated as diagram bellow.

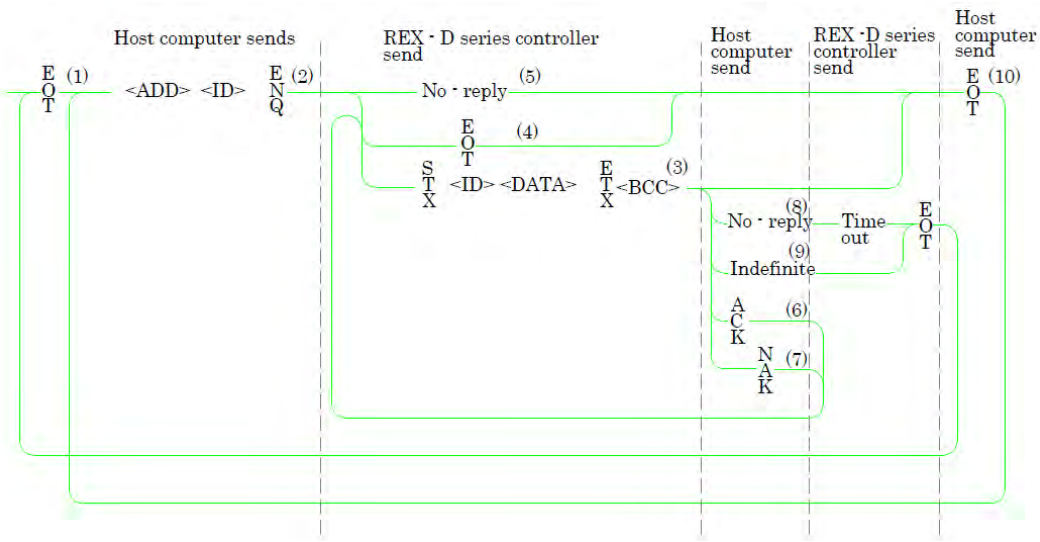

ADD : Address

ID : Identifier

3.2.2.1. Selection Procedure

Selection is an operation in which the host computer selects one set from among the controllers multiconnected and thus steering the data that must be received. The procedure is as the following.

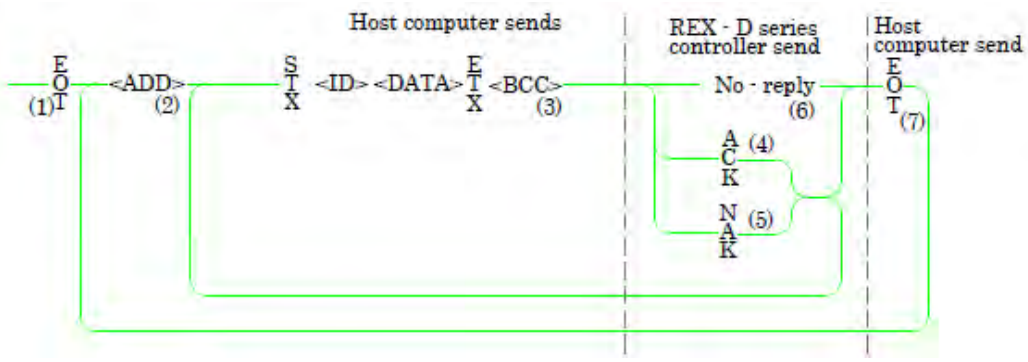

3.3. SOURCE–METER UNIT (SMU–KEITHLEY 2602A)

The main work that has been done in this thesis is to characterize the degradation of light–emitting diodes aged under stress conditions. To evaluate evolution of devices under stress, one of the main methods consists to follow electrical parameters (as I–V curves, discrete equivalents elements, etc…) that allow detecting the changes of LED parameters. I–V characteristics can allow us to reveal the failure mode of the LED die contact. I–V characteristics of LED,

including reverse bias and forward bias for both low level injected current or high level injected current, are intrinsic information that allows to judge the degradation state of LEDs. However, as at reverse bias current and low level injected current of LED, the LED current is very low in the range of of 10^{-8} A to 10^{-10} A; so, it is necessary to use a high precision equipment to perform the measurement. In this regard, the Keithley 2602A source–meter unit is utilized due to its high accuracy of measurement. The detail of functionality of the device can be found in [71], and some main feature and parameters are briefly descripted in the following section.

3.3.1. 2–Wires and 4–Wires Feature

Two–wires local sensing measurements, Figure III.12, can be used for the following source–measure conditions: 1) sourcing and measuring cur-rent, 2) sourcing and measuring voltage in high impedance (more than 1 kΩ) test circuits. When sourcing and/or measuring voltage in a low–impedance test circuit, there can be errors associated with IR drops in the test leads.

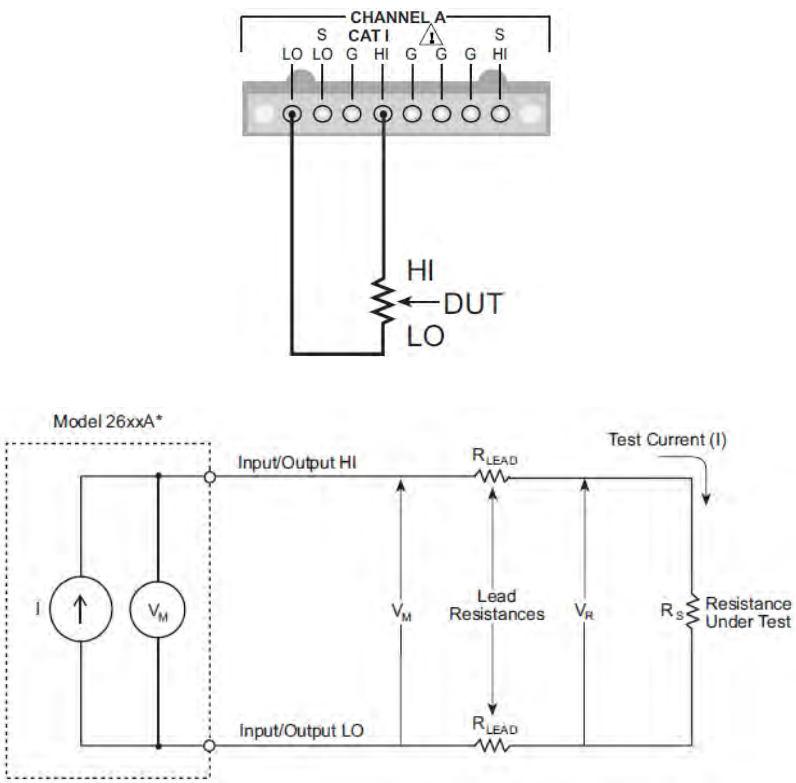

Figure III.12: Two–wires connections.

In the case of LED measured device, that has a variable impedance characteristic in nature in a small range value of impedance, voltage source and measure accuracy are optimized by using 4–wires remote sense connections (Figure III.13). When sourcing voltage, 4–wires remote sensing ensures that the programmed voltage is delivered to the device under test (DUT). When measuring voltage, only the voltage drop across the DUT is measured.

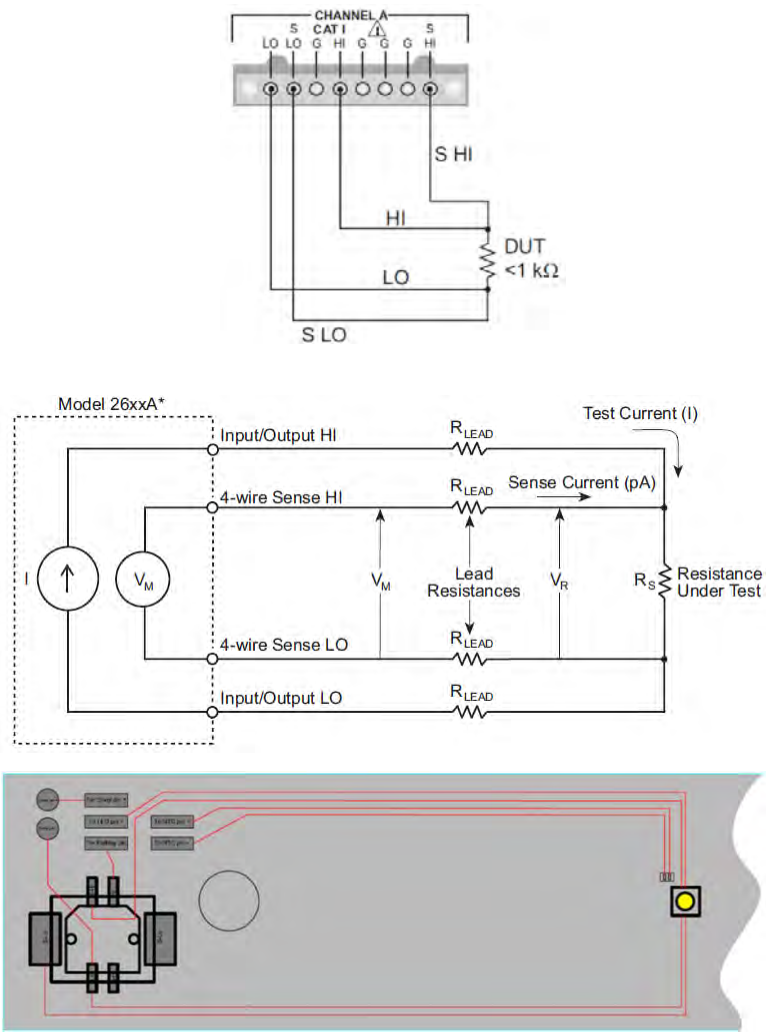

Figure III.13: Four–wires connections.

3.3.2. Software Program Measurement for SMU–Keithley 2602A

In order to measure electrical characteristic of large amount of LED samples during the experiment, an effort has been done on developing an application program named "**Keithley 2602A**", Figure III.14. This program enables to set a large

number of necessary parameters easily. It was also developed in visual basic platform as a user interface and the description of its utilization is briefly presented as following.

From the inherent feature of Keithley SMU device, the program is designed proving two group channels to perform independent measurement that comes along with Keithley. They are channel A and channel B (called *"Channel A"* and *"Channel B"* in the interface) and are applied to hold all the necessary setup parameters of each channel. Some of these parameters can be either enable or disable when selection of a specific source sweep mode has been selected to perform a particular source and measurement mode. So, when the parameters are disabled, the remained parameters are required to set these values and to complete the test.

The two channels have the same setup parameter; this is why only one of these will be briefly described here. Staring from up to down of the panel, *"Source Sweep Mode"* dropdown list is use to select one of various type of sweep mode of source and measure including Pulse, DC linear staircase sweep, Pulsed linear staircase sweep, DC logarithmic staircase sweep, Pulsed logarithmic staircase sweep, DC list sweep and Pulsed list sweep (Figure III.15). And the mode of source and measurement can be interchanged between voltage source–measure current and current source – measure voltage for each sweep mode. Then *"Bias Level"* textbox give the value at which the base of pulse can be offset. *"Source Start Value"* textbox sets the value of starting point of source sweep. *"Source Stop Value"* sets the value of stop point of source sweep. *"Source Limit"* sets the limit value of source to protect DUT for specific measurement condition. *"Source Rangei"*, *"Source Rangev"*, *"Meas Rangei"*, *"Meas Rangev"* textbox field are set compliant to the maximum limit SMU's power, in our case KI–2602A is 40W. *"Ton"* and *"Toff"* gives the time of the pulse and it will be disabled for *"Toff"* in case of DC sweep mode.

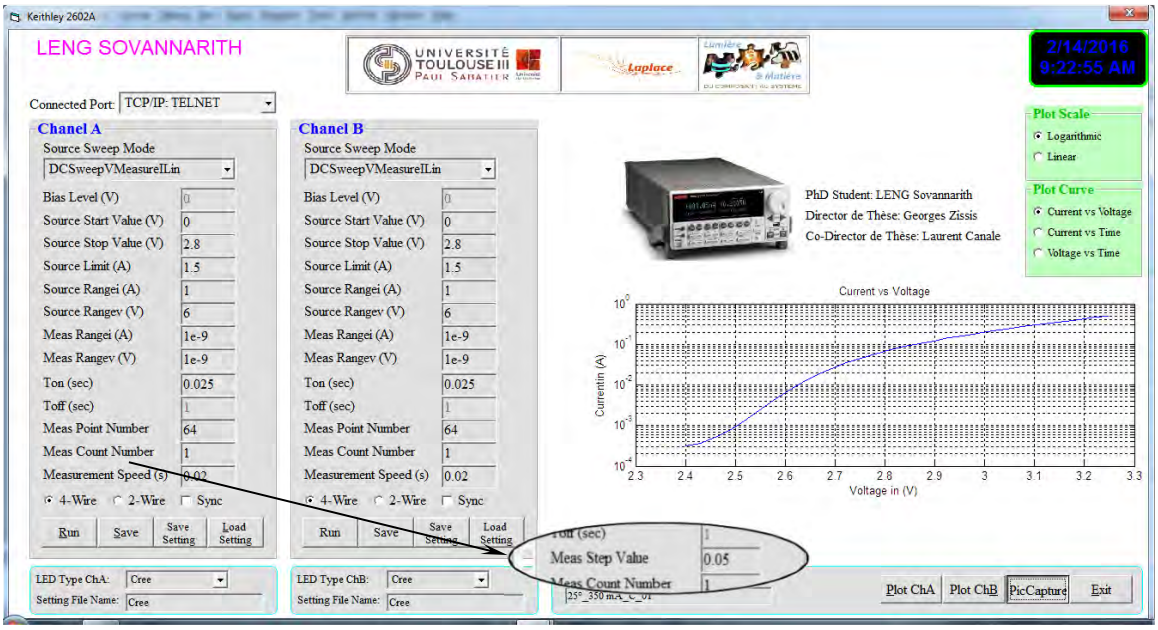

Figure III.14: Application program for SMU–Kethley 2602A.

"Meas Point Number" sets the number of measurement's points that will be performed and, by clicking on this text label, it will allow to set a specific value of step of current or voltage source (instead of the previous number of points that the measurement will performed as indicated in Figure III.14. Then *"Meas Count Number"* allows to repeat the measurement as many time as needed and all these measured data will be saved to spreadsheet file. *"Measurement Speed"* is the speed of SMU device to perform the measurement. This value is converted from Number of Power Line Cycles (NPLC) which is detected by the device and either 50Hz or 60Hz, where 1 PLC for 60 Hz is 16.67 ms (1/60) and 1 PLC for 50 Hz is 20 ms (1/50). The fastest integration time (0.001 PLC) of the device results in the fastest reading rate, but also causes increased reading noise and fewer usable digits. The slowest integration time (25 PLC) provides the best common–mode and normal–mode noise rejection, but has the slowest reading rate. Settings between the fastest and slowest integration times are a compromise between speed and noise. So the converted time of measurement speed is between 0.02ms to 0.5s in the case 50Hz power line. Bellow this, there are ratio buttons *"4–Wires"* and *"2–Wires"* that allow to select either 4–Wires or 2–Wires measurement mode which is descripted in the section V.3.1 above. Next, there is a *"Sync"* checkbox that allows to synchronize the source–measure device to a spectrometer (Specbos 1201) that will mention in the next

section. This function permits to activate the spectrometer to perform the optical measurement while the sourcemeter unit supplies the device.

"Run" to run the program after all parameters are completely setup. *"Save"* to save all measurement data including source and time to a spreadsheet that allows performing further data analyses. "*Save Setting"* allows to save all set parameter values in to a spreadsheet file that can be reloaded to use in the next measurement by loading the file with *"Load Setting"*. Below the Panel group *"LED Type"*, by selecting item in the list down (a specific list of LED type used in this work), it will load the predefine setup parameter value of LED type including Cree, Osram, Philips and Seoul. However, the value can be manually set for each field descripted above. *"Setting File Name"* helps to display the name of the setting file that currently loaded.

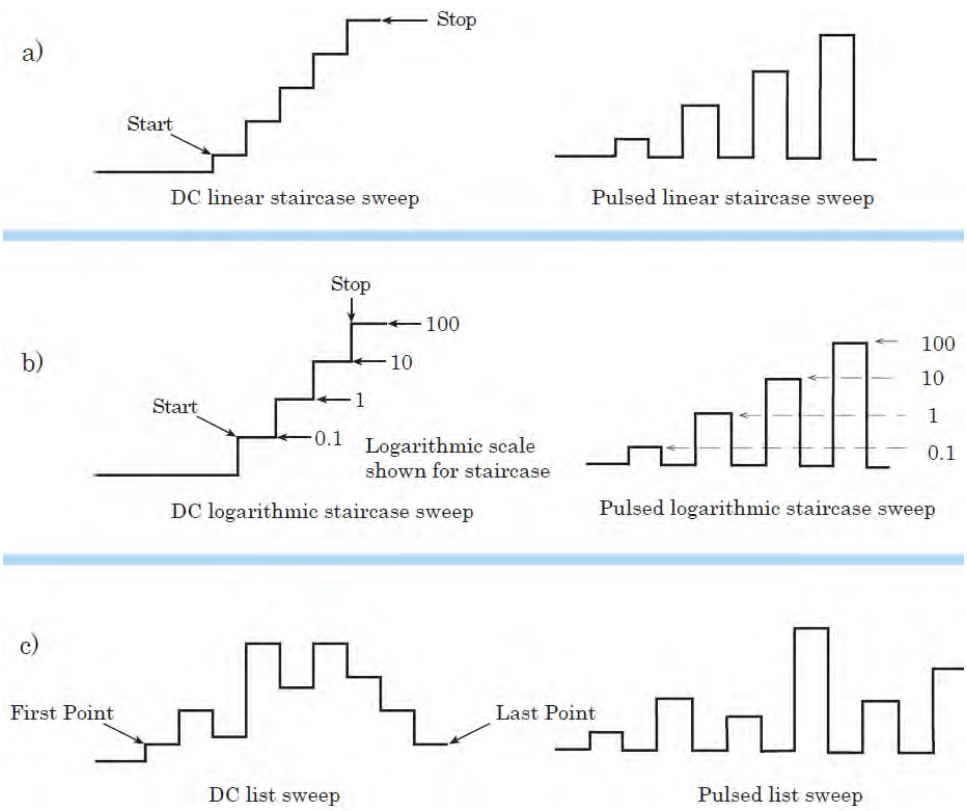

Figure III.15: Sweep modes a) linear, b) logarithmic and c) list.

In the right side of panel groups from the top, there are two panel groups "Plot Scale" and "Plot Curve". *"Plot Scale"* provides two scales of axis, linear and logarithmic, and *"Plot Curve"* provides different electrical variables to be plotted either current versus voltage, current versus time or voltage versus time. At the

right bottom, there are four buttons *"Plot ChA"* and *"Plot ChB"* to plot the curve, for each specific channel, that is performed by the measurements and the curve is displayed in the area above these buttons. There is also *"PicCapture"* button to capture the screen picture of the program and *"Exit"* button to quit the program. The complete source code of the "Keithley 2602A" is provided in Appendix D.

3.4. IMPEDANCE ANALYZER (SOLARTRON MODULAB)

Other parameters including capacitance–voltage characteristic, series resistance and parallel resistance of the LED are also the main candidate to help evaluate the degradation of the device [17]. These parameters can be extracted by the using of Solartron ModuLab. It is an impedance analyzer that provides a flexibility to measure variety of mate-rial, including LED, OLED and other display materials, ferroelectrics, pie-zoelectrics, polymers, ceramics, superconductors, due to modular design of the system where appropriate modules may be configured depending on the application. A number of modules are combined into a single chassis. The modules are arranged in groups, known as instrument groups. The de-tail functionality of the Solartron ModuLab can be found in [72].

3.4.1. Instrument Group Modules

Modules of instrument group including: 1. MFRA 1MHz module is a Frequency response analyzer (FRA) and can perform in the range of 10 µHz to 1 MHz, 2. MAT 1MHz module is a core module for voltage generation and voltage/current measurement. Maximum data capture rate: 1M samples/second Voltage span: ±8 V at up to ±100 mA. 3. MHV 100 is high voltage module that can provide the output voltage span: ±100 V at up to ±100 mA, 4. MFA is a femto ammeter that allows to measure a low current in the range of 3 pA to 100 mA, 5. MREF is a reference module reduces systematic errors due to cables and instrumentation and 6. MBST 2A is a power booster module that can provide current output: ±2A at voltage to match the core module (MAT 1MHz) or using the high voltage module (MHV 100) up to maximum voltage ±20 V.

To perform different measurement tasks, the modules of instrument group have to be properly configured based on its specific function. In this work, the configuration of the measurement task is conducted by using the combination of four principle modules including a conjunction of MAT core module, MBST module and MHV module to perform the measure of capacitance–voltage characteristic of LED samples in the range of current larger than 100 mA provided by MAT core module only. The MFRA module is used to perform the scanning of measured device's impedance. The hardware connection configuration of the tested LED is shown in Figure III.16. The connection also provides the 4 wires configuration that can be controlled in the ModuLab software control.

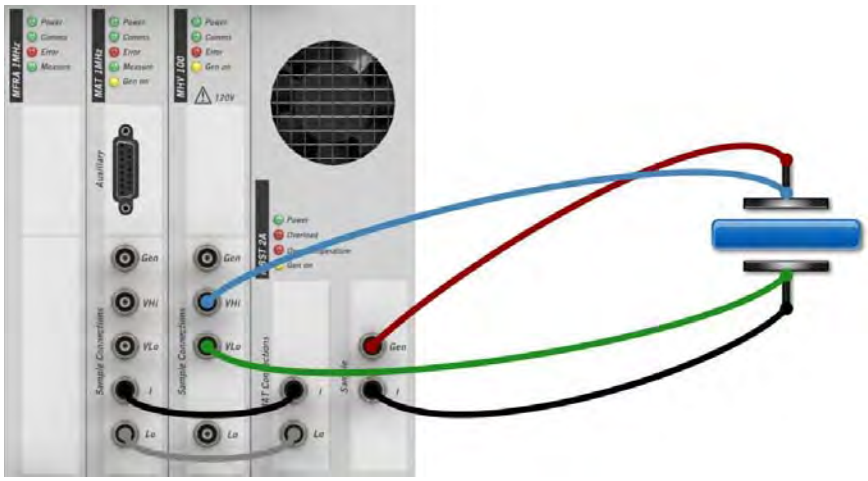

Figure III.16: LED measurement configuration.

3.4.2. PC Communication Setup

Communications to the impedance analyser "Solartron" can be established with the computer through an Ethernet port by using RJ–45 "straight through" cable between the PC and the ModuLab XM chassis Figure III.17. Communication is done by setting appropriate IP address of PC to a predefined IP of Solartron ModuLab. In this case, PC's IP "10.20.40.X" is used to communicate to the same network configuration of ModuLab device.

Figure III.17: Networking to PC.

3.4.3. Software Program Control of Solartron ModuLab

For control and performance of the measurement with this device, measurements can be easily accomplished with the help of accompanied software. The ModuLab XM MTS system is controlled by a PC running with the ModuLab XM software, which has been installed as shown in Figure III.18. The detail of configuration and utilization of the software can found in [72]. However, in this work the measurement of capacitance and voltage (C–V) characteristic is done and the setting of parameter has been configured differently depend on specific reference data of LED type. Figure III.19 is showing a C–V measurement of LEDs from Cree. The voltage scan is in the range –3 V to 3.2 V with as single scan frequency of 1 kHz.

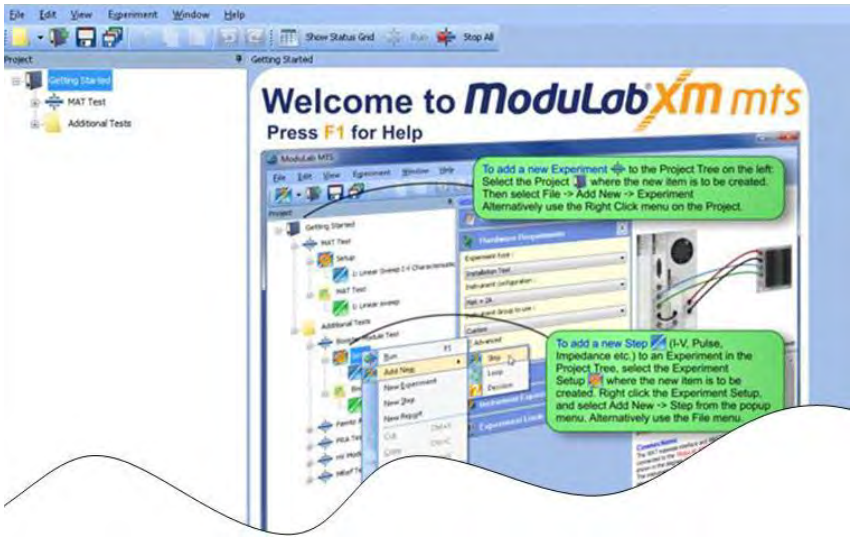

Figure III.18: Software control of ModuLab.

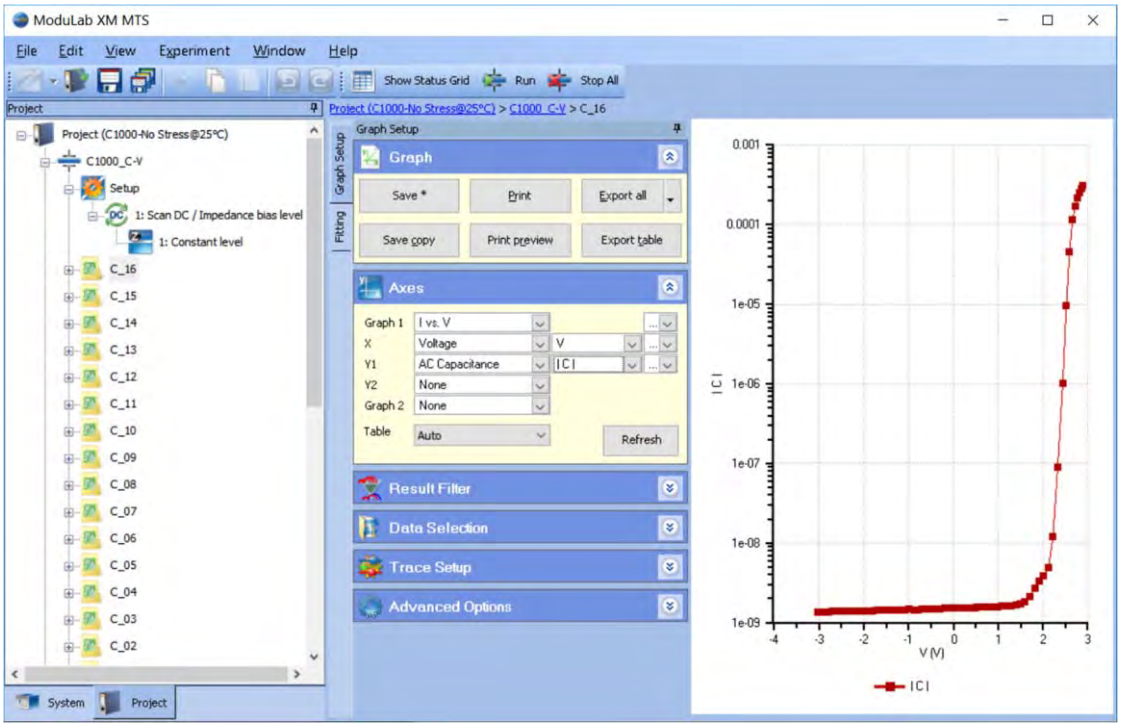

Figure III.19: C–V Characteristic measurement.

The measurement of LED's impedance can also be done at various bi-as voltage levels with the sweep frequency defined from 1 Hz to 1 MHz. and Figure III.20 shows the scanned impedance of LED with the bias volt-age from 0.5 V to 3.2V.

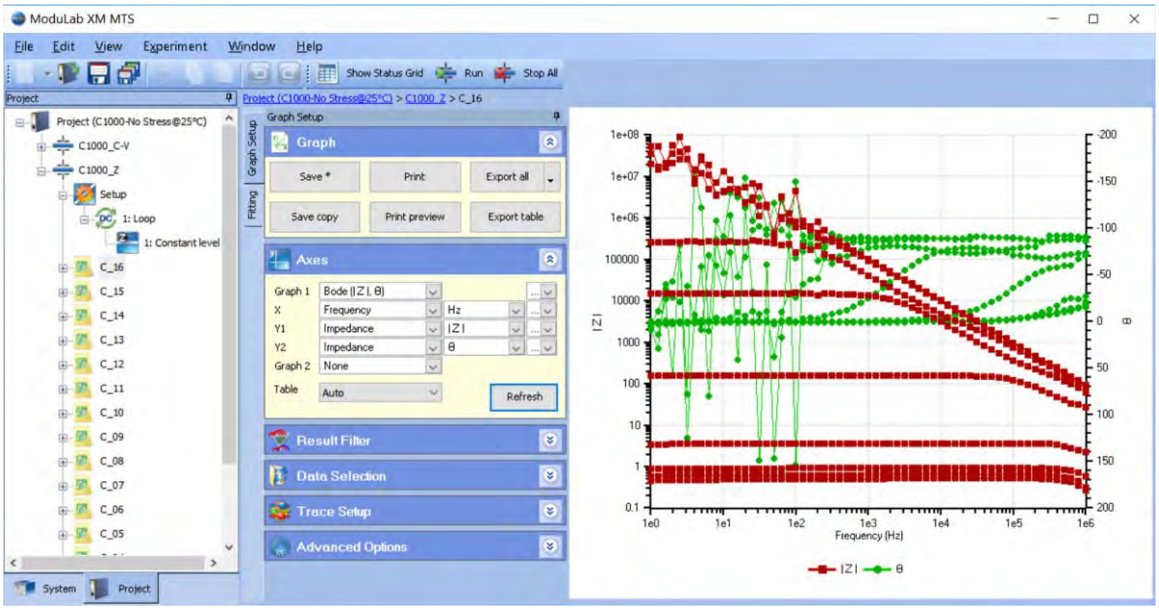

Figure III.20: Impedance measurement.

After impedance of the sample has been measured, the impedance curve along the frequency sweep can be fitted inherently in the software and the corresponding value of series resistance, parallel resistance and capacitance of the measured device along with its equivalent circuit can be extracted as illustrated in Figure III.21. This figure shows also the equivalent circuit and fitting curve of a measured sample with a bias voltage 2.4 V.

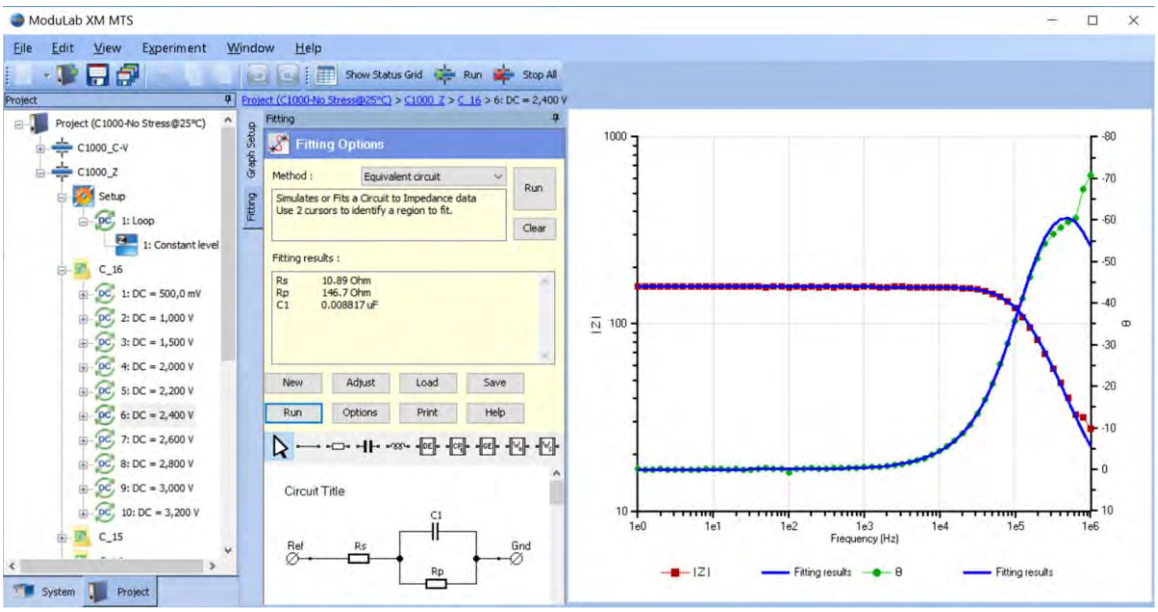

Figure III.21: Fitting and equivalent circuit of a measured sample.

3.5. SPECTROMETER (SPECBOS 1201)

Another important characteristic that can indicate the depreciation of LED is its optical characteristics. Optical parameters are crucial parameters that can indicate the degradation of LED. In this work, these optical parameters are measured since the first time before sending the devices to stress condition, and then successive measurement of the parameters is done along the stressed time to compare to the initial state. The optical parameters are obtained by the help of a spectrometer. “Specbos 1201” spectrometer is used to measure various optical parameters including luminance, radiance, CCT, chromaticity coordinate, spectrum and so on.

3.5.1. Optical Measurement Hardware Setup

In order to measure the optical parameters of the tested device, the setup of the measurement procedure is done by putting the spectrometer straight forward to the LED in the predefined distance, one meter in this case, between the spectrometer and the measured LED (Figure III.22). This distance will still the same for all measurements.

Figure III.22: Setup measured distance.

The target of the measured device and the area at which the spectrometer performs the computation of the measured parameters is provided inherently in the spectrometer with help of program software Jeti LiVal. As shown in Figure III.23, a pointing laser is directly stroked on the measured target where the LED is placed. And the pointing laser is attached with the base circle of the cone at which the light from the measured LED is collected by the spectrometer to perform internally calculation of measured parameters. After setup is completely done, the photometric characterizations are then carried out in a dark environment.

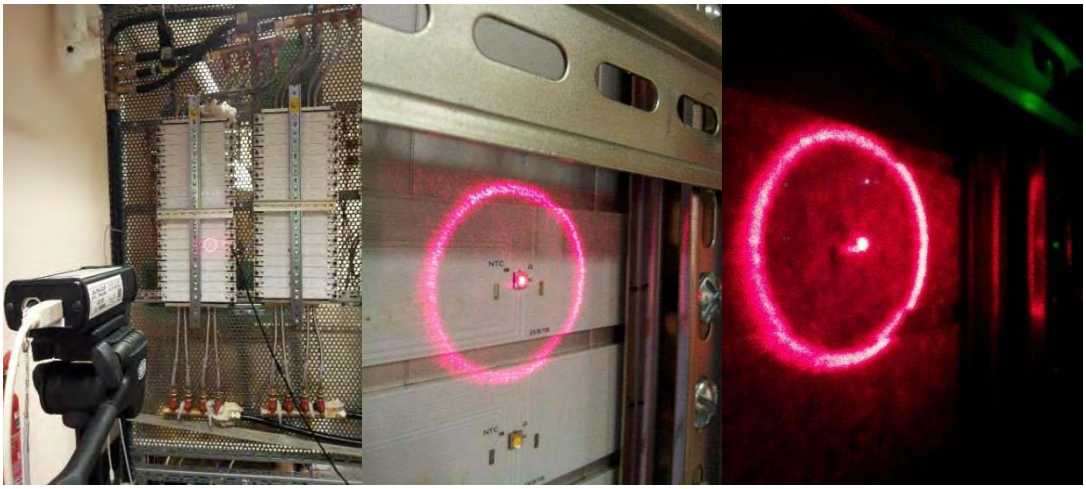

Figure III.23: Photometrical measurement setup.

3.5.2. Software Program Measurement of Specbos 1201

The photometrical measurement is accomplished by the use of Jeti Lival software program that comes along with the spectrometer (Figure III.24).

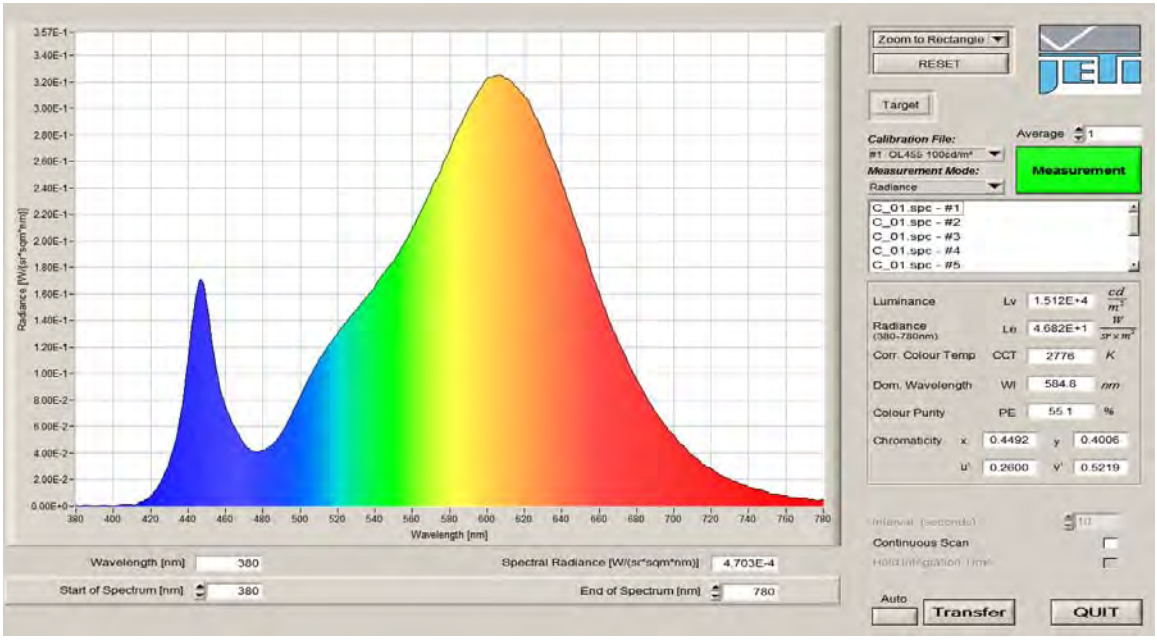

Figure III.24: Jeti Lival program for Specbos 1201 control and measure.

The measurement is performed for different current levels from 0 to 1000 mA with the step of 100 mA. The Keithley 2602A source–meter unit provides the current source. For each level of current source given by sourcemeter, the spectrometer is activated automatically by the trigger control signal from SMU to

implement the measure consequently. Then, all measurements are exported to a spreadsheet; (Appendix E) that allows to further process of data analysis.

3.6. LED's Driver

The supply from SMU is only able to supply each LED with a high current quality during the measurement period. However, to power all 128 LED samples for a long period of stress time, custom–made LED's driver circuits have been built (Figure III.25). The LED samples are supplied by a high accuracy (less than 1%) and very stable DC current source. This can allow us to admit that there is no variability on degradations in connection with the power supplies. LEDs are always supplied with a DC current source because a small voltage variation leads to a large variation of current due to the exponential I–V characteristic of the LED.

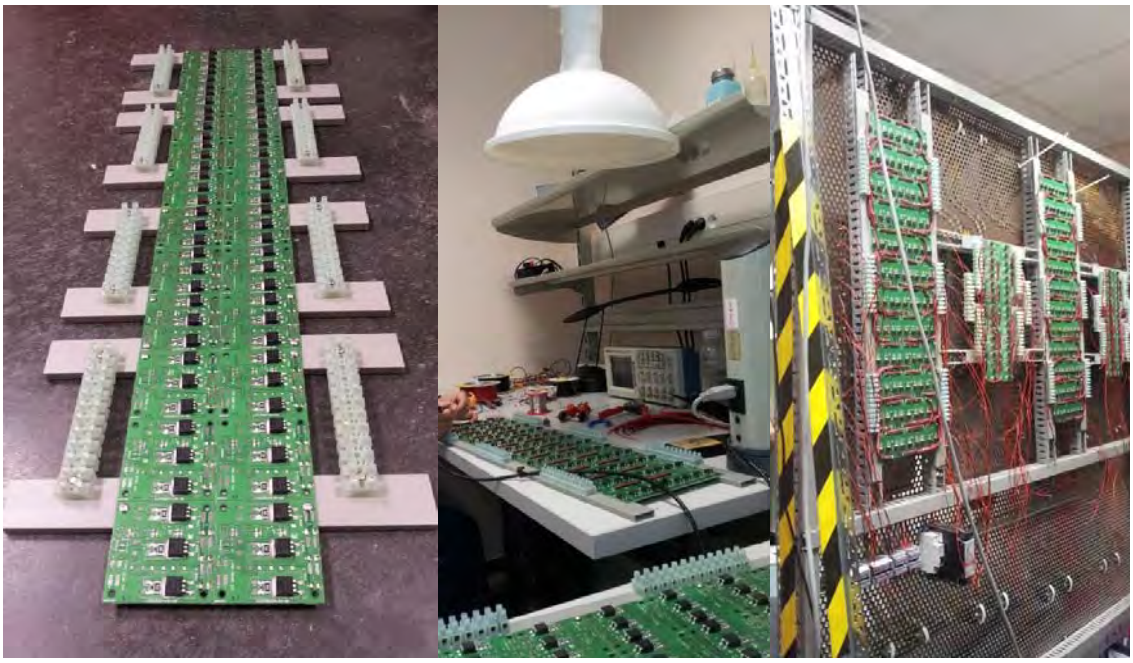

Figure III.25: Drivers of LED samples.

The DC current source is built with a LM317 Current Regulator. The design of the regulator, used to supply the LED samples, is following the circuit provided in Figure III.26.

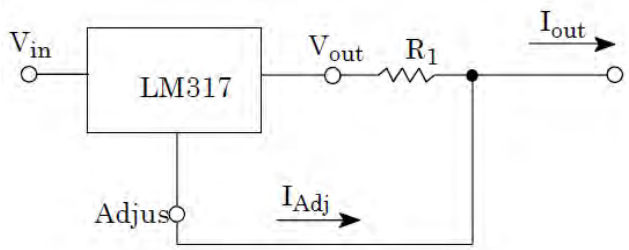

Figure III.26: Current regulator circuit.

In this circuit, the value of resistance R_1 has been selected to obtain the output current needed to supply the LED. The current accuracy is directly link to the resistance accuracy; this is why each resistance is selected and tested one by one to reach the best performances. This can be well defined as explained with the Eq. III.1.

$$I = \left(\frac{V_{ref}}{R_1}\right) + I_{adj} = \left(\frac{1.25V}{R_1}\right) \qquad For\ 10\,\text{mA} \le I_{out} \le 1.5A \qquad \text{(Eq. III.1)}$$

So, by selecting a standard resistance of 3.6Ω, it can provide a con-stant output current of 1.25V/3.6Ω = 0.34722 A = 347.22mA that is nearly the same as nominal value characteristic of LED samples to be use for one stress condition namely 350mA stress condition in this experiment work (error is less than 0.8%). However, there is another stress condition intended to perform for the experiment namely 1000 mA stress condition by combined in parallel of three constant current outputs form each LM317 current regulator so that can provide actually 347.22 x 3 = 1041 mA for each LED sample powered with high current stresses. All data treat-ments and curves plotting were taken into account the real value of 1041 mA but for an easy reading, this value is rounded to 1000 mA in the text.

Since LM317 is a linear current regulator, it inherently draws as much current as its supply. When this current is multiplied by the voltage difference between input and output, a significant heat can be generated. So, the optimization of the

difference between these voltages has to be considered. To select the smallest input voltage (to reduce self–heating), it is computed as as Eq. III.2 [73].

$$\text{Input voltage} = \text{drop in LM317} + \text{drop in load due to constant current} \quad \text{(Eq. III.2)}$$

Where the "drop in LM317" is 3V and the "drop in load due to con-stant current", in the case of tested LED samples, is in the range of 2.8 to 4V. So, the selected input source voltage is chosen around the value of 3V + 4V = 7V.

Another consideration of input source selection is the large current drawn by all LED samples. To properly supply all combined LED samples, which is necessary to power the 4 panel groups as descripted in the last part of section V.1, the supply has to be able to handle the current of "32 LEDs" x "1. 041A/LED" = 33.3 A for 1000mA current stress groups and "32 LEDs" x "0.34722A/LED" = 11.1 A. So, there are three of power supplies of Switch Mode Power Supply (SMPS) which can provide the DC voltage regulated from 6 to 9V and the supported current 40A, Figure III.27. Two of these are used for two panel groups of 1000mA stress current with the output voltage for LM317 current regulator is 6.67V, and another is used for two panel groups of 350mA stress current with the output voltage for LM317 current regulator is 6.51V.

Figure III.27: Switch mode Power supply for LED drivers up to 40A.

4.

EVALUATION OF FAILURE MECHANISMS FOR LEDS STUDIED

In this chapter, the experimental observation of temperature influence on LED electrical characteristics has been highlighted and explained based on the theory and literature. Then, the issue on self–heating effect during the measurement setup has been discussed. After that, various electrical characteristics of LED samples have been reported from their initial state to an aged state under accelerated aging stress conditions. Subsequently, the electrical characteristics of those LED stressed samples have been presented and compared to their initial state in order to reach the conclusion on device degradations.

4.1. Effect of Temperature on LED Performance

The first studied case is on the effect of temperature on powered LED in operation. In this case, current–voltage (I–V) characteristics have been measured for three different temperature conditions 15°C, 25°C and 35°C to evaluate the effect of temperature on LED in operation. The measurement is implemented by using a source–meter unit (Keithley–2602A). The measurement data of these temperature conditions are inserted on the same graph as shown in Figure IV.1 for linear scale and Figure IV.2 for semi–logarithm scale. The plot reveals that, when the LED working temperature is increased, there is a reducing of operation voltage by shifting the curves to the left along the rising of temperature. And the lowering of forward voltage due to the increase of temperature as reported in [74, p. 198], is maybe caused by the following factors:

(i) a decrease of the resistivity of the p–type and n–type layers.

(ii) an increase in the injection of holes from p–type of diodes to the active layer.

(iii) a decrease in the resistivity of the ohmic contacts.

Another interpretation is that, at the same voltage, the current will be greater and induce an augmentation of carriers's energy. When the carriers get more energy, they move more actively as mentioned by Liu and Luo , [75].

In Figure IV.3, we plot the forward voltages of LED versus various setting temperatures and it shows that there is a linear relationship. This feature is well ex-plained by the equation of temperature dependence with forward voltage (Eq.

II.24). It has been detailed in section 2.1.1 in Chapter 2 and recapitulated in Eq. IV.1.

$$\frac{dV_f}{dT} = \underbrace{\frac{k}{e}\ln\left(\frac{N_D N_A}{N_C N_V}\right)}_{\text{T dependence of } n_i} - \underbrace{\frac{\alpha T(T+2\beta)}{e(T+\beta)^2}}_{\text{T dependence of bandgap energy}} - \underbrace{\frac{3k}{e}}_{\text{T dependence of effective densities of state}} \qquad \text{(Eq. IV.1)}$$

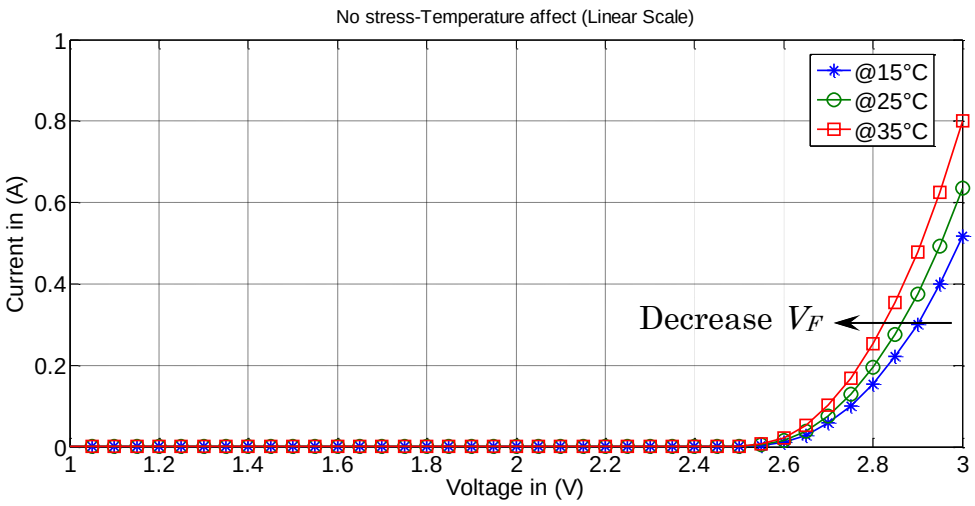

Figure IV.1: Temperature effect on LED, linear scale.

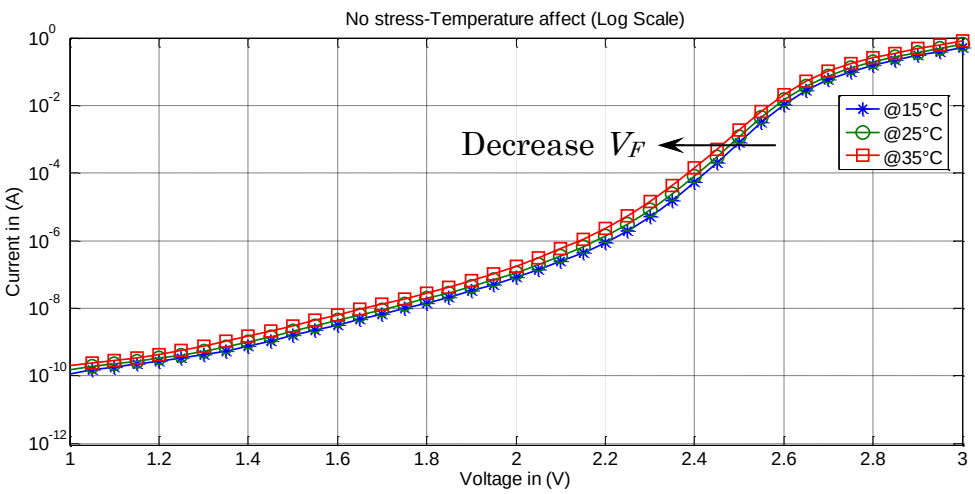

Figure IV.2: Temperature effect on LED, semi–log scale.

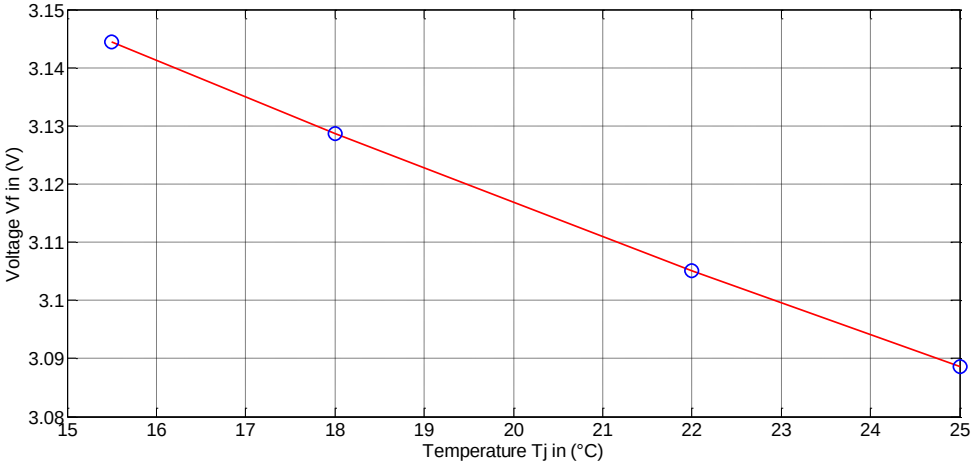

Figure IV.3: Linearity of forward voltage to temperature.

4.2. Self–Heating Test

An observation is done on the self–heating issue of LEDs that maybe occurs during operation or measurements because self–heating can alter characteristic of the device comparing to the case without self–heating. Not only during the operation but also during the measurement, LED must be biased with a current or voltage source for further proceeding. When LED is biased, there may be self–heating caused by the current injection especially in the region of high current level. So, in this case study, there is a test to verify and restrain the self–heating effect on the measurement data.

The test was performed by two different modes of voltage source provided by the source–measurement unit (Keithley–2602A). The two source modes, Figure IV.4, are the pulsed linear staircase sweep mode and a DC linear staircase sweep voltage source. The former is done by providing a very short pulse of 25ms with a small duty cycle of the pulse (0.5%) and assimilates as the case that there is no self–heating during the measurement due to a short pulse compared to a long period time, whereas the latter is powered by a DC linear staircase sweep (the LED is not switch off during the whole process of measurement points) to confirm the concerned case of self–heating process.

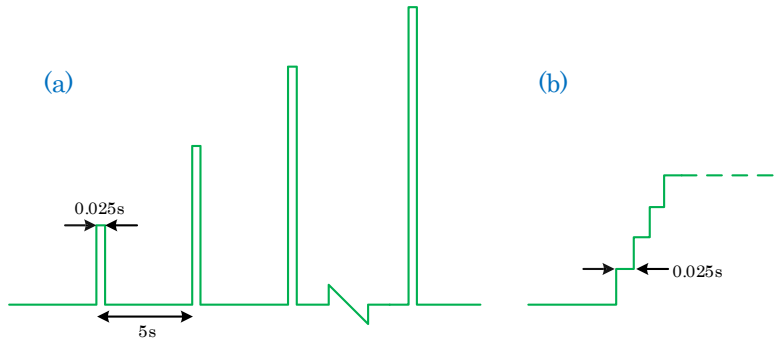

Figure IV.4: Source mode (a) Linear pulse, (b) Linear DC sweep.

From the test result, it shows that there is no difference between values of the measurement data for the both cases of the two source modes. Figure IV.5 illustrates the I–V characteristic and shows the consistency of the two sets of data. This can allow us to conclude that for a short period of time scale of meas-urement performed in the test, the process used to characterize the devices doesn't affect substantially the results. Thus, in the following sections, the measurement protocol to characterize the LED behavior can be performed by one of the aforementioned source modes.

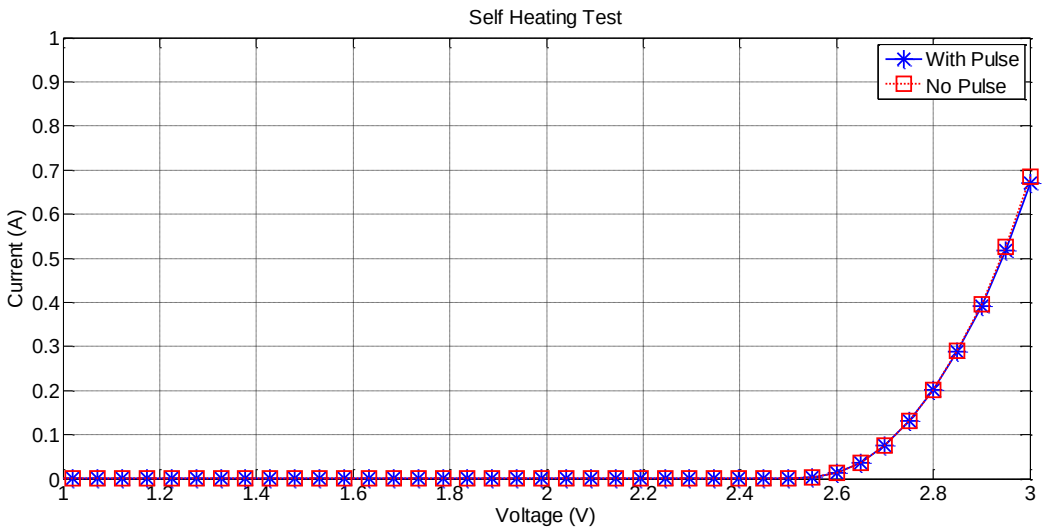

Figure IV.5: I–V Curve, self–heating test.

4.3. Initial State Of Electrical Characterizations

This case study attempts to report the electrical characteristics of initial state of all LED samples that are used for the degradation failure analysis. The measurement characteristics of samples are classified into four groups of different

LED types including Cree, Osram, Philips and Seoul groups. And for each group of LED types, there are two separately group characteristics to be identified based on the two different electrical stresses (350mA and 1000mA). In addition, for every group of current stress condition, there are 16 LED samples.

The case study also tries to illustrate the electrical characteristics separately be-tween forward bias characteristics and reverse bias characteristics of each sam-ple because these two bias modes will act as main candidates to evaluate or characterize the degradation behavior of LEDs. The following figures will illustrate the measurement data of each specific group. The following figures will illustrate the measurement data of each specific group and all the measurement have been done at the room temperature (25°C).

The Cree LED samples are firstly reported. Figure IV.6 and Figure IV.7 show the current–voltage (I–V) characteristics of 350mA current stress condition of all 16 samples of Cree LEDs plotted on the same graph on a linear scale and semi–log scale, respectively.

Figure IV.8 and Figure IV.9 show the current–voltage (I–V) characteristics of 1000mA current stress condition of all 16 samples of Cree plotted on the same graph on a linear scale and semi–log scale, respectively.

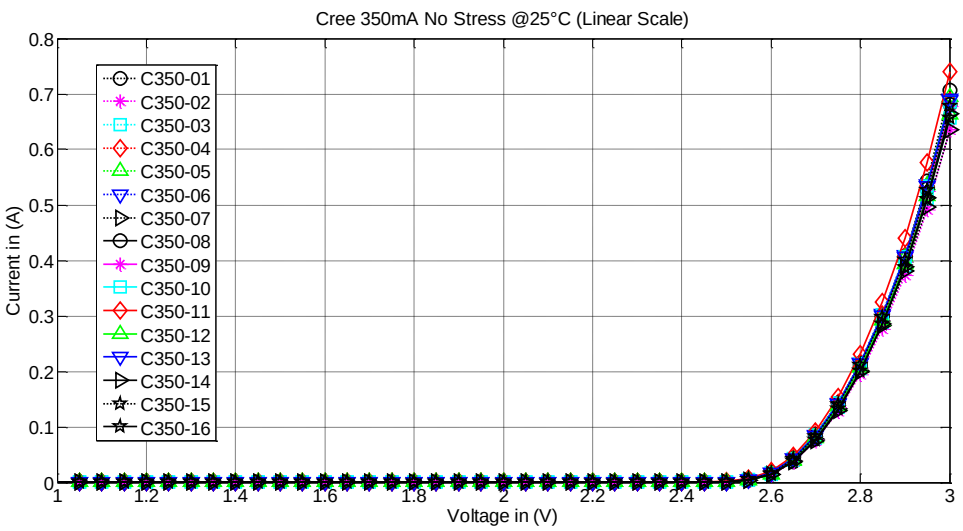

Figure IV.6: I–V characteristic of Cree@350mA, linear.

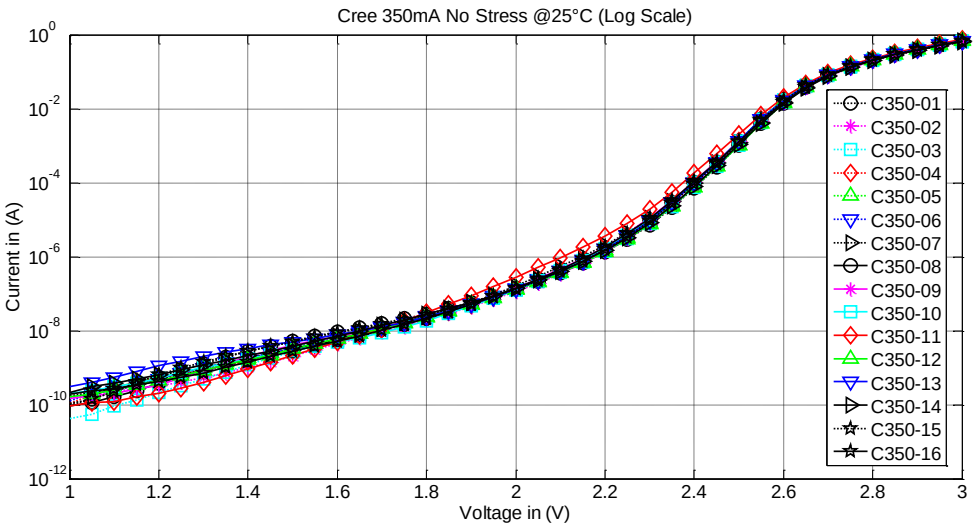

Figure IV.7: I–V characteristic of Cree@350mA, semi–log.

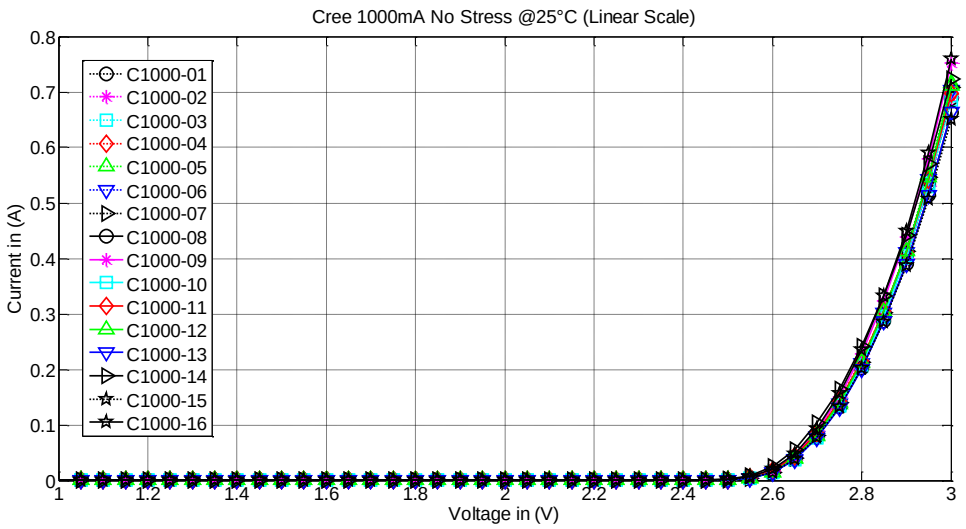

Figure IV.8: I–V characteristic of Cree@1000mA, linear.

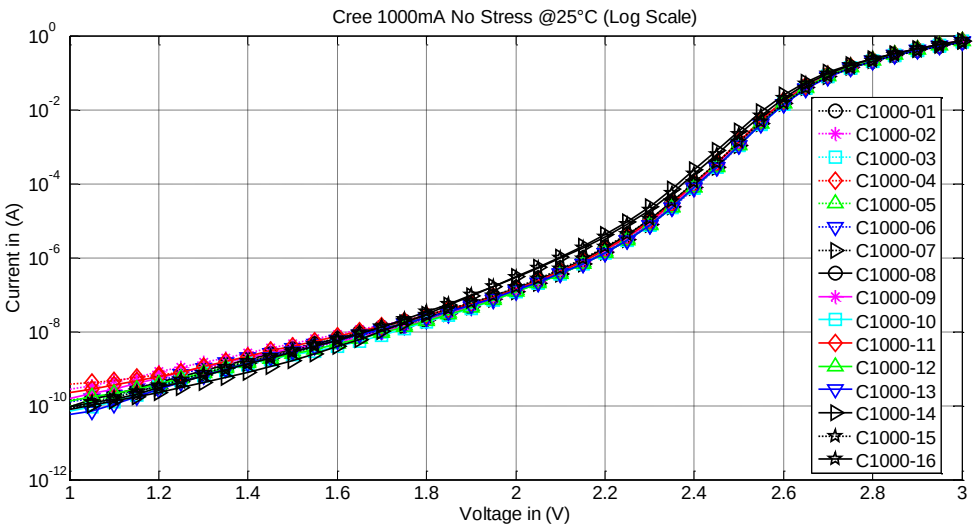

Figure IV.9: I–V characteristic of Cree@1000mA, semi–log.

The measurement results shown in those figures (Figure IV.6, Figure IV.7, Figure IV.8 and Figure IV.9), reveal good binning product because there is a small variation of I–V characteristic for all the samples from the same manufacturer and also clarified by the values as indicated in Table IV.1 – the computed error deviation of I–V characteristic of 16 samples of each LED group, Cree, Osram, Philips and Seoul.

However, the result shows that there should be a different characteristic among all of the LED samples, even they come from the same manufacturer with the same LED material and technology. The differences take place for the whole well–known LED's operation zone that is indicated clearly in Figure IV.10 for 350mA stress group and Figure IV.11 for 1000mA stress group.

These figures (Figure IV.10 and Figure IV.11) show the I–V characteristic that is an average of all 16 LEDs samples along with the error bar to emphasize the deviation characteristic among the LED samples. In these semi–log scale plots, it can show clearly the error in the zone of low injected current level, zone I and in the zone of ideal diode characteristic, zone II.

Table IV.1: dispersion of I–V characteristic of 16 Samples each LED group computed at V=2.9V.

Cree	Osram	Philips	Seoul
1.81%	6.66%	2.27%	2.43%

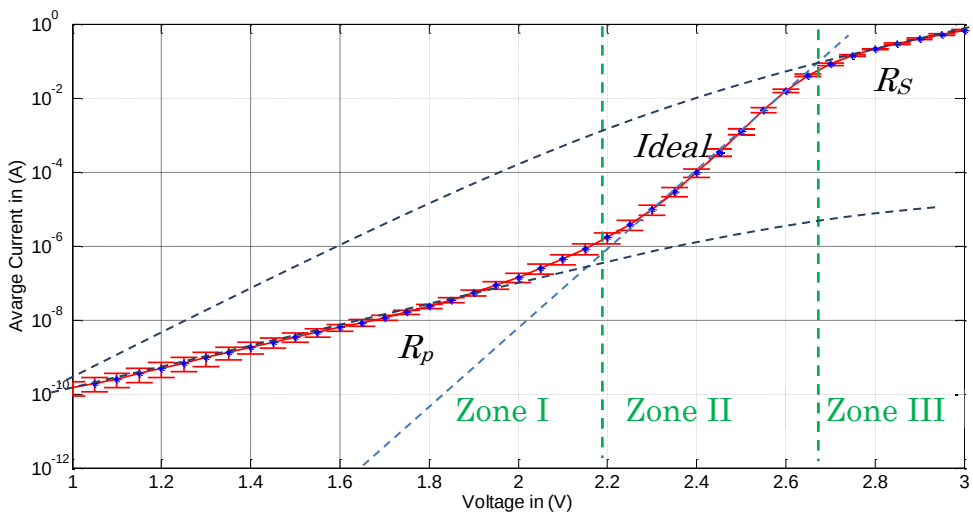

Figure IV.10: Error bar around average value of 16 samples Cree@350mA, semi–log.

However, for the zone of high injected current level, zone III, the error or the deviation is clearly shown in the linear scale plotted in the Figure IV.12 for 350mA stress group and Figure IV.13 for 1000mA stress group.

From the result, it shows that Nitride–based LED's electrical characteristics are different from those of conventional diodes, such as p–n or Schottky diodes. So the LED's electrical characteristics have to take into account the parasitic resistances.

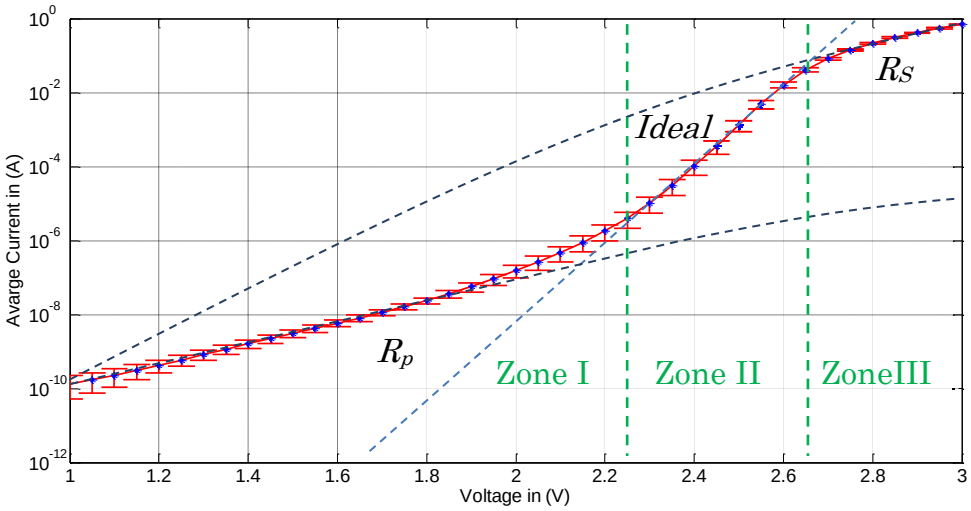

Figure IV.11: Error bar around *average value of 16 samples Cree@1000mA, semi–log.*

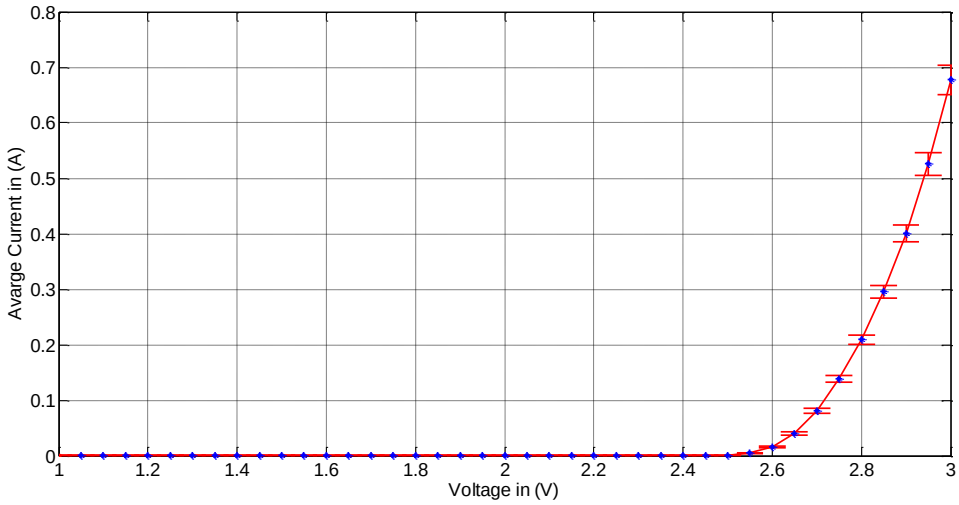

Figure IV.12: Error bar around *average value of 16 samples Cree@350mA, linear.*

From Schubert , [17], these parasitic resistance effects divide the forward bias electrical characteristic of LED into three different zones as being described previously including:

Zone I that is the effect of parasitic parallel resistance caused by leakage path of low level current. This leakage path is ascribed by the damage of bulk or surface imperfections of semiconductor which is mediated by surface or bulk point defects and dislocations.

Zone II is the ideal operation zone of LED.

Zone III demonstrates the effect of series resistance that is imputed by the excessive contact resistance or by the resistance of the neutral regions during high–injected current.

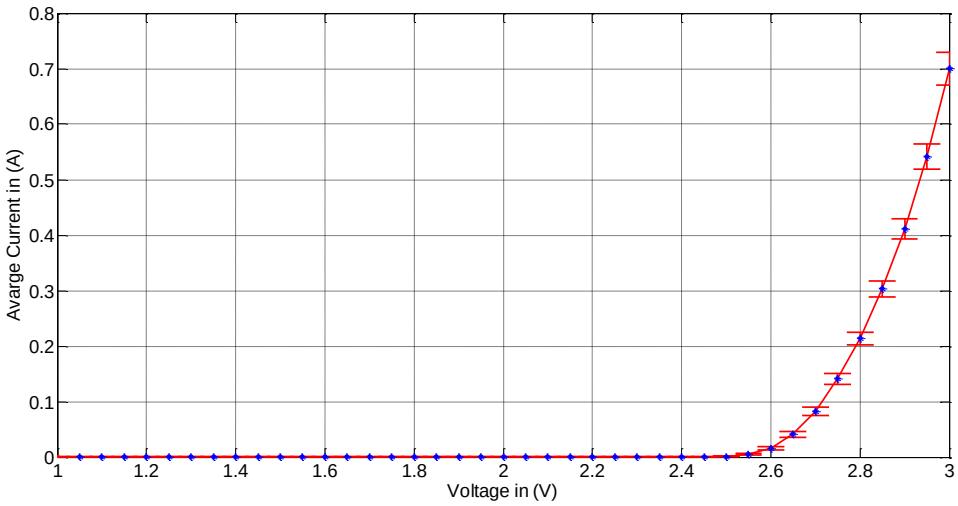

Figure IV.13: Error bar around *average value of 16 samples Cree@1000mA, linear.*

The I–V curves in semi–logarithmic scale in either Figure IV.10 or Figure IV.11 reveal the presence of different conduction mechanismstransport phenomenons that is compatible to the previous results mentioned in [74, p. 198], in the low voltage level, zone I, current has a nearly exponential dependence on voltage. In this zone, the I–V curve does not significantly depend on temperature and the main mechanism responsible for current conduction is a field–dependent process such as tunneling rather than a thermally activated process. For GaN–based LEDs, forward–bias tunneling components are usually represented in Eq. IV.2.

$$I \approx I_0 e^{\left(\frac{eV}{E}\right)} \qquad \text{(Eq. IV.2)}$$

Where I_0 is saturation current, E represents an energy barrier to tunneling carriers, and has negligible temperature dependence and can be expressed as

$$E = \frac{4\hbar e\sqrt{N_D}}{\pi\sqrt{m^* \varepsilon}} \qquad \text{(Eq. IV.3)}$$

Where e is the electron charge, $\hbar$ is the Planck's constant divided by 2π, m^* is the effective mass of the electrons, and N_D represents the doping concentration.

So, zone I is the zone that current conduction is dominated by tunneling. Thus, we can assert that tunneling processes of GaN–based LEDs can be caused by:

(i) tunneling of holes into the active region.

(ii) tunneling of electrons to deep levels located within the barriers or the p–GaN region with subsequent recombination.

(iii) tunneling recombination via multiple–step processes.

(iv) diagonal tunneling.

Zone II is a thermoelectronic effect. While for high current densities, zone III, the presence of the series resistance results in a significant decrease in the slope of the I–V curves: series resistance originates from the non–ideal conductivity of the ohmic contacts and of the quasi–neutral regions.

We also report the electrical characteristic of other sample groups–Osram, Philips and Seoul. Among these groups, the result reveals that, as shown in Figure IV.14 and Figure IV.15, the samples coming from Philips present a good similarity with the characteristics from manufacturer datasheets that means good binning devices. On the other hand, the samples from Osram exhibit two different devices characteristic depicted in Figure IV.16 and Figure IV.17. The samples from Seoul show the existence of a moderate deviation range among the devices in both high–injected current and low–injected current as illustrated in Figure IV.18 and Figure IV.19, respectively. The binning quality of these different products can be also

evaluated referring to Table IV.1 – the computed error deviation of I–V characteristic of 16 samples of each LED group, Cree, Osram, Philips and Seoul.

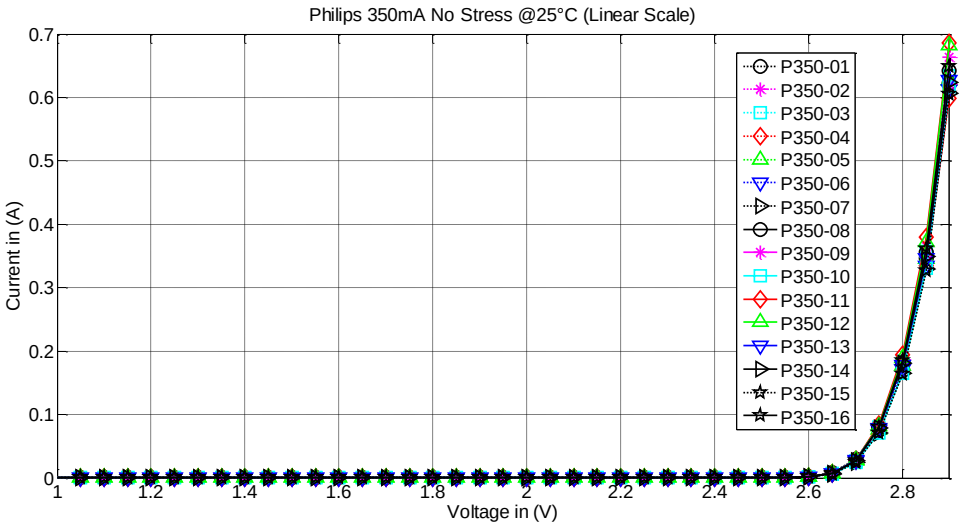

Figure IV.14: I–V characteristic of Philips, linear.

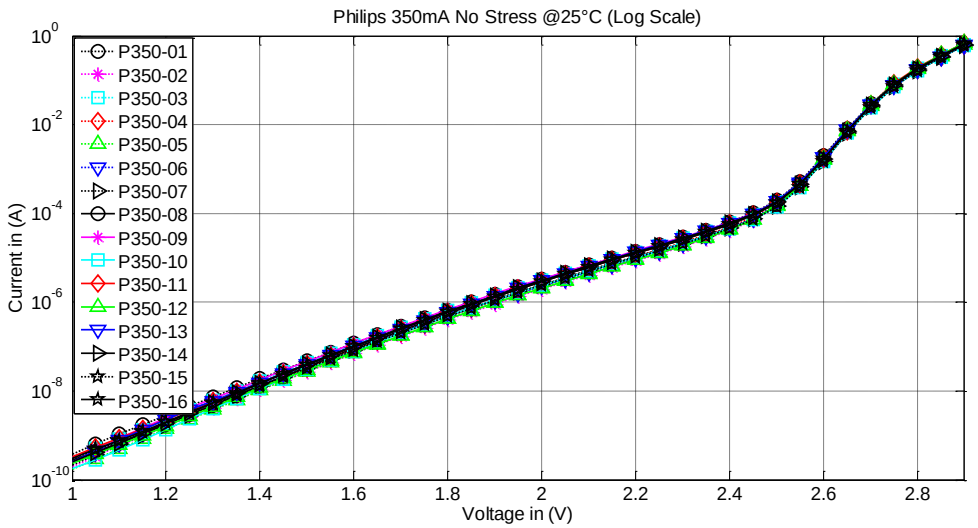

Figure IV.15: I–V characteristic of Philips, semi–log scale.

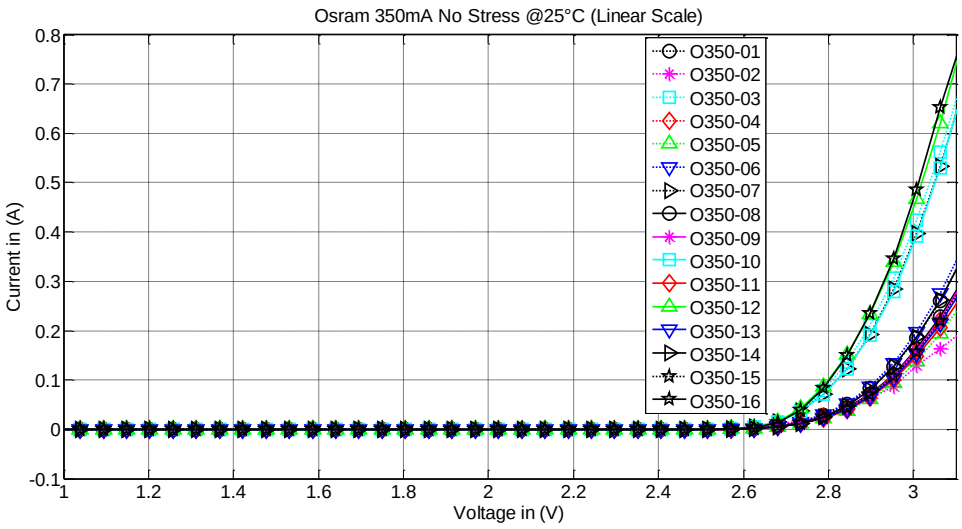

Figure IV.16: I–V characteristic of Osram, linear scale.

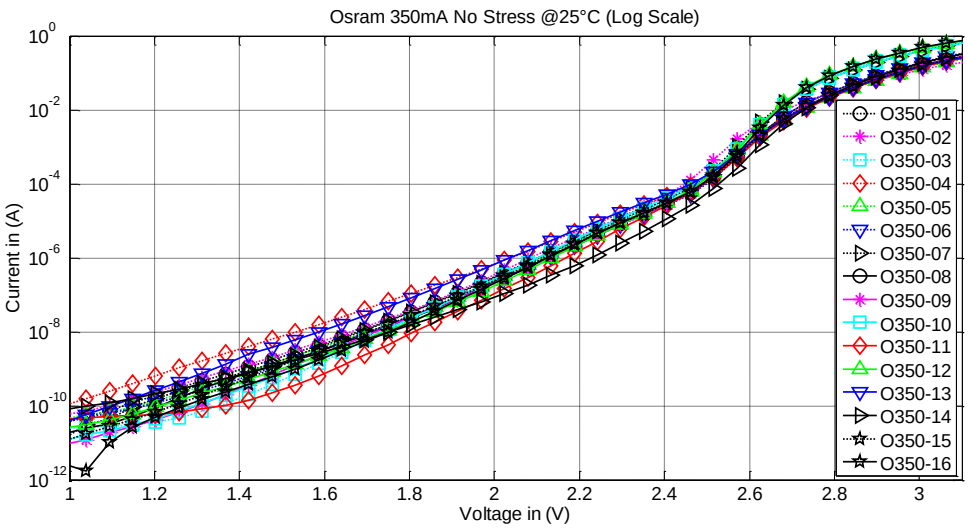

Figure IV.17: I–V characteristic of Osram, semi–log scale.

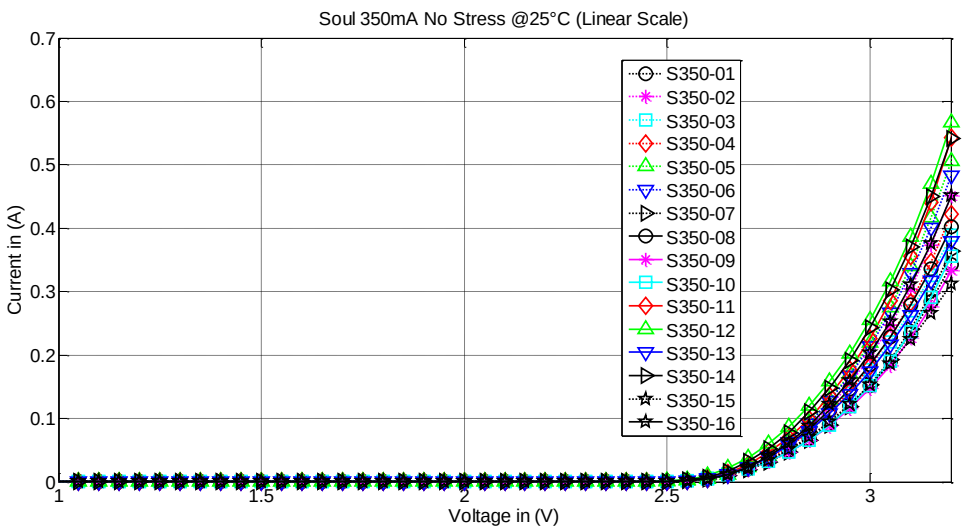

Figure IV.18: I–V characteristic of Seoul, linear scale.

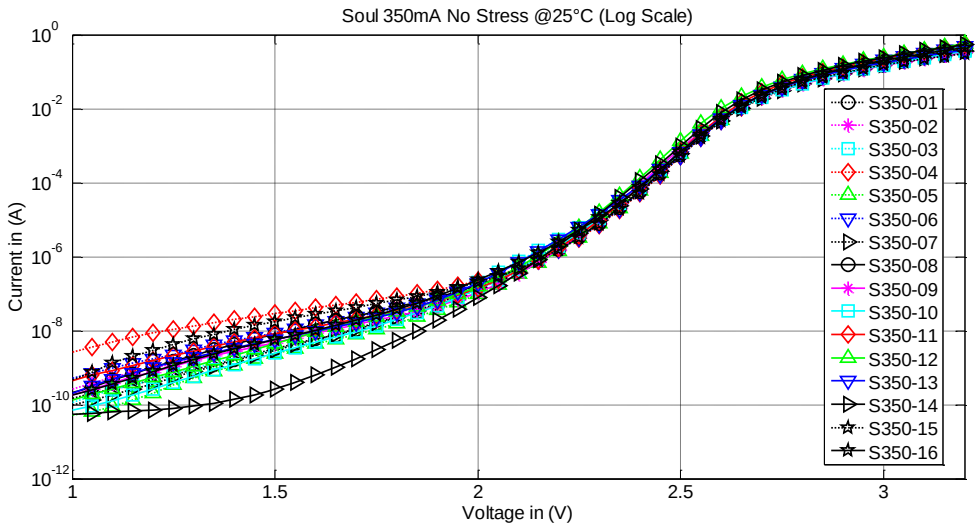

Figure IV.19: I–V characteristic of Seoul, semi–log scale.

4.4. ELECTRICAL FAILURE SIGNATURES

The detailed characteristics of initial state of each LED group are reported in the above section. They are the main starting point used as a refer-ence for the analysis of device degradation before submitting a sequential period of stress time.

In this section, we will demonstrate the main behaviors and the main degradation mechanisms of the tested devices used in the study. In the aging study of LEDs related to their aging process, there are two main methods that have been used to evaluate the characteristic gradual changes of its performance after the stress conditions. Those methods include what we call the "primary method" of evaluation based on measurements data including electrical and optical characterizations and the another method namely "secondary method" of evaluation based on the observation of its structural and chemical characterizations by the aid of microscopic scanning equipment such as Scanning Electron Microscope (SEM), Energy Dispersive X–Ray (EDX) Spectros-copy, Transmission Electron Microscope (TEM), Electron Beam Induced Current (EBIC) or Electron Beam Induced Voltage (EBIV) etc. In this study, we mainly focus on the first aforementioned method for the degradation mechanism evalu-ation of the devices and the relevant measurement data are reported as the fol-lowing sections. However, due to the different behavior in response to the deg-radation process of the four different LED types, we found that, within the stress time of the study up

to 2160 hours, some of the devices have exhibited an insignificant degradation characteristic with a very slight modification that make some difficulties to distinguish the degradation modification from the ac-curacy of the measurement tools or a small error during measurement setup.

There are many researchers who have studied on degradation mechanisms of LEDs [76]–[82], and it is revealed that electrical characteristics are one of the main indicators in evaluation the degradation of light emitting diodes. It can specially reflect the defect of LEDs at chip level and also indicate the variation of ohmic contact at the p–side. In this section, we also indicate the various electrical characteristics of tested LEDs and provide the conclusion on the causes of degradation mechanisms.

The electrical aging characteristics of LEDs are mainly investigated at different operation zones, as reported in section 4.3, in order to evaluate the degradation site of LEDs when they are subjected to the stress conditions. The I–V characteristics of reverse bias and low injected current can figure out defects produced in the active region while the I–V characteristic of the high–injected current shows the effects of the stress on the degradation of the ohmic contacts, p–type regions and other parts of LEDs.

4.4.1. Electrical Aging Characteristic of Cree's Devices

The results of the device's I–V characteristic from Cree shown in the Figure IV.20 and Figure IV.21 for the case of low electrical current stress (350mA) and high electrical current stress (1000mA), respectively, reveal that at the zone of high–injected current measurement, the forward voltages of the device are slightly modified along the stress time. In addition, we find that the trend of these changes is the increase of its forward voltage operation. From these results, we can say that there should be a degradation of devices that can be extrapolated to the worsening of their p–type ohmic contact layer that can lead to the increase of series resistance and eventually caused the increase of forward voltage. The increase of series resistance can be interfered to various failure mechanisms such as,

(i) the interaction between magnesium as the acceptor dopant and the hydrogen containing in semiconductor or in the passivation layer which is unavoidable during metal–organic chemical vapor deposition (MOCVD) process where trimethyl–gallium ($Ga(CH_3)_3$) and ammonia (NH_3) which contain hydrogen is used as precursor molecules [83],

(ii) electromigration of metal contacts through the threading dislocations or

(iii) breaking of current spread layer that leads to non–uniformed current distribution.

The increase of parasitic series resistance after subjected to stress can be clarified in the Figure IV.22. In this figure, the series resistances at high–injected current level of unstressed device and stressed device at 2160h, are plotted in the same graph of I–V characteristic. The graph shows that the series resistance is increased after the stress and it is consistent to the increase of forward voltage.

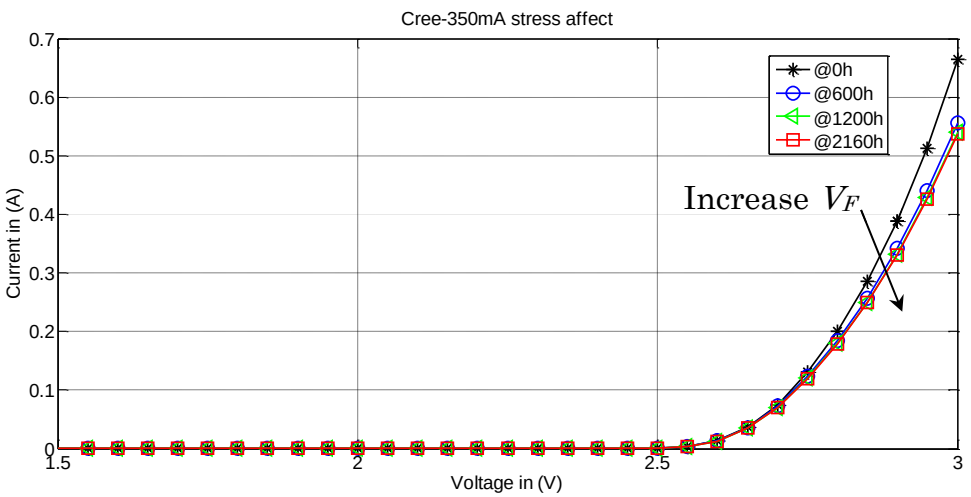

Figure IV.20: Aging I–V characteristic, Cree@stress350mA.

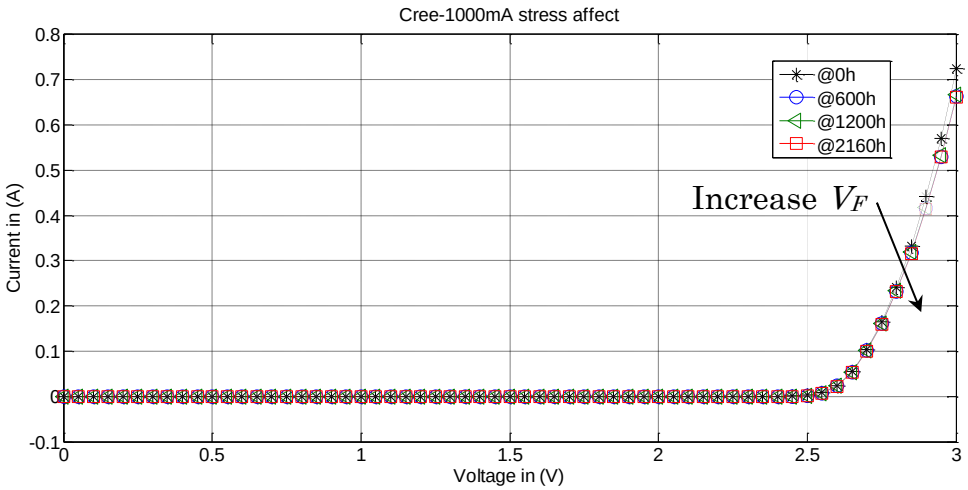

Figure IV.21: Aging I–V characteristic, Cree@stres1000mA.

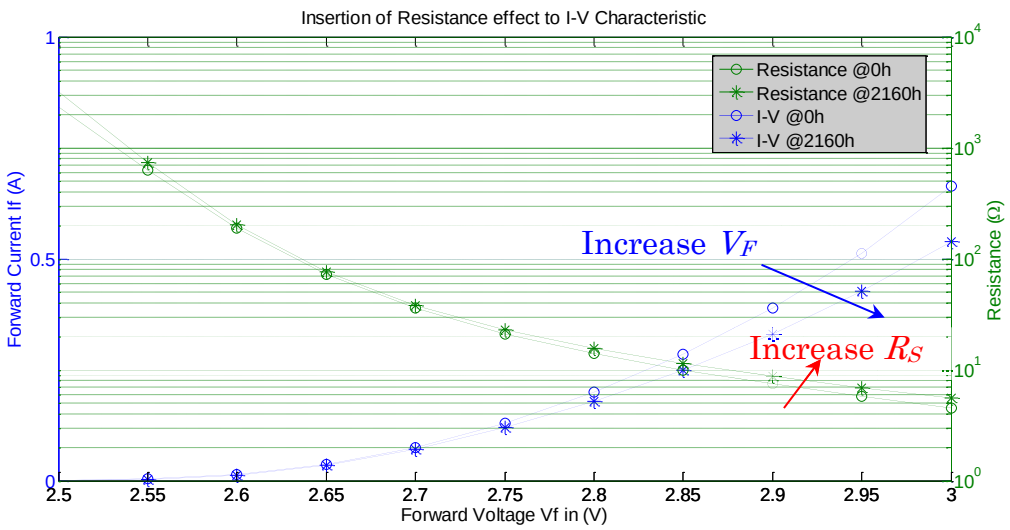

Figure IV.22: Effect of series resistance RS after stress (Cree@stress350mA).

The results of I–V characteristics of the devices under the reverse bias illustrated in Figure IV.23 and Figure IV.24 for low current stress (350mA) and high current stress (1000mA), respectively, show that the reverse currents are slightly decrease with the stress time. This can conclude that, after subjected to a period of stress, the devices have increased their parallel parasitic effects (figure IV.31). In the previous chapters, we have seen that junction degradation (like diffusion…) will induce junction leakage current symbolized by a decrease of R_P that drive, among others things, to a drop of the efficiency. In our case, the increase of the parallel resistance R_P indicates that the efficiency seems to be enhanced for Cree LED groups. We need further investigation to explain this phenomenon.

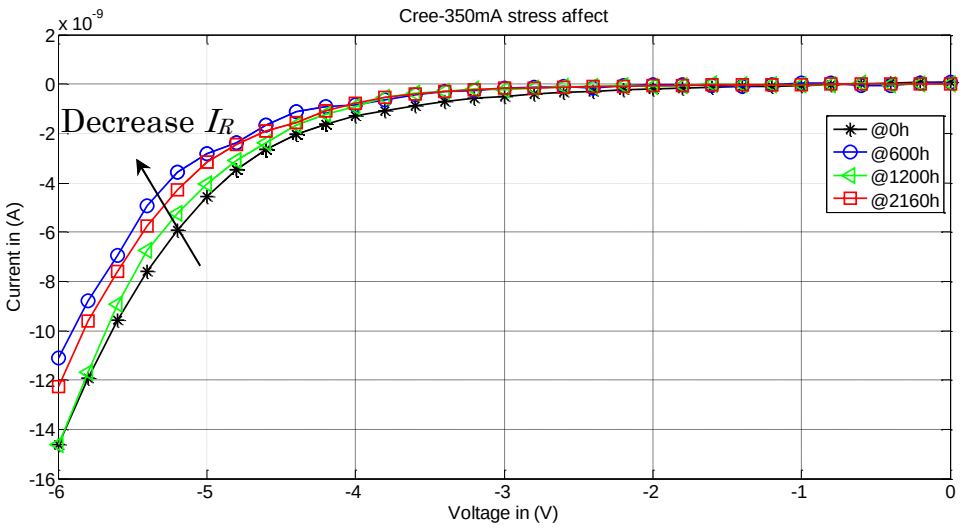

Figure IV.23: Aging reverse bias I−V characteristic (Cree@stress350mA).

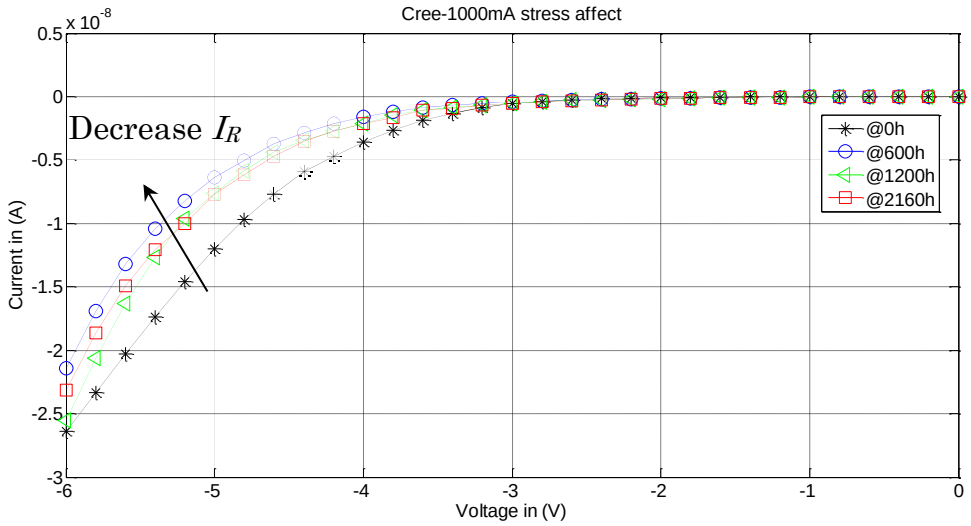

Figure IV.24: Aging reverse bias I−V characteristic (Cree@stress1000mA).

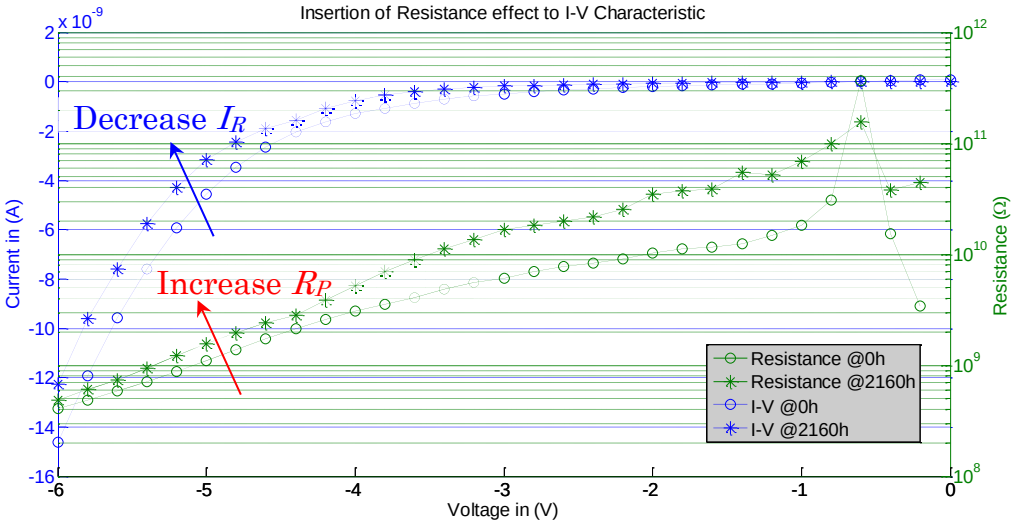

Figure IV.25: Effect of parallel resistance RP after stress (Cree@stress350mA).

4.4.2. Electrical Aging Characteristic of Osram's Devices

In contrast to the characteristics of Cree's devices, the devices coming from Osram show the decrease of their forward voltage along the stress time at high level injected current of I–V characteristic as shown in Figure IV.26 and Figure IV.27 for both low current stress (350mA) and high current stress (1000mA), respectively, and these characteristic are also reported in previous studies such as [77], [78]. The decreasing of the forward voltage of the devices during the aging process can be explained by the possibility of disruption of electrons to the residual complexes magnesium–hydrogen that can release hydrogen from the complexes increasing the Mg acceptor concentration and leading to improving of the ohmic contact of the devices. The enhancement of ohmic contact can be justified by the plot in Figure IV.28 that shows the decrease value of series resistance effect (R_S) after the stress time.

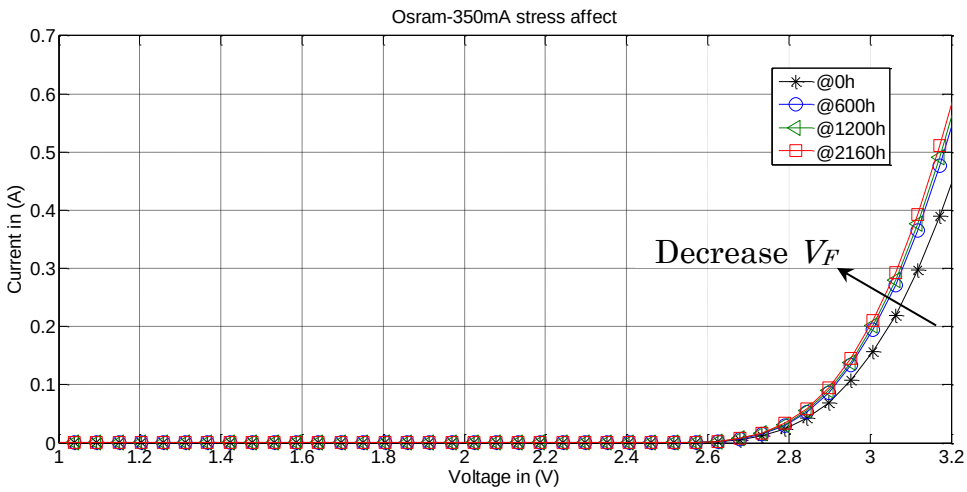

Figure IV.26: Aging I–V characteristic (Osram@stress350mA, linear scale).

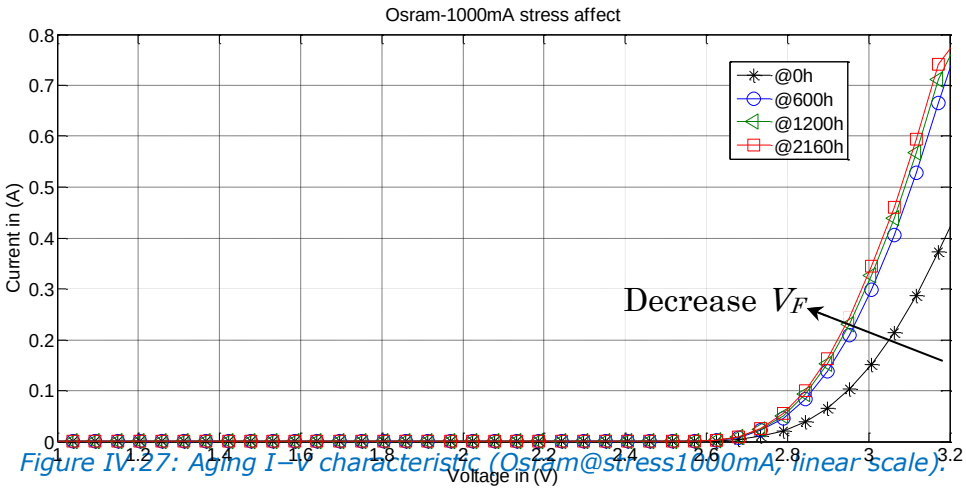

Figure IV.27: Aging I–V characteristic (Osram@stress1000mA, linear scale).

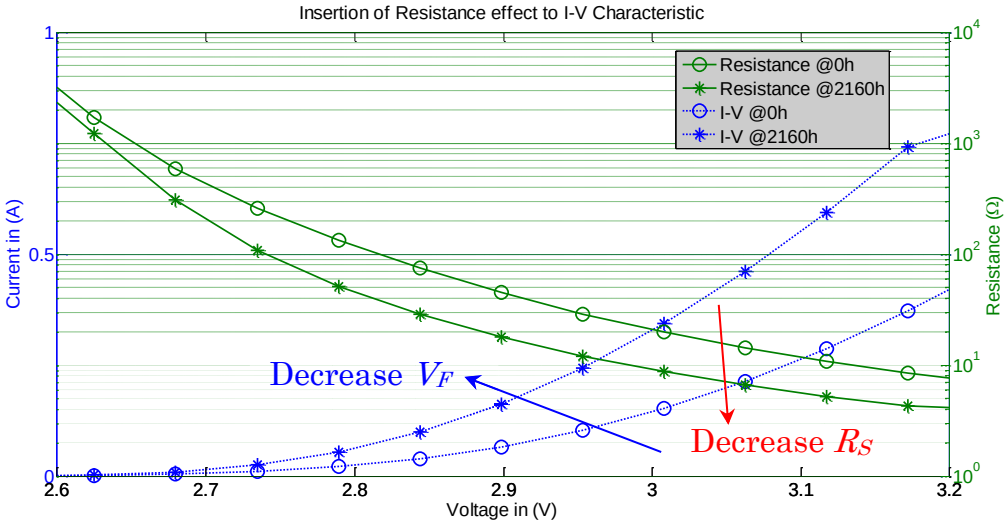

Figure IV.28: Effect of series resistance R_S after stress (Osram@stress1000mA).

However, after the stress, in the zone of low injected currents of I–V characteristics in Figure IV.29 and Figure IV.30 (for low current stress (350mA) and high current stress (1000mA) conditions, respectively), the forward current increases slightly. Furthermore, the increasing rate of forward current of the device under the higher current stress (1000mA) is higher than the one under low current stress (350mA). In the zone I (low injected current level) and after stress, the increasing of current can be due to the creation of point defects or dislocation defects inside the active region of the chip. That can lead to trap more injected charge carriers and then, induce an increase of leakage path of current flow. The increase of leakage path can be also confirmed by the reduction of device's parallel resistance (R_P) as illustrated in the Figure IV.31.

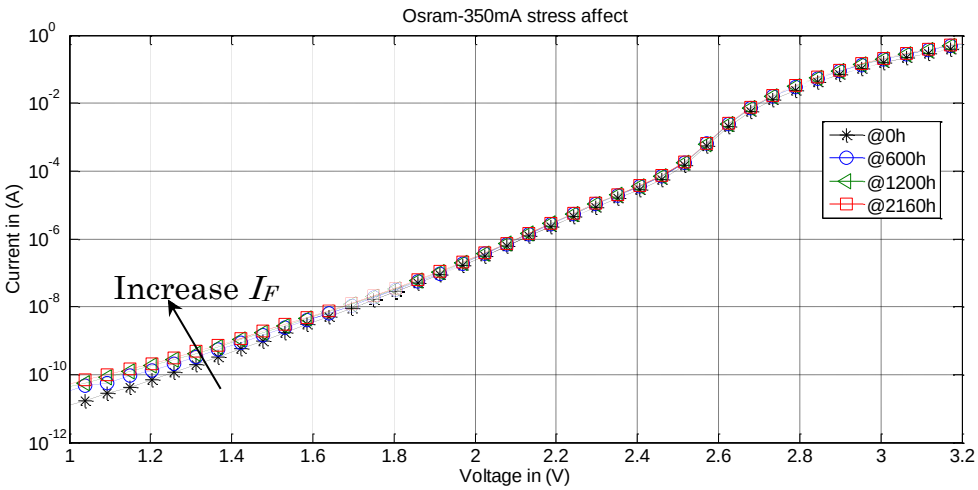

Figure IV.29: Aging I–V characteristic (Osram@stress350mA, semi–log scale).

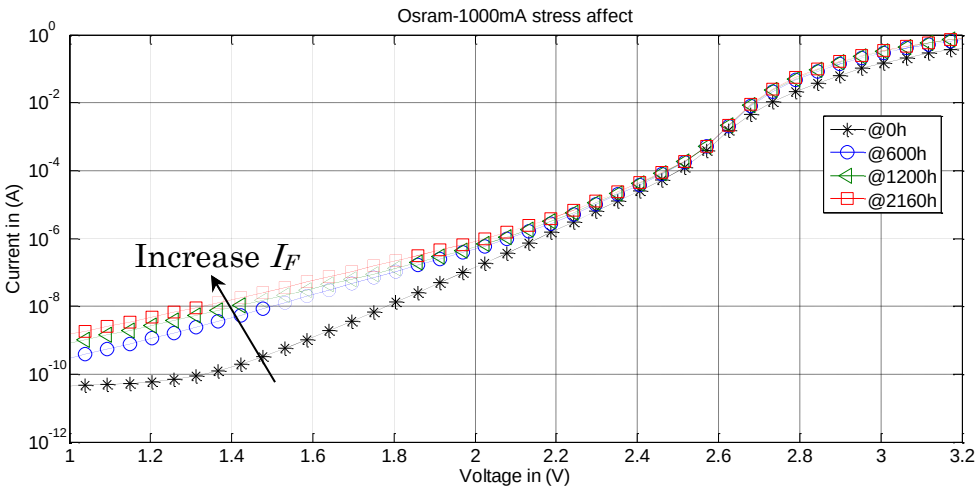

Figure IV.30: Aging I–V characteristic (Osram@stress1000mA, semi–log scale).

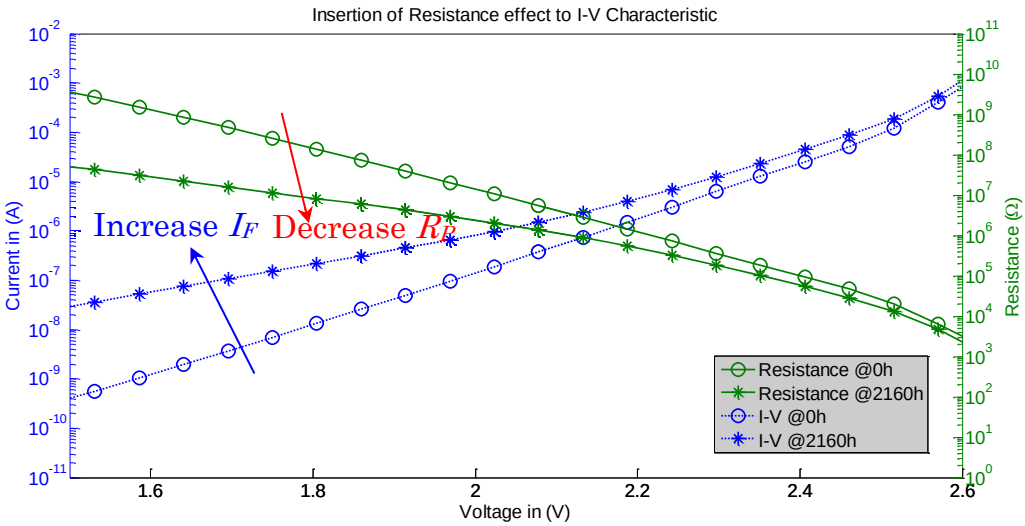

Figure IV.31: Effect of parallel resistance R_P after stress (Osram@stress1000mA).

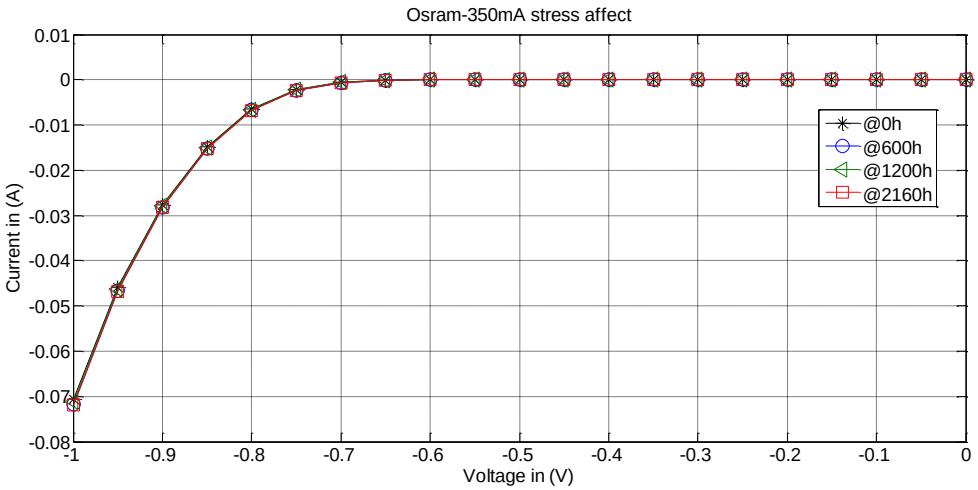

Figure IV.32: Aging reverse bias I–V characteristic (Osram@stress350mA).

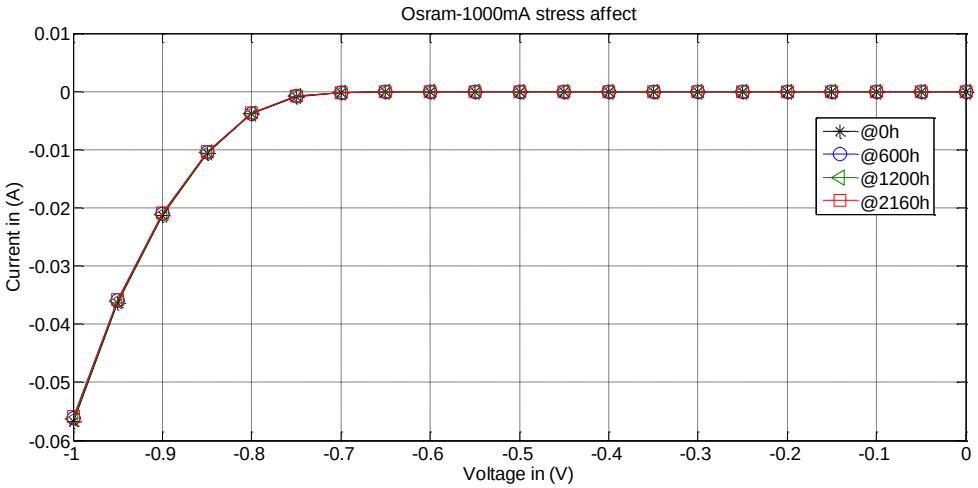

Figure IV.33: Aging reverse bias I–V characteristic (Osram@stres1000mA).

The reverse bias characteristics of the Osram's devices are shown in Figure IV.32 and Figure IV.33 for low current stress (350mA) and high current stress (1000mA), respectively. From the figures, any evolution was unable to be observed during the stress period for both current stress conditions. This is probably due to the reverse protection's component integrated in the devices described previously in section 4.4.

4.4.3. Electrical Aging Characteristic of Philips's Devices

Observing to the results from Philips's devices in Figure IV.34 and Figure IV.35 that are the forward bias I–V characteristics of the devices for low current stress (350mA) and high current stress (1000mA), respectively, it shows that they

have a good stability of their I–V characteristic in the zone III (high–injected current) measured along the stressed time 0h, 600h, 1200h and 2160h. This result can be ascribed to the stable characteristic of devices ohmic contact due to a good optimization of growth or passivation process during devices fabrication. To confirm the good stability of ohmic contact of the device after subjecting to the stress, we compare the series resistance of the unstressed device and the same resistance with stressed during 2160h as shown in Figure IV.36. At the zone III (high–injected current), it shows that the series resistances R_S of the unstressed and stressed device don't exhibit any change during the stressed time.

Meanwhile, they show very stable characteristics of their series resistance effect in the zone III during stress conditions. The result of I–V characteristic at the zone of low injection current (FigureIV.37 and Figure IV.38 for low current stress–350mA and high current stress–1000mA, respectively) and the result of I–V characteristic of reverse bias (Figure IV.39 and Figure IV.40 for low current stress–350mA and high current stress–1000mA, respectively), show a notably increase of injected current along the sequential stressed time. The increase of the injected current can be again attributed to degradation of the devices at their chip level due to the creation of point defects (such as vacancies, interstitial defects, impurity atoms) or dislocation defects inside the active region of the devices that can trap more injected charge carriers or there should be damage parts of devices that can lead to the increase of leakage path of current flow.

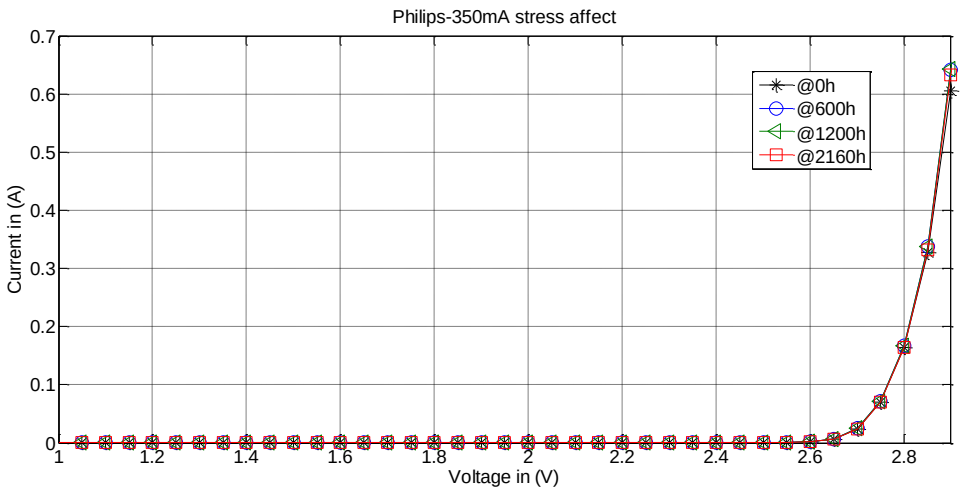

Figure IV.34: Aging I–V characteristic (Philips@stress350mA, linear scale).

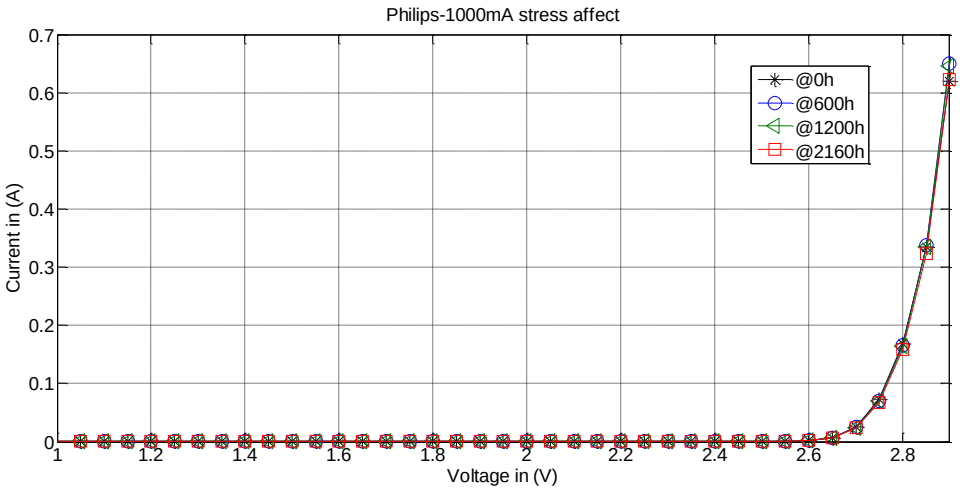

Figure IV.35: Aging I−V characteristic (Philips@stress1000mA, linear scale).

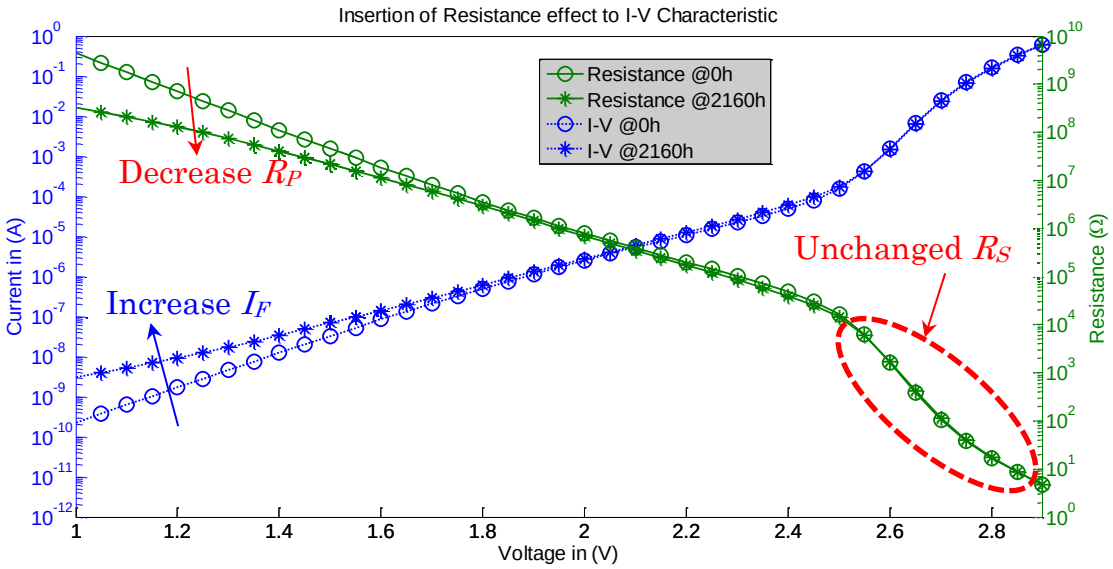

Figure IV.36: Effect of resistance RP and RS after stress (Philips@stress1000mA).

Figure IV.36 (at the zone of low level current) and Figure IV.41, illustrate the effect of decreasing parallel resistance (R_P) of the devices that is correlated to the increase of both forward injected current (I_F) at the zone of low level current (Figure IV.36) and reversed injected current (I_R) (Figure IV.41).

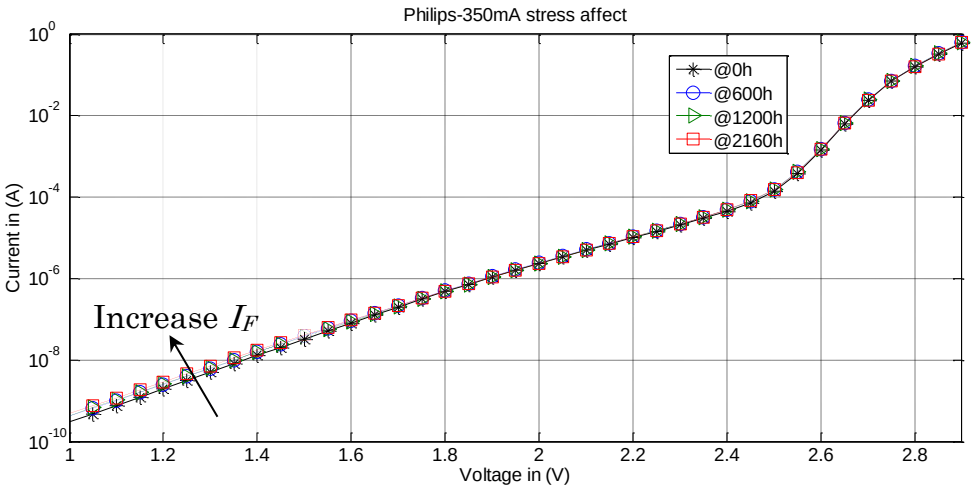

Figure IV.37: Aging I–V characteristic (Philips@stress350mA, semi–log scale).

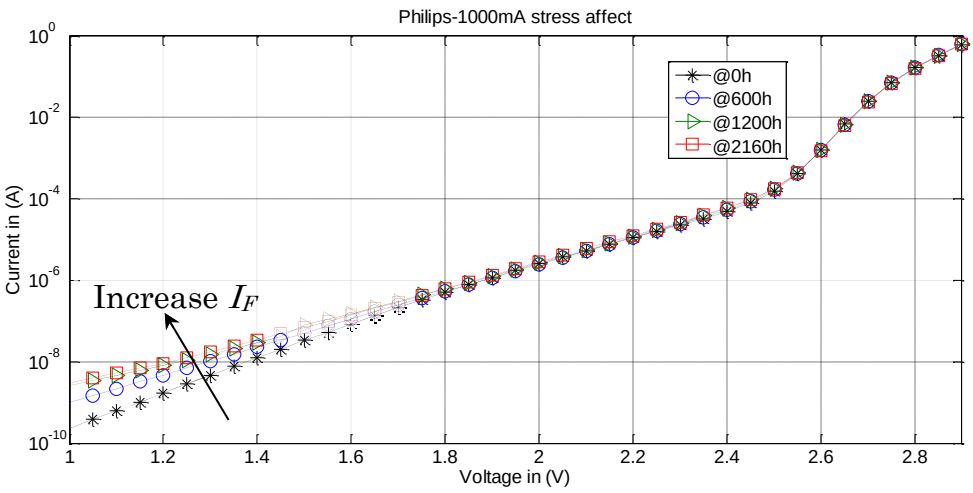

Figure IV.38: Aging I–V characteristic (Philips@stress1000mA, semi–log scale).

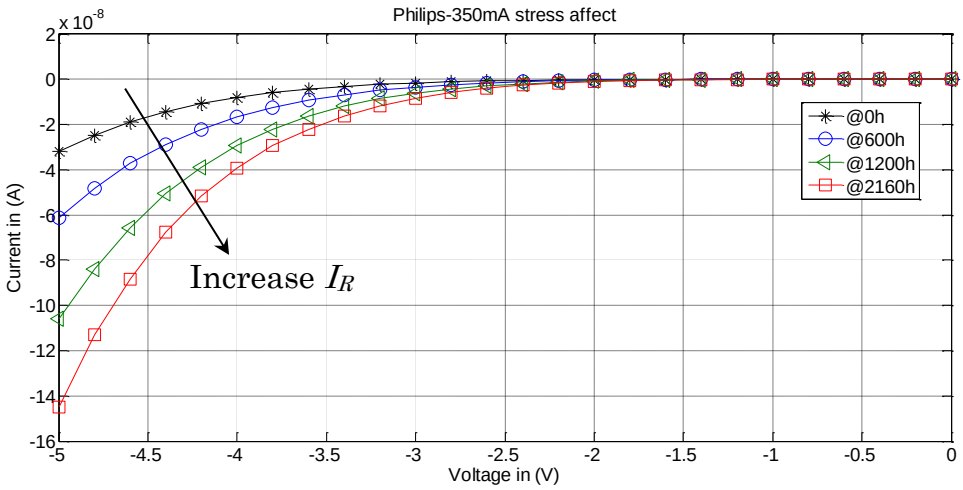

Figure IV.39: Aging reverse bias I–V characteristic (Philips@stress350mA).

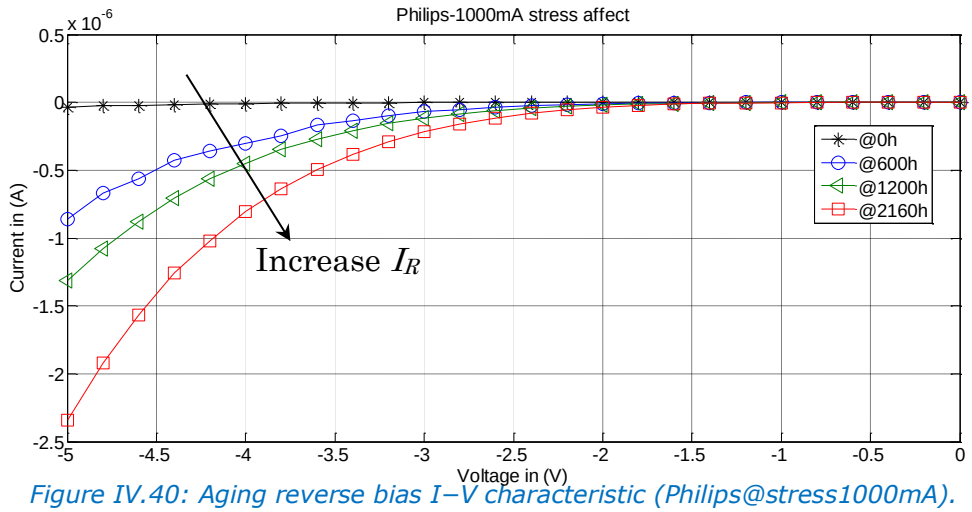

Figure IV.40: Aging reverse bias I–V characteristic (Philips@stress1000mA).

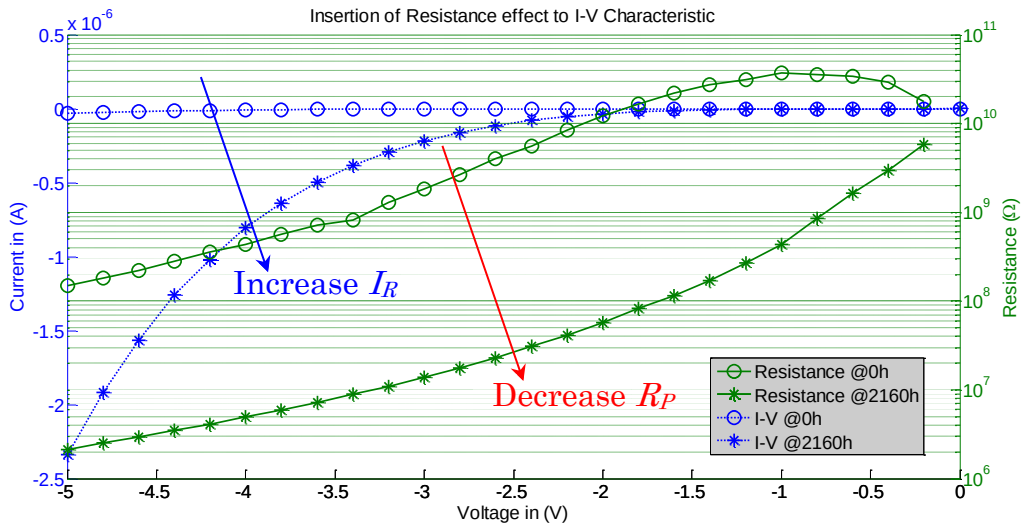

Figure IV.41: Effect of resistance RP after stress (Philips@stress1000mA).

4.4.4. Electrical Aging Characteristic of Seoul's Devices

The electrical aging characteristics of the Seoul Semiconductor devices are slightly differents in terms of degradation rates between the aging characteristics of the devices under low current stress (350mA) and higher current stress (1000mA) for all operation zones of forward bias LEDs as well as reverse bias.

The results reveal that the aging devices under the higher current stress (1000mA) have a slight higher degradation rate than those under the low current stress condition along the stressed time. That can be connected exclusively at the impact of the electrical stress. As shown in Figure IV.42 (I–V characteristic for low

current stress–350mA) and Figure IV.43 (I–V characteristic for high current stress–1000mA), the aging characteristics at zone III show the decrease of forward voltage that is similar to the devices behavior of the Osram group. The cause of this decrease is due to the possibility of disruption of electrons in the residual complexes magnesium–hydrogen that can release hydrogen from the complexes increasing the Mg acceptor concentration and leading to improving the ohmic contact of the devices. This phenomenon has for consequence to reduce the series resistance (R_S) at high level injected current as depicted in Figure IV.44.

The results also reveal that the devices under the low current stress condition (350mA) do not show any effects caused by parallel parasitic resistance along the studied period of stress as indicated by their low injected current measurements (Figure IV.45) and reverse bias measurements (Figure IV.46). Unlikely, the devices under higher stress current (1000mA) exhibit the degradation after subjected to a sequential of stress time with increase of current at their low injected current level and reverse bias. The plot in the Figure IV.47 confirme the increasing of forward current at low injected current level and the increase of reverse current is shown by the plot in Figure IV.48. The increase of injected currents for the both low injected current level and reverse bias are also correlated to their decrease of parallel resistance (R_P) as illustrated in Figure IV.49 and Figure IV.50, respectively.

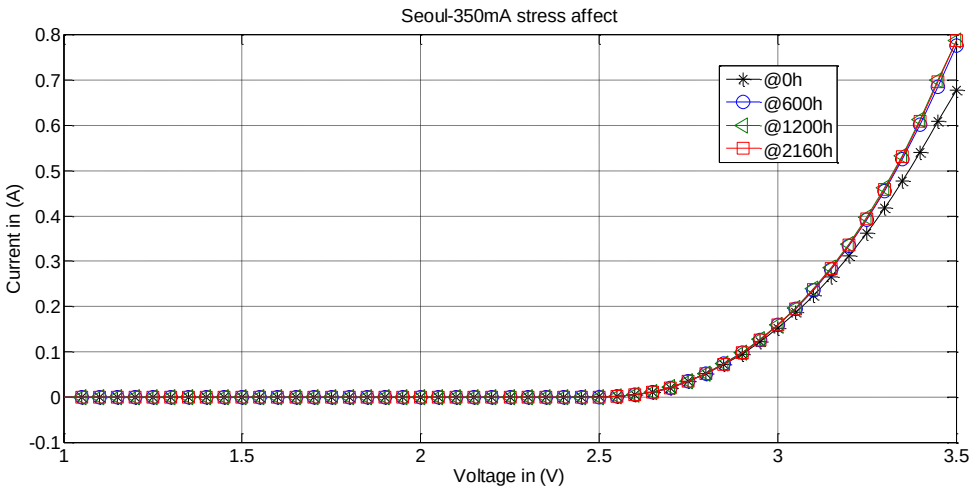

Figure IV.42: Aging I–V characteristic, Seoul@stress350mA, linear scale.

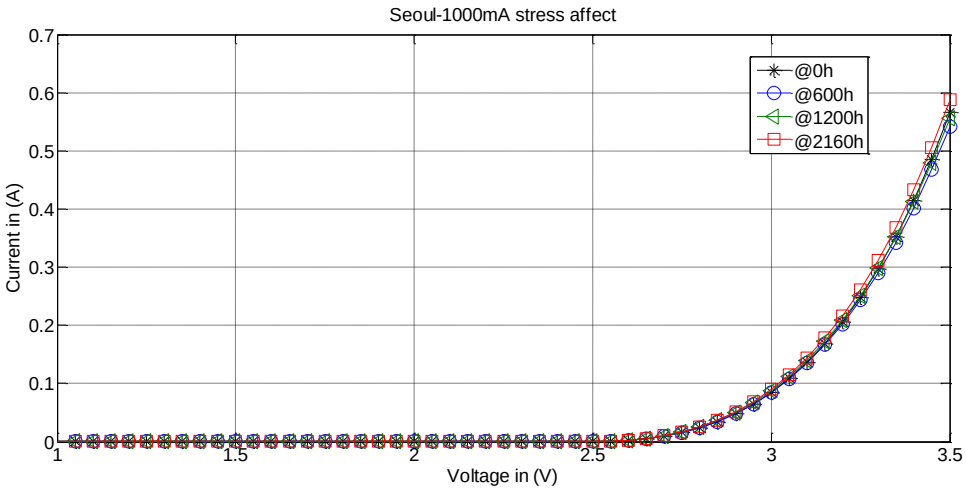

Figure IV.43: Aging I−V characteristic, Seoul@stress1000mA, linear scale.

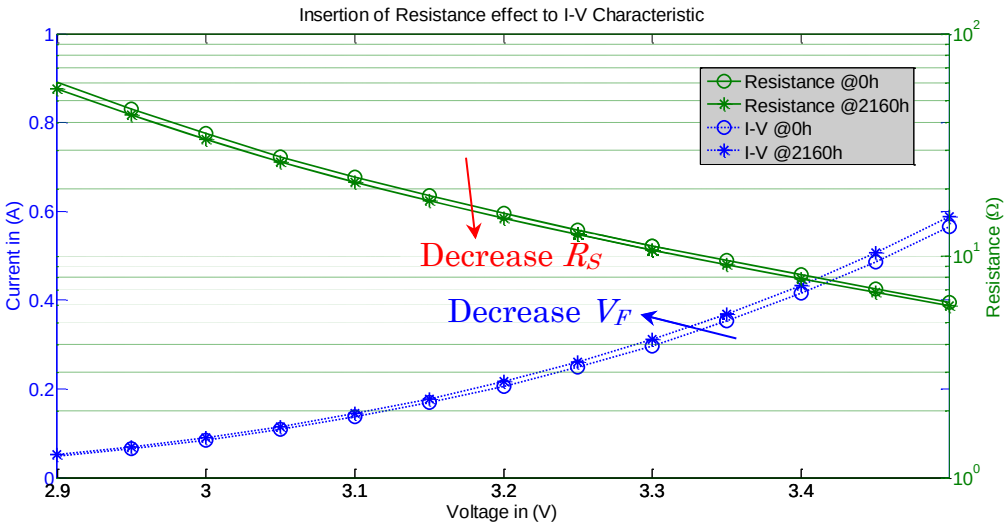

Figure IV.44: Effect of series resistance RS after stress (Seoul@stress1000mA).

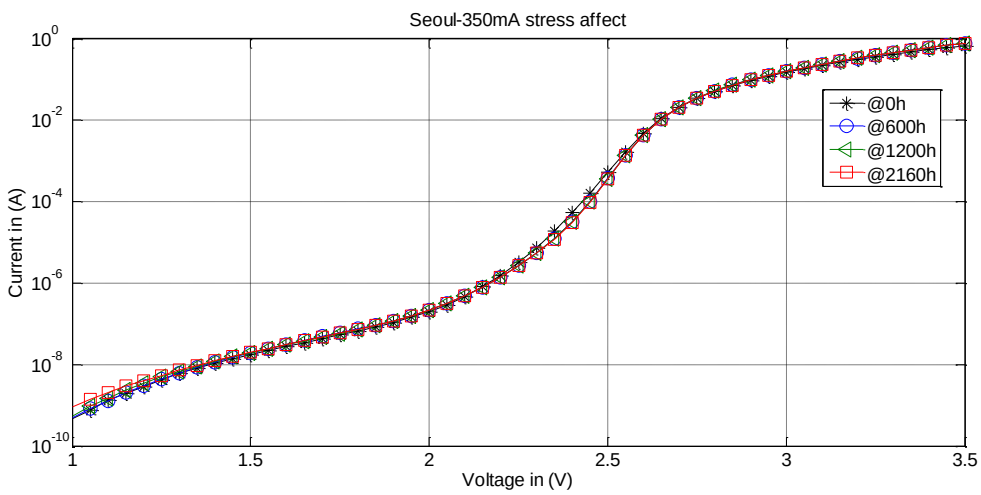

Figure IV.45: Aging I−V characteristic, Seoul@stress350mA, semi−log scale.

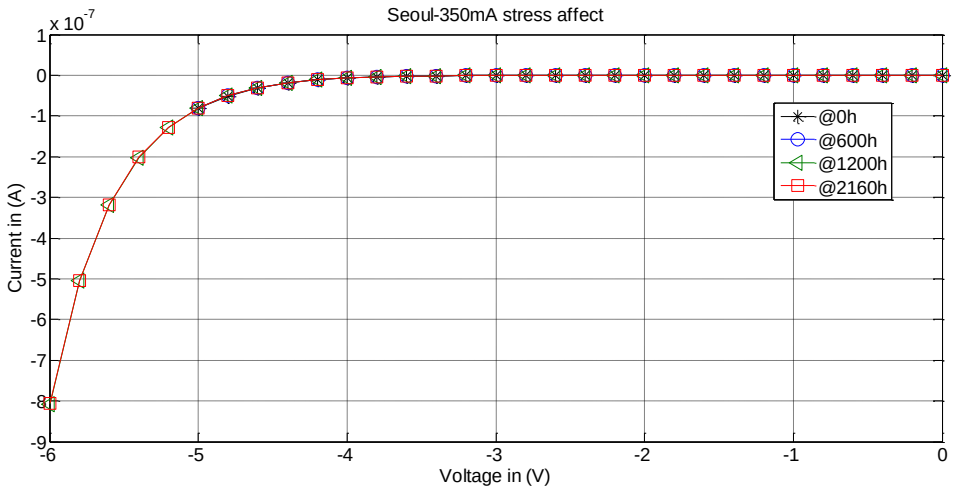

Figure IV.46: Aging reverse bias I−V characteristic, Seoul@stress350mA.

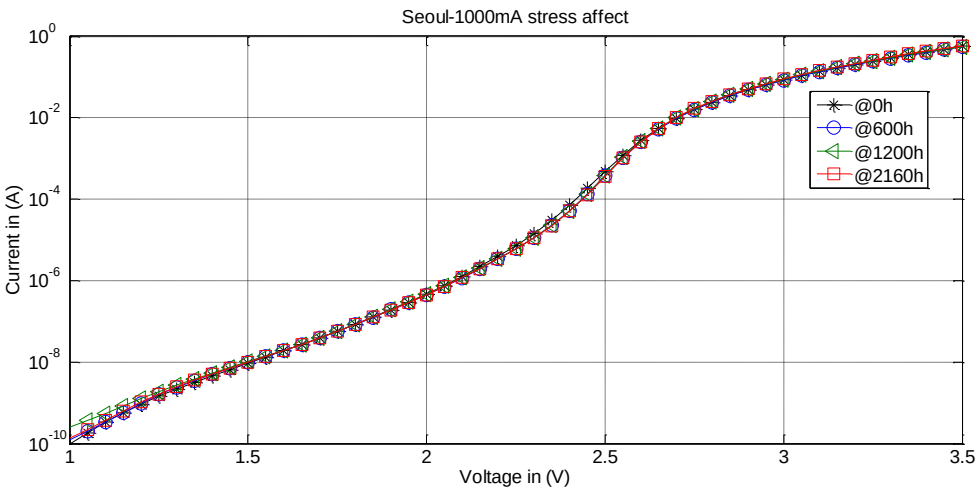

Figure IV.47: Aging I−V characteristic, Seoul@stress1000mA, semi−log scale.

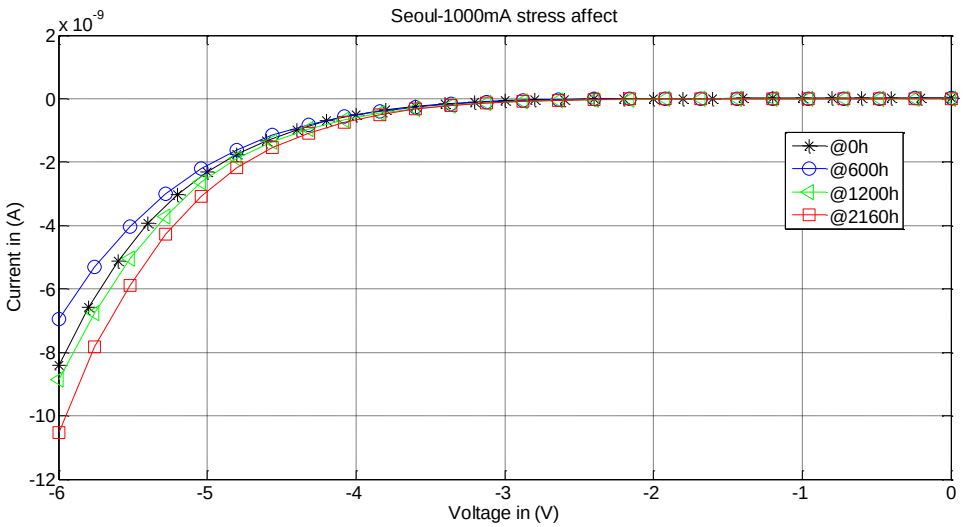

Figure IV.48: Aging reverse bias I−V characteristic, Seoul@stress1000mA.

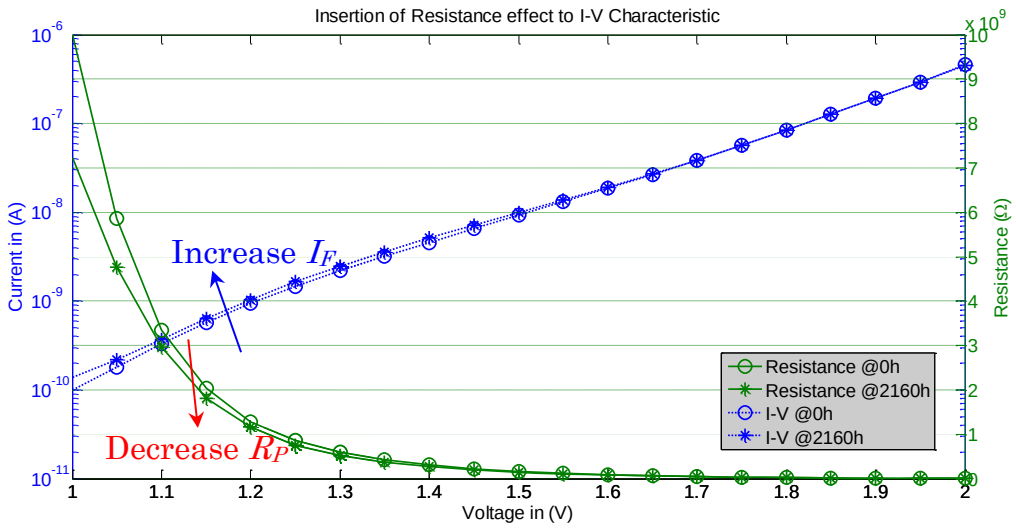

Figure IV.49: Effect of parallel resistance RP after stress (Seoul@stress1000mA).

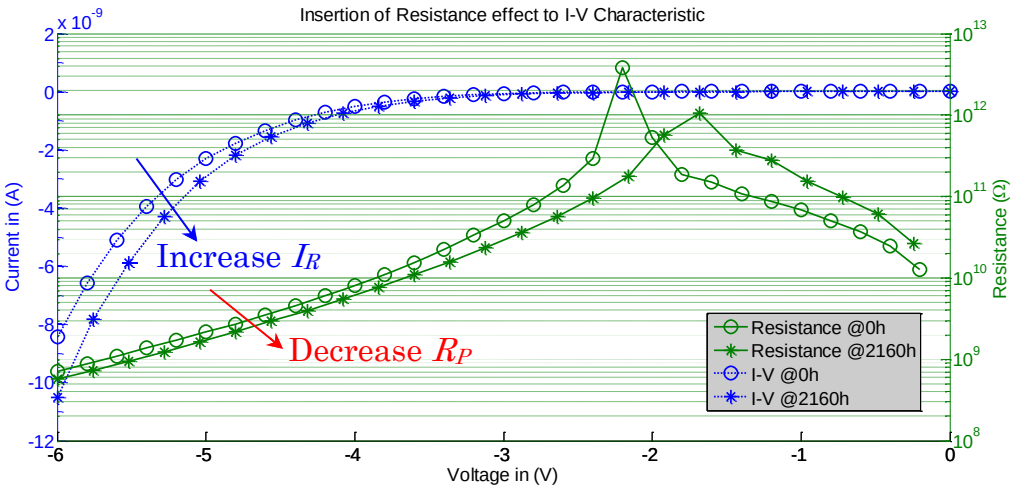

Figure IV.50: Effect of resistance RP after stress (Seoul@stress1000mA).

4.5. OPTICAL FAILURE SIGNATURES

In the previous chapter, we have reported the degradation analysis of High–Power White LEDs (HPW LEDs) inferring from their electrical properties point of view. Likewise, in this chapter, the degradation of the devices has been confirmed by observing their photometric properties. Photometrical characterizations of the devices are also the main primary method that can allow evaluating their failure modes. In this chapter, we firstly report the photometrical properties of each LED group in their initial state. Similar to the studying of their electrical characterizations, the LEDs photometrical properties have been characterized and compared among the large amount of each group of the same manufacturer's

product and also compared across the different products–Cree, Osram, Philips and Seoul Semiconductor. Finally, the photometrical properties of LEDs after being submitted to stresses (thermal and electrical) have been recorded and compared to their initial state in order to figure out the degradation mechanisms.

4.5.1. Initial State of Photometric Characterization

In this section, we report the photometrical characteristics at initial state of LED samples from each group.

In Figure IV.51, Figure IV.52, Figure IV.53 and Figure IV.54, we show respectively Cree, Osram, Philips and Seoul Semiconductor's luminance characteristics measured at various current levels from 100mA to 1000mA with 100mA step. It is shown that the luminance is nearly linear in the range of applied current between 100mA to 1000mA.

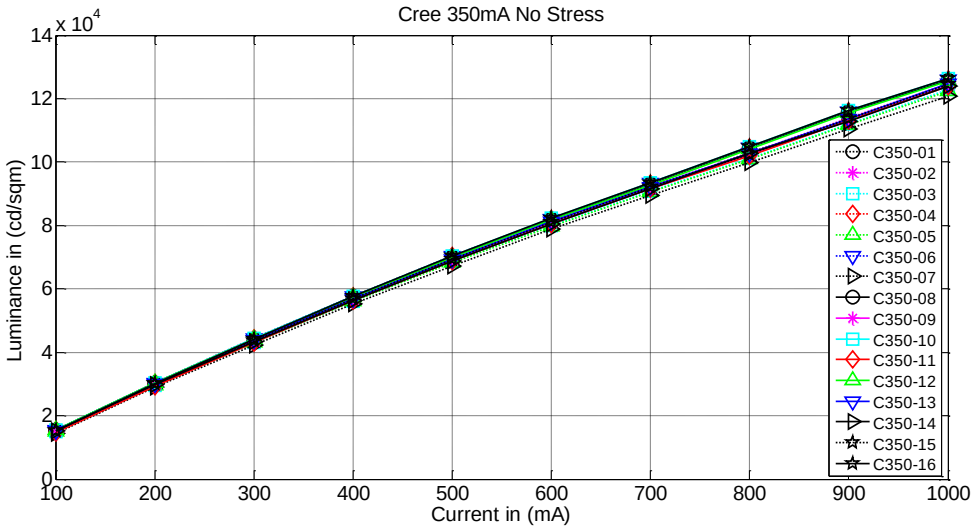

Figure IV.51: L–I characteristic (unstressed Cree@350mA).

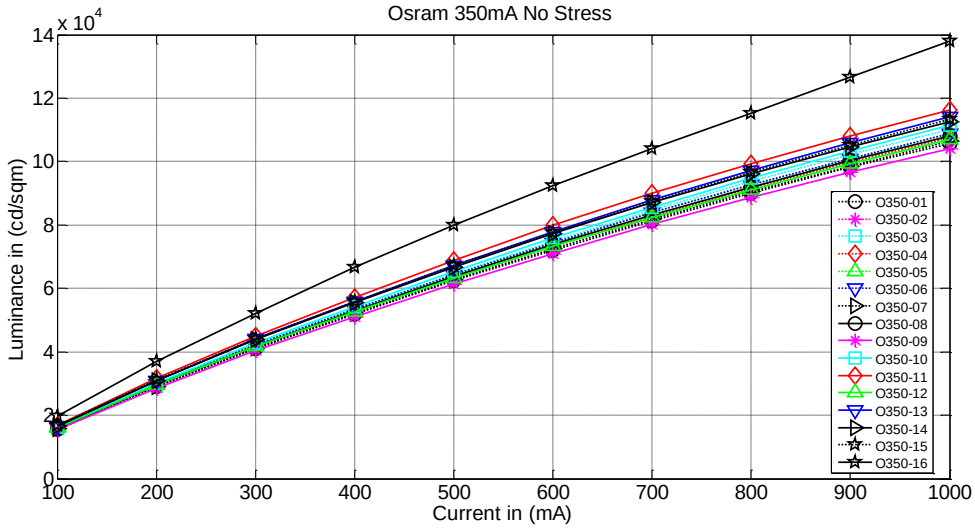

Figure IV.52: L−I characteristic (unstressed Osram@350mA).

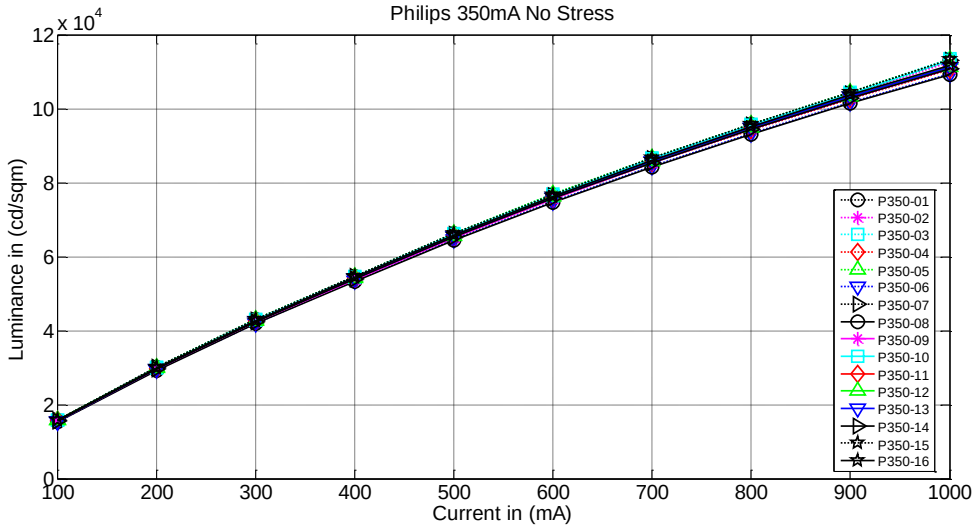

Figure IV.53: L−I characteristic (unstressed Philips@350mA).

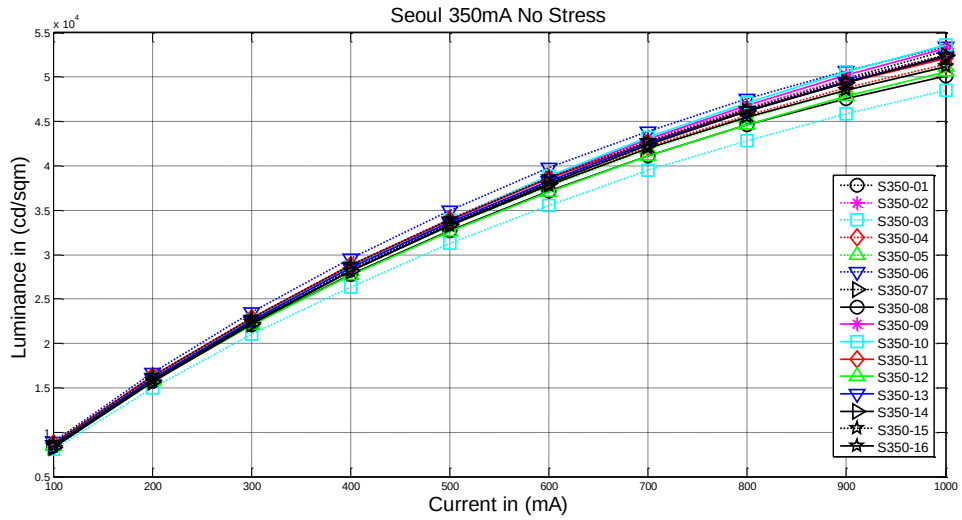

Figure IV.54: L−I characteristic (unstressed Seoul@350mA).

We also report the optical spectrum of each group in Figure IV.55 (Cree), Figure IV.56 (Osram), Figure IV.57 (Philips) and Figure IV.58 (Seoul Semiconductor). The spectrum is measured in the range of visible wavelength 380nm to 780nm with 2 degree of observer.

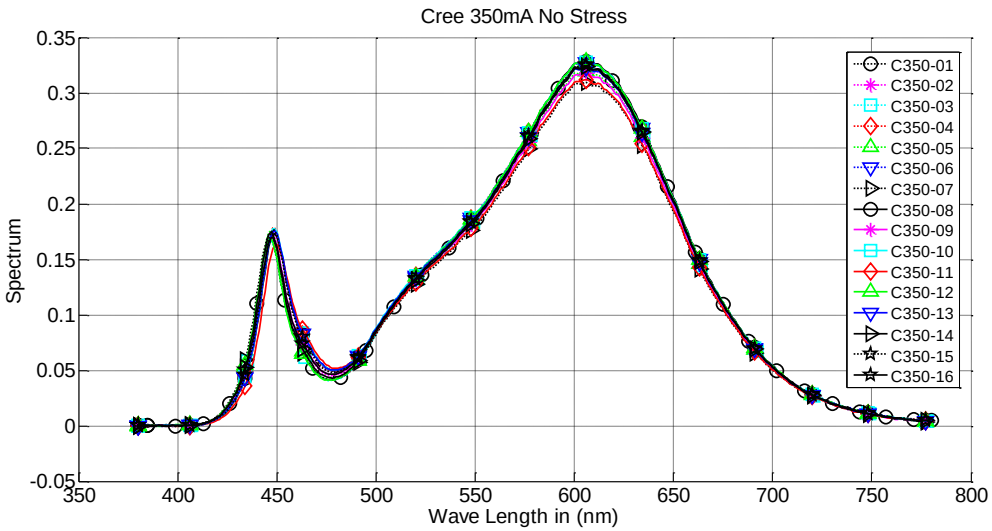

Figure IV.55: Spectrum (unstressed Cree@350mA).

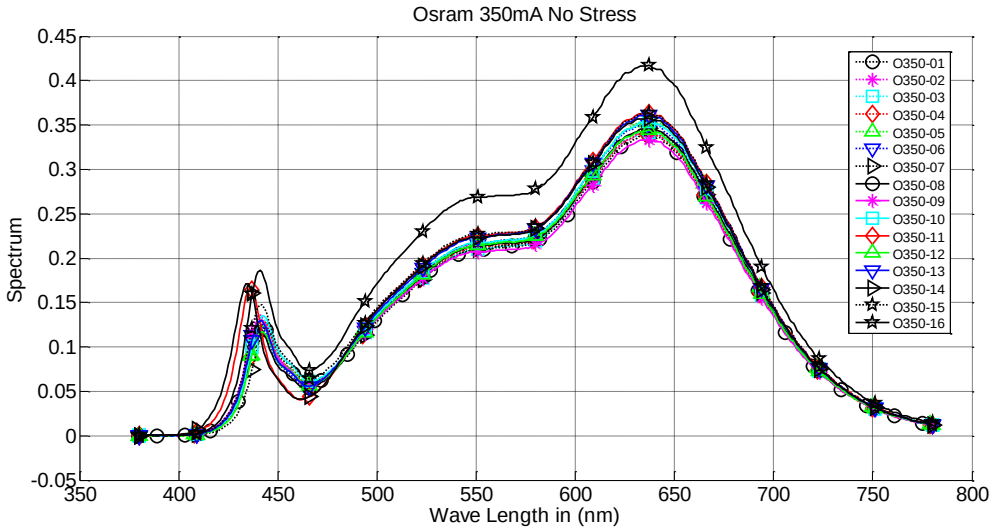

Figure IV.56: Spectrum (unstressed Osram@350mA).

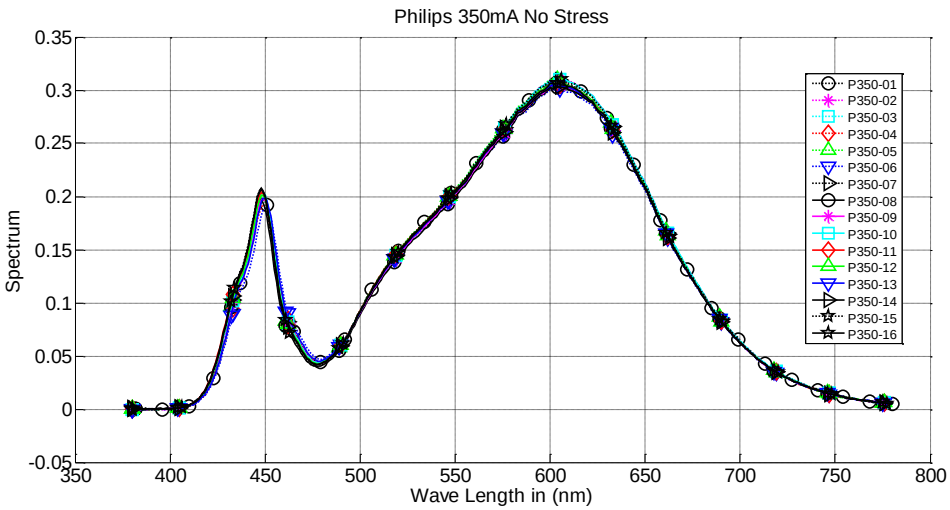

Figure IV.57: Spectrum (unstressed Philips@350mA).

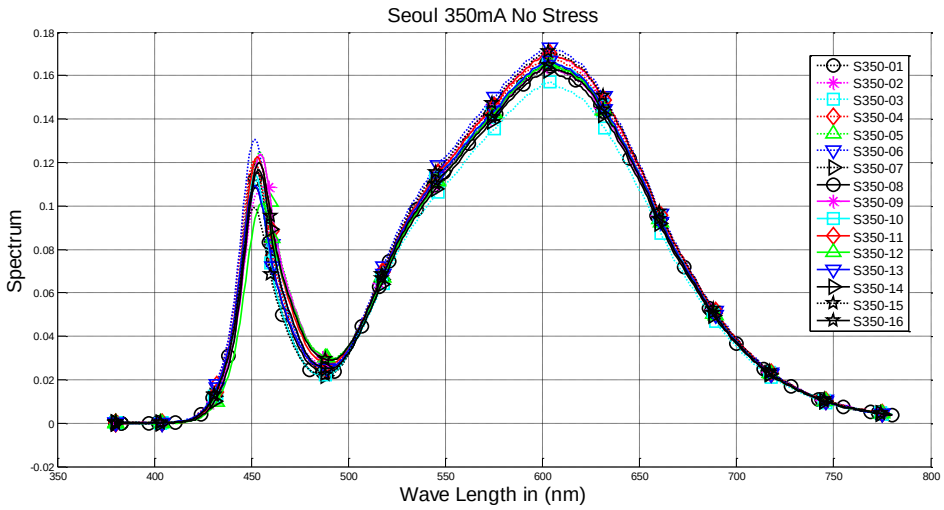

Figure IV.58: Spectrum (unstressed Seoul@350mA).

Similar to the electrical characterization, the photometric characterizations of the LED samples of Cree and Philips groups exhibit only a slight deviation of characteristics among the devices while the samples from Seoul show a bigger range deviation. Samples from Osram have the highest deviation and the variation around the mean value is indicated in Table IV.2. The table shows the error deviation of measured luminance and spectrum of 16 LED samples of each LED group – Cree, Osram, Philips and Seoul. The deviation of each 16 samples is also illustrated by the plot of their average along with their standard deviation bar as depicted in Figure IV.59 to Figure IV.62 for their luminance, respectively for Cree, Osram, Philips and Seoul Semiconductor, and Figure IV.63 to Figure IV.66 for their spectrum in the same order.

Table IV.2: Error of variation of luminance and spectrum of 16 samples each unstressed LED group @350mA.

	Cree	Osram	Philips	Seoul
Luminance @1000mA	1.26%	12.84%	1.26%	2.59%
Spectrum @600nm	1.77%	6.01%	0.96%	2.40%

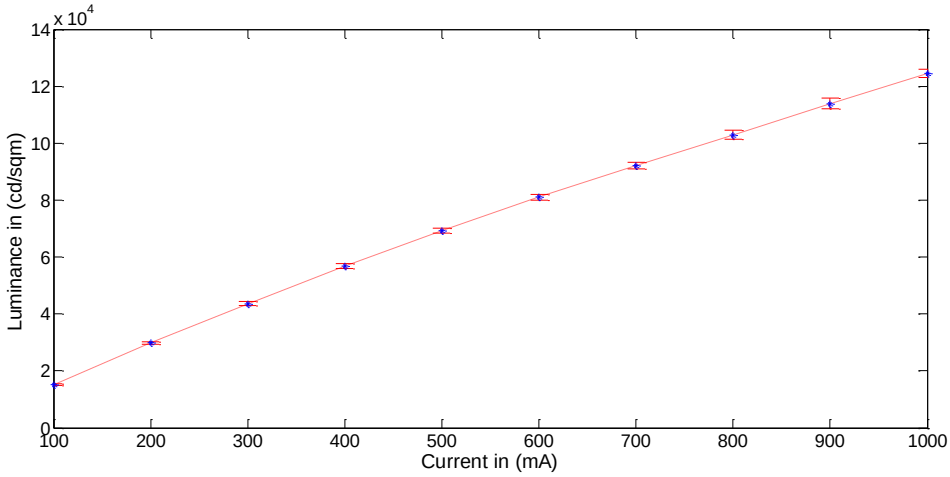

Figure IV.59: Average L–I of 16 samples (unstressed Cree@350mA).

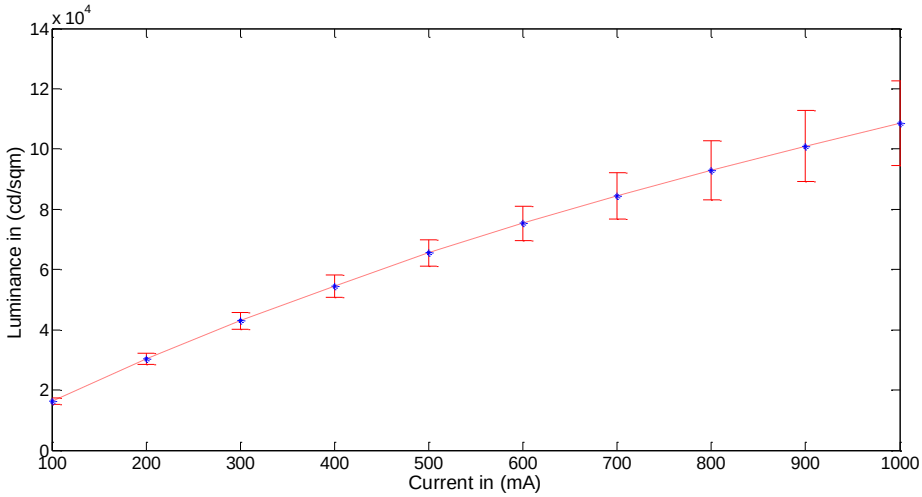

Figure IV.60: Average L–I of 16 samples (unstressed Osram@350mA).

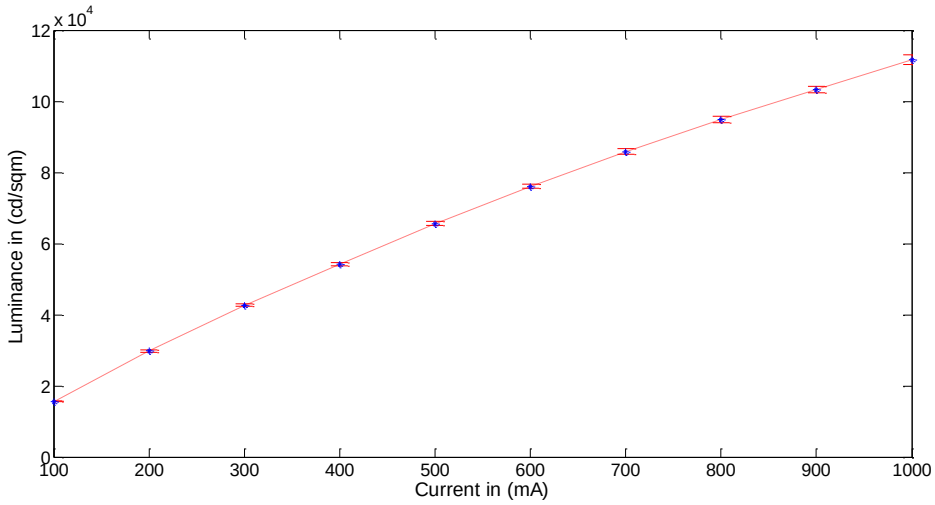

Figure IV.61: Average L–I of 16 samples (unstressed Philips@350mA).

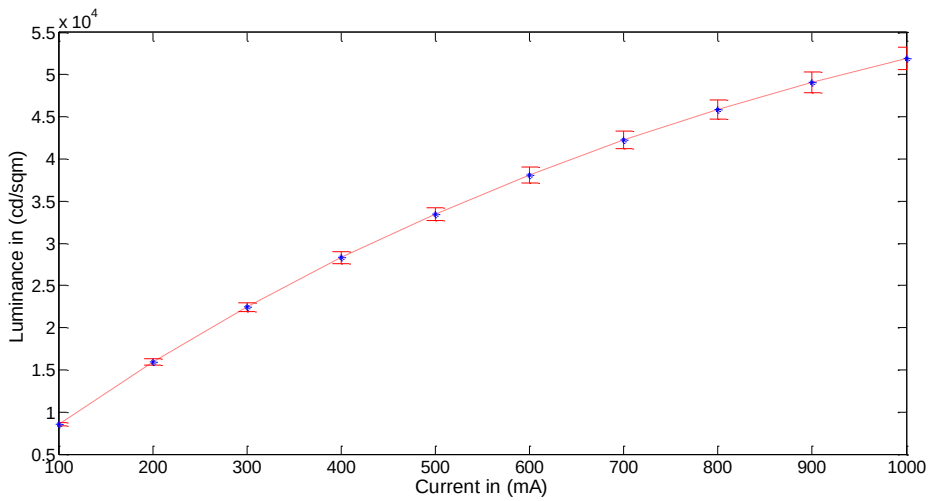

Figure IV.62: Average L–I of 16 samples (unstressed Seoul@350mA).

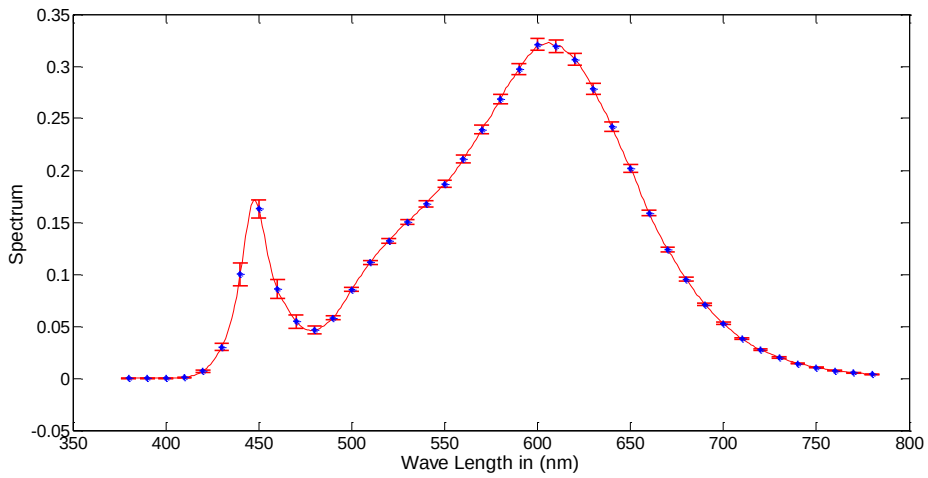

Figure IV.63: Average spectrum of 16 samples (unstressed Cree@350mA).

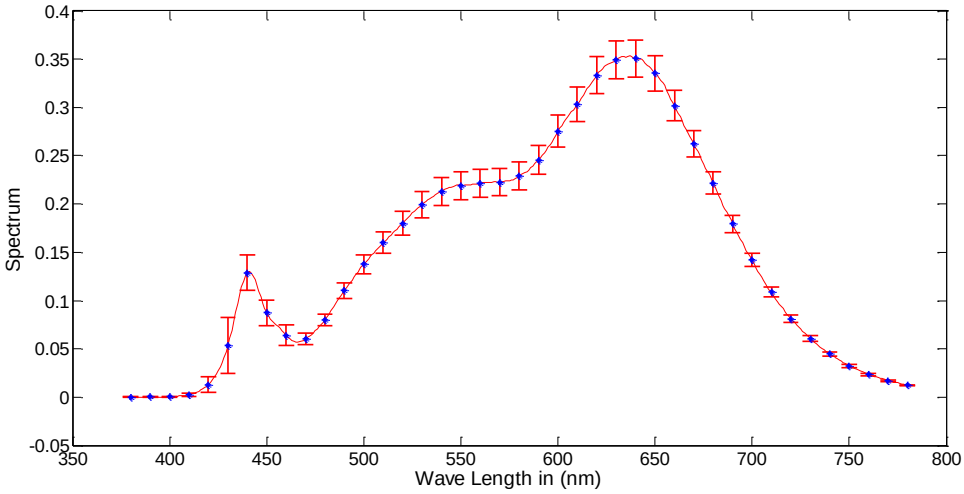

Figure IV.64: Average spectrum of 16 samples (unstressed Osram@350mA).

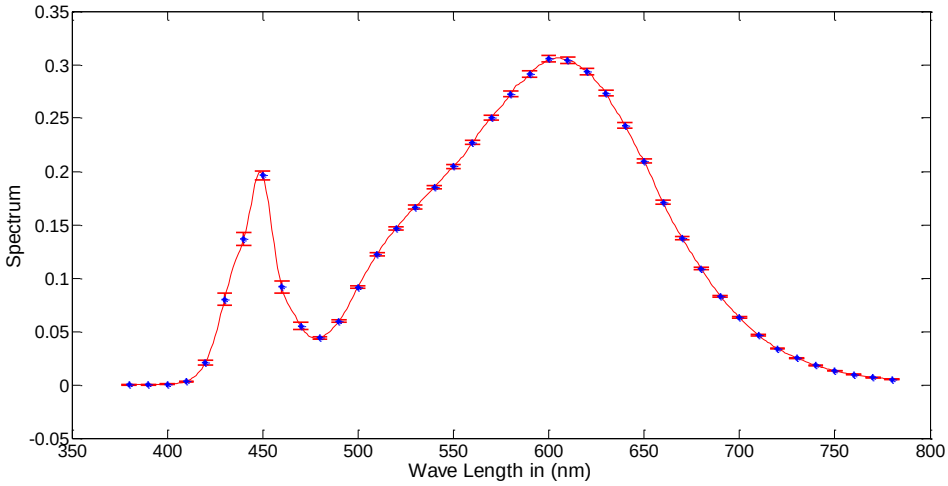

Figure IV.65: Average spectrum of 16 samples (unstressed Philips@350mA).

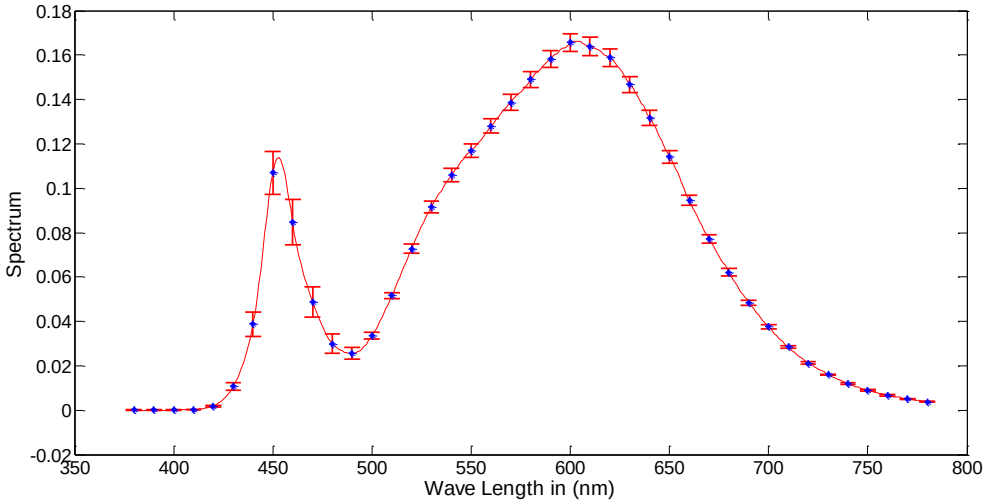

Figure IV.66: Average spectrum of 16 samples (unstressed Seoul@350mA).

Figure IV.67 and Figure IV.68 illustrate the both plots of current vs. luminance and spectrum, respectively, with the four types of LED−Cree, Osram, Philips and Seoul over–plotted on the same charts. The result shows that the product of manufacturers Cree, Philips and Osram nearly have the same level of quality with a slight different level of luminance arranged from the upper to lower order Cree, Philips and Osram. While the products coming from Seoul show a large lowest luminance comparing to the other groups as shown in Figure IV.67, in Figure IV.68, the Cree's device shows the highest peak value of the optical spectrum at yellow–red region and the devices of Osram and Philips have the same peak spectrum level at yellow–red region but the peak spectrum of Osram shifts to further red spectrum than the peak spectrum of Philips. It also shows that the Seoul's device has the lowest peak spectrum at this yellow–red spectrum. Furthermore, observing to the region of blue spectrum (around 450 nm), the two devices from Cree and Philips are nearly the same peak spectrum and much higher than that of devices from Osram and Seoul which also nearly have the same peak spectrum level.

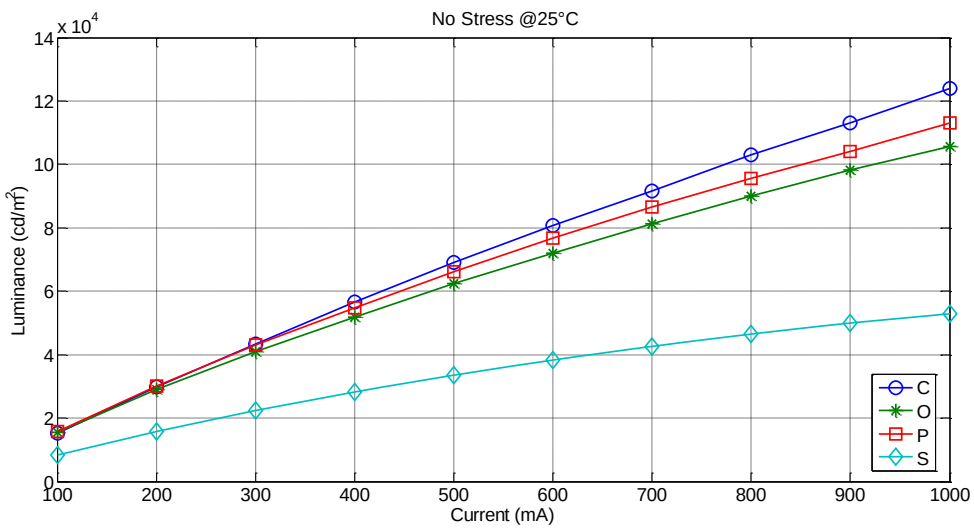

Figure IV.67: L−I characteristic (unstressed COPS LEDs@350mA).

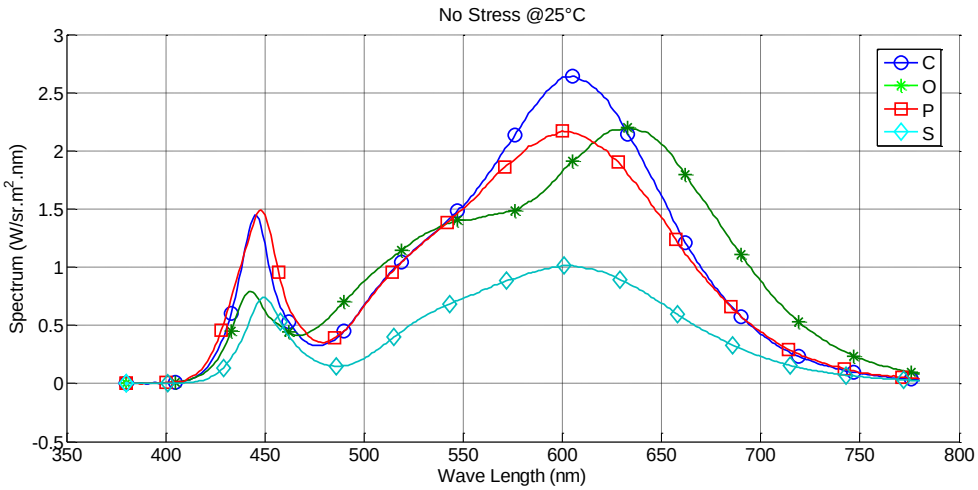

Figure IV.68: Spectrum (unstressed COPS LEDs@350mA).

Another result from the photometrical measurements shows that although the luminance level of these LED groups is quite different specially for Seoul but as shown in Figure IV.69, the chromatic coordinate of all LED groups locate close to each other and very close to the Planckian locus and this is due to all the products are selected as in the same range of correlated color temperature as a warm–white LED.

Figure IV.70 shows the measured value of spectral reflectivity $R_i(\lambda)$ and the value of general color rendering index (CRI) R_a that can be also computed from these $R_i(\lambda)$ for each LED group as in Eq. IV.4.

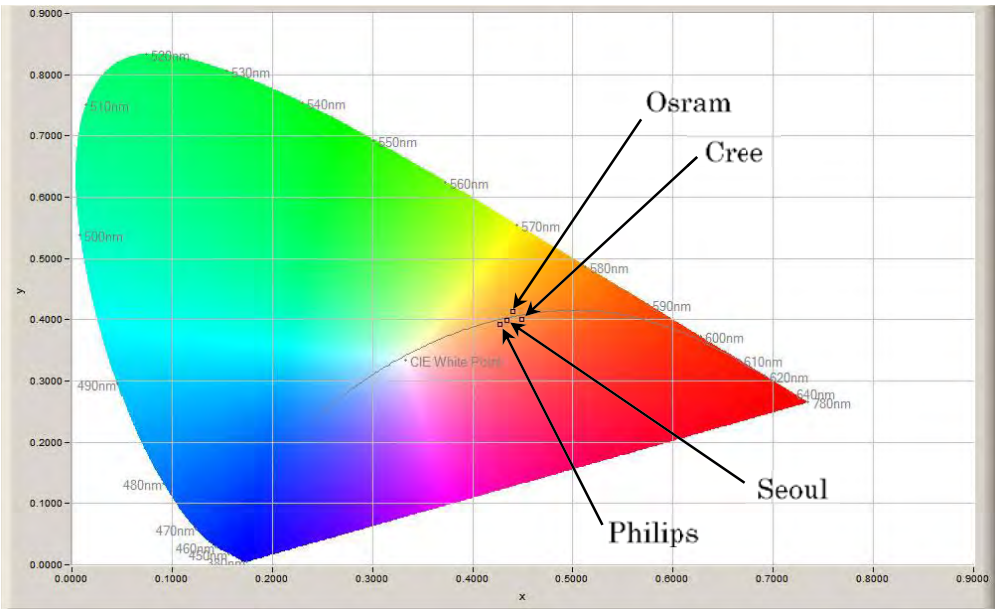

Figure IV.69: Chromaticity (unstressed COPS LEDs).

Figure IV.70: Color rendering index a) Cree, b) Osram, c) Philips and d) Seoul.

$$CRI_{general} = R_a = \frac{1}{8}\sum_{i=1}^{8} R_i \qquad \text{(Eq. IV.4)}$$

The result reveals that the CRI of Osram product has the best render performance with the its color rendering Ra = 96.61 comparing to the other groups– Philips (Ra = 82.87), Cree (Ra = 81.93) and Seoul (Ra = 80.10).

4.5.2. Photometrical Characterizations of LEDs under accelerated aging conditions

The changes of photometrical characteristic data of LED can be affected by all aging modes from the chip, the ohmic contact to the LED packages including phosphor material that is integrated to convert the blue emitted light (around 450 nm) to a white light. So, the photometrical measurements will allow us to identify the degradation of the devices after they undergo stresses. In this chapter, the photometrical characterizations of the devices including the modifications of their luminance, optical spectrum, optical power and chromaticity after they operate 2160 hours have been reported. Again, the photometrical characteristics of stressed

devices have been compared to their initial state in order to evaluate their degradation evolution.

From the result, it is found that the photometrical characterizations of the devices coming from Cree and Philips do not significantly change along the stress period. We can perceive a beginning of a little alteration of these devices' characteristics but not yet enough significant to validate unarguable evolutions for both cases of DC current stress conditions, 350mA and 1000mA as shown in Figure IV.71 to Figure IV.78 (aging luminance or spectrum of Cree and Philips under nominal current, 350mA, or stressed current, 1000mA).

From these results, we can conclude that the package and phosphors layer of the devices are not notably degraded with the stress current or heat generation during the stress time of the study.

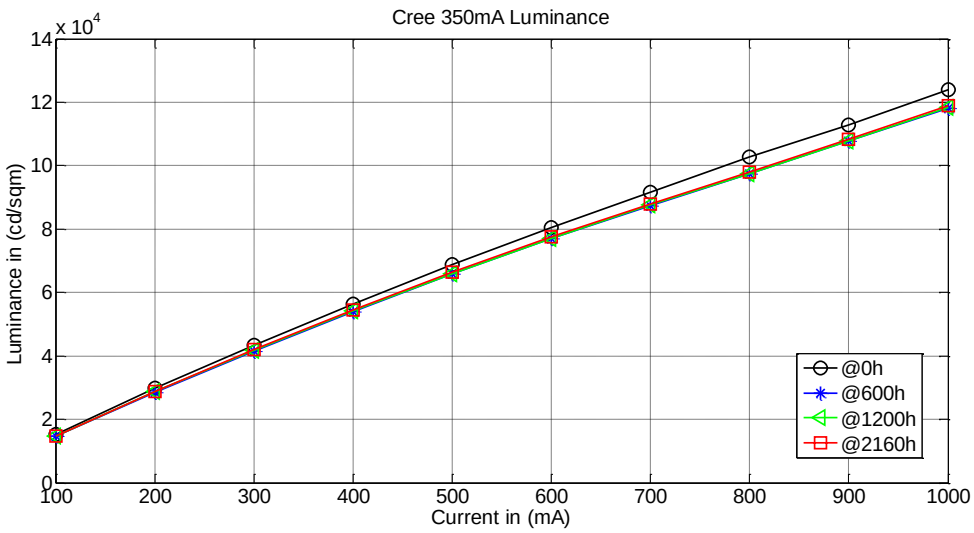

Figure IV.71: Aging luminance (350mA–stressed Cree).

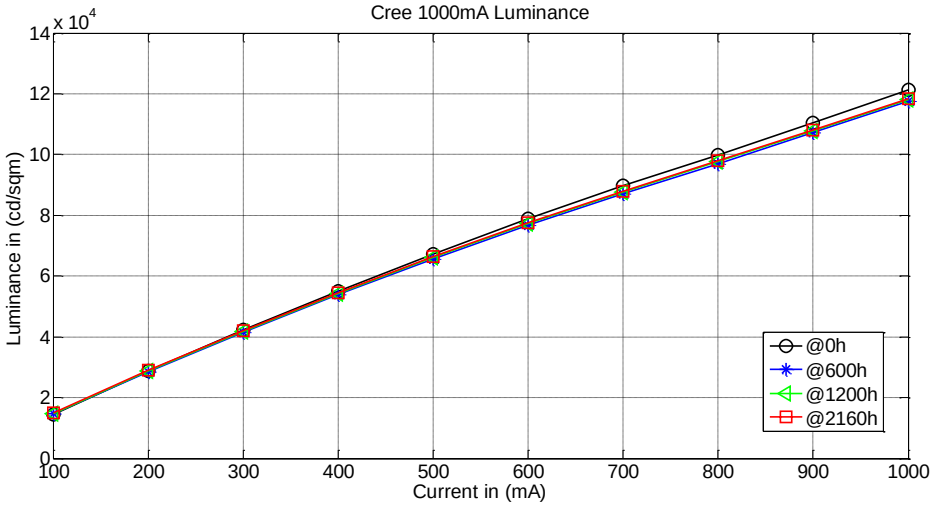

Figure IV.72: Aging luminance (1000mA–stressed Cree).

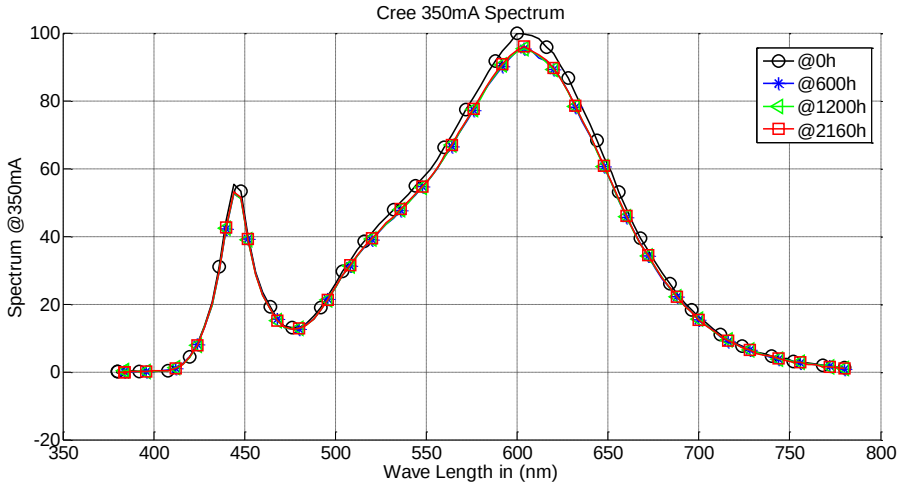

Figure IV.73: Aging spectrum (350mA–stressed Cree).

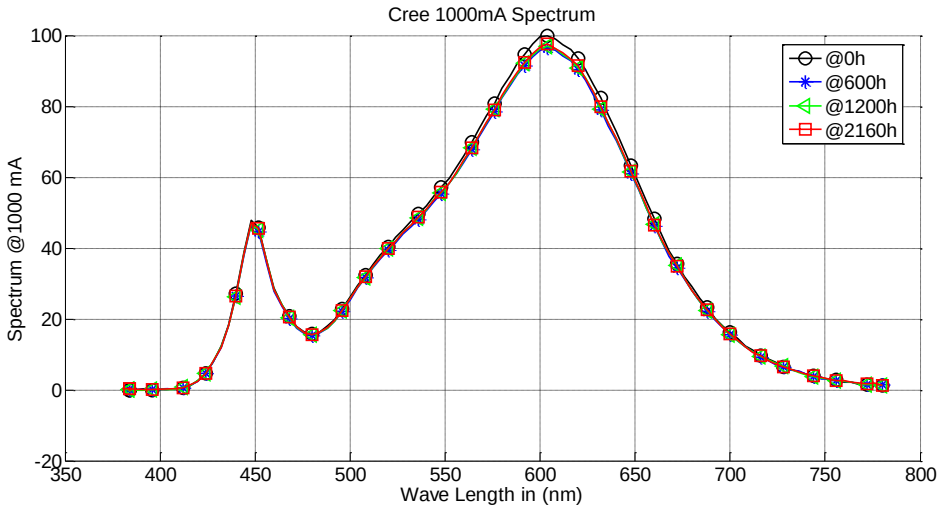

Figure IV.74: Aging spectrum (1000mA–stressed Cree).

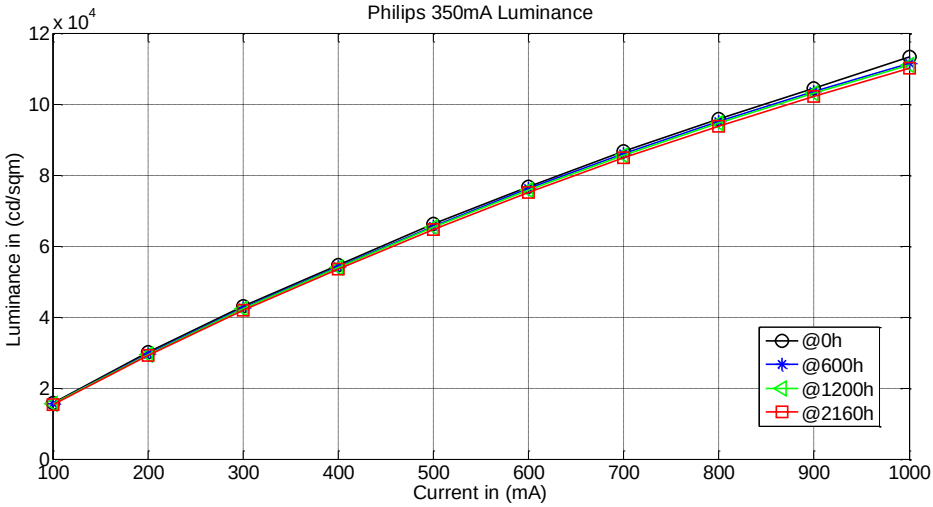

Figure IV.75: Aging luminance (1000mA–stressed Philips).

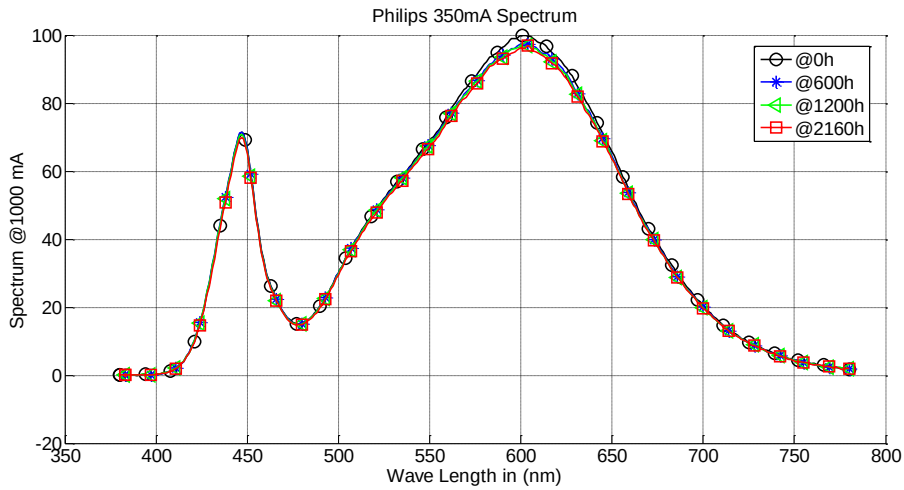

Figure IV.76: Aging spectrum (1000mA–stressed Philips).

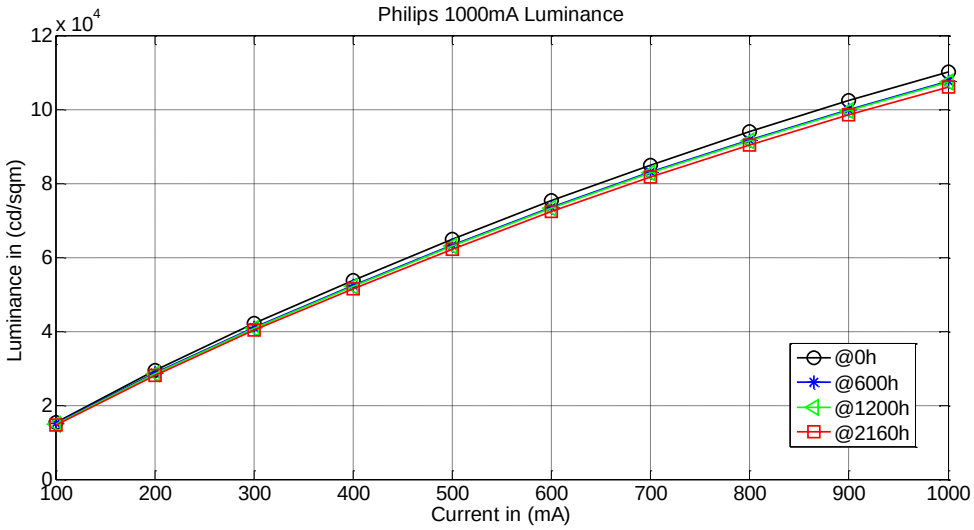

Figure IV.77: Aging luminance (1000mA–stressed Philips).

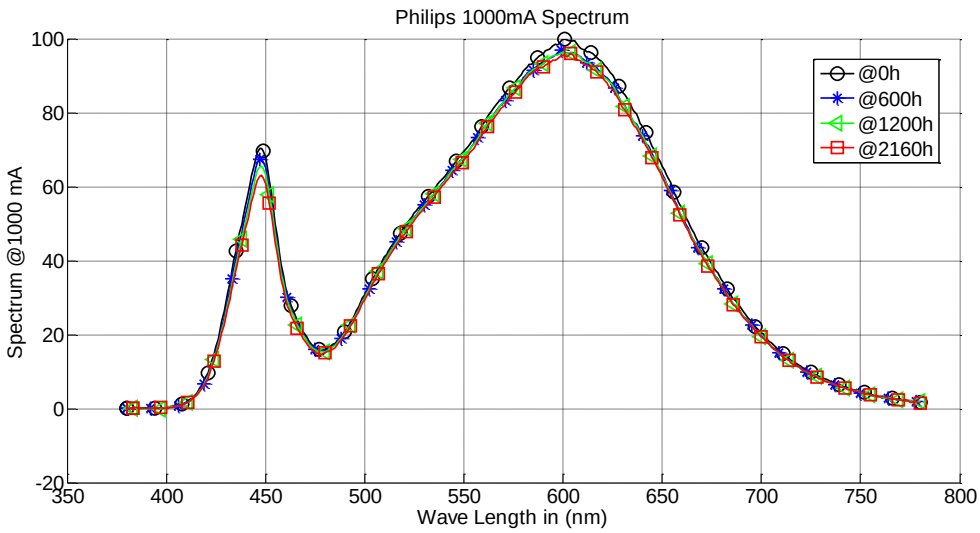

Figure IV.78: Aging spectrum (1000mA–stressed Philips).

In contrast, we find that the photometrical data of Osram are seriously changed along the stress time. It shows a drastically subsequent degradation of its luminance along the stress time as illustrated in Figure IV.79 (aging current vs. luminance at nominal current, 350mA). In Figure IV.80 (aging spectrum under at nominal current, 350mA), it shows a significant modification of the spectral output of the devices for both blue luminescence peak around 440nm and broaden yellow–red peak. We find that the intensity of yellow–red spectrum of phosphor–related electroluminescence is quickly reduced following the increase of stress time, while the intensity of blue electroluminescence exhibits a notably increase. This certifies the decrease of efficiency of the stressed samples and the change of chromaticity by shifting the chromatic coordinate to blueish light output and it is clearly verified by the chromatic plot in Figure IV.81.

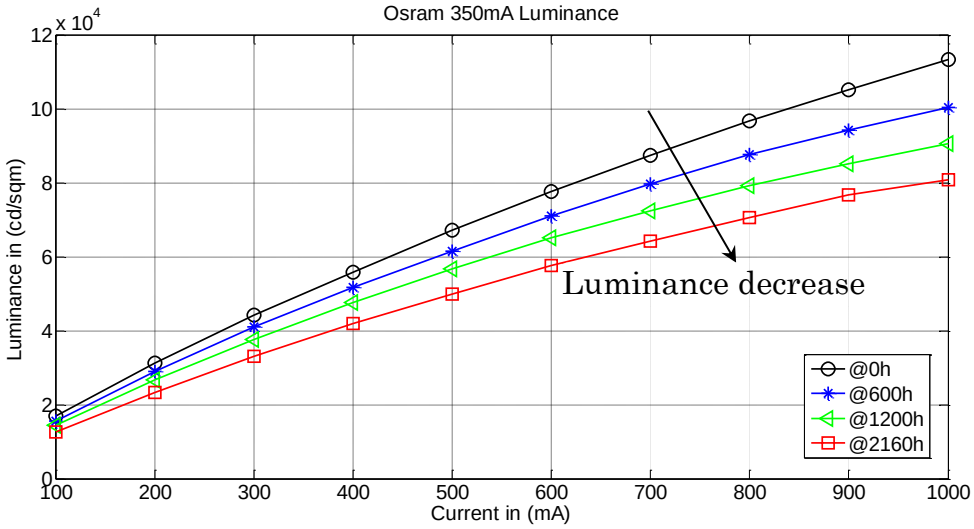

Figure IV.79: Aging luminance (350mA–stressed Osram).

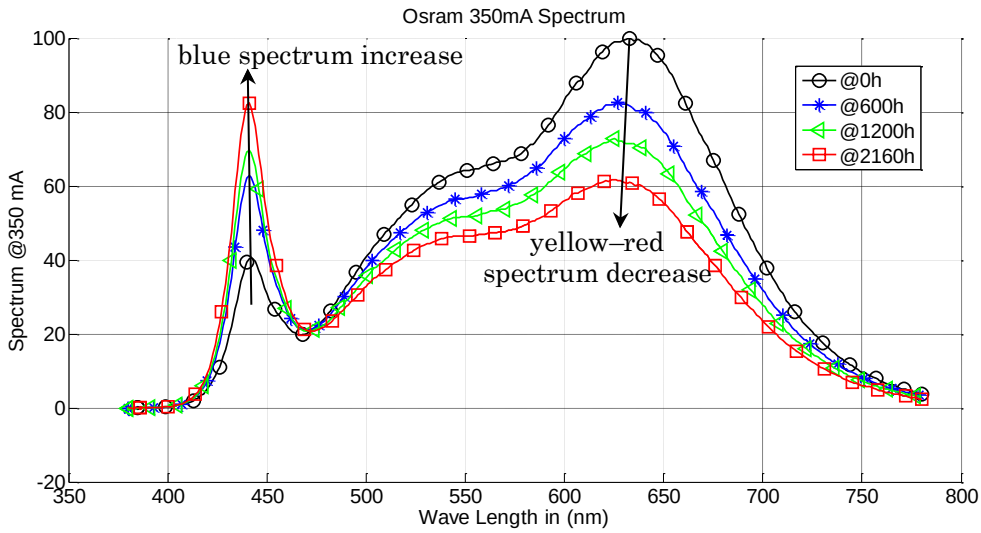

Figure IV.80: Aging spectrum (350mA–stressed Osram).

The result of the device's degradation from this group is surprisingly observed on the samples that are subjected to the low stress current 350mA, while the result from the same Osram group samples which are operated under the higher stressed current of 1000mA does not encounter any significant changes in their optical characteristic for both luminance and spectral power distribution (SDP) as indicated in Figure IV.82 and Figure IV.83, respectively. Based on these results, we cannot conclude that the decrease of external efficiency of the Osram LEDs is caused by degradation of devices due to the current or thermal stresses.

However, the degradation of these devices can be ascribed to the dirtiness of the package and possibly due to the accidental misting of silicon oil on the device's package during experimental setup and this may alter the property of the phosphor layer of the devices.

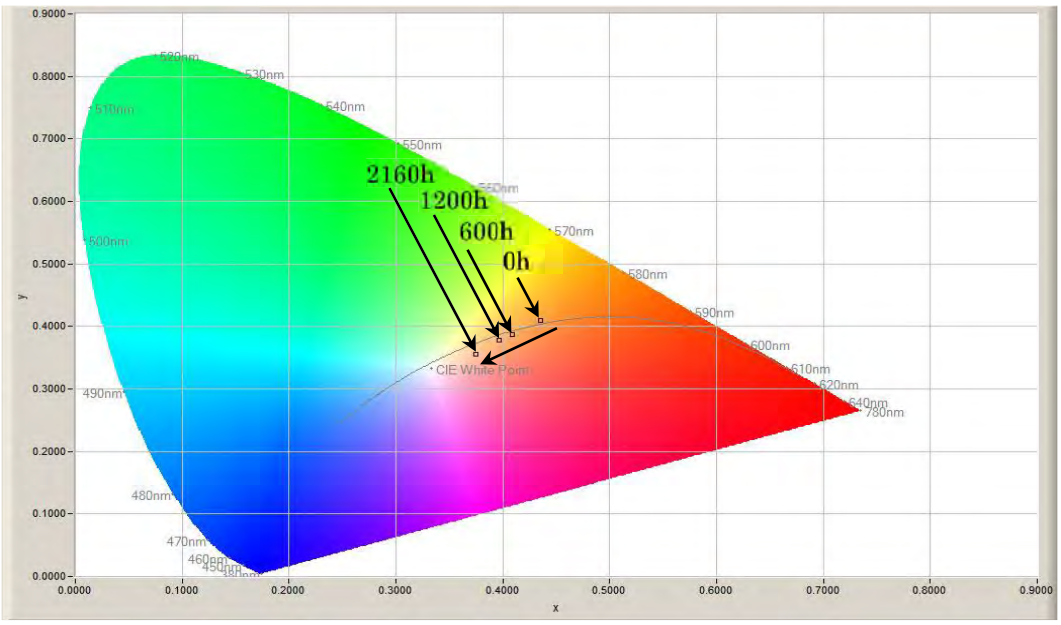

Figure IV.81: Aging chromaticity to blueish light (350mA–stressed Osram).

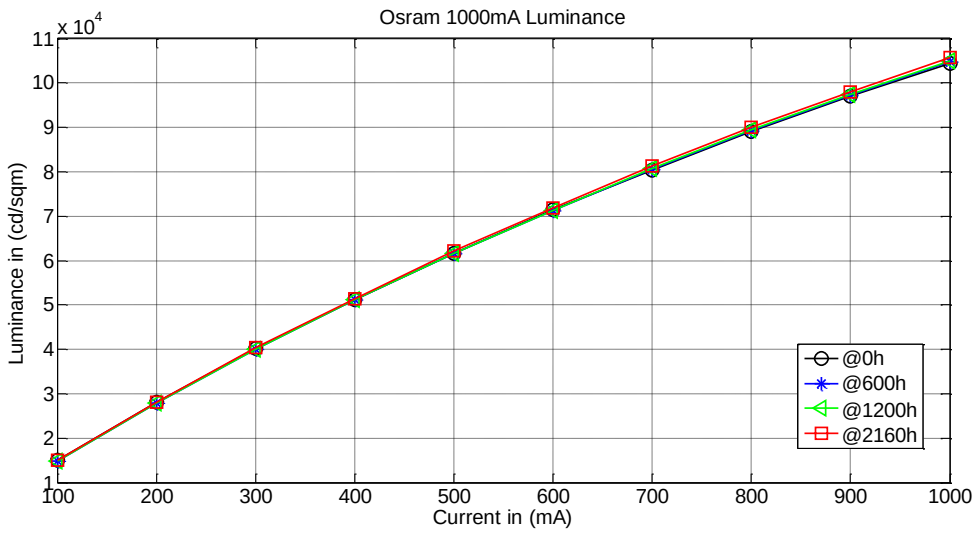

Figure IV.82: Aging luminance (1000mA–stressed Osram).

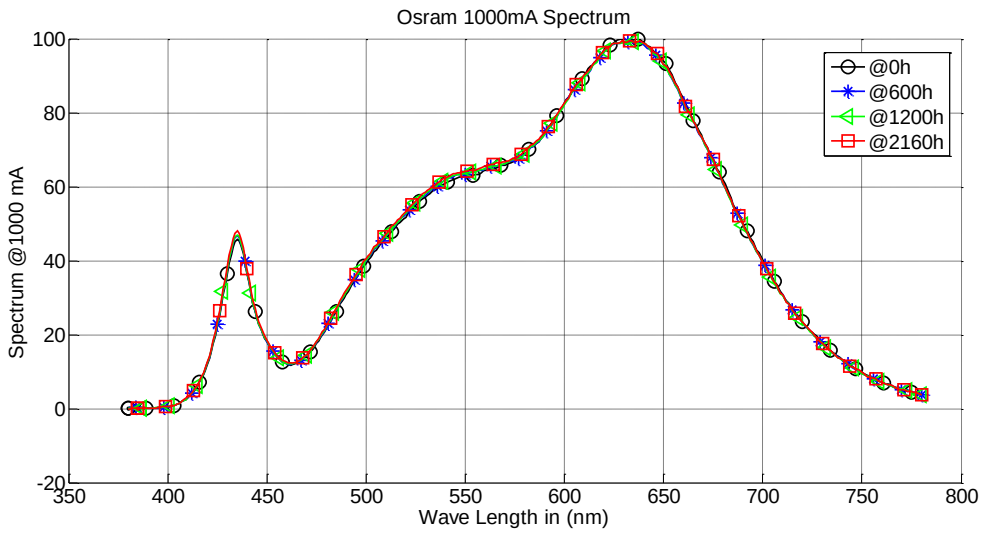

Figure IV.83: Aging spectrum (1000mA–stressed Osram).

Another interesting notice has been observed on the degradation of aged devices from Seoul Semiconductor's LEDs. From the result indicated in the Figure IV.84 and Figure IV.85, we find that the devices under the electrical current stress of 350mA are slightly reduced their luminance and electroluminescence peak spectrum at yellow–red region, respectively. The result of the same measured photometrical parameters of the devices under the higher electrical stress condition, at 1000mA, shows a faster rate of the degradation as illustrated in the Figure IV.86 (aging luminance of Seoul at 1000mA current stress) and Figure IV.87 (aging spectrum of Seoul at 1000mA current stress). The result reveals that the devices are more susceptible when they are under the higher current stress. This should be extrapolated to be caused by the higher thermal activated effect and/or by the exposure to the higher intensity of the short wave length of the blue light that is generated by the higher current on encapsulation package and/or on the phosphorous material of the device. The effect of current stress levels on the degradation rate is clearly emphasized on the plot of its normalized optical power in Figure IV.88. In this figure, we superimpose all the normalized optical power of LED groups to describe their difference of degradation rate. For a stress time of 2160 hours, we see that the largest percentage of degradation of the Osram's device reaches nearly 25%, followed by the device coming from Seoul Semiconductor under the high current stress, which reaches more than 10%, and finally, the LEDs from Philips present a decrease of 6%. It is noticed that the devices coming from Cree show the less modification behavior along the aging time.

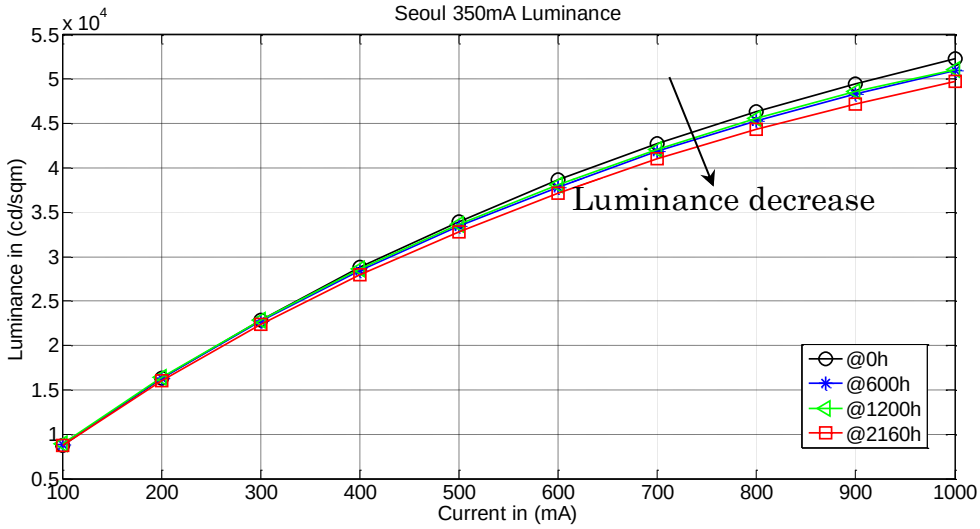

Figure IV.84: Aging luminance (350mA–stressed Seoul).

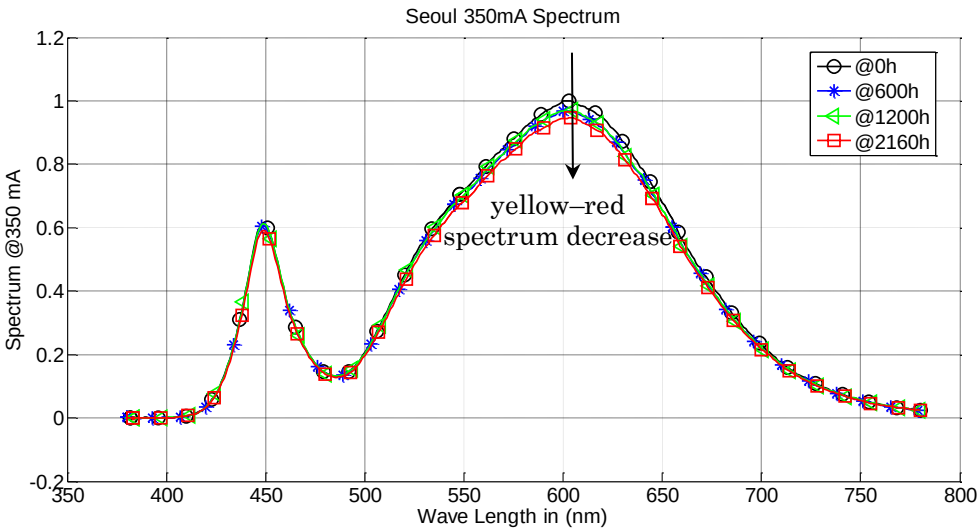

Figure IV.85: Aging spectrum (350mA–stressed Seoul).

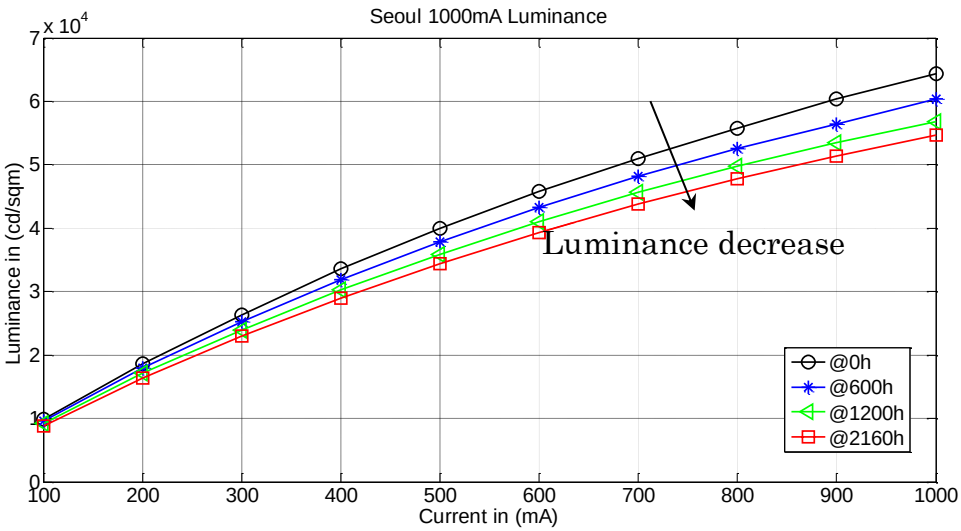

Figure IV.86: Aging luminance (1000mA–stressed Seoul).

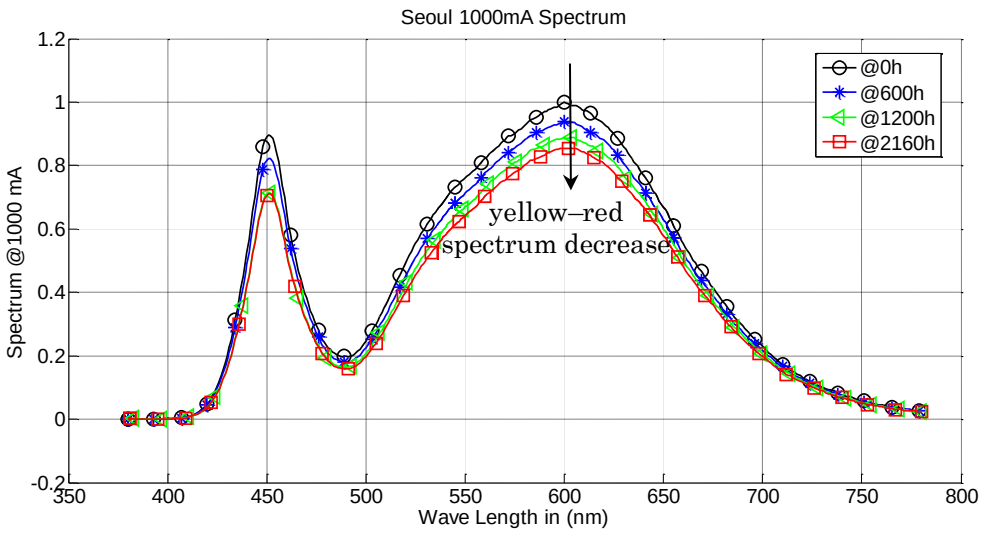

Figure IV.87: Aging spectrum (1000mA–stressed Seoul).

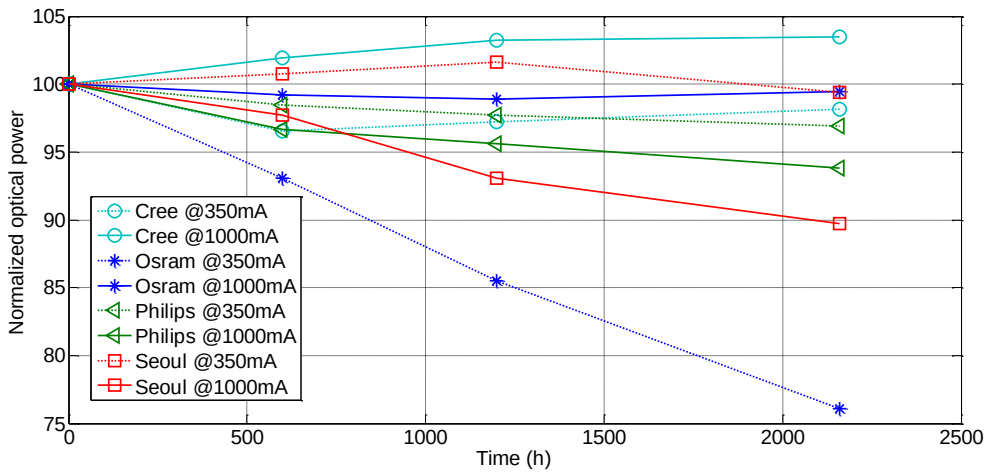

Figure IV.88: Aging optical power (COPS LEDs).

4.6. CONCLUSION– CHAPTER 4

In this chapter, we have reported various results corresponding to LED's electrical characteristics of the four different types of LED group from Cree, Osram, Philips and Seoul Semiconductor before submitting to stress conditions.

The primary method based on electrical characterization of devices has been used to evaluate the degradation after submitting to the stress. From electrical measurements, the aging characteristic gradual changes of each LED group have been described and it is shown that the devices from Cree exhibit an increase of the forward voltage in the zone III of high injected level after the stress while the devices from Osram and Seoul Semiconductor indicate a decrease of their forward voltage. The increase and decrease of this forward voltage of LEDs is clearly justified by their increase and decrease of parasitic series resistance (R_S), respectively. The modification of parasitic series resistances is extrapolated to the modification of ohmic contact of the device that can allow identifying the degradation of LED devices.

The degradation mode of LED chip or die is inferred by the study of the parallel resistance R_P evolution that is linked to the I–V characteristic in the zone of low injection level of forward bias or the I–V characteristic of reverse bias. The decline of R_P is related to the increase of injected current and is correlated to the formation of point defects or dislocation defects inside semiconductor. In addition, the stress level can affect the degradation rate of the devices. When the highest stress is subjected to the device, the faster degradation rate, they undergo.

The photometrical characterizations of devices of all LED groups have been reported. At their initial state, the statistical property of all LED samples in each LED group have been demonstrated and it shows that the devices coming from Osram have the highest statistical difference with its coefficient of variation of luminance and spectrum is 12.84% and 6.01%, respectively, comparing to that of Osram (2.59%–luminance, 2.40%–spectrum), Cree (1.26%–luminance, 1.77%–spectrum) and Philips (1.26%–luminance, 0.96%–spectrum). The initial state characteristics of their photometrical properties also show that the devices coming

from Cree exhibits the highest luminance flux followed by Philips, Osram and Seoul Semiconductor. However, Osram's devices show the best rendering index among the other groups.

The result of the stressed devices reveals that, based on the selection of many LED products to be tested, there are various different degradation results can be observed from each device group. It is shown that the devices coming from Osram exhibit the largest degradation of their luminance and spectrum comparing to the other products. However, the mechanism of this failure mode could not be associated to the level of stressed current or heat generation during the stressed time because the result of this 350mA–low current stress device contrasts to the result obtained from the devices under 1000mA–high current stress which shows insignificant change after the stress period.

It is similar to the result of the high–current stress Osram's device, the photometrical measurements from Cree and Philips also indicate an unnoted degradation after subjected the stress during the stressed time of study (up to 2160h). So, in order to be able to observe any degradation of these devices it should be required longer stressed time of study.

However, the study results of the device coming from Seoul Semiconductor can be observed to have a small degradation with the reduction of its photometrical performances under low level of current stress (350mA) and even faster degradation rate under the high current stressed (1000mA). The photometrical degradation of the device during the same stressed period comparing to the other devices allow to conclude that this device (note that this is an old technology chosen specially for this study to promote degradations observation) presents a low quality of Seoul's product package comparing to those of other products. Furthermore, the different degradation rate of Seoul's devices between the stress under low current level and high current level leads to the conclusion that the dominant effect on failure mode in this case seems to be linked to current's density effects. The higher stressed of operated current level we have the faster failure of LED package is.

GENERAL CONCLUSION AND PERSPECTIVES

This work deals with characterizations and analyses of light emitting diode's degradations by using the so–called primary method that is based on the LED's electrical and photometrical characterizations.

Firstly, we have introduced this thesis by a brief history of lighting system followed by the LED's technology and the failure modes. Theory of the chapter 2 was used to understand and analyze the results obtained. The experimental part was described and exploited in the last two chapters introduced by the description of the aging bench and followed by characterizations and measurements. This is the heart of this work.

The characterizations of the four different types of LED group from Cree, Osram, Philips and Seoul Semiconductor before submitting to stressed condition reveal that, for both electrical and optical measurement, the binning quality of the devices from Osram presents the largest dispersion comparing to the other group. The dispersion of Osram's I–V characteristic is 6.66% comparing to Seoul 2.43%, Cree 1.81%, and Philips 2.27%. The dispersion of luminance of Osram is 12.84% comparing to Seoul 2.59%, Cree 1.26%, and Philips 1.26%. Likewise, the error deviation of spectrum of Osram is 6.01% comparing to Seoul 2.40%, Cree 1.77%, and Philips 0.96%.

Based on the electrical characterization of aging devices, it allows concluding about the degradation of semiconductor chip and ohmic contact of the devices. I–V characteristic of reverse bias and low injection level allow evaluating the degradation characteristic of LED chip and the result shows that the reverse current of Philips and Seoul Semiconductor's devices has increase after subjected to the stress which can be concluded that LED chip presents the appearance of degradation after subjected to the stress. While the devices from Cree show the decrease of their reverse bias current and this should be inferred the enhancement of defect formation after they subject to the stress. It is impossible to conclude the degradation characteristic of the devices from Osram based on their reverse bias current due to the function of reverse bias protection which cause their reverse bias

current unchanged after subjected to the stress. However, the low injection level characteristic can allow concluding that the devices also degrade as their current at this region increase after stress. Degradation characteristic of the devices is also illustrated by linking to modification of parasitic parallel resistance (R_P) as the degraded devices experience to the decrease of parallel resistance of leakage path.

The degradation of device's ohmic contact can be evaluated at high level injection of I–V characteristic that can also be associated to the modification of series resistance R_S. Cree's devices exhibit degradation of its ohmic contact as seen by the increase of forward voltage at the zone of high injected level after the stress while the ohmic contact of devices from Osram and Seoul Semiconductor is enhanced after experience to the stress as shown by the decrease of their forward voltage and the devices from Philips show the stability of their ohmic contact as their forward voltage is unchanged along the stress period.

While, in this work, the electrical characteristic is used to characterize the degradation property of LED's semiconductor chip and the ohmic contact of the LED device, the optical is used to indicate the degradation property of device's package. After subjected to the stress, the LED package of most of the devices coming from Cree, Philips and Osram is not affected by the stress during the stressed time (2160 hours) although the results of optical property of some devices coming from Osram under low current stress present the modification. However, the optical property modification of those devices is attributed to effect of external influence of dirt of silicon oil on the devices' package and should not cause by the effect of the stress current because most of the devices under the high current stress do not show notably changes of their optical property. In contrast, the optical property of Seoul Semiconductor's devices shows the degradation of their package as clarified by the decrease of their optical property under both low and high current stress.

As perspectives for this work, the primary method based on characterization of electrical and optical property allows to evaluate the degradation characteristic in various part of LED componence including semiconductor chip, ohmic contact and device's package. However, due to high reliability of state–of–art high brightness LED, it requires longer time period of study in order to obtain better result of

degradation evaluation of some LED devices. Furthermore, the result based on the primary method cannot give all degradation or failure modes indication and failure mechanism that can experience to the LED devices and it cannot neither provide clear image of defects or damage as in the case of secondary method that incorporates cost effective and high technology equipment such as Scanning Electron Microscope (SEM), Energy Dispersive X–Ray (EDX) Spectroscopy, Transmission Electron Microscope (TEM), Electron Beam Induced Current (EBIC) or Electron Beam Induced Voltage (EBIV) that can be used to provide clear physical symptom of the devices at different part of LED. So, the next step for the future project should be the experimental prototype based on the secondary evaluation method in order to provide the result of LED failure modes and mechanisms as a compliment to the method that has been used in this work.

REFERENCES

[1] V. K. Khanna, *Fundamentals of solid-state lighting: LEDs, OLEDs, and their applications in illumination and displays*. Boca Raton: CRC Press, Taylor & Francis Group, 2014.

[2] S. Kitsinelis, *Light sources: basics of lighting technologies and applications / Spiros Kitsinelis*, 2nd ed. Boca Raton : CRC Press, 2015.

[3] S. P. Denbaars, "Gallium-nitride-based materials for blue to ultraviolet optoelectronics devices," *Proc. IEEE*, vol. 85, no. 11, pp. 1740–1749, Nov. 1997.

[4] C. E. Webb and J. D. C. Jones, Eds., *Handbook of laser technology and applications*. Bristol: Philadelphia : Institute of Physics, 2004.

[5] Y.-H. Lo, Ed., *Emerging optoelectronic technologies and applications*. Singapore ; River Edge, NJ: World Scientific, 1997.

[6] P. Mottier, Ed., *LEDs for lighting applications*. London : Hoboken, NJ: ISTE ; Wiley, 2009.

[7] T. Ueda *et al.*, "Vertical InGaN-based blue light emitting diode with plated metal base fabricated using laser lift-off technique," *Phys. Status Solidi C*, vol. 0, no. 7, pp. 2219–2222, Dec. 2003.

[8] T. Ueda, M. Ishida, and M. Yuri, "Separation of Thin GaN from Sapphire by Laser Lift-Off Technique," *Jpn. J. Appl. Phys.*, vol. 50, no. 4, p. 41001, Apr. 2011.

[9] S. C. Hsu and C. Y. Liu, "Fabrication of Thin-GaN LED Structures by Au–Si Wafer Bonding," *Electrochem. Solid-State Lett.*, vol. 9, no. 5, p. G171, 2006.

[10] W. S. Wong, T. Sands, and N. W. Cheung, "Damage-free separation of GaN thin films from sapphire substrates," *Appl. Phys. Lett.*, vol. 72, no. 5, p. 599, 1998.

[11] V. Haerle *et al.*, "High brightness LEDs for general lighting applications Using the new ThinGaN™-Technology," *Phys Stat Sol A*, vol. 201, no. 12, pp. 2736–2739, Sep. 2004.

[12] S. Zhang, B. Feng, Q. Sun, and H. Zhao, "Preparation of GaN-on-Si based thin-film flip-chip LEDs," *J. Semicond.*, vol. 34, no. 5, p. 53006, May 2013.

[13] Yen-Chih Chiang, Bing-Cheng Lin, Kuo-Ju Chen, Chien-Chung Lin, Po-Tsung Lee, and Hao-Chung Kuo, "Innovative Fabrication of Wafer-Level InGaN-Based Thin-Film Flip-Chip Light-Emitting Diodes," *IEEE Photonics Technol. Lett.*, vol. 27, no. 13, pp. 1457–1460, Jul. 2015.

[14] C. B. Soh *et al.*, "Enhancement in light extraction efficiency from GaN based LEDs with nanopores ITO p-contact grown on patterned sapphire substrate," *Phys. Status Solidi B*, vol. 247, no. 7, pp. 1757–1760, Jun. 2010.

[15] T. Fujii, Y. Gao, R. Sharma, E. L. Hu, S. P. DenBaars, and S. Nakamura, "Increase in the extraction efficiency of GaN-based light-emitting diodes via surface roughening," *Appl. Phys. Lett.*, vol. 84, no. 6, p. 855, 2004.

[16] C. L. Lin *et al.*, "Light enhancement by the formation of an Al oxide honeycomb nanostructure on the n-GaN surface of thin-GaN light-emitting diodes," *Appl. Phys. Lett.*, vol. 90, no. 24, p. 242106, 2007.

[17] E. F. Schubert, *Light-emitting diodes*. Cambridge; New York: Cambridge University Press, 2006.

[18] S. W. R. Lee, R. Zhang, K. Chen, and J. C. C. Lo, "Emerging trend for LED wafer level packaging," *Front. Optoelectron.*, vol. 5, no. 2, pp. 119–126, Jun. 2012.

[19] "Constitution d'une LED." [Online]. Available: http://www.led-fr.net/caracteristiques-led.htm.

[20] "Seoul Semiconductor Package-less LED Gaining Traction in Lighting Market Applications." [Online]. Available: http://www.ledinside.com/news/2015/10/seoul_semiconductor_package_less_led_gaining_traction_in_lighting_market_applications.

[21] "Oslon Black Flat: Making two from one." [Online]. Available: http://www.osram-os.com/osram_os/en/press/press-releases/led-for-automotive,-consumer,-industry/2013/oslon-black-flat-making-two-from-one/index.jsp?mkturl=pr-oslon-black-flat.

[22] J.-K. Sim, K. Ashok, Y.-H. Ra, H.-C. Im, B.-J. Baek, and C.-R. Lee, "Characteristic enhancement of white LED lamp using low temperature co-fired ceramic-chip on board package," *Curr. Appl. Phys.*, vol. 12, no. 2, pp. 494–498, Mar. 2012.

[23] Byung-Ho Kim and Cheol-Hee Moon, "Comparison of the Thermal Performance of the Multichip LED Packages," *IEEE Trans. Compon. Packag. Manuf. Technol.*, vol. 2, no. 11, pp. 1832–1837, Nov. 2012.

[24] Min Seok Ha, "THERMAL ANALYSIS OF HIGH POWER LED ARRAYS," Georgia Institute of Technology, 2009.

[25] G. Lu, S. Yang, and Y. Huang, "Analysis on failure modes and mechanisms of LED," *Reliab. Maintainab. Saf.*, pp. 1237–1241, 2009.

[26] J. Tharian, "Degradation- and Failure Mode Analysis of III-V Nitride Devices," 2007, pp. 284–287.

[27] T. Yanagisawa, "The degradation of GaAlAs red light-emitting diodes under continuous and low-speed pulse operations," *Microelectron. Reliab.*, vol. 38, no. 10, pp. 1627–1630, Oct. 1998.

[28] A. Uddin, A. C. Wei, and T. G. Andersson, "Study of degradation mechanism of blue light emitting diodes," *Thin Solid Films*, vol. 483, no. 1–2, pp. 378–381, Jul. 2005.

[29] G. Meneghesso *et al.*, "Failure Modes and Mechanisms of DC-Aged GaN LEDs," *Phys. Status Solidi A*, vol. 194, no. 2, pp. 389–392, Dec. 2002.

[30] Y. Chen *et al.*, "Pit formation in GaInN quantum wells," *Appl. Phys. Lett.*, vol. 72, no. 6, p. 710, 1998.

[31] H. M. Hobgood *et al.*, "Large diameter 6H-SiC for microwave device applications," *J. Cryst. Growth*, vol. 137, no. 1–2, pp. 181–186, Mar. 1994.

[32] Y.-J. Yoon, B.-K. Kim, and M. Kim, "Nanostructure origin of leakage current in GaN/InGaN lighting emitting diode using patterned sapphire substrate," *Microsc. Microanal.*, vol. 14, no. S2, pp. 634–635, Aug. 2008.

[33] F. C. Frank, "Capillary equilibria of dislocated crystals," *Acta Crystallogr.*, vol. 4, no. 6, pp. 497–501, Nov. 1951.

[34] Z. Liliental-Weber, Y. Chen, S. Ruvimov, and J. Washburn, "Nanotubes and Pinholes in GaN and their Formation Mechanism," *Mater. Sci. Forum*, vol. 258–263, pp. 1659–1664, 1997.

[35] T. Egawa, H. Ishikawa, T. Jimbo, and M. Umeno, "Optical degradation of InGaN/AlGaN light-emitting diode on sapphire substrate grown by metalorganic chemical vapor deposition," *Appl. Phys. Lett.*, vol. 69, no. 6, p. 830, 1996.

[36] B. Cotterell, Z. Chen, J.-B. Han, and N.-X. Tan, "The Strength of the Silicon Die in Flip-Chip Assemblies," *J. Electron. Packag.*, vol. 125, no. 1, p. 114, 2003.

[37] M. Ranjan, L. Gopalakrishnan, K. Srihari, and C. Woychik, "Die cracking in flip chip assemblies," in *Electronic Components & Technology Conference, 1998. 48th IEEE*, 1998, pp. 729–733.

[38] J. D. Wu, C. Y. Huang, and C. C. Liao, "Fracture strength characterization and failure analysis of silicon dies," *Microelectron. Reliab.*, vol. 43, no. 2, pp. 269–277, 2003.

[39] K. Köhler *et al.*, "Control of the Mg doping profile in III-N light-emitting diodes and its effect on the electroluminescence efficiency," *J. Appl. Phys.*, vol. 97, no. 10, p. 104914, 2005.

[40] D. L. Barton *et al.*, "Degradation of blue AlGaN/InGaN/GaN LEDs subjected to high current pulses," in *Reliability Physics Symposium, 1995. 33rd Annual Proceedings., IEEE International*, 1995, pp. 191–199.

[41] H. Kim, H. Yang, C. Huh, S.-W. Kim, S.-J. Park, and H. Hwang, "Electromigration-induced failure of GaN multi-quantum well light emitting diode," *Electron. Lett.*, vol. 36, no. 10, p. 908, 2000.

[42] W. D. Van Driel, *Solid state lighting reliability: components to systems*. New York: Springer, 2012.

[43] F. Wu, W. Zhao, S. Yang, and C. Zhang, "Failure modes and failure analysis of white LEDs," in *Electronic Measurement & Instruments, 2009. ICEMI'09. 9th International Conference on*, 2009, pp. 4–978.

[44] M.-H. Chang, D. Das, P. V. Varde, and M. Pecht, "Light emitting diodes reliability review," *Microelectron. Reliab.*, vol. 52, no. 5, pp. 762–782, May 2012.

[45] Hongping Zhao, "III-Nitride Light-Emitting Diodes for Solid-State Lighting," 09-Apr-2012.

[46] G. Meneghesso, C. Crosato, F. Garat, G. Martines, A. Paccagnella, and E. Zanoni, "Failure mechanisms of Schottky gate contact degradation and deep traps creation in AlGaAs/InGaAs PM-HEMTs submitted to accelerated life tests," *Microelectron. Reliab.*, vol. 38, no. 6–8, pp. 1227–1232, Jun. 1998.

[47] M. Dammann, A. Leuther, F. Benkhelifa, T. Feltgen, and W. Jantz, "Reliability and degradation mechanism of AlGaAs/InGaAs and InAlAs/InGaAs HEMTs," *Phys. Status Solidi A*, vol. 195, no. 1, pp. 81–86, Jan. 2003.

[48] K. Mizuishi, H. Kurono, H. Sato, and H. Kodera, "Degradation mechanism of GaAs MESFET's," *IEEE Trans. Electron Devices*, vol. 26, no. 7, pp. 1008–1014, Jul. 1979.

[49] Z. Jian-Ming *et al.*, "High power and high reliability GaN/InGaN flip-chip light-emitting diodes," *Chin. Phys.*, vol. 16, no. 4, p. 1135, 2007.

[50] S. J. Chang *et al.*, "Improved ESD protection by combining InGaN-GaN MQW LEDs with GaN Schottky diodes," *IEEE Electron Device Lett.*, vol. 24, no. 3, pp. 129–131, Mar. 2003.

[51] S.-C. Shei, J.-K. Sheu, and C.-F. Shen, "Improved Reliability and ESD Characteristics of Flip-Chip GaN-Based LEDs With Internal Inverse-Parallel Protection Diodes," *IEEE Electron Device Lett.*, vol. 28, no. 5, pp. 346–349, May 2007.

[52] M. Meneghini *et al.*, "High temperature electro-optical degradation of InGaN/GaN HBLEDs," *Microelectron. Reliab.*, vol. 47, no. 9–11, pp. 1625–1629, Sep. 2007.

[53] M. Meneghini, A. Tazzoli, G. Mura, G. Meneghesso, and E. Zanoni, "A Review on the Physical Mechanisms That Limit the Reliability of GaN-Based LEDs," *IEEE Trans. Electron Devices*, vol. 57, no. 1, pp. 108–118, Jan. 2010.

[54] J. Hu, L. Yang, and M. Whan Shin, "Mechanism and thermal effect of delamination in light-emitting diode packages," *Microelectron. J.*, vol. 38, no. 2, pp. 157–163, Feb. 2007.

[55] L. Zhou, B. An, Y. Wu, and S. Liu, "Analysis of delamination and darkening in high power LED packaging," in *2009 16th IEEE International Symposium on the Physical and Failure Analysis of Integrated Circuits*, 2009, pp. 656–660.

[56] Xiaobing Luo, Bulong Wu, and Sheng Liu, "Effects of Moist Environments on LED Module Reliability," *IEEE Trans. Device Mater. Reliab.*, vol. 10, no. 2, pp. 182–186, Jun. 2010.

[57] Jianzheng Hu, Lianqiao Yang, and Moo Whan Shin, "Thermal Effects of Moisture Inducing Delamination in Light-Emitting Diode Packages," 2006, pp. 1957–1962.

[58] Philips-Lumileds-Luxeon, "Reliability Datasheet RD25," 2006.

[59] G. Zhang, S. Feng, H. Zhu, J. liu, J. Li, and C. Guo, "Determination of Thermal Fatigue Delamination of Die Attach Materials for High-Brightness LEDs," *IEEE Photonics Technol. Lett.*, vol. 24, no. 5, pp. 398–400, Mar. 2012.

[60] M. Royer, R. Tuttle, S. Rosenfeld, and N. Miller, "Color Maintenance of LEDs in Laboratory and Field Applications," U.S. Department of Energy, Sep. 2013.

[61] G. Meneghesso, M. Meneghini, and E. Zanoni, "Recent results on the degradation of white LEDs for lighting," *J. Phys. Appl. Phys.*, vol. 43, no. 35, p. 354007, Sep. 2010.

[62] J.-H. Hwang, Y.-D. Kim, J.-W. Kim, S.-J. Jung, H.-K. Kwon, and T.-H. Oh, "Study on the effect of the relative position of the phosphor layer in the LED package on the high power LED lifetime," *Phys. Status Solidi C*, vol. 7, no. 7–8, pp. 2157–2161, Jun. 2010.

[63] B. Fan, H. Wu, Y. Zhao, Y. Xian, and G. Wang, "Study of Phosphor Thermal-Isolated Packaging Technologies for High-Power White Light-Emitting Diodes," *IEEE Photonics Technol. Lett.*, vol. 19, no. 15, pp. 1121–1123, Aug. 2007.

[64] J. K. Kim, H. Luo, E. F. Schubert, J. Cho, C. Sone, and Y. Park, "Strongly Enhanced Phosphor Efficiency in GaInN White Light-Emitting Diodes Using Remote Phosphor Configuration and Diffuse Reflector Cup," *Jpn. J. Appl. Phys.*, vol. 44, no. No. 21, pp. L649–L651, May 2005.

[65] H. Deng, S. Feng, C. Guo, Y. Qiao, and G. Zhang, "Reliability of solder joints in High-power LED package in power cycling tests," 2010, pp. 1683–1685.

[66] Y. Liu, F. Sun, L. Luo, C. A. Yuan, and G. Zhang, "Microstructure Evolution and Shear Behavior of the Solder Joints for Flip-Chip LED on ENIG Substrate," *J. Electron. Mater.*, vol. 44, no. 7, pp. 2450–2457, Jul. 2015.

[67] G. Elger, S. V. Kandaswamy, R. Derix, and F. Conti, "Detection of solder joint cracking of high power leds on AI-IMS during temperature shock test by transient thermal analysis," 2014, pp. 1–6.

[68] W. Yuan and P. Altieri-Weimar, "Modeling of LED solder joint cracking during temperature cycling with Finite Element," in *Thermal, Mechanical and Multi-Physics Simulation and Experiments in Microelectronics and Microsystems (EuroSimE), 2015 16th International Conference on*, 2015, pp. 1–5.

[69] Y. Xi and E. F. Schubert, "Junction–temperature measurement in GaN ultraviolet light-emitting diodes using diode forward voltage method," *Appl. Phys. Lett.*, vol. 85, no. 12, p. 2163, 2004.

[70] Y. P. Varshni, "Temperature dependence of the energy gap in semiconductors," *Physica*, vol. 34, no. 1, pp. 149–154, Jan. 1967.

[71] "Series 2600A System SourceMeter Reference Manual." Keithley Instruments, Inc., 2011-2008.

[72] "ModuLab XM MTS User Guide." Solartron Analytical Ltd.

[73] "Design a constant current source using LM317 voltage regulator," *Help2Educate*. [Online]. Available: http://www.help2educate.com/constant-current-source-using-lm317/.

[74] T.-Y. Seong, Ed., *III-nitride based light emitting diodes and applications*. Dordrecht: Springer, 2013.

[75] S. Liu and X. Luo, *LED packaging for lighting applications: design, manufacturing and testing*. Beijing: Chemical Industry Press, 2011.

[76] M. Meneghini, A. Tazzoli, G. Mura, G. Meneghesso, and E. Zanoni, "A Review on the Physical Mechanisms That Limit the Reliability of GaN-Based LEDs," *IEEE Trans. Electron Devices*, vol. 57, no. 1, pp. 108–118, Jan. 2010.

[77] M. Dal Lago, M. Meneghini, N. Trivellin, G. Meneghesso, and E. Zanoni, "Degradation mechanisms of high-power white LEDs activated by current and temperature," *Microelectron. Reliab.*, vol. 51, no. 9–11, pp. 1742–1746, Sep. 2011.

[78] H. Chen *et al.*, "Failure analysis of electrical-thermal-optical characteristics of LEDs based on AlGaInP and InGaN/GaN," *Semiconductors*, vol. 46, no. 10, pp. 1310–1315, Oct. 2012.

[79] Y. Deshayes, L. Bechou, F. Verdier, and Y. Danto, "Long-term Reliability Prediction of 935 nm LEDs Using Failure Laws and Low Acceleration Factor Ageing Tests," *Qual. Reliab. Eng. Int.*, vol. 21, no. 6, pp. 571–594, Oct. 2005.

[80] G. Meneghesso, M. Meneghini, and E. Zanoni, "Recent results on the degradation of white LEDs for lighting," *J. Phys. Appl. Phys.*, vol. 43, no. 35, p. 354007, Sep. 2010.

[81] S. Levada, M. Meneghini, E. Zanoni, S. Buso, G. Spiazzi, and G. Meneghesso, "High brightness InGaN LEDs degradation at high injection current bias," in *Reliability Physics Symposium Proceedings, 2006. 44th Annual., IEEE International*, 2006, pp. 615–616.

[82] M. Meneghini *et al.*, "Chip and package-related degradation of high power white LEDs," *Microelectron. Reliab.*, vol. 52, no. 5, pp. 804–812, May 2012.

[83] J. K. Lee *et al.*, "Electrochemical removal of hydrogen atoms in Mg-doped GaN epitaxial layers," *J. Appl. Phys.*, vol. 117, no. 18, p. 185702, May 2015.

ANNEXES

APPENDIX A: COMMUNICATION IDENTIFIER LIST OF REX–D100

Name	Identifier	Number of digits	Data range	Initial value	User setting value	R/W
Measured–value(PV)	M1	6	Scaling low–limit to scaling high–limit	–		R/0
First current transformer input value (CT1)	M2	6	0.0 to 100. 0A	–		R/0
Second current transformer input value (CT2)	M3	6	0.0 to 100. 0A	–		R/0
First alarm output	AA	6	0 : OFF 1 : ON	–		R/0
Second alarm output	AB	6	0 : OFF 1 : ON	–		R/0
Heater break alarm output 1	AC	6	0 : OFF 1 : ON	–		R/0
Heater break alarm output 2	AD	6	0 : OFF 1 : ON	–		R/0
Control loop break alarm	AE	6	0 : OFF 1 : ON	–		R/0
Burnout	B1	6	0 : OFF 1 : ON	–		R/0
Manipulated output 1 (Heating–side)	O1	6	–5.0 to 105. 0%	–		R/0
Manipulated output 1 (Cooling–side)	O2	6	–5.0 to 105. 0%	–		R/0
Set–value (SV) monitoring	MS	6	Scaling low–limit to scaling high–limit	–		R/0
Error data	ER	6	0 to 255	–		R/0
AUTO/MAN transfer	J1	6	0 : AUTO mode 1 : MAN mode	AUTO mode		R/W
RUN/STOP transfer	SR	6	0 : RUN 1 : STOP	RUN		R/W
PID/Auto–tuning transfer	G1	6	0 : PID control 1 : Auto–tuning	PID (control)		R/W
Set–value (SV1)	S1	6	Scaling low–limit to scaling high–limit	0(0.0)		R/W
Manipulated output value (MV)	ON	6	Low–limit output range to high–limit output range	–5.0		R/W
Step set–value (SV2)	S2	6	Scaling low–limit to scaling high–limit	0(0.0)		R/W
First alarm setting	A1	6	–1999 to 9999 (The decimal–point position is the same as that of PV)	50(50.0)		R/W
Second alarm setting	A2	6	–1999 to 9999 (The decimal–point position is the same as that of PV)	–50(–50. 0)		R/W
First heater break alarm setting	A3	6	0.0 to 100. 0A (0.0 : HBA1 OFF)	0.0		R/W
Second heater break alarm setting	A4	6	0.0 to 100. 0A (0.0 : HBA2 OFF)	0.0		R/W
PV bias	PB	6	Temperature input : –1999 (–199.9) to –9999 (999.9)°C [°F] Voltage input : –1999 to 9999 (The decimal–point position is the same as that of PV)	0(0.0)		R/W
SV change rate limit	HH	6	Temperature input : 0(0.0) to input span (or 9999 [999.9])°C [°F] /min Voltage input : 0.0 to 100.0%/min of span	0(0.0)		R/W
First alarm action selection	XA	6	0 to 14	5		R/W
First alarm differential gap	HA	6	Temperature input : 0(0.0) to 100(100.0)°C [°F] Voltage input: 0.0 to 10.0% of span	Temperature input:2(2.0) Voltage input : 0.2		R/W
First alarm timer setting	TD	6	0 to 600 sec	0		R/W
Control loop break alarm setting	A5	6	0 to 7200 sec (0 : LBA OFF)	0		R/W
LBA deadband	V3	6	Temperature input : 0 to 9999 °C [°F] (0 : LBA OFF) Voltage input : 0 to 10.0% of span	0		R/W
Second alarm action selection	XB	6	0 to 14	6		R/W
Second alarm differential gap setting	HB	6	Temperature input : 0(0.0) to 100(100.0)°C [°F] Voltage input: 0.0 to 10.0% of span	Temperature input:2(2.0) Voltage input : 0.2		R/W

Name	Identifier	Number of digits	Data range	Initial value	User setting value	R/W
Second alarm timer setting	TG	6	0 to 600 sec	0		R/W
HBA delay timer	TH	6	0 to 600 sec	3		R/W
Proportional band (Heating–side)	P1	6	Temperature input : 0(0.0) to input span (or 9999 [999.9])°C [°F] Voltage input : 0.0 to l00.0% of span	Temperature input 30(30.0) Voltage input 3. 0		R/W
Integral time	I1	6	0 to 3600 sec (0:Integral action OFF)	240		R/W
Derivative time	D1	6	0 to 3600 sec (0:Derivative action OFF)	60		R/W
Anti–reset windup (ARW)	W1	6	1 to 100% of proportional band	100		R/W
Cooling–side proportional band	P2	6	1 to 3000% of proportional band	100		R/W
Overlap/deadband	V1	6	Temperature input : –10(–10.0) to 10(10.0)°C [°F] Voltage input : –10.0 to 10.0% of span	0(0.0)		R/W
ON/OFF action differential gap	MH	6	Temperature input : 0(0.0) to 50(50.0)°C [°F] Voltage input : 0.0 to 10.0% of span	Temperature input 2(2.0) Voltage input 0.2		R/W
Manual reset	MR	6	–50.0 to 50.0% (Heating/cooling –100.0 to 100.0%)	0.0		R/W
Fazzy	XP	6	0: OFF 1 :ON	ON		R/W
Proportioning cycle (OUTl)	TO	6	1 to 100 sec	20		R/W
Output limit (High–limit)	OH	6	Low limit output range to 105.0% (Heating/cooling 0. to 105.0%)	105.0		R/W
Output limit (Low–limit)	OL	6	–5.0% to high limit output range	–5.0		R/W
Direct/reverse action selection	XE	6	0: Direct action 1 : Reverse action	1		R/W
Proportioning cycle (OUT2)	T1	6	1 to 100 sec	20		R/W
Output limit[high–limit](OUT2)	OI	6	0.0 to 105.0% (Cooling–side output)	105.0		R/W
Analog output specification selection	LA	6	0 to 4 (See page 24. of manual)	0		R/W
High limit analog output range	HV	6	(See page 23. of manual)	–		R/W
Low limit analog output range	HW	6	(See page 23. of manual)	–		R/W
Input type selection	XI	6	0 to 37 (See page 24. of manual)	0		R/W
Scaling high–limit	XV	6	Scaling low–limit to 9999	999.9		R/W
Scaling low–limit	XW	6	–1999 to scaling high–limit	–199.9		R/W
Decimal–point position selection	XU	6	0 to 3	1		R/W
AUTO/MAN function selection	PQ	6	0 : Not provided 1 : Provided	0		R/W
Control RUN/STOP display selection	DH	6	0 : Not provided 1 : Provided	0		R/W
Current transformer type selection	XR	6	0 : CTL–6–P–N 1 : CTL–12–S56–10L–N	0		R/W
Air cooling/water cooling selection	XQ	6	0 :Air cooling 1 : Water cool1ng (H/C)	0		R/W
Auto–tuning (AT) differential gap	GH	6	0 to 3600 sec	10		R/W
Action selection at input abnormality	WH	6	0 : No alarm action when abnormal input 1 : Output OFF 2 : Output ON	0		R/W
Universal output selection	XO	6	0 : Relay contact output 1 : Voltage pulse output 2 : Continuous current output	0		R/W

APPENDIX B: CONTROLLER SCANNED PARAMETER

Device Number				01	02	03	04
N°	Identifier	Description	Data Range	Parameter's Value			
1	M1	Measured-value (PV)	Low->High	25.1	25.2	25.8	27.1
2	M2	First current transformer input value (CT1)	0->100A				
3	M3	Second current transformer input value (CT2)	0->100A				
4	AA	First alarm output	0:OFF 1:ON	0	0	0	0
5	AB	Second alarm output	0:OFF 1:ON	0	0	0	0
6	AC	Heater break alarm output 1	0:OFF 1:ON				
7	AD	Heater break alarm output 2	0:OFF 1:ON				
8	AE	Control loop break alarm	0:OFF 1:ON				
9	B1	Burnout	0:OFF 1:ON	0	0	0	0
10	O1	Manipulated output1 (Heating Side)	-5.0 to 105.0%	10	10	10	10
11	O2	Manipulated output2 (Cooling Side)	-5.0 to 105.0%				
12	MS	Set-value (SV) monitoring	Low->High	26	50	60	70
13	ER	Error data	0->255	0	0	0	0
14	J1	AUTO/MAN transfer	0:Auto 1:MAN	0	0	0	0
15	SR	RUN/STOP transfer	0:RUN 1:STOP	0	0	0	0
16	G1	PID/Auto-tuning transfer	0:PID 1:Auto-tuning	1	1	1	1
17	S1	Set-value (SV1) monitoring	Low->High	26	50	60	70
18	ON	Manipulated output value (MV)	Low->High	10	10	10	10
19	S2	Step set-value (SV2)	Low->High				
20	A1	First alarm setting	-1999->9999°C	50	50	50	50
21	A2	Second alarm setting	-1999->9999°C	-50	-50	-50	-50
22	A3	First heater break alarm setting	0->100A				
23	A4	Second heater break alarm setting	0->100A				
24	PB	PV bias	-1999->9999°C	0	0	0	0
25	HH	SV change rate limit	0->9999°C/min	0	0	0	0
26	XA	First alarm action selection	0->14	5	5	5	5
27	HA	First alarm differential gap	0->100°C	2	2	2	2
28	TD	First alarm timer setting	0->600sec	0	0	0	0
29	A5	Control loop break alarm setting	0->7200sec	0	0	0	0
30	V3	Control loop break alarm setting	0->9999°C	0	0	0	0
31	XB	Second alarm action selection	0->14	6	6	6	6
32	HB	Second alarm action selection	0->100°C	2	2	2	2
33	TG	Second alarm timer setting	0->600sec	0	0	0	0
34	TH	HBA delay timer	0->600sec				
35	P1	Proportional band (Heating-side)	0->9999°C/min	30	30	30	30
36	I1	Intergral time	0->3600sec	240	240	240	240
37	D1	Derivative time	0->3600sec	60	60	60	60
38	W1	Anti-reset windup (ARW)	1->100% of proportional band	100	100	100	100
39	P2	Cooling-side proportional band	1->3000% of proportional band				
40	V1	Overlap/deadband	-10->10°C				
41	MH	ON/OFF action differential gap	0->50°C	2	2	2	2
42	MR	Manual reset	-50->50%	0	0	0	0
43	XP	Fazzy	0:OFF 1:ON	1	1	1	1
44	TO	Proportioning cycle (OUT1)	1->100sec				
45	OH	Output limit (High-limit)	Low->105%	100	100	100	100
46	OL	Output limit (Low-limit)	-5%->High	10	10	10	10
47	XE	Direct/reverse action selection	0:Dir 1:Rev	0	0	0	0
48	T1	Proportioning cycle (OUT2)	0->100sec				
49	OI	Output limit[high-limit](OUT2)	0->105%				
50	LA	Analog output specification selection	0->4				
51	HV	High limit analog output range	*7 See page 23				
52	HW	Low limit analog output range	*7 See page 23				
53	XE	Input type selection	0->37	0	0	0	0
54	XV	Scaling high-limit	Low->9999	999.9	999.9	999.9	999.9
55	XW	Scaling low-limit	-1999->High	-199.9	-199.9	-199.9	-199.9
56	XU	Decimal-point position selection	0->3				
57	PQ	AUTO/MAN function selection	0:not provided 1:provided	1	1	1	1
58	DH	Control RUN/STOP display selection	0:not provided 1:provided	1	1	1	1
59	XR	Current transformer type selection	0:CTL-6-P-N 1:CTL-12-S56-10L-N				
60	XQ	Air cooling/water cooling selection	0:Air cooling 1:Water cooling (H/C)				
61	GH	Auto-tuning (AT) differential	0->3600sec	10	10	10	10
62	WH	Action selection at input abnormality	0:No alarm action when abnormal input 1:Output OFF 2:Output ON	0	0	0	0
63	XO	Universal output selection	REX- D100 has no universal output & no identifier appears				

APPENDIX C: PROGRAM CODE FOR REX–D100

```
Option Explicit
Private StoredReply$
Private iScan%

Private Sub Form_Load()
    Me.Left = 5000
    Me.Top = 2500
    'Detect Exist ComPort-----------------------------------------------------
    Dim i%
    With COMPort
        For i = 1 To 100
            On Error Resume Next
            .CommPort = i
            On Error Resume Next
            .PortOpen = True
            On Error Resume Next
            .PortOpen = False
            If Err.Number = 0 Then
                cmbPort.AddItem "COM" + CStr(i)
            End If
        Next i
    End With
    '-------------------------------------------------------------------------
    If COMPort.PortOpen = True Then
        COMPort.PortOpen = False
    End If

    'For Setting Parameters*****************************************************
    cmbIden_Get.List(0) = "M1,Measured-value (PV),Low->High" ' (R/O)
    cmbIden_Get.List(1) = "M2,First current transformer input value (CT1),0->100A" ' (R/O)
    cmbIden_Get.List(2) = "M3,Second current transformer input value (CT2),0->100A" ' (R/O)
    cmbIden_Get.List(3) = "AA,First alarm output, 0:OFF 1:ON" '(R/O)
    cmbIden_Get.List(4) = "AB,Second alarm output, 0:OFF 1:ON" '(R/O)
    cmbIden_Get.List(5) = "AC,Heater break alarm output 1, 0:OFF 1:ON" '(R/O)
    cmbIden_Get.List(6) = "AD,Heater break alarm output 2, 0:OFF 1:ON" '(R/O)
    cmbIden_Get.List(7) = "AE,Control loop break alarm, 0:OFF 1:ON" '(R/O)
    cmbIden_Get.List(8) = "B1,Burnout, 0:OFF 1:ON" '(R/O)
    cmbIden_Get.List(9) = "O1,Manipulated output1 (Heating Side),-5.0 to 105.0%" '% of output
(R/O)
    cmbIden_Get.List(10) = "O2,Manipulated output2 (Cooling Side),-5.0 to 105.0%" '% of output
(R/O)
    cmbIden_Get.List(11) = "MS,Set-value (SV) monitoring,Low->High" '(R/O)
    cmbIden_Get.List(12) = "ER,Error data, 0->255" '(R/O)
    cmbIden_Get.List(13) = "J1,AUTO/MAN transfer,0:Auto 1:MAN"  '(R/W)
    cmbIden_Get.List(14) = "SR,RUN/STOP transfer,0:RUN 1:STOP"  '(R/W)
    cmbIden_Get.List(15) = "G1,PID/Auto-tuning transfer,0:PID 1:Auto-tuning"    '(R/W)
    cmbIden_Get.List(16) = "S1,Set-value (SV1) monitoring,Low->High"  ' (R/W)
    cmbIden_Get.List(17) = "ON,Manipulated output value (MV),Low->High" '(R/W)
    cmbIden_Get.List(18) = "S2,Step set-value (SV2),Low->High" '(R/W)
    cmbIden_Get.List(19) = "A1,First alarm setting,-1999->9999°C" '(R/W)
    cmbIden_Get.List(20) = "A2,Second alarm setting,-1999->9999°C" '(R/W)
    cmbIden_Get.List(21) = "A3,First heater break alarm setting,0->100A" '(R/W)
    cmbIden_Get.List(22) = "A4,Second heater break alarm setting,0->100A" '(R/W)
    cmbIden_Get.List(23) = "PB,PV bias,-1999->9999°C" '-199.9->999.9°F,Voltage input:-1999->9999V
(R/W)
    cmbIden_Get.List(24) = "HH,SV change rate limit,0->9999°C/min"  '0->999.9°F,Voltage input:0-
>100%/min (R/W)
    cmbIden_Get.List(25) = "XA,First alarm action selection,0->14" '(R/W)
    cmbIden_Get.List(26) = "HA,First alarm differential gap,0->100°C" '0->100°F,Voltage input:0-
>10% (R/W)
    cmbIden_Get.List(27) = "TD,First alarm timer setting,0->600sec" '(R/W)
    cmbIden_Get.List(28) = "A5,Control loop break alarm setting,0->7200sec" '(R/W)
    cmbIden_Get.List(29) = "V3,Control loop break alarm setting,0->9999°C" '0->9999°F,Voltage
input:0->100% (R/W)
    cmbIden_Get.List(30) = "XB,Second alarm action selection,0->14" '(R/W)
    cmbIden_Get.List(31) = "HB,Second alarm action selection,0->100°C" '0->100°F,Voltage input:0-
>10% (R/W)
    cmbIden_Get.List(32) = "TG,Second alarm timer setting,0->600sec" '(R/W)
    cmbIden_Get.List(33) = "TH,HBA delay timer,0->600sec" '(R/W)
    cmbIden_Get.List(34) = "P1,Proportional band (Heating-side),0->9999°C/min" '0-
>999.9°F,Voltage input:0->100% (R/W)
    cmbIden_Get.List(35) = "I1,Intergral time,0->3600sec" '(R/W)
```

```
    cmbIden_Get.List(36) = "D1,Derivative time,0->3600sec" '(R/W)
    cmbIden_Get.List(37) = "W1,Anti-reset windup (ARW),1->100% of proportional band" '(R/W)
    cmbIden_Get.List(38) = "P2,Cooling-side proportional band,1->3000% of proportional band"
'(R/W)
    cmbIden_Get.List(39) = "V1,Overlap/deadband,-10->10°C" '-10->10°F,Voltage input:-10->10% of
span(R/W)
    cmbIden_Get.List(40) = "MH,ON/OFF action differential gap,0->50°C" '0->50°F,Voltage input:0-
>10% of span(R/W)
    cmbIden_Get.List(41) = "MR,Manual reset,-50->50%" '(Heating/cooling -100.0 to 100.0%) (R/W)
    cmbIden_Get.List(42) = "XP,Fazzy,0:OFF 1:ON" ' (R/W)
    cmbIden_Get.List(43) = "TO,Proportioning cycle (OUT1),1->100sec" ' (R/W)
    cmbIden_Get.List(44) = "OH,Output limit (High-limit),Low->105%" ' (Heating/cooling 0. to
105.0%)(R/W)
    cmbIden_Get.List(45) = "OL,Output limit (Low-limit),-5%->High" ' (R/W)
    cmbIden_Get.List(46) = "XE,Direct/reverse action selection,0:Dir 1:Rev" ' (R/W)
    cmbIden_Get.List(47) = "T1,Proportioning cycle (OUT2),0->100sec" ' (R/W)
    cmbIden_Get.List(48) = "OI,Output limit[high-limit](OUT2),0->105%" '(Cooling-side output)
(R/W)
    cmbIden_Get.List(49) = "LA,Analog output specification selection,0->4" ' (R/W)
    cmbIden_Get.List(50) = "HV,High limit analog output range,*7 See page 23" ' (R/W)
    cmbIden_Get.List(51) = "HW,Low limit analog output range,*7 See page 23" ' (R/W)
    cmbIden_Get.List(52) = "XI, Input type selection,0->37" ' (R/W)
    cmbIden_Get.List(53) = "XV,Scaling high-limit,Low->9999" ' (R/W)
    cmbIden_Get.List(54) = "XW,Scaling low-limit,-1999->High" ' (R/W)
    cmbIden_Get.List(55) = "XU,Decimal-point position selection,0->3" ' (R/W)
    cmbIden_Get.List(56) = "PQ,AUTO/MAN function selection,0:not provided 1:provided" ' (R/W)
    cmbIden_Get.List(57) = "DH,Control RUN/STOP display selection,0:not provided 1:provided" '
(R/W)
    cmbIden_Get.List(58) = "XR,Current transformer type selection,0:CTL-6-P-N 1:CTL-12-S56-10L-N"
' (R/W)
    cmbIden_Get.List(59) = "XQ,Air cooling/water cooling selection,0:Air cooling 1:Water cooling
(H/C)" ' (R/W)
    cmbIden_Get.List(60) = "GH,Auto-tuning (AT) differential,0->3600sec" ' (R/W)
    cmbIden_Get.List(61) = "WH,Action selection at input abnormality,0:No alarm action when
abnormal input 1:Output OFF 2:Output ON" ' (R/W)
    cmbIden_Get.List(62) = "XO,Universal output selection,REX- D100 has no universal output & no
identifier appears" ' (R/W)
    cmbIden_Get.ListIndex = 0   'default active M1 command

    'For Setting Parameters*********************************************************
    cmbIden_Set.List(0) = "J1,AUTO/MAN transfer,0:Auto 1:MAN"  '(R/W)
    cmbIden_Set.List(1) = "SR,RUN/STOP transfer,0:RUN 1:STOP"  '(R/W)
    cmbIden_Set.List(2) = "G1,PID/Auto-tuning transfer,0:PID 1:Auto-tuning"    '(R/W)
    cmbIden_Set.List(3) = "S1,Set-value (SV1) monitoring,Low->High"  ' (R/W)
    cmbIden_Set.List(4) = "ON,Manipulated output value (MV),Low->High" '(R/W)
    cmbIden_Set.List(5) = "S2,Step set-value (SV2),Low->High" '(R/W)
    cmbIden_Set.List(6) = "A1,First alarm setting,-1999->9999°C" '(R/W)
    cmbIden_Set.List(7) = "A2,Second alarm setting,-1999->9999°C" '(R/W)
    cmbIden_Set.List(8) = "A3,First heater break alarm setting,0->100A" '(R/W)
    cmbIden_Set.List(9) = "A4,Second heater break alarm setting,0->100A" '(R/W)
    cmbIden_Set.List(10) = "PB,PV bias,-1999->9999°C" '-199.9->999.9°F,Voltage input:-1999->9999V
(R/W)
    cmbIden_Set.List(11) = "HH,SV change rate limit,0->9999°C/min"  '0->999.9°F,Voltage input:0-
>100%/min (R/W)
    cmbIden_Set.List(12) = "XA,First alarm action selection,0->14" '(R/W)
    cmbIden_Set.List(13) = "HA,First alarm differential gap,0->100°C" '0->100°F,Voltage input:0-
>10% (R/W)
    cmbIden_Set.List(14) = "TD,First alarm timer setting,0->600sec" '(R/W)
    cmbIden_Set.List(15) = "A5,Control loop break alarm setting,0->7200sec" '(R/W)
    cmbIden_Set.List(16) = "V3,Control loop break alarm setting,0->9999°C" '0->9999°F,Voltage
input:0->100% (R/W)
    cmbIden_Set.List(17) = "XB,Second alarm action selection,0->14" '(R/W)
    cmbIden_Set.List(18) = "HB,Second alarm action selection,0->100°C" '0->100°F,Voltage input:0-
>10% (R/W)
    cmbIden_Set.List(19) = "TG,Second alarm timer setting,0->600sec" '(R/W)
    cmbIden_Set.List(20) = "TH,HBA delay timer,0->600sec" '(R/W)
    cmbIden_Set.List(21) = "P1,Proportional band (Heating-side),0->9999°C/min" '0-
>999.9°F,Voltage input:0->100% (R/W)
    cmbIden_Set.List(22) = "I1,Intergral time,0->3600sec" '(R/W)
    cmbIden_Set.List(23) = "D1,Derivative time,0->3600sec" '(R/W)
    cmbIden_Set.List(24) = "W1,Anti-reset windup (ARW),1->100% of proportional band" '(R/W)
    cmbIden_Set.List(25) = "P2,Cooling-side proportional band,1->3000% of proportional band"
'(R/W)
    cmbIden_Set.List(26) = "V1,Overlap/deadband,-10->10°C" '-10->10°F,Voltage input:-10->10% of
span(R/W)
    cmbIden_Set.List(27) = "MH,ON/OFF action differential gap,0->50°C" '0->50°F,Voltage input:0-
>10% of span(R/W)
    cmbIden_Set.List(28) = "MR,Manual reset,-50->50%" '(Heating/cooling -100.0 to 100.0%) (R/W)
```

```
    cmbIden_Set.List(29) = "XP,Fazzy,0:OFF 1:ON" ' (R/W)
    cmbIden_Set.List(30) = "TO,Proportioning cycle (OUT1),1–>100sec" ' (R/W)
    cmbIden_Set.List(31) = "OH,Output limit (High–limit),Low–>105%" ' (Heating/cooling 0. to
105.0%)(R/W)
    cmbIden_Set.List(32) = "OL,Output limit (Low–limit),–5%–>High" ' (R/W)
    cmbIden_Set.List(33) = "XE,Direct/reverse action selection,0:Dir 1:Rev" ' (R/W)
    cmbIden_Set.List(34) = "T1,Proportioning cycle (OUT2),0–>100sec" ' (R/W)
    cmbIden_Set.List(35) = "OI,Output limit[high–limit](OUT2),0–>105%" '(Cooling–side output)
(R/W)
    cmbIden_Set.List(36) = "LA,Analog output specification selection,0–>4" ' (R/W)
    cmbIden_Set.List(37) = "HV,High limit analog output range" ' (R/W)
    cmbIden_Set.List(38) = "HW,Low limit analog output range" ' (R/W)
    cmbIden_Set.List(39) = "XI, Input type selection,0–>37" ' (R/W)
    cmbIden_Set.List(40) = "XV,Scaling high–limit,Low–>9999" ' (R/W)
    cmbIden_Set.List(41) = "XW,Scaling low–limit,–1999–>High" ' (R/W)
    cmbIden_Set.List(42) = "XU,Decimal–point position selection,0–>3" ' (R/W)
    cmbIden_Set.List(43) = "PQ,AUTO/MAN function selection,0:not provided 1:provided" ' (R/W)
    cmbIden_Set.List(44) = "DH,Control RUN/STOP display selection,0:not provided 1:provided" '
(R/W)
    cmbIden_Set.List(45) = "XR,Current transformer type selection,0:CTL–6–P–N 1:CTL–12–S56–10L–N"
' (R/W)
    cmbIden_Set.List(46) = "XQ,Air cooling/water cooling selection,0:Air cooling 1:Water cooling
(H/C)" ' (R/W)
    cmbIden_Set.List(47) = "GH,Auto–tuning (AT) differential,0–>3600sec" ' (R/W)
    cmbIden_Set.List(48) = "WH,Action selection at input abnormality,0:No alarm action when
abnormal input 1:Output OFF 2:Output ON" ' (R/W)
    cmbIden_Set.List(49) = "XO,Universal output selection,REX– D100 has no universal output & no
identifier appears" ' (R/W)
    cmbIden_Set.ListIndex = 3  'default active S1 command

End Sub

Private Sub cmbPort_click()
    If COMPort.PortOpen = True Then
        COMPort.PortOpen = False
    End If
    COMPort.CommPort = Mid(cmbPort.List(cmbPort.ListIndex), 4, 1) 'take last character as com
number
End Sub

Private Sub cmdGetValue_Get_Click()
    If Not cmbPort.DataChanged Then
        MsgBox "Please select port before continue!", vbOKOnly, "Port Configure"
    Else
        'Request data ----------------------------------------------------------------------
        Dim DAdd_Get$, Iden_Get$, dataRX_Get$
        DAdd_Get = txtDAdd_Get.Text
        Iden_Get = Mid(cmbIden_Get.List(cmbIden_Get.ListIndex), 1, 2)   'Talk first two
characters of cmbIden_Get's list content

        If Len(DAdd_Get) <= 1 Or Len(DAdd_Get) > 2 Or Val(DAdd_Get) > 32 Then
            MsgBox "Address is two digit and less than 32 device!", vbOKOnly, "Set Device
Address"
            txtDAdd_Get.SetFocus
        End If

        If COMPort.PortOpen = False Then  'Open port
            COMPort.PortOpen = True
        End If
        COMPort.Output = Chr(EOT)
        COMPort.Output = DAdd_Get + Iden_Get + Chr(ENQ)

'        COMPort.PortOpen = False 'Close port
        TmrRX_Get.Enabled = True
    End If
End Sub
Private Sub cmdScan_Get_Click()
    Dim DAdd_Get$, Iden_Get$, dataRX_Get$
'    Static i%
    If Not cmbPort.DataChanged Then
        MsgBox "Please select port before continue!", vbOKOnly, "Port Configure"
    Else
    'Request data ----------------------------------------------------------------------
        DAdd_Get = txtDAdd_Get.Text
        Iden_Get = Mid(cmbIden_Get.List(iScan), 1, 2)   'Talk first two characters of
cmbIden_Get's list content

        If Len(DAdd_Get) <= 1 Or Len(DAdd_Get) > 2 Or Val(DAdd_Get) > 32 Then
```

```
            MsgBox "Address is two digit and less than 32 device!", vbOKOnly, "Set Device
Address"
            txtDAdd_Get.SetFocus
        End If

        If COMPort.PortOpen = False Then  'Open port
            COMPort.PortOpen = True
        End If
        COMPort.Output = Chr(EOT)
        COMPort.Output = DAdd_Get + Iden_Get + Chr(ENQ)

        TmrScanData.Enabled = True
    End If
End Sub

Private Sub TmrScanData_Timer()
    Dim dataRX_Get$, DataStored$, DAdd_Get$
'    Static i%

    DAdd_Get = txtDAdd_Get.Text
    On Error Resume Next
    Open App.Path + "\" + "Parameter Setting Device N° " + DAdd_Get + ".csv" For Output As #1
    If iScan = 0 Then
        Print #1, "Device Number " + DAdd_Get
        Print #1, "N°,Identifier,Description,Data Range,Parameter's Value"
    End If


        dataRX_Get = COMPort.Input 'Data Receive from device
        txtReply_Get.Text = Mid(dataRX_Get, 4, 6)
        DataStored = Mid(dataRX_Get, 4, 6)
        Print #1, CStr(iScan + 1) + "," + cmbIden_Get.List(iScan) + "," + DataStored
        iScan = iScan + 1
    If iScan < cmbIden_Get.ListCount Then
        Call cmdScan_Get_Click
    Else
        TmrScanData.Enabled = False
        MsgBox "Scaning Finised", vbInformation, "Scaning Process"
        Close #1
        iScan = 0
    End If

End Sub

Private Sub TmrRX_Get_Timer()
    Dim dataRX_Get$

    If COMPort.PortOpen = False Then  'Open port
        COMPort.PortOpen = True
    End If

    dataRX_Get = COMPort.Input 'Data Receive from device
specified/Data has been sent", vbOKOnly, "EOT Reply"
    Call cmdGetValue_Get_Click
End Sub
Private Sub TmrClock_Timer()
    lblDate = Format$(Now, "dddd mm-dd-yyyy")
    lblTime = Time
End Sub
Private Sub cmdStop_Get_Click()
    TmrRX_Get.Enabled = False
    If COMPort.PortOpen = True Then
        COMPort.PortOpen = False
    End If
End Sub

Private Function BCC()
    Dim i%
    Dim Chstr$  'a character of BCC check string
    Dim AccBCC$  'Accumulative of BCC compute
    Dim B$
    AccBCC = Chr(0) 'initial for doing Xor
    For i = 1 To Len(BCCChStr)
        Chstr = Mid(BCCChStr, i, 1)
        AccBCC = Asc(AccBCC) Xor Asc(Chstr)
        AccBCC = Chr(AccBCC)    'convert Decimal form to Ascii character
    Next i
    BCC = AccBCC
```

```
End Function

Private Sub cmdBackSelMode_Click()
    If COMPort.PortOpen = True Then
        MsgBox "Please stop get value before leaving.", vbOKOnly
    Else
        Selection_Mode.Show
        Me.Hide
    End If
End Sub

Private Sub mnuHelp_Click()
    frmHelp.Show
End Sub

Private Sub cmdExit_Click()
    End
End Sub

'*****************************************************************************************
'                                    Setting Parameters                                  *
'*****************************************************************************************
Private Sub cmdSetValue_Click()
    If Not cmbPort.DataChanged Then
        MsgBox "Please select port before continue!", vbOKOnly, "Port Configure"
    Else
        'Sent data selection-------------------------------------------------------------
        Dim DAdd_Set$, Iden$, VSet$
        DAdd_Set = txtDAdd_Set.Text
        Iden = Mid(cmbIden_Set.List(cmbIden_Set.ListIndex), 1, 2)
        VSet = txtVSet.Text
        txtReply.Text = ""

        If Len(DAdd_Set) <= 1 Or Len(DAdd_Set) > 2 Or Val(DAdd_Set) > 32 Then
            MsgBox "Address is two digit and less than 32 devices!", vbOKOnly, "Set Device
Address"
            txtDAdd_Set.SetFocus
        End If
        BCCChStr = Iden + VSet + Chr(ETX)

        If COMPort.PortOpen = False Then  'Open port
            COMPort.PortOpen = True
        End If

        COMPort.Output = Chr(EOT)
        COMPort.Output = DAdd_Set
        COMPort.Break = False 'Clear break signal on transmission line
        COMPort.Output = Chr(STX) + BCCChStr + BCC
        txtDataSent.Text = Chr(STX) + BCCChStr + BCC

        TmrRX_Set.Enabled = True
    End If
End Sub

Private Sub TmrRX_Set_Timer()

    'Receice Reply-------------------------------------------------------------------
    Dim dataRX$, DAdd_Set$
    DAdd_Set = txtDAdd_Set.Text
    dataRX = COMPort.Input
    If (dataRX = Chr(ACK)) Then
        txtReply.Text = "ACK"
        COMPort.Output = DAdd_Set + Chr(STX) + BCCChStr + BCC
    ElseIf (dataRX = Chr(NAK)) Then
        txtReply.Text = "NAK"
        COMPort.Output = Chr(STX) + BCCChStr + BCC
    Else
        txtReply.Text = "No Reply"
    End If

    COMPort.PortOpen = False 'Close port
    TmrRX_Set.Enabled = False

End Sub
```

For “Define_Parameters Module”

```
Option Explicit
```

```
Public Const STX = &H2
Public Const EOT = &H4
Public Const ENQ = &H5
Public Const ACK = &H6
Public Const NAK = &H15
Public Const ETX = &H3
Public BCCChStr$    'Extracted string used for BCC Check
Public TimeOut As Boolean
Public TimeLimit As Integer
```

APPENDIX D: PROGRAM CODE FOR SMU KEITHLEY 2602A

```
Option Explicit
'For Picture Capture
Private Declare Sub keybd_event Lib "user32" (ByVal bVk As Byte, ByVal bScan As Byte, ByVal
dwFlags _
    As Long, ByVal dwExtraInfo As Long)

'Global Variables*******************************
Private comPort&
Private ilist_A$, vlist_A$
Private MeasDate_A$, MeasTime_A
Private MeasPointorStep_A As Boolean
Private MeasPoint_A&, MeasCountNumber_A&
Private SyncOut_A&
Private DataReply_A$

Private ilist_B$, vlist_B$
Private MeasDate_B$, MeasTime_B
Private MeasPointorStep_B As Boolean
Private MeasPoint_B&, MeasCountNumber_B&
Private SyncOut_B&
Private DataReply_B$
Private ton_A#, ton_B#

'For Matlab Automation Server
Private objMatLab As Object
Private Result As String

Dim LState As Boolean

Private Sub chkSync_A_Click()
    If chkSync_A.Value = Checked Then
        txtToff_A = 5 '5 second waitting time of spectrometer operation
        txtTon_A = 1
        SyncOut_A = 1
    Else
        SyncOut_A = 0
    End If
End Sub

Private Sub cmbLedType_A_Click()
    Call cmbSourceMode_A_Click
    txtUserParameter_A.Text = cmbLedType_A.List(cmbLedType_A.ListIndex)
End Sub

Private Sub cmbPort_Click()

    If Mid(cmbPort.List(cmbPort.ListIndex), 9) = "RAW-SOCKET" Then
        TCPSock.Close
        comPort = 5025    'Reserve for global variable Port number
    ElseIf Mid(cmbPort.List(cmbPort.ListIndex), 9) = "TELNET" Then
        TCPSock.Close
        comPort = 23
    ElseIf Mid(cmbPort.List(cmbPort.ListIndex), 9) = "DST" Then
        TCPSock.Close
        comPort = 5030
    End If

    TCPSock.RemotePort = comPort
    TCPSock.Connect
End Sub

Private Sub cmbSourceMode_A_Click()
    Select Case cmbSourceMode_A.ListIndex
        Case 0
            Call SRC_I_A
            txtBiasLevel_A.Enabled = True
            txtSourceStart_A.Enabled = False
            txtToff_A.Enabled = True
        Case 2, 4
            Call SRC_I_A
```

```
            txtBiasLevel_A.Enabled = True
            txtSourceStart_A.Enabled = True
            txtToff_A.Enabled = True
        Case 6, 8
            Call SRC_I_A
            txtBiasLevel_A.Enabled = False
            txtSourceStart_A.Enabled = True
            txtToff_A.Enabled = False
        Case 1
            Call SRC_V_A
            txtBiasLevel_A.Enabled = True
            txtSourceStart_A.Enabled = False
            txtToff_A.Enabled = True
        Case 3, 5
            Call SRC_V_A
            txtBiasLevel_A.Enabled = True
            txtSourceStart_A.Enabled = True
            txtToff_A.Enabled = True
        Case 7, 9
            Call SRC_V_A
            txtBiasLevel_A.Enabled = False
            txtSourceStart_A.Enabled = True
            txtToff_A.Enabled = False
        Case 10
            Call SRC_I_A
            ilist_A = InputBox("Please enter your list of each current value seperated by ,
(comma)", _
            "Current List")
        Case 11
            vlist_A = InputBox("Please enter your list of each voltage value seperated by ,
(comma)" _
            , "Voltage List")
    End Select
End Sub

Private Sub cmdExit_Click()
    End
End Sub

Private Sub cmdLoadSetting_A_Click()
    Dim FullPath$, Filename$, sName$, ValLoad$, State As Variant

    cdlFile_A.Filter = "Apps (*.csv)|*.csv|All files (*.*)|*.*"
    cdlFile_A.DefaultExt = "csv"
    cdlFile_A.DialogTitle = "Load File"
    cdlFile_A.Filename = ""
    cdlFile_A.ShowOpen
    On Error GoTo OnError 'In case when save file is cancel
    'The FileName property gives you the variable of full path name need to use
    FullPath = cdlFile_A.Filename 'Return a full pathname and filename of an opened or saved file
    Filename = cdlFile_A.FileTitle

    Open FullPath For Input As #1

    Input #1, sName, ValLoad
    cmbSourceMode_A.ListIndex = ValLoad
    Input #1, sName, ValLoad
    txtBiasLevel_A.Text = ValLoad
    Input #1, sName, ValLoad
    txtSourceStart_A.Text = ValLoad
    Input #1, sName, ValLoad
    txtSourceStop_A.Text = ValLoad
    Input #1, sName, ValLoad
    txtSourceLimit_A.Text = ValLoad
    Input #1, sName, ValLoad
    txt_Source_Rangei_A.Text = ValLoad
    Input #1, sName, ValLoad
    txt_Source_Rangev_A.Text = ValLoad
    Input #1, sName, ValLoad
    txt_Meas_Rangei_A.Text = ValLoad
    Input #1, sName, ValLoad
    txt_Meas_Rangev_A.Text = ValLoad
    Input #1, sName, ValLoad
    txtTon_A.Text = ValLoad
    Input #1, sName, ValLoad
    txtToff_A.Text = ValLoad
    Input #1, sName, ValLoad
    txtMeasPointNum_A.Text = ValLoad
```

```
    Input #1, sName, ValLoad
    txtMeasCountNumber_A.Text = ValLoad
    Input #1, sName, ValLoad
    txtMeasSpeed_A.Text = ValLoad
    Input #1, sName, ValLoad
    opt4Wire_A.Value = ValLoad
    Input #1, sName, ValLoad
    opt2Wire_A.Value = ValLoad
    Close #1

    txtUserParameter_A.Text = Filename

OnError:
    Exit Sub
End Sub

Private Sub cmdPicCapure_Click()
    Static i%
    Capture_Picture App.Path + "\Picture 0" + CStr(i) + ".bmp"
    i = i + 1
End Sub
Public Function Capture_Picture(ByVal Destination$) As Boolean
On Error GoTo errl
    DoEvents
        Call keybd_event(vbKeySnapshot, 1, 0, 0) 'Get the screen and copy it to clipboard
    DoEvents 'let computer catch up
        SavePicture Clipboard.GetData(vbCFBitmap), Destination$ ' saves the clipboard data to a
BMP file
        Capture_Picture = True
    Exit Function
errl:
    MsgBox "Error number: " & Err.Number & ". " & Err.Description
    Capture_Picture = False
End Function

Private Sub cmdPlot_A_Click()

    tmrPlot_A.Enabled = True

End Sub

Private Sub cmdRun_A_Click()
    Dim bias_A#, start_A#, stop_A#, level_A#, limit_A#, SourceRangei_A#, SourceRangev_A#, _
    MeasRangei_A#, MeasRangev_A#, toff_A#
    Dim T_MeasSpeed_A#, nplc_A#
    Const tag_A = 1
    Const Freq = 50
    Dim MeasTime$
    Dim iMeasCount&

    'Get parameter values ------------------------------
        bias_A = Val(txtBiasLevel_A.Text)
        start_A = Val(txtSourceStart_A.Text)
        stop_A = Val(txtSourceStop_A.Text)
        level_A = stop_A
        limit_A = Val(txtSourceLimit_A.Text)
        SourceRangei_A = Val(txt_Source_Rangei_A.Text)
        SourceRangev_A = Val(txt_Source_Rangev_A.Text)
        MeasRangei_A = Val(txt_Meas_Rangei_A.Text)
        MeasRangev_A = Val(txt_Meas_Rangev_A.Text)
        ton_A = Val(txtTon_A.Text)
        toff_A = Val(txtToff_A.Text)
        If lblMeasPointNum_A.Caption = "Meas Step Value" Then
            MeasPoint_A = (Val(txtSourceStop_A.Text) - Val(txtSourceStart_A.Text)) /
Val(txtMeasPointNum_A.Text) + 1
        Else
            MeasPoint_A = Val(txtMeasPointNum_A.Text)
        End If
        MeasCountNumber_A = Val(txtMeasCountNumber_A.Text)
        T_MeasSpeed_A = Val(txtMeasSpeed_A.Text) 'in second

    If Not cmbPort.DataChanged Then
        MsgBox "Please select port before continue!", vbOKOnly, "Configure Port"
        On Error GoTo ErrorConnection
    Else

    ' Send Command-----------------------------------------------------------------
        For iMeasCount = 1 To MeasCountNumber_A 'Repeat Measurement
```

```
            On Error GoTo ErrorConnection
            TCPSock.SendData "reset()" + vbLf
            TCPSock.SendData "smua.nvbuffer1.clear()" + vbLf
            Select Case cmbSourceMode_A.ListIndex
                Case 0, 1, 2, 3, 4, 5
                    TCPSock.SendData "smua.source.rangei =" + CStr(SourceRangei_A) + vbLf
                    TCPSock.SendData "smua.source.rangev =" + CStr(SourceRangev_A) + vbLf
                    TCPSock.SendData "smua.measure.rangei =" + CStr(MeasRangei_A) + vbLf
                    TCPSock.SendData "smua.measure.rangev =" + CStr(MeasRangev_A) + vbLf

                    TCPSock.SendData "smua.measure.autozero = smua.AUTOZERO_ONCE" + vbLf
                    TCPSock.SendData "smua.nvbuffer1.appendmode = 1" + vbLf

                Case 6, 7, 8, 9, 10, 11
                    TCPSock.SendData "smua.measure.autorangev = smua.AUTORANGE_ON" + vbLf
                    TCPSock.SendData "smua.measure.autorangei = smua.AUTORANGE_ON" + vbLf
                    TCPSock.SendData "smua.source.autorangev = smua.AUTORANGE_ON" + vbLf
                    TCPSock.SendData "smua.source.autorangei = smua.AUTORANGE_ON" + vbLf
            End Select

            TCPSock.SendData "smua.nvbuffer1.collectsourcevalues = 1" + vbLf
            TCPSock.SendData "smua.nvbuffer1.collecttimestamps = 1" + vbLf
            TCPSock.SendData "smua.source.delay = 1" + vbLf 'Sourec delay
            TCPSock.SendData "smua.measure.delay = smua.DELAY_AUTO" + vbLf 'Measure delay
            TCPSock.SendData "smua.measure.interval = 0.1" + vbLf 'Measure interval
            TCPSock.SendData "digio.trigger [1].mode = 1" + vbLf 'digio.TRIG_FALLING
            TCPSock.SendData "digio.trigger [1].pulsewidth =" + CStr(toff_A + ton_A / 2) + vbLf
'5 sec waitting time of spectrometer operation
            'Wire Mode-----------------------------------------------------------------
                If opt2Wire_A.Value = True Then
                    TCPSock.SendData "smua.sense=smua.SENSE_LOCAL" + vbLf
                ElseIf opt4Wire_A.Value = True Then
                    TCPSock.SendData "smua.sense=smua.SENSE_REMOTE" + vbLf
                End If
            'Set Measurement Speed Chanel A--------------------------------------------
                nplc_A = Freq * T_MeasSpeed_A
                TCPSock.SendData "smua.measure.nplc=" + CStr(nplc_A) + vbLf
            'Start Measure Mode
                TCPSock.SendData "smua.source.output = smua.OUTPUT_ON" + vbLf

                If cmbSourceMode_A.ListIndex = 0 Then
                    TCPSock.SendData "ConfigPulseIMeasureV(smua," + CStr(bias_A) + "," +
CStr(level_A) _
                    + "," + CStr(limit_A) + "," + CStr(ton_A) + "," + CStr(toff_A) + "," _
                    + CStr(MeasPoint_A) + "," + "smua.nvbuffer1" + "," + CStr(tag_A) + ",nil," +
CStr(SyncOut_A) + ")" + vbLf
                ElseIf cmbSourceMode_A.ListIndex = 1 Then
    '                TCPSock.SendData "digio.writeport(0)"
                    TCPSock.SendData "ConfigPulseVMeasureI(smua," + CStr(bias_A) + "," +
CStr(level_A) _
                    + "," + CStr(limit_A) + "," + CStr(ton_A) + "," + CStr(toff_A) + "," _
                    + CStr(MeasPoint_A) + "," + "smua.nvbuffer1" + "," + CStr(tag_A) + ",nil," +
CStr(SyncOut_A) + ")" + vbLf
                ElseIf cmbSourceMode_A.ListIndex = 2 Then
                    TCPSock.SendData "ConfigPulseIMeasureVSweepLin(smua," + CStr(bias_A) + "," _
                    + CStr(start_A) + "," + CStr(stop_A) + "," + CStr(limit_A) + "," +
CStr(ton_A) + "," _
                    + CStr(toff_A) + "," + CStr(MeasPoint_A) + "," + "smua.nvbuffer1" + "," +
CStr(tag_A) + ",nil," + CStr(SyncOut_A) + ")" + vbLf
                ElseIf cmbSourceMode_A.ListIndex = 3 Then
                    TCPSock.SendData "ConfigPulseVMeasureISweepLin(smua," + CStr(bias_A) + "," _
                    + CStr(start_A) + "," + CStr(stop_A) + "," + CStr(limit_A) + "," +
CStr(ton_A) + "," _
                    + CStr(toff_A) + "," + CStr(MeasPoint_A) + "," + "smua.nvbuffer1" + "," +
CStr(tag_A) + ",nil," + CStr(SyncOut_A) + ")" + vbLf
                ElseIf cmbSourceMode_A.ListIndex = 4 Then
                    TCPSock.SendData "ConfigPulseIMeasureVSweepLog(smua," + CStr(bias_A) + "," _
                    + CStr(start_A) + "," + CStr(stop_A) + "," + CStr(limit_A) + "," +
CStr(ton_A) + "," _
                    + CStr(toff_A) + "," + CStr(MeasPoint_A) + "," + "smua.nvbuffer1" + "," +
CStr(tag_A) + ",nil," + CStr(SyncOut_A) + ")" + vbLf
                ElseIf cmbSourceMode_A.ListIndex = 5 Then
                    TCPSock.SendData "ConfigPulseVMeasureISweepLog(smua," + CStr(bias_A) + "," _
                    + CStr(start_A) + "," + CStr(stop_A) + "," + CStr(limit_A) + "," +
CStr(ton_A) + "," _
                    + CStr(toff_A) + "," + CStr(MeasPoint_A) + "," + "smua.nvbuffer1" + "," +
CStr(tag_A) + ",nil," + CStr(SyncOut_A) + ")" + vbLf
                ElseIf cmbSourceMode_A.ListIndex = 6 Then
```

```
                    TCPSock.SendData "smua.source.limitv = " + CStr(limit_A) + vbLf
                    TCPSock.SendData "SweepILinMeasureV(smua," + CStr(start_A) + "," +
CStr(stop_A) + "," _
                    + CStr(ton_A) + "," + CStr(MeasPoint_A) + ")" + vbLf
                ElseIf cmbSourceMode_A.ListIndex = 7 Then
                    TCPSock.SendData "smua.source.limiti = " + CStr(limit_A) + vbLf
                    TCPSock.SendData "SweepVLinMeasureI(smua," + CStr(start_A) + "," +
CStr(stop_A) + "," _
                    + CStr(ton_A) + "," + CStr(MeasPoint_A) + ")" + vbLf
                ElseIf cmbSourceMode_A.ListIndex = 8 Then
                    TCPSock.SendData "smua.source.limitv = " + CStr(limit_A) + vbLf
                    TCPSock.SendData "SweepILogMeasureV(smua," + CStr(start_A) + "," +
CStr(stop_A) + "," _
                    + CStr(ton_A) + "," + CStr(MeasPoint_A) + ")" + vbLf
                ElseIf cmbSourceMode_A.ListIndex = 9 Then
                    TCPSock.SendData "smua.source.limiti = " + CStr(limit_A) + vbLf
                    TCPSock.SendData "SweepVLogMeasureI(smua," + CStr(start_A) + "," +
CStr(stop_A) + "," _
                    + CStr(ton_A) + "," + CStr(MeasPoint_A) + ")" + vbLf
                ElseIf cmbSourceMode_A.ListIndex = 10 Then
                    TCPSock.SendData "smua.source.limitv = " + CStr(limit_A) + vbLf
                    TCPSock.SendData "SweepIListMeasureV(smua," + "{" + ilist_A + "}" + "," +
CStr(ton_A) _
                    + "," + CStr(MeasPoint_A) + ")" + vbLf
                ElseIf cmbSourceMode_A.ListIndex = 10 Then
                    TCPSock.SendData "smua.source.limiti = " + CStr(limit_A) + vbLf
                    TCPSock.SendData "SweepVListMeasureI(smua," + "{" + vlist_A + "}" + "," +
CStr(ton_A) _
                    + "," + CStr(MeasPoint_A) + ")" + vbLf
                End If

                TCPSock.SendData "InitiatePulseTest(" + CStr(tag_A) + ")" + vbLf
                ' Store Measured Data
                Select Case cmbSourceMode_A.ListIndex
                    Case 0, 2, 4, 6, 8, 10
                        TCPSock.SendData "printbuffer(1, smua.nvbuffer1.n,
smua.nvbuffer1.readings)" + vbLf
                        'TCPSock.SendData "print(""\n"")" + vbLf
                        TCPSock.SendData "waitcomplete()" + vbLf

                        TCPSock.SendData "printbuffer(1, smua.nvbuffer1.n,
smua.nvbuffer1.sourcevalues)" + vbLf
                        'TCPSock.SendData "print(""\n"")" + vbLf
                        TCPSock.SendData "waitcomplete()" + vbLf

                        TCPSock.SendData "printbuffer(1, smua.nvbuffer1.n,
smua.nvbuffer1.timestamps)" + vbLf
                        TCPSock.SendData "waitcomplete()" + vbLf
                    Case 1, 3, 5, 7, 9, 11
                        TCPSock.SendData "printbuffer(1, smua.nvbuffer1.n,
smua.nvbuffer1.sourcevalues)" + vbLf
                        'TCPSock.SendData "print(""\n"")" + vbLf
                        TCPSock.SendData "waitcomplete()" + vbLf

                        TCPSock.SendData "printbuffer(1, smua.nvbuffer1.n,
smua.nvbuffer1.readings)" + vbLf
                        'TCPSock.SendData "print(""\n"")" + vbLf
                        TCPSock.SendData "waitcomplete()" + vbLf

                        TCPSock.SendData "printbuffer(1, smua.nvbuffer1.n,
smua.nvbuffer1.timestamps)" + vbLf
                        'TCPSock.SendData "print(""\n"")" + vbLf
                        TCPSock.SendData "waitcomplete()" + vbLf
                End Select

                TCPSock.SendData "smua.source.output = smua.OUTPUT_OFF" + vbLf
        Next iMeasCount
    End If
    TCPSock.SendData "beeper.enable = beeper.ON" + vbLf
    TCPSock.SendData "beeper.beep(1,300)" + vbLf
'    TCPSock.SendData "beeper.enable = beeper.OFF" + vbLf

    MeasDate_A = Format(Date, "yyyy-mm-dd")
    MeasTime_A = Format(Time, "hh-mm-ss AM/PM")

ErrorConnection:
'        MsgBox "Please select port before continue!", vbOKOnly, "Configure Port"
```

```
End Sub

Private Sub cmdSave_A_Click()
    tmrReadData_A.Enabled = True
End Sub

Private Sub cmdSaveSetting_A_Click()
    Dim FullPath$, Filename$

    cdlFile_A.Filter = "Apps (*.csv)|*.csv|All files (*.*)|*.*"
    cdlFile_A.DefaultExt = "csv"
    cdlFile_A.DialogTitle = "Save File"
    cdlFile_A.Filename = txtUserParameter_A.Text
    cdlFile_A.ShowSave
    On Error Resume Next 'In case when save file is cancel
    'The FileName property gives you the variable of full path name need to use
    FullPath = cdlFile_A.Filename 'Return a full pathname and filename of an opened or saved file
    Filename = cdlFile_A.FileTitle

    Open FullPath For Output As #1
    Print #1, "Select Source Mode," + CStr(cmbSourceMode_A.ListIndex)
    Print #1, "Bias Level (A)," + txtBiasLevel_A.Text
    Print #1, "Source Start Value (A)," + txtSourceStart_A.Text
    Print #1, "Source Stop Value (A)," + txtSourceStop_A.Text
    Print #1, "Source-Limit (V)," + txtSourceLimit_A.Text

    Print #1, "Source-Rangei (A)," + txt_Source_Rangei_A.Text
    Print #1, "Source-Rangev (V)," + txt_Source_Rangev_A.Text
    Print #1, "Meas-Rangei (A)," + txt_Meas_Rangei_A.Text
    Print #1, "Meas-Rangev (A)," + txt_Meas_Rangev_A.Text

    Print #1, "Ton (sec)," + txtTon_A.Text
    Print #1, "Toff (sec)," + txtToff_A.Text
    Print #1, "Meas Point Number," + txtMeasPointNum_A.Text
    Print #1, "Meas Count Number," + txtMeasCountNumber_A.Text
    Print #1, "Measurement Speed (s)," + txtMeasSpeed_A.Text
    Print #1, "opt4Wire_A," + CStr(opt4Wire_A.Value)
    Print #1, "opt2Wire_A," + CStr(opt2Wire_A.Value)
    Close #1
    txtUserParameter_A.Text = Filename
End Sub

Private Sub Form_Activate()
    Me.Top = 50
    TCPSock.RemoteHost = InputBox("Please enter device's IP Address:", " Setup IP Address",
"10.20.40.20")
End Sub

Private Sub Form_Deactivate()
    TCPSock.Close
End Sub

Private Sub Form_Load()
    'Port Selection ---------------------------------------------------------
    cmbPort.AddItem "TCP/IP: RAW-SOCKET"
    cmbPort.AddItem "TCP/IP: TELNET"
    cmbPort.AddItem "TCP/IP: DST"   ' (dead socket termination)
'    cmbPort.ListIndex = 0   'RAW-SOCKET Port
'    comPort = 5025  'RAW-SOCKET Port

    'Chanel A-----------------------------------------------------------------
    'f, msg = ConfigPulseIMeasureV(smu, bias, level, limit, ton, toff, points, buffer,tag,
sync_in, sync_out, sync_in_timeout, sync_in_abort)
    cmbSourceMode_A.List(0) = "PulseIMeasureV"
    'f, msg = ConfigPulseVMeasureI(smu, bias, level, limit, ton, toff, points, buffer, tag,
sync_in, sync_out, sync_in_timeout, sync_in_abort)
    cmbSourceMode_A.List(1) = "PulseVMeasureI"
    'f, msg = ConfigPulseIMeasureVSweepLin(smu, bias, start, stop, limit, ton, toff, points,
buffer, tag, sync_in, sync_out, sync_in_timeout, sync_in_abort)
    cmbSourceMode_A.List(2) = "PulsedIMeasureVLin"
    'f, msg = ConfigPulseVMeasureISweepLin(smu, bias, start, stop, limit, ton, toff, points,
buffer, tag, sync_in, sync_out, sync_in_timeout, sync_in_abort)
    cmbSourceMode_A.List(3) = "PulsedVMeasureILin"
    'f, msg = ConfigPulseIMeasureVSweepLog(smu, bias, start, stop, limit, ton, toff, points,
buffer, tag, sync_in, sync_out, sync_in_timeout, sync_in_abort)
    cmbSourceMode_A.List(4) = "PulsedIMeasureVLog"
    'f, msg = ConfigPulseVMeasureISweepLog(smu, bias, start, stop, limit, ton, toff, points,
buffer, tag, sync_in, sync_out, sync_in_timeout, sync_in_abort)
```

```
    cmbSourceMode_A.List(5) = "PulsedVMeasureILog"
    'SweepILinMeasureV(smu, starti, stopi, stime, points)
    cmbSourceMode_A.List(6) = "DCSweepIMeasureVLin"
    'SweepVLinMeasureI(smu, startv, stopv, stime, points)
    cmbSourceMode_A.List(7) = "DCSweepVMeasureILin"
    'SweepILogMeasureV(smu, starti, stopi, stime, points)
    cmbSourceMode_A.List(8) = "DCSweepIMeasureVLog"
    'SweepVLogMeasureI(smu, startv, stopv, stime, points)
    cmbSourceMode_A.List(9) = "DCSweepVMeasureILog"
    'SweepIListMeasureV(smu, ilist, stime, points)
    cmbSourceMode_A.List(10) = "ListIMeasureV"
    'SweepVListMeasureI(smu, ilist, stime, points)
    cmbSourceMode_A.List(11) = "ListVMeasureI"
    cmbSourceMode_A.ListIndex = 7
    cmbLedType_A.ListIndex = 0

    'Chanel B-----------------------------------------------------------------
    'f, msg = ConfigPulseIMeasureV(smu, bias, level, limit, ton, toff, points, buffer,tag,
sync_in, sync_out, sync_in_timeout, sync_in_Bbort)
    cmbSourceMode_B.List(0) = "PulseIMeasureV"
    'f, msg = ConfigPulseVMeasureI(smu, bias, level, limit, ton, toff, points, buffer, tag,
sync_in, sync_out, sync_in_timeout, sync_in_Bbort)
    cmbSourceMode_B.List(1) = "PulseVMeasureI"
    'f, msg = ConfigPulseIMeasureVSweepLin(smu, bias, start, stop, limit, ton, toff, points,
buffer, tag, sync_in, sync_out, sync_in_timeout, sync_in_Bbort)
    cmbSourceMode_B.List(2) = "PulsedIMeasureVLin"
    'f, msg = ConfigPulseVMeasureISweepLin(smu, bias, start, stop, limit, ton, toff, points,
buffer, tag, sync_in, sync_out, sync_in_timeout, sync_in_Bbort)
    cmbSourceMode_B.List(3) = "PulsedVMeasureILin"
    'f, msg = ConfigPulseIMeasureVSweepLog(smu, bias, start, stop, limit, ton, toff, points,
buffer, tag, sync_in, sync_out, sync_in_timeout, sync_in_Bbort)
    cmbSourceMode_B.List(4) = "PulsedIMeasureVLog"
    'f, msg = ConfigPulseVMeasureISweepLog(smu, bias, start, stop, limit, ton, toff, points,
buffer, tag, sync_in, sync_out, sync_in_timeout, sync_in_Bbort)
    cmbSourceMode_B.List(5) = "PulsedVMeasureILog"
    'SweepILinMeasureV(smu, starti, stopi, stime, points)
    cmbSourceMode_B.List(6) = "DCSweepIMeasureVLin"
    'SweepVLinMeasureI(smu, startv, stopv, stime, points)
    cmbSourceMode_B.List(7) = "DCSweepVMeasureILin"
    'SweepILogMeasureV(smu, starti, stopi, stime, points)
    cmbSourceMode_B.List(8) = "DCSweepIMeasureVLog"
    'SweepVLogMeasureI(smu, startv, stopv, stime, points)
    cmbSourceMode_B.List(9) = "DCSweepVMeasureILog"
    'SweepIListMeasureV(smu, ilist, stime, points)
    cmbSourceMode_B.List(10) = "ListIMeasureV"
    'SweepVListMeasureI(smu, ilist, stime, points)
    cmbSourceMode_B.List(11) = "ListVMeasureI"
    cmbSourceMode_B.ListIndex = 7
    cmbLedType_B.ListIndex = 0

    Set objMatLab = CreateObject("Matlab.Application")
    Result = objMatLab.MinimiZeCommandWindow()
    Result = objMatLab.quit

End Sub

Private Sub lblMeasPointNum_A_Click()
    Dim Step#, MeasPoint_A&
    If Not MeasPointorStep_A And (cmbSourceMode_A.ListIndex = 2 Or cmbSourceMode_A.ListIndex = 3
_
                        Or cmbSourceMode_A.ListIndex = 6 Or cmbSourceMode_A.ListIndex = 7) Then
        lblMeasPointNum_A.Caption = "Meas Step Value"
        MeasPointorStep_A = Not MeasPointorStep_A
        Step = (Val(txtSourceStop_A.Text) - Val(txtSourceStart_A.Text)) /
(Val(txtMeasPointNum_A.Text) - 1)
        txtMeasPointNum_A.Text = Step
    ElseIf MeasPointorStep_A And (cmbSourceMode_A.ListIndex = 2 Or cmbSourceMode_A.ListIndex = 3
_
                        Or cmbSourceMode_A.ListIndex = 6 Or cmbSourceMode_A.ListIndex = 7) Then
        lblMeasPointNum_A.Caption = "Meas Point Number"
        MeasPointorStep_A = Not MeasPointorStep_A
        MeasPoint_A = (Val(txtSourceStop_A.Text) - Val(txtSourceStart_A.Text)) /
Val(txtMeasPointNum_A.Text) + 1
        txtMeasPointNum_A.Text = MeasPoint_A
    End If
End Sub

Private Sub tmrClock_Timer()
```

```
    lblDate = Date
    lblTime = Time
End Sub

Private Sub tmrFlashName_Timer()
    If LState = True Then
        lblMyName.Visible = True
    Else
        lblMyName.Visible = False
    End If
    LState = Not LState
End Sub

Private Sub tmrPlot_A_Timer()
    Dim dataRead$, DataReply_A_Local$
    Dim i%
    Dim MlabPath$

    On Error GoTo ErrorCom
    TCPSock.GetData DataReply_A_Local
    If DataReply_A_Local$ <> "" Then
        DataReply_A = DataReply_A_Local
    End If

    Open App.Path + "\SavePlotData_A.csv" For Output As #1
    Print #1, DataReply_A 'stored data to global variable DataReply_A
    Close #1
ErrorCom:
    MlabPath = App.Path
    Result = objMatLab.execute("clear all")
    Result = objMatLab.PutCharArray("MlabPath", "base", MlabPath)
    Result = objMatLab.execute("data=xlsread(strcat(MlabPath,'\SavePlotData_A.csv'));")
    Result = objMatLab.execute("Legend_A=[];")
    For i = 1 To MeasCountNumber_A
        Result = objMatLab.PutWorkspaceData("i", "base", i)
        Result = objMatLab.execute("Voltage(:,i)=data(3*i-2,:);")
        Result = objMatLab.execute("Current(:,i)=data(3*i-1,:);")
        Result = objMatLab.execute("Time(:,i)=data(3*i,:);")
        Result = objMatLab.execute("Legend_A=[Legend_A,strcat({strcat(num2str(i),'
Measure')})];")
    Next

    Result = objMatLab.PutWorkspaceData("Ton", "base", ton_A)

    If optPlotCurve(0).Value = True And optPlotScale(0).Value = True Then 'Case Current vs
Voltage & Log Scale
        Result = objMatLab.execute("semilogy(Voltage,abs(Current));")
        Result = objMatLab.execute("title('Current vs Voltage'),xlabel('Voltage in
(V)'),ylabel('Currentin (A)'),legend(Legend_A),grid")
    ElseIf optPlotCurve(0).Value = True And optPlotScale(1).Value = True Then 'Case Current vs
Voltage & Log Linear
        Result = objMatLab.execute("plot(Voltage,abs(Current));")
        Result = objMatLab.execute("title('Current vs Voltage'),xlabel('Voltage in
(V)'),ylabel('Currentin (A)'),legend(Legend_A),grid")
    ElseIf optPlotCurve(1).Value = True And optPlotScale(0).Value = True Then 'Case Current vs
Time & Log Scale
        Result = objMatLab.execute("semilogy(Time,abs(Current));")
        Result = objMatLab.execute("title('Current vs Voltage'),xlabel('Time in
(s)'),ylabel('Currentin (A)'),legend(Legend_A),grid")
    ElseIf optPlotCurve(1).Value = True And optPlotScale(1).Value = True Then 'Case Current vs
Time & Log Linear
        Result = objMatLab.execute("plot(Time,abs(Current));")
        Result = objMatLab.execute("title('Current vs Voltage'),xlabel('Time in
(s)'),ylabel('Currentin (A)'),legend(Legend_A),grid")
    ElseIf optPlotCurve(2).Value = True And optPlotScale(0).Value = True Then 'Case Voltage vs
Time & Log Scale
        Result = objMatLab.execute("semilogy(Time,Voltage);")
        Result = objMatLab.execute("title('Current vs Voltage'),xlabel('Time in
(s)'),ylabel('Voltage (V)'),legend(Legend_A),grid")
    ElseIf optPlotCurve(2).Value = True And optPlotScale(1).Value = True Then 'Case Voltage vs
Time & Log Linear
        Select Case cmbSourceMode_A.ListIndex
            Case 0, 1, 2, 3, 4, 5
                Result = objMatLab.execute("bar(Time,Voltage,Ton);")
            Case 6, 7, 8, 9
                Result = objMatLab.execute("stairs(Time,Voltage);")
        End Select
```

```
        Result = objMatLab.execute("title('Current vs Voltage'),xlabel('Time in
(s)'),ylabel('Voltage (V)'),legend(Legend_A),grid")
    End If

    Result = objMatLab.execute("set(gcf,'Visible','off')")
    Result = objMatLab.execute("set(gcf, 'Position', [0, 0, 550, 250])")
    Result = objMatLab.execute("hgexport(gcf,'-clipboard')")
    ImgPlot.Picture = Clipboard.GetData()

'    Clipboard.Clear

    tmrPlot_A.Enabled = False

End Sub

Private Sub txtMeasSpeed_A_lostfocus()
    If Val(txtMeasSpeed_A.Text) < 0.00002 Or Val(txtMeasSpeed_A.Text) > 0.5 Then
'0.001<nplc<25
        MsgBox "Measurement speed range is between 0.00002 sec 0.5 sec", vbOKOnly, _
        "Speed Configuration"
        txtMeasSpeed_A.SetFocus
    End If
End Sub

Private Sub SRC_I_A()
    If cmbLedType_A.List(cmbLedType_A.ListIndex) = "Cree" Then
        lblBiasLevel_A.Caption = "Bias Level (A)"
        txtBiasLevel_A = 0
        lblSourceStart_A.Caption = "Source Start Value (A)"
        txtSourceStart_A.Text = 0 'Format(1, "1e-6")
        lblSourceStop_A.Caption = "Source Stop Value (A)"
        txtSourceStop_A = 0.35
        lblSourceLimit_A.Caption = "Source Limit (V)"
        txtSourceLimit_A.Text = 3.15
    ElseIf cmbLedType_A.List(cmbLedType_A.ListIndex) = "Osram" Then
        lblBiasLevel_A.Caption = "Bias Level (A)"
        txtBiasLevel_A = 0
        lblSourceStart_A.Caption = "Source Start Value (A)"
        txtSourceStart_A.Text = 0 'Format(1, "1e-6")
        lblSourceStop_A.Caption = "Source Stop Value (A)"
        txtSourceStop_A = 0.35
        lblSourceLimit_A.Caption = "Source Limit (V)"
        txtSourceLimit_A.Text = 3.5
    ElseIf cmbLedType_A.List(cmbLedType_A.ListIndex) = "Philips" Then
        lblBiasLevel_A.Caption = "Bias Level (A)"
        txtBiasLevel_A = 0
        lblSourceStart_A.Caption = "Source Start Value (A)"
        txtSourceStart_A.Text = 0 'Format(1, "1e-6")
        lblSourceStop_A.Caption = "Source Stop Value (A)"
        txtSourceStop_A = 0.35
        lblSourceLimit_A.Caption = "Source Limit (V)"
        txtSourceLimit_A.Text = 3
    ElseIf cmbLedType_A.List(cmbLedType_A.ListIndex) = "Seoul" Then
        lblBiasLevel_A.Caption = "Bias Level (A)"
        txtBiasLevel_A = 0
        lblSourceStart_A.Caption = "Source Start Value (A)"
        txtSourceStart_A.Text = 0 'Format(1, "1e-6")
        lblSourceStop_A.Caption = "Source Stop Value (A)"
        txtSourceStop_A = 0.35
        lblSourceLimit_A.Caption = "Source Limit (V)"
        txtSourceLimit_A.Text = 4
    End If

End Sub
Private Sub SRC_V_A()
    If cmbLedType_A.List(cmbLedType_A.ListIndex) = "Cree" Then
        lblBiasLevel_A.Caption = "Bias Level (V)"
        txtBiasLevel_A = 0
        lblSourceStart_A.Caption = "Source Start Value (V)"
        txtSourceStart_A.Text = 0 'Format(1, "1e-6")
        lblSourceStop_A.Caption = "Source Stop Value (V)"
        txtSourceStop_A.Text = 2.8
        lblSourceLimit_A.Caption = "Source Limit (A)"
        txtSourceLimit_A.Text = 1.5
    ElseIf cmbLedType_A.List(cmbLedType_A.ListIndex) = "Osram" Then
        lblBiasLevel_A.Caption = "Bias Level (V)"
        txtBiasLevel_A = 0
        lblSourceStart_A.Caption = "Source Start Value (V)"
```

```
        txtSourceStart_A.Text = 0 'Format(1, "1e-6")
        lblSourceStop_A.Caption = "Source Stop Value (V)"
        txtSourceStop_A.Text = 3.2
        lblSourceLimit_A.Caption = "Source Limit (A)"
        txtSourceLimit_A.Text = 0.8
    ElseIf cmbLedType_A.List(cmbLedType_A.ListIndex) = "Philips" Then
        lblBiasLevel_A.Caption = "Bias Level (V)"
        txtBiasLevel_A = 0
        lblSourceStart_A.Caption = "Source Start Value (V)"
        txtSourceStart_A.Text = 0 'Format(1, "1e-6")
        lblSourceStop_A.Caption = "Source Stop Value (V)"
        txtSourceStop_A.Text = 2.76
        lblSourceLimit_A.Caption = "Source Limit (A)"
        txtSourceLimit_A.Text = 1
    ElseIf cmbLedType_A.List(cmbLedType_A.ListIndex) = "Seoul" Then
        lblBiasLevel_A.Caption = "Bias Level (V)"
        txtBiasLevel_A = 0
        lblSourceStart_A.Caption = "Source Start Value (V)"
        txtSourceStart_A.Text = 0 'Format(1, "1e-6")
        lblSourceStop_A.Caption = "Source Stop Value (V)"
        txtSourceStop_A.Text = 3.25
        lblSourceLimit_A.Caption = "Source Limit (A)"
        txtSourceLimit_A.Text = 0.8
    End If

End Sub
Private Sub tmrReadData_A_Timer()
    Dim FullPath$, Filename$
    Dim DataReply_A_Local$

    cdlFile_A.Filter = "Apps (*.csv)|*.csv|All files (*.*)|*.*"
    cdlFile_A.DefaultExt = "csv"
    cdlFile_A.DialogTitle = "Save File"
    cdlFile_A.Filename = txtFileName.Text
    cdlFile_A.ShowSave
    On Error Resume Next  'In case when save file is cancel
    'The Filename property gives you the variable of full path name need to use
    FullPath = cdlFile_A.Filename 'Return a full pathname including filename of an opened or
saved file
    Filename = cdlFile_A.FileTitle

    'Read Data------------------
    TCPSock.GetData DataReply_A_Local$
    If DataReply_A_Local$ <> "" Then
        DataReply_A = DataReply_A_Local$
    End If
    Open FullPath For Output As #1
    Print #1, DataReply_A
    Close #1

    txtFileName.Text = Filename

    tmrReadData_A.Enabled = False
End Sub


'*****************************************************************************************
'                                                                                         *
'                                          Channel B                                      *
'                                                                                         *
'*****************************************************************************************

Private Sub chkSync_B_Click()
    If chkSync_B.Value = Checked Then
        txtToff_B = 5 '5 second waitting time of spectrometer operation
        txtTon_B = 1
        SyncOut_B = 1
    Else
        SyncOut_B = 0
    End If
End Sub

Private Sub cmbLedType_B_Click()
    Call cmbSourceMode_B_Click
    txtUserParameter_B.Text = cmbLedType_B.List(cmbLedType_B.ListIndex)
End Sub

Private Sub cmbSourceMode_B_Click()
```

```
    Select Case cmbSourceMode_B.ListIndex
        Case 0
            Call SRC_I_B
            txtBiasLevel_B.Enabled = True
            txtSourceStart_B.Enabled = False
            txtToff_B.Enabled = True
        Case 2, 4
            Call SRC_I_B
            txtBiasLevel_B.Enabled = True
            txtSourceStart_B.Enabled = True
            txtToff_B.Enabled = True
        Case 6, 8
            Call SRC_I_B
            txtBiasLevel_B.Enabled = False
            txtSourceStart_B.Enabled = True
            txtToff_B.Enabled = False
        Case 1
            Call SRC_V_B
            txtBiasLevel_B.Enabled = True
            txtSourceStart_B.Enabled = False
            txtToff_B.Enabled = True
        Case 3, 5
            Call SRC_V_B
            txtBiasLevel_B.Enabled = True
            txtSourceStart_B.Enabled = True
            txtToff_B.Enabled = True
        Case 7, 9
            Call SRC_V_B
            txtBiasLevel_B.Enabled = False
            txtSourceStart_B.Enabled = True
            txtToff_B.Enabled = False
        Case 10
            Call SRC_I_B
            ilist_B = InputBox("Please enter your list of each current value seperated by ,
(comma)", _
            "Current List")
        Case 11
            vlist_B = InputBox("Please enter your list of each voltage value seperated by ,
(comma)" _
            , "Voltage List")
    End Select
End Sub

Private Sub cmdLoadSetting_B_Click()
    Dim FullPath$, Filename$, sName$, ValLoad$, State As Variant

    cdlFile_B.Filter = "Apps (*.csv)|*.csv|All files (*.*)|*.*"
    cdlFile_B.DefaultExt = "csv"
    cdlFile_B.DialogTitle = "Load File"
    cdlFile_B.Filename = ""
    cdlFile_B.ShowOpen
    On Error GoTo OnError 'In case when save file is cancel
    'The FileName property gives you the variable of full path name need to use
    FullPath = cdlFile_B.Filename 'Return a full pathname and filename of an opened or saved file
    Filename = cdlFile_B.FileTitle

    Open FullPath For Input As #1

    Input #1, sName, ValLoad
    cmbSourceMode_B.ListIndex = ValLoad
    Input #1, sName, ValLoad
    txtBiasLevel_B.Text = ValLoad
    Input #1, sName, ValLoad
    txtSourceStart_B.Text = ValLoad
    Input #1, sName, ValLoad
    txtSourceStop_B.Text = ValLoad
    Input #1, sName, ValLoad
    txtSourceLimit_B.Text = ValLoad
    Input #1, sName, ValLoad
    txt_Source_Rangei_B.Text = ValLoad
    Input #1, sName, ValLoad
    txt_Source_Rangev_B.Text = ValLoad
    Input #1, sName, ValLoad
    txt_Meas_Rangei_B.Text = ValLoad
    Input #1, sName, ValLoad
    txt_Meas_Rangev_B.Text = ValLoad
    Input #1, sName, ValLoad
    txtTon_B.Text = ValLoad
```

```
    Input #1, sName, ValLoad
    txtToff_B.Text = ValLoad
    Input #1, sName, ValLoad
    txtMeasPointNum_B.Text = ValLoad
    Input #1, sName, ValLoad
    txtMeasCountNumber_B.Text = ValLoad
    Input #1, sName, ValLoad
    txtMeasSpeed_B.Text = ValLoad
    Input #1, sName, ValLoad
    opt4Wire_B.Value = ValLoad
    Input #1, sName, ValLoad
    opt2Wire_B.Value = ValLoad
    Close #1

    txtUserParameter_B.Text = Filename

OnError:
    Exit Sub
End Sub

Private Sub cmdPlot_B_Click()

    tmrPlot_B.Enabled = True

End Sub

Private Sub cmdRun_B_Click()
    Dim bias_B#, start_B#, stop_B#, level_B#, limit_B#, SourceRangei_B#, SourceRangev_B#, _
    MeasRangei_B#, MeasRangev_B#, toff_B#
    Dim T_MeasSpeed_B#, nplc_B#
    Const tag_B = 1
    Const Freq = 50
    Dim MeasTime$
    Dim iMeasCount&

    'Get parameter values ------------------------------
        bias_B = Val(txtBiasLevel_B.Text)
        start_B = Val(txtSourceStart_B.Text)
        stop_B = Val(txtSourceStop_B.Text)
        level_B = stop_B
        limit_B = Val(txtSourceLimit_B.Text)
        SourceRangei_B = Val(txt_Source_Rangei_B.Text)
        SourceRangev_B = Val(txt_Source_Rangev_B.Text)
        MeasRangei_B = Val(txt_Meas_Rangei_B.Text)
        MeasRangev_B = Val(txt_Meas_Rangev_B.Text)
        ton_B = Val(txtTon_B.Text)
        toff_B = Val(txtToff_B.Text)
        If lblMeasPointNum_B.Caption = "Meas Step Value" Then
            MeasPoint_B = (Val(txtSourceStop_B.Text) – Val(txtSourceStart_B.Text)) /
Val(txtMeasPointNum_B.Text) + 1
        Else
            MeasPoint_B = Val(txtMeasPointNum_B.Text)
        End If
        MeasCountNumber_B = Val(txtMeasCountNumber_B.Text)
        T_MeasSpeed_B = Val(txtMeasSpeed_B.Text) 'in second

    If Not cmbPort.DataChanged Then
        MsgBox "Please select port before continue!", vbOKOnly, "Configure Port"
        On Error GoTo ErrorConnection
    Else

    ' Send Command-----------------------------------------------------------------
        For iMeasCount = 1 To MeasCountNumber_B 'Repeat Measurement
            On Error GoTo ErrorConnection
            TCPSock.SendData "reset()" + vbLf
            TCPSock.SendData "smub.nvbuffer1.clear()" + vbLf
            Select Case cmbSourceMode_B.ListIndex
                Case 0, 1, 2, 3, 4, 5
                    TCPSock.SendData "smub.source.rangei =" + CStr(SourceRangei_B) + vbLf
                    TCPSock.SendData "smub.source.rangev =" + CStr(SourceRangev_B) + vbLf
                    TCPSock.SendData "smub.measure.rangei =" + CStr(MeasRangei_B) + vbLf
                    TCPSock.SendData "smub.measure.rangev =" + CStr(MeasRangev_B) + vbLf

                    TCPSock.SendData "smub.measure.autozero = smub.AUTOZERO_ONCE" + vbLf
                    TCPSock.SendData "smub.nvbuffer1.appendmode = 1" + vbLf
                Case 6, 7, 8, 9, 10, 11
                    TCPSock.SendData "smub.measure.autorangev = smub.AUTORANGE_ON" + vbLf
                    TCPSock.SendData "smub.measure.autorangei = smub.AUTORANGE_ON" + vbLf
```

```
                    TCPSock.SendData "smub.source.autorangev = smub.AUTORANGE_ON" + vbLf
                    TCPSock.SendData "smub.source.autorangei = smub.AUTORANGE_ON" + vbLf
            End Select
            TCPSock.SendData "smub.nvbuffer1.collectsourcevalues = 1" + vbLf
            TCPSock.SendData "smub.nvbuffer1.collecttimestamps = 1" + vbLf
            TCPSock.SendData "smub.source.delay = 0.1" + vbLf 'Sourec delay
            TCPSock.SendData "smub.measure.delay = smub.DELAY_AUTO" + vbLf 'Measure delay
            TCPSock.SendData "smub.measure.interval = 0.1" + vbLf 'Measure interval
            TCPSock.SendData "digio.trigger [1].mode = 1" + vbLf 'digio.TRIG_FALLING
            TCPSock.SendData "digio.trigger [1].pulsewidth =" + CStr(toff_B + ton_B / 2) + vbLf
'5 sec waitting time of spectrometer operation
            'Wire Mode-----------------------------------------------------------------
                If opt2Wire_B.Value = True Then
                    TCPSock.SendData "smub.sense=smub.SENSE_LOCAL" + vbLf
                ElseIf opt4Wire_B.Value = True Then
                    TCPSock.SendData "smub.sense=smub.SENSE_REMOTE" + vbLf
                End If
            'Set Measurement Speed Chanel A-------------------------------------------
                nplc_B = Freq * T_MeasSpeed_B
                TCPSock.SendData "smub.measure.nplc=" + CStr(nplc_B) + vbLf
            'Start Measure Mode
                TCPSock.SendData "smub.source.output = smub.OUTPUT_ON" + vbLf

                If cmbSourceMode_B.ListIndex = 0 Then
                    TCPSock.SendData "ConfigPulseIMeasureV(smub," + CStr(bias_B) + "," +
CStr(level_B) _
                    + "," + CStr(limit_B) + "," + CStr(ton_B) + "," + CStr(toff_B) + "," _
                    + CStr(MeasPoint_B) + "," + "smub.nvbuffer1" + "," + CStr(tag_B) + ",nil," +
CStr(SyncOut_B) + ")" + vbLf
                ElseIf cmbSourceMode_B.ListIndex = 1 Then
    '                TCPSock.SendData "digio.writeport(0)"
                    TCPSock.SendData "ConfigPulseVMeasureI(smub," + CStr(bias_B) + "," +
CStr(level_B) _
                    + "," + CStr(limit_B) + "," + CStr(ton_B) + "," + CStr(toff_B) + "," _
                    + CStr(MeasPoint_B) + "," + "smub.nvbuffer1" + "," + CStr(tag_B) + ",nil," +
CStr(SyncOut_B) + ")" + vbLf
                ElseIf cmbSourceMode_B.ListIndex = 2 Then
                    TCPSock.SendData "ConfigPulseIMeasureVSweepLin(smub," + CStr(bias_B) + "," _
                    + CStr(start_B) + "," + CStr(stop_B) + "," + CStr(limit_B) + "," +
CStr(ton_B) + "," _
                    + CStr(toff_B) + "," + CStr(MeasPoint_B) + "," + "smub.nvbuffer1" + "," +
CStr(tag_B) + ",nil," + CStr(SyncOut_B) + ")" + vbLf
                ElseIf cmbSourceMode_B.ListIndex = 3 Then
                    TCPSock.SendData "ConfigPulseVMeasureISweepLin(smub," + CStr(bias_B) + "," _
                    + CStr(start_B) + "," + CStr(stop_B) + "," + CStr(limit_B) + "," +
CStr(ton_B) + "," _
                    + CStr(toff_B) + "," + CStr(MeasPoint_B) + "," + "smub.nvbuffer1" + "," +
CStr(tag_B) + ",nil," + CStr(SyncOut_B) + ")" + vbLf
                ElseIf cmbSourceMode_B.ListIndex = 4 Then
                    TCPSock.SendData "ConfigPulseIMeasureVSweepLog(smub," + CStr(bias_B) + "," _
                    + CStr(start_B) + "," + CStr(stop_B) + "," + CStr(limit_B) + "," +
CStr(ton_B) + "," _
                    + CStr(toff_B) + "," + CStr(MeasPoint_B) + "," + "smub.nvbuffer1" + "," +
CStr(tag_B) + ",nil," + CStr(SyncOut_B) + ")" + vbLf
                ElseIf cmbSourceMode_B.ListIndex = 5 Then
                    TCPSock.SendData "ConfigPulseVMeasureISweepLog(smub," + CStr(bias_B) + "," _
                    + CStr(start_B) + "," + CStr(stop_B) + "," + CStr(limit_B) + "," +
CStr(ton_B) + "," _
                    + CStr(toff_B) + "," + CStr(MeasPoint_B) + "," + "smub.nvbuffer1" + "," +
CStr(tag_B) + ",nil," + CStr(SyncOut_B) + ")" + vbLf
                ElseIf cmbSourceMode_B.ListIndex = 6 Then
                    TCPSock.SendData "smub.source.limitv = " + CStr(limit_B) + vbLf
                    TCPSock.SendData "SweepILinMeasureV(smub," + CStr(start_B) + "," +
CStr(stop_B) + "," _
                    + CStr(ton_B) + "," + CStr(MeasPoint_B) + ")" + vbLf
                ElseIf cmbSourceMode_B.ListIndex = 7 Then
                    TCPSock.SendData "smub.source.limiti = " + CStr(limit_B) + vbLf
                    TCPSock.SendData "SweepVLinMeasureI(smub," + CStr(start_B) + "," +
CStr(stop_B) + "," _
                    + CStr(ton_B) + "," + CStr(MeasPoint_B) + ")" + vbLf
                ElseIf cmbSourceMode_B.ListIndex = 8 Then
                    TCPSock.SendData "smub.source.limitv = " + CStr(limit_B) + vbLf
                    TCPSock.SendData "SweepILogMeasureV(smub," + CStr(start_B) + "," +
CStr(stop_B) + "," _
                    + CStr(ton_B) + "," + CStr(MeasPoint_B) + ")" + vbLf
                ElseIf cmbSourceMode_B.ListIndex = 9 Then
                    TCPSock.SendData "smub.source.limiti = " + CStr(limit_B) + vbLf
```

```
                    TCPSock.SendData "SweepVLogMeasureI(smub," + CStr(start_B) + "," +
CStr(stop_B) + "," _
                    + CStr(ton_B) + "," + CStr(MeasPoint_B) + ")" + vbLf
                ElseIf cmbSourceMode_B.ListIndex = 10 Then
                    TCPSock.SendData "smub.source.limitv = " + CStr(limit_B) + vbLf
                    TCPSock.SendData "SweepIListMeasureV(smub," + "{" + ilist_B + "}" + "," +
CStr(ton_B) _
                    + "," + CStr(MeasPoint_B) + ")" + vbLf
                ElseIf cmbSourceMode_B.ListIndex = 10 Then
                    TCPSock.SendData "smub.source.limiti = " + CStr(limit_B) + vbLf
                    TCPSock.SendData "SweepVListMeasureI(smub," + "{" + vlist_B + "}" + "," +
CStr(ton_B) _
                    + "," + CStr(MeasPoint_B) + ")" + vbLf
                End If

                TCPSock.SendData "InitiatePulseTest(" + CStr(tag_B) + ")" + vbLf
                ' Store Measured Data
                Select Case cmbSourceMode_B.ListIndex
                    Case 0, 2, 4, 6, 8, 10
                        TCPSock.SendData "printbuffer(1, smub.nvbuffer1.n,
smub.nvbuffer1.readings)" + vbLf
                        'TCPSock.SendData "print(""\n"")" + vbLf
                        TCPSock.SendData "waitcomplete()" + vbLf

                        TCPSock.SendData "printbuffer(1, smub.nvbuffer1.n,
smub.nvbuffer1.sourcevalues)" + vbLf
                        'TCPSock.SendData "print(""\n"")" + vbLf
                        TCPSock.SendData "waitcomplete()" + vbLf

                        TCPSock.SendData "printbuffer(1, smub.nvbuffer1.n,
smub.nvbuffer1.timestamps)" + vbLf
                        TCPSock.SendData "waitcomplete()" + vbLf
                    Case 1, 3, 5, 7, 9, 11
                        TCPSock.SendData "printbuffer(1, smub.nvbuffer1.n,
smub.nvbuffer1.sourcevalues)" + vbLf
                        'TCPSock.SendData "print(""\n"")" + vbLf
                        TCPSock.SendData "waitcomplete()" + vbLf

                        TCPSock.SendData "printbuffer(1, smub.nvbuffer1.n,
smub.nvbuffer1.readings)" + vbLf
                        'TCPSock.SendData "print(""\n"")" + vbLf
                        TCPSock.SendData "waitcomplete()" + vbLf

                        TCPSock.SendData "printbuffer(1, smub.nvbuffer1.n,
smub.nvbuffer1.timestamps)" + vbLf
                        'TCPSock.SendData "print(""\n"")" + vbLf
                        TCPSock.SendData "waitcomplete()" + vbLf
                End Select

                TCPSock.SendData "smub.source.output = smub.OUTPUT_OFF" + vbLf
        Next iMeasCount
    End If
    TCPSock.SendData "beeper.enable = beeper.ON" + vbLf
    TCPSock.SendData "beeper.beep(1,300)" + vbLf
'    TCPSock.SendData "beeper.enable = beeper.OFF" + vbLf

    MeasDate_B = Format(Date, "yyyy-mm-dd")
    MeasTime_B = Format(Time, "hh-mm-ss AM/PM")

ErrorConnection:
'        MsgBox "Please select port before continue!", vbOKOnly, "Configure Port"
End Sub

Private Sub cmdSave_B_Click()
    tmrReadData_B.Enabled = True
End Sub

Private Sub cmdSaveSetting_B_Click()
    Dim FullPath$, Filename$

    cdlFile_B.Filter = "Apps (*.csv)|*.csv|All files (*.*)|*.*"
    cdlFile_B.DefaultExt = "csv"
    cdlFile_B.DialogTitle = "Save File"
    cdlFile_B.Filename = txtUserParameter_B.Text
    cdlFile_B.ShowSave
    On Error Resume Next 'In case when save file is cancel
    'The FileName property gives you the variable of full path name need to use
    FullPath = cdlFile_B.Filename 'Return a full pathname and filename of an opened or saved file
```

```
    Filename = cdlFile_B.FileTitle

    Open FullPath For Output As #1
    Print #1, "Select Source Mode," + CStr(cmbSourceMode_B.ListIndex)
    Print #1, "Bias Level (A)," + txtBiasLevel_B.Text
    Print #1, "Source Start Value (A)," + txtSourceStart_B.Text
    Print #1, "Source Stop Value (A)," + txtSourceStop_B.Text
    Print #1, "Source-Limit (V)," + txtSourceLimit_B.Text

    Print #1, "Source-Rangei (A)," + txt_Source_Rangei_B.Text
    Print #1, "Source-Rangev (V)," + txt_Source_Rangev_B.Text
    Print #1, "Meas-Rangei (A)," + txt_Meas_Rangei_B.Text
    Print #1, "Meas-Rangev (A)," + txt_Meas_Rangev_B.Text

    Print #1, "Ton (sec)," + txtTon_B.Text
    Print #1, "Toff (sec)," + txtToff_B.Text
    Print #1, "Meas Point Number," + txtMeasPointNum_B.Text
    Print #1, "Meas Count Number," + txtMeasCountNumber_B.Text
    Print #1, "Measurement Speed (s)," + txtMeasSpeed_B.Text
    Print #1, "opt4Wire_B," + CStr(opt4Wire_B.Value)
    Print #1, "opt2Wire_B," + CStr(opt2Wire_B.Value)
    Close #1
    txtUserParameter_B.Text = Filename
End Sub

Private Sub lblMeasPointNum_B_Click()
    Dim Step#, MeasPoint_B&
    If Not MeasPointorStep_B And (cmbSourceMode_B.ListIndex = 2 Or cmbSourceMode_B.ListIndex = 3
_
                        Or cmbSourceMode_B.ListIndex = 6 Or cmbSourceMode_B.ListIndex = 7) Then
        lblMeasPointNum_B.Caption = "Meas Step Value"
        MeasPointorStep_B = Not MeasPointorStep_B
        Step = (Val(txtSourceStop_B.Text) - Val(txtSourceStart_B.Text)) /
(Val(txtMeasPointNum_B.Text) - 1)
        txtMeasPointNum_B.Text = Step
    ElseIf MeasPointorStep_B And (cmbSourceMode_B.ListIndex = 2 Or cmbSourceMode_B.ListIndex = 3
_
                        Or cmbSourceMode_B.ListIndex = 6 Or cmbSourceMode_B.ListIndex = 7) Then
        lblMeasPointNum_B.Caption = "Meas Point Number"
        MeasPointorStep_B = Not MeasPointorStep_B
        MeasPoint_B = (Val(txtSourceStop_B.Text) - Val(txtSourceStart_B.Text)) /
Val(txtMeasPointNum_B.Text) + 1
        txtMeasPointNum_B.Text = MeasPoint_B
    End If
End Sub

Private Sub tmrPlot_B_Timer()
    Dim dataRead$, DataReply_B_Local$
    Dim i%
    Dim MlabPath$

    On Error GoTo ErrorCom
    TCPSock.GetData DataReply_B_Local
    If DataReply_B_Local$ <> "" Then
        DataReply_B = DataReply_B_Local
    End If

    Open App.Path + "\SavePlotData_B.csv" For Output As #1
    Print #1, DataReply_B 'stored data to global variable DataReply_B
    Close #1
ErrorCom:
    MlabPath = App.Path
    Result = objMatLab.execute("clear all")
    Result = objMatLab.PutCharArray("MlabPath", "base", MlabPath)
    Result = objMatLab.execute("data=xlsread(strcat(MlabPath,'\SavePlotData_B.csv'));")
    Result = objMatLab.execute("Legend_B=[];")
    For i = 1 To MeasCountNumber_B
        Result = objMatLab.PutWorkspaceData("i", "base", i)
        Result = objMatLab.execute("Voltage(:,i)=data(3*i-2,:);")
        Result = objMatLab.execute("Current(:,i)=data(3*i-1,:);")
        Result = objMatLab.execute("Time(:,i)=data(3*i,:);")
        Result = objMatLab.execute("Legend_B=[Legend_B,strcat({strcat(num2str(i),'
Measure')})];")
    Next

    Result = objMatLab.PutWorkspaceData("Ton", "base", ton_B)
```

```
    If optPlotCurve(0).Value = True And optPlotScale(0).Value = True Then 'Case Current vs
Voltage & Log Scale
        Result = objMatLab.execute("semilogy(Voltage,abs(Current));")
        Result = objMatLab.execute("title('Current vs Voltage'),xlabel('Voltage in
(V)'),ylabel('Currentin (A)'),legend(Legend_B),grid")
    ElseIf optPlotCurve(0).Value = True And optPlotScale(1).Value = True Then 'Case Current vs
Voltage & Log Linear
        Result = objMatLab.execute("plot(Voltage,abs(Current));")
        Result = objMatLab.execute("title('Current vs Voltage'),xlabel('Voltage in
(V)'),ylabel('Currentin (A)'),legend(Legend_B),grid")
    ElseIf optPlotCurve(1).Value = True And optPlotScale(0).Value = True Then 'Case Current vs
Time & Log Scale
        Result = objMatLab.execute("semilogy(Time,abs(Current));")
        Result = objMatLab.execute("title('Current vs Voltage'),xlabel('Time in
(s)'),ylabel('Currentin (A)'),legend(Legend_B),grid")
    ElseIf optPlotCurve(1).Value = True And optPlotScale(1).Value = True Then 'Case Current vs
Time & Log Linear
        Result = objMatLab.execute("plot(Time,abs(Current));")
        Result = objMatLab.execute("title('Current vs Voltage'),xlabel('Time in
(s)'),ylabel('Currentin (A)'),legend(Legend_B),grid")
    ElseIf optPlotCurve(2).Value = True And optPlotScale(0).Value = True Then 'Case Voltage vs
Time & Log Scale
        Result = objMatLab.execute("semilogy(Time,Voltage);")
        Result = objMatLab.execute("title('Current vs Voltage'),xlabel('Time in
(s)'),ylabel('Voltage (V)'),legend(Legend_B),grid")
    ElseIf optPlotCurve(2).Value = True And optPlotScale(1).Value = True Then 'Case Voltage vs
Time & Log Linear
        Select Case cmbSourceMode_B.ListIndex
            Case 0, 1, 2, 3, 4, 5
                Result = objMatLab.execute("bar(Time,Voltage,Ton);")
            Case 6, 7, 8, 9
                Result = objMatLab.execute("stairs(Time,Voltage);")
        End Select
        Result = objMatLab.execute("title('Current vs Voltage'),xlabel('Time in
(s)'),ylabel('Voltage (V)'),legend(Legend_B),grid")
    End If

    Result = objMatLab.execute("set(gcf,'Visible','off')")
    Result = objMatLab.execute("set(gcf, 'Position', [0, 0, 750, 250])")
    Result = objMatLab.execute("hgexport(gcf,'-clipboard')")
    ImgPlot.Picture = Clipboard.GetData()
'    Clipboard.Clear

    tmrPlot_B.Enabled = False
End Sub

Private Sub txtMeasSpeed_B_lostfocus()
    If Val(txtMeasSpeed_B.Text) < 0.00002 Or Val(txtMeasSpeed_B.Text) > 0.5 Then
'0.001<nplc<25
        MsgBox "Measurement speed range is between 0.00002 sec 0.5 sec", vbOKOnly, _
        "Speed Configuration"
        txtMeasSpeed_B.SetFocus
    End If
End Sub

Private Sub SRC_I_B()
    If cmbLedType_B.List(cmbLedType_B.ListIndex) = "Cree" Then
        lblBiasLevel_B.Caption = "Bias Level (A)"
        txtBiasLevel_B = 0
        lblSourceStart_B.Caption = "Source Start Value (A)"
        txtSourceStart_B.Text = 0 'Format(1, "1e-6")
        lblSourceStop_B.Caption = "Source Stop Value (A)"
        txtSourceStop_B = 0.35
        lblSourceLimit_B.Caption = "Source Limit (V)"
        txtSourceLimit_B.Text = 3.15
    ElseIf cmbLedType_B.List(cmbLedType_B.ListIndex) = "Osram" Then
        lblBiasLevel_B.Caption = "Bias Level (A)"
        txtBiasLevel_B = 0
        lblSourceStart_B.Caption = "Source Start Value (A)"
        txtSourceStart_B.Text = 0 'Format(1, "1e-6")
        lblSourceStop_B.Caption = "Source Stop Value (A)"
        txtSourceStop_B = 0.35
        lblSourceLimit_B.Caption = "Source Limit (V)"
        txtSourceLimit_B.Text = 3.5
    ElseIf cmbLedType_B.List(cmbLedType_B.ListIndex) = "Philips" Then
        lblBiasLevel_B.Caption = "Bias Level (A)"
        txtBiasLevel_B = 0
        lblSourceStart_B.Caption = "Source Start Value (A)"
```

```
        txtSourceStart_B.Text = 0 'Format(1, "1e-6")
        lblSourceStop_B.Caption = "Source Stop Value (A)"
        txtSourceStop_B = 0.35
        lblSourceLimit_B.Caption = "Source Limit (V)"
        txtSourceLimit_B.Text = 3
    ElseIf cmbLedType_B.List(cmbLedType_B.ListIndex) = "Seoul" Then
        lblBiasLevel_B.Caption = "Bias Level (A)"
        txtBiasLevel_B = 0
        lblSourceStart_B.Caption = "Source Start Value (A)"
        txtSourceStart_B.Text = 0 'Format(1, "1e-6")
        lblSourceStop_B.Caption = "Source Stop Value (A)"
        txtSourceStop_B = 0.35
        lblSourceLimit_B.Caption = "Source Limit (V)"
        txtSourceLimit_B.Text = 4
    End If

End Sub
Private Sub SRC_V_B()
    If cmbLedType_B.List(cmbLedType_B.ListIndex) = "Cree" Then
        lblBiasLevel_B.Caption = "Bias Level (V)"
        txtBiasLevel_B = 0
        lblSourceStart_B.Caption = "Source Start Value (V)"
        txtSourceStart_B.Text = 0 'Format(1, "1e-6")
        lblSourceStop_B.Caption = "Source Stop Value (V)"
        txtSourceStop_B.Text = 2.8
        lblSourceLimit_B.Caption = "Source Limit (A)"
        txtSourceLimit_B.Text = 1.5
    ElseIf cmbLedType_B.List(cmbLedType_B.ListIndex) = "Osram" Then
        lblBiasLevel_B.Caption = "Bias Level (V)"
        txtBiasLevel_B = 0
        lblSourceStart_B.Caption = "Source Start Value (V)"
        txtSourceStart_B.Text = 0 'Format(1, "1e-6")
        lblSourceStop_B.Caption = "Source Stop Value (V)"
        txtSourceStop_B.Text = 3.2
        lblSourceLimit_B.Caption = "Source Limit (A)"
        txtSourceLimit_B.Text = 0.8
    ElseIf cmbLedType_B.List(cmbLedType_B.ListIndex) = "Philips" Then
        lblBiasLevel_B.Caption = "Bias Level (V)"
        txtBiasLevel_B = 0
        lblSourceStart_B.Caption = "Source Start Value (V)"
        txtSourceStart_B.Text = 0 'Format(1, "1e-6")
        lblSourceStop_B.Caption = "Source Stop Value (V)"
        txtSourceStop_B.Text = 2.76
        lblSourceLimit_B.Caption = "Source Limit (A)"
        txtSourceLimit_B.Text = 1
    ElseIf cmbLedType_B.List(cmbLedType_B.ListIndex) = "Seoul" Then
        lblBiasLevel_B.Caption = "Bias Level (V)"
        txtBiasLevel_B = 0
        lblSourceStart_B.Caption = "Source Start Value (V)"
        txtSourceStart_B.Text = 0 'Format(1, "1e-6")
        lblSourceStop_B.Caption = "Source Stop Value (V)"
        txtSourceStop_B.Text = 3.25
        lblSourceLimit_B.Caption = "Source Limit (A)"
        txtSourceLimit_B.Text = 0.8
    End If

End Sub
Private Sub tmrReadData_B_Timer()
    Dim FullPath$, Filename$
    Dim DataReply_B_Local$

    cdlFile_B.Filter = "Apps (*.csv)|*.csv|All files (*.*)|*.*"
    cdlFile_B.DefaultExt = "csv"
    cdlFile_B.DialogTitle = "Save File"
    cdlFile_B.Filename = txtFileName.Text
    cdlFile_B.ShowSave
    On Error Resume Next  'In case when save file is cancel
    'The Filename property gives you the variable of full path name need to use
    FullPath = cdlFile_B.Filename 'Return a full pathname including filename of an opened or
saved file
    Filename = cdlFile_B.FileTitle

    'Read Data------------------
    TCPSock.GetData DataReply_B_Local$
    If DataReply_B_Local$ <> "" Then
        DataReply_B = DataReply_B_Local$
    End If
    Open FullPath For Output As #1
```

```
    Print #1, DataReply_B
    Close #1

    txtFileName.Text = Filename

    tmrReadData_B.Enabled = False
End Sub
```

Appendix E: Spectrophotometer Specbos Spreadsheet Data Export.

Name	#1	#2	#3	#4	#5	#6	#7	#8	#9	#10
Correction										
Date	04-11-15	04-11-15	04-11-15	04-11-15	04-11-15	04-11-15	04-11-15	04-11-15	04-11-15	04-11-15
Time	6:30:50 PM	6:30:56 PM	6:31:02 PM	6:31:08 PM	6:31:14 PM	6:31:20 PM	6:31:26 PM	6:31:32 PM	6:31:38 PM	6:31:44 PM
Integration Time [ms]	33.000	16.000	12.000	8.000	7.000	6.000	6.000	4.000	4.000	3.000
Luminance [cd/sqm]	1.512E+04	2.975E+04	4.345E+04	5.660E+04	6.904E+04	8.074E+04	9.173E+04	1.030E+05	1.132E+05	1.241E+05
Radiance [W/(sr*sqm)] (380-780nm)	4.682E+01	9.212E+01	1.346E+02	1.753E+02	2.139E+02	2.501E+02	2.844E+02	3.191E+02	3.509E+02	3.844E+02
Correlated Colour Temp. (CCT) [K]	2776	2784	2794	2796	2802	2808	2817	2813	2820	2820
Dominant Wavelength (DWl) [nm]	584.8	584.9	584.9	584.9	585.0	585.0	585.0	585.1	585.0	585.1
Colour Purity (PE) [%]	55.1	54.5	54.1	53.8	53.4	53.1	52.7	52.6	52.4	52.2
Chromaticity Coordinates										
x	0.4492	0.4482	0.4473	0.4468	0.4461	0.4456	0.4447	0.4448	0.4442	0.4440
y	0.4006	0.3998	0.3992	0.3987	0.3981	0.3978	0.3973	0.3969	0.3966	0.3963
u'	0.2600	0.2598	0.2594	0.2594	0.2592	0.2590	0.2587	0.2589	0.2586	0.2586
v'	0.5219	0.5214	0.5210	0.5207	0.5204	0.5202	0.5199	0.5197	0.5195	0.5194
CIE XYZ										
X	16952	33353	48687	63437	77358	90442	102691	115420	126804	139027
Y	15121	29750	43455	56599	69036	80741	91731	102985	113213	124082
Z	5668	11309	16717	21935	27002	31800	36475	41088	45446	49984
Colour Rendering Index										
Reference Illuminant	Planckian radiator	Planckian radiator	Planckian radiator	Planckian radiator	Planckian radiator	Planckian radiator	Planckian radiator	Planckian radiator	Planckian radiator	Planckian radiator
CCT [K]	2776	2784	2794	2796	2802	2808	2817	2813	2820	2820
R1	80.6	80.4	80.4	80.1	80.0	79.8	79.8	79.5	79.4	79.3
R2	90.0	89.8	89.6	89.5	89.3	89.2	89.2	89.1	89.0	88.9
R3	96.3	96.2	96.1	96.0	96.0	95.9	95.8	95.8	95.7	95.7
R4	80.0	79.8	79.8	79.5	79.4	79.2	79.2	78.8	78.7	78.6
R5	80.4	80.2	80.1	79.9	79.8	79.6	79.6	79.3	79.2	79.1
R6	87.6	87.3	87.0	86.8	86.6	86.4	86.3	86.2	86.0	86.0
R7	81.9	81.8	81.9	81.7	81.6	81.5	81.6	81.3	81.3	81.1
R8	58.6	58.5	58.5	58.1	58.1	57.9	58.1	57.4	57.4	57.2
R9	8.9	8.3	8.3	7.4	7.2	6.8	7.0	5.7	5.6	5.0
R10	76.8	76.4	76.0	75.7	75.4	75.2	75.0	74.8	74.6	74.5
R11	79.1	78.9	78.9	78.6	78.3	78.2	78.2	77.7	77.5	77.3
R12	72.5	72.5	72.4	72.2	72.1	72.0	72.0	71.9	71.8	71.8
R13	82.6	82.4	82.3	82.1	81.9	81.8	81.8	81.5	81.4	81.2
R14	98.2	98.1	98.0	97.9	97.9	97.8	97.8	97.8	97.7	97.7
R15	73.9	73.8	73.8	73.5	73.5	73.3	73.4	73.0	73.0	72.8
Ra	81.93	81.75	81.67	81.46	81.34	81.21	81.21	80.92	80.85	80.72
DC	2.8E-03	3.0E-03	3.2E-03	3.3E-03	3.5E-03	3.5E-03	3.6E-03	3.8E-03	3.9E-03	4.0E-03
Photosynthetically Active Radiation										
Begin Wavelength [nm]	400	400	400	400	400	400	400	400	400	400
End Wavelength [nm]	700	700	700	700	700	700	700	700	700	700
Ephot (Begin..End) [uMol/s sqm]	2.2014E+02	4.3293E+02	6.3233E+02	8.2294E+02	1.0039E+03	1.1734E+03	1.3338E+03	1.4959E+03	1.6443E+03	1.8013E+03
Circadian Metrics										
Lec [W/(sr*sqm)]	7.391E+0	1.465E+1	2.156E+1	2.818E+1	3.456E+1	4.058E+1	4.641E+1	5.214E+1	5.758E+1	6.323E+1
acv	3.339E-1	3.364E-1	3.388E-1	3.400E-1	3.419E-1	3.433E-1	3.455E-1	3.458E-1	3.474E-1	3.480E-1
CCT [K]	2776	2784	2794	2796	2802	2808	2817	2813	2820	2820
LED Values										
Peak Wavelength [nm]	606.0	607.0	605.0	606.0	606.0	605.0	605.0	606.0	605.0	605.0
PEAK FWHM [nm]	121.1	120.9	121.8	121.5	121.7	121.8	122.5	121.3	121.5	121.2
Centroid Wavelength [nm]	585.8	585.4	585.1	584.9	584.6	584.4	584.2	584.0	583.9	583.7
RGB Values										
RGB Space	manual	manual	manual	manual	manual	manual	manual	manual	manual	manual
R	23914.9	46976.8	68451.7	89135.9	108561.7	126791.8	143738.9	161617.7	177352.0	194412.2
G	13341.8	26264.1	38396.3	50013.7	61034.6	71417.8	81201.6	91110.2	100223.0	109834.8
B	5586.8	11151.2	16488.1	21638.5	26643.3	31381.5	36002.9	40559.7	44867.7	49352.3
Ratio Values										
Wavelength Range Dividend [nm]	380 - 400	380 - 400	380 - 400	380 - 400	380 - 400	380 - 400	380 - 400	380 - 400	380 - 400	380 - 400
Wavelength Range Divisor [nm]	400 - 420	400 - 420	400 - 420	400 - 420	400 - 420	400 - 420	400 - 420	400 - 420	400 - 420	400 - 420
Ratio Value	0.1060	0.0630	0.0666	0.1112	0.1132	0.0925	0.0346	0.0143	0.0476	0.0667
Wavelength [nm]	*Le [W/(sr*sqm*nm)]*	*Le [W/(sr*sqm*nm)]*	*Le [W/(sr*sqm*nm)]*	*Le [W/(sr*sqm*nm)]*	*Le [W/(sr*sqm*nm)]*	*Le [W/(sr*sqm*nm)]*	*Le [W/(sr*sqm*nm)]*	*Le [W/(sr*sqm*nm)]*	*Le [W/(sr*sqm*nm)]*	*Le [W/(sr*sqm*nm)]*
380	4.70260E-04	-2.60471E-04	4.42860E-04	4.84464E-03	1.06878E-04	-1.41075E-03	6.97158E-04	4.88196E-03	4.21217E-03	-2.31602E-04
381	6.42582E-05	-5.53240E-05	3.24868E-04	3.20065E-03	1.99298E-04	1.27198E-03	-9.02857E-04	2.73892E-03	-3.35628E-04	3.39573E-03
382	-2.04056E-04	2.50508E-04	3.83524E-04	1.46297E-03	8.53552E-04	3.05867E-03	-2.23049E-03	2.59899E-04	-3.73760E-03	5.22025E-03
383	-2.58373E-05	8.16532E-04	8.46427E-04	8.99717E-04	1.71734E-03	2.64634E-03	-1.72434E-03	-5.74455E-04	-2.33288E-03	3.00897E-03
384	3.86285E-04	1.33154E-03	1.36852E-03	1.11333E-03	2.56746E-03	1.25769E-03	-1.03227E-04	-8.38209E-05	1.22933E-03	-3.82477E-04
385	[illegible]	[illegible]	1.42618E-03	1.16843E-03	3.22490E-03	9.06552E-04	1.16321E-03	6.42621E-04	2.29502E-03	-5.22455E-04
⋮										
775	4.93828E-03	8.87573E-03	1.26829E-02	1.95609E-02	[illegible]	[illegible]	[illegible]	[illegible]	3.58079E-02	4.07348E-02
776	4.32276E-03	8.99885E-03	1.38177E-02	2.00431E-02	2.18851E-02	2.20659E-02	2.79485E-02	3.49352E-02	3.52911E-02	3.67784E-02
777	3.96883E-03	8.79017E-03	1.41780E-02	1.93178E-02	1.91262E-02	2.21383E-02	2.60880E-02	3.34631E-02	3.41432E-02	3.44811E-02
778	4.09127E-03	8.01694E-03	1.33344E-02	1.73327E-02	1.72781E-02	2.26082E-02	2.52621E-02	3.09581E-02	3.26654E-02	3.31402E-02
779	4.48313E-03	7.20492E-03	1.25042E-02	1.55329E-02	1.76695E-02	1.92520E-02	2.33953E-02	2.82373E-02	3.30271E-02	2.91224E-02
780	4.77623E-03	6.74233E-03	1.14292E-02	1.47948E-02	1.87238E-02	1.58500E-02	2.29337E-02	2.51942E-02	3.24325E-02	2.65542E-02

APPENDIX F: DATASHEET OF LEDS

- Datasheet of Cree
- Datasheet of Osram
- Datasheet of Philips
- Datasheet of Seoul Semiconductor

Cree® XLamp® XP-G2 LEDs

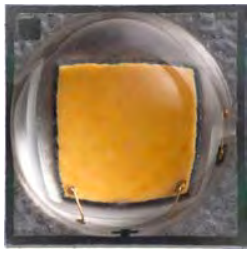

PRODUCT DESCRIPTION

The XLamp XP-G2 LED builds on the unprecedented performance of the original XP-G by increasing lumen output up to 20% while providing a single die LED point source for precise optical control. The XP-G2 LED shares the same footprint as the original XP-G, providing a seamless upgrade path and shortening the design cycle.

XLamp XP-G2 LEDs are the ideal choice for lighting applications where high light output and maximum efficacy are required, such as LED light bulbs, outdoor lighting, portable lighting, indoor lighting and solar-powered lighting.

FEATURES

- Available in white, outdoor white and 80-, 85- and 90-CRI white
- ANSI-compatible chromaticity bins
- Binned at 85 °C
- Maximum drive current: 1500 mA
- Low thermal resistance: 4 °C/W
- Wide viewing angle: 115°
- Unlimited floor life at ≤ 30 ºC/85% RH
- Reflow solderable - JEDEC J-STD-020C
- Electrically neutral thermal path
- RoHS- and REACh- compliant
- UL-recognized component (E349212)

TABLE OF CONTENTS

Characteristics 2
Flux Characteristics..... 3
Relative Spectral Power Distribution..... 4
Relative Flux vs. Junction Temperature 4
Electrical Characteristics..... 5
Relative Flux vs. Current 5
Relative Chromaticity vs Current and Temperature 6
Typical Spatial Distribution..... 7
Thermal Design 7
Reflow Soldering Characteristics .. 8
Notes..... 9
Mechanical Dimensions.....10
Tape and Reel 11
Packaging.....12

Copyright © 2012-2013 Cree, Inc. All rights reserved. The information in this document is subject to change without notice. Cree®, the Cree logo and XLamp® are registered trademarks of Cree, Inc.

Cree, Inc.
4600 Silicon Drive
Durham, NC 27703
USA Tel: +1.919.313.5300

CHARACTERISTICS

Characteristics	Unit	Minimum	Typical	Maximum
Thermal resistance, junction to solder point	°C/W		4	
Viewing angle (FWHM)	degrees		115	
Temperature coefficient of voltage	mV/°C		-1.8	
ESD withstand voltage (HBM per Mil-Std-883D)	V			8000
DC forward current	mA			1500
Reverse voltage	V			5
Forward voltage (@ 350 mA, 85 °C)	V		2.8	3.15
Forward voltage (@ 700 mA, 85 °C)	V		2.9	
Forward voltage (@ 1000 mA, 85 °C)	V		3.0	
Forward voltage (@ 1500 mA, 85 °C)	V		3.1	
LED junction temperature	°C			150

Copyright © 2012-2013 Cree, Inc. All rights reserved. The information in this document is subject to change without notice. Cree®, the Cree logo and XLamp® are registered trademarks of Cree, Inc.

FLUX CHARACTERISTICS (T_J = 85 °C)

The following table provides several base order codes for XLamp XP-G2 LEDs. It is important to note that the base order codes listed here are a subset of the total available order codes for the product family.

Color	CCT Range		Base Order Codes Min. Luminous Flux @ 350 mA			Calculated Minimum Luminous Flux (lm)** @ 85 °C			Order Code
	Min.	Max.	Group	Flux (lm) @ 85 °C	Flux (lm) @ 25 °C*	700 mA	1.0 A	1.5 A	
Cool White	5000 K	8300 K	R3	122	138	223	297	402	XPGBWT-L1-0000-00F51
			R4	130	147	237	316	429	XPGBWT-L1-0000-00G51
			R5	139	158	254	338	458	XPGBWT-L1-0000-00H51
Outdoor White	3200 K	5300 K	R2	114	129	208	277	376	XPGBWT-01-0000-00EC2
			R3	122	138	223	297	402	XPGBWT-01-0000-00FC2
			R4	130	147	237	316	429	XPGBWT-01-0000-00GC2
Neutral White	3700 K	5300 K	Q5	107	121	195	260	353	XPGBWT-L1-0000-00DE4
			R2	114	129	208	277	376	XPGBWT-L1-0000-00EE4
			R3	122	138	223	297	402	XPGBWT-L1-0000-00FE4
80-CRI White	2600 K	4300 K	Q4	100	113	182	243	330	XPGBWT-H1-0000-00CE7
			Q5	107	121	195	260	353	XPGBWT-H1-0000-00DE7
			R2	114	129	208	277	376	XPGBWT-H1-0000-00EE7
			R3	122	138	223	297	402	XPGBWT-H1-0000-00FE7
Warm White	2600 K	3700 K	Q4	100	113	182	243	330	XPGBWT-L1-0000-00CE7
			Q5	107	121	195	260	353	XPGBWT-L1-0000-00DE7
			R2	114	129	208	277	376	XPGBWT-L1-0000-00EE7
			R3	122	138	223	297	402	XPGBWT-L1-0000-00FE7
			R4	130	147	237	316	429	XPGBWT-L1-0000-00GE7
85-CRI White	2600 K	3200 K	P3	73.9	83.8	135	180	244	XPGBWT-P1-0000-008E7
			P4	80.6	91.4	147	196	266	XPGBWT-P1-0000-009E7
			Q2	87.4	99.1	160	213	288	XPGBWT-P1-0000-00AE7
			Q3	93.9	106	172	228	310	XPGBWT-P1-0000-00BE7
90-CRI White	2600 K	3200 K	P3	73.9	83.8	135	180	244	XPGBWT-U1-0000-008E7
			P4	80.6	91.4	147	196	266	XPGBWT-U1-0000-009E7
			Q2	87.4	99.1	160	213	288	XPGBWT-U1-0000-00AE7

Notes:

- Cree maintains a tolerance of ±7% on flux and power measurements, ±0.005 on chromaticity (CCx, CCy) measurements and ±2 on CRI measurements.
- Typical CRI for Cool White (5000 K - 8300 K CCT) is 70.
- Typical CRI for Neutral White (3700 K - 5300 K CCT) is 75.
- Typical CRI for Outdoor White (4000 K - 5300 K CCT) is 70.
- Typical CRI for Warm White (2600 K - 3700 K CCT) is 80.
- Flux values @ 25 °C are calculated and for reference only.
- Minimum CRI for 80-CRI White is 80.
- Minimum CRI for 85-CRI White is 85.
- Minimum CRI for 90-CRI White is 90.

** Calculated flux values at 700 mA, 1 A and 1.5 A are for reference only.

Copyright © 2012-2013 Cree, Inc. All rights reserved. The information in this document is subject to change without notice. Cree®, the Cree logo and XLamp® are registered trademarks of Cree, Inc.

RELATIVE SPECTRAL POWER DISTRIBUTION

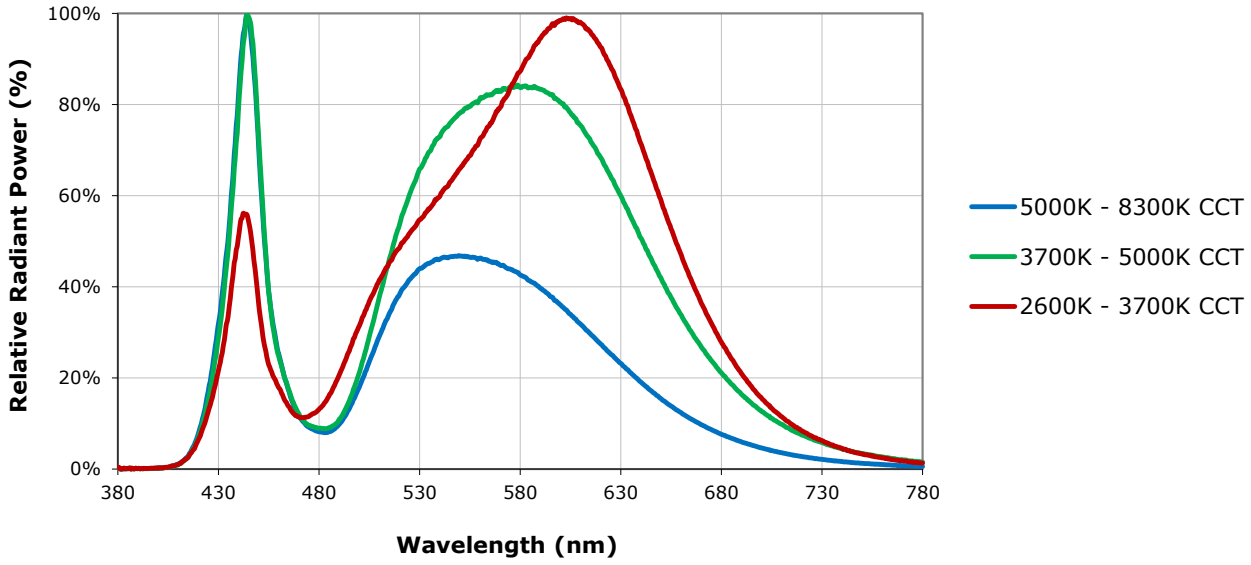

RELATIVE FLUX VS. JUNCTION TEMPERATURE (I_F = 350 mA)

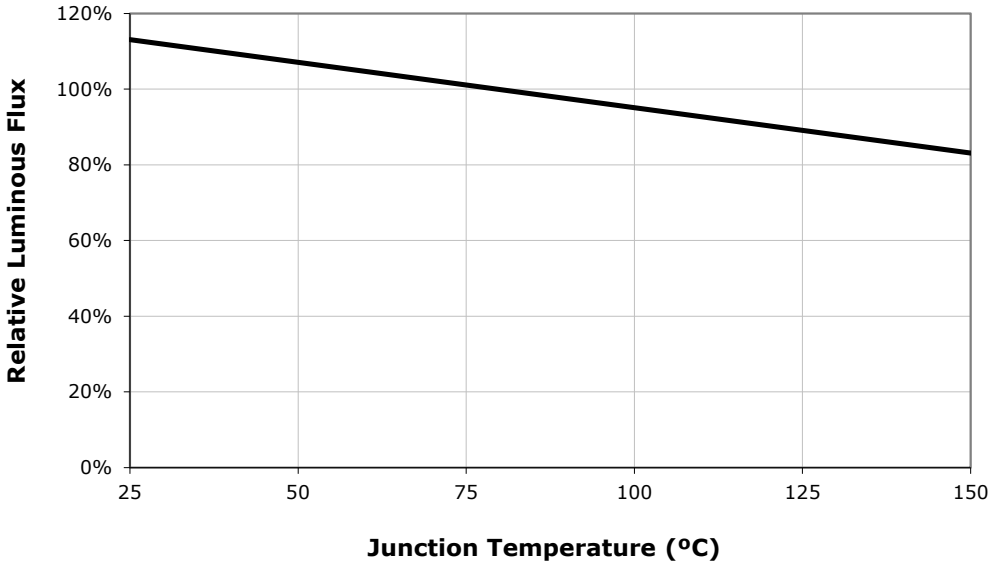

Copyright © 2012-2013 Cree, Inc. All rights reserved. The information in this document is subject to change without notice. Cree®, the Cree logo and XLamp® are registered trademarks of Cree, Inc.

ELECTRICAL CHARACTERISTICS (T_J = 85 °C)

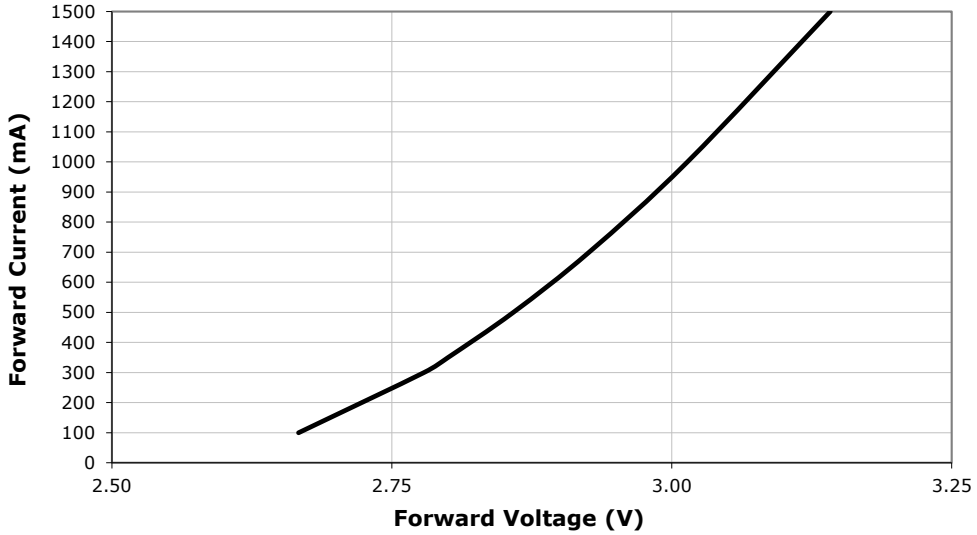

RELATIVE FLUX VS. CURRENT (T_J = 85 °C)

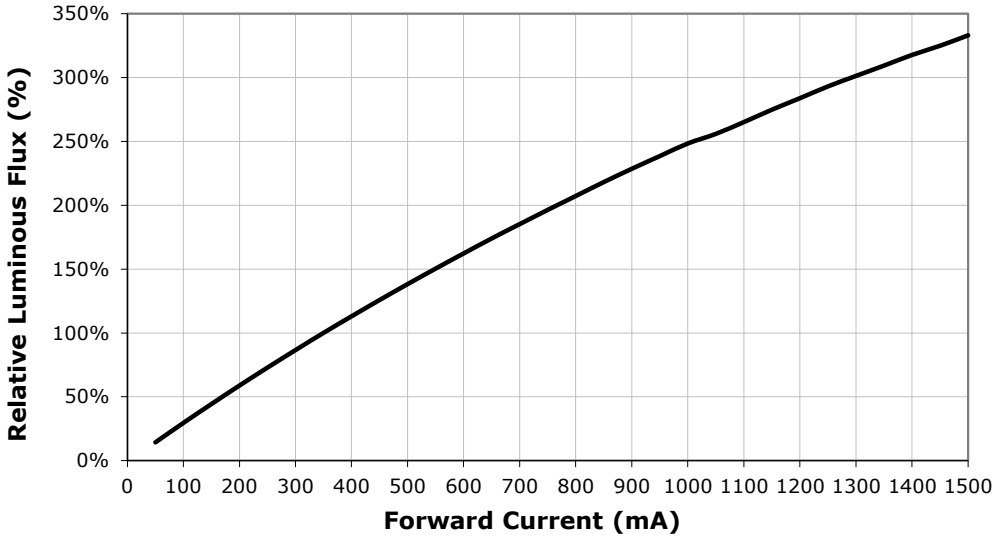

Copyright © 2012-2013 Cree, Inc. All rights reserved. The information in this document is subject to change without notice. Cree®, the Cree logo and XLamp® are registered trademarks of Cree, Inc.

RELATIVE CHROMATICITY VS CURRENT AND TEMPERATURE (WARM WHITE*)

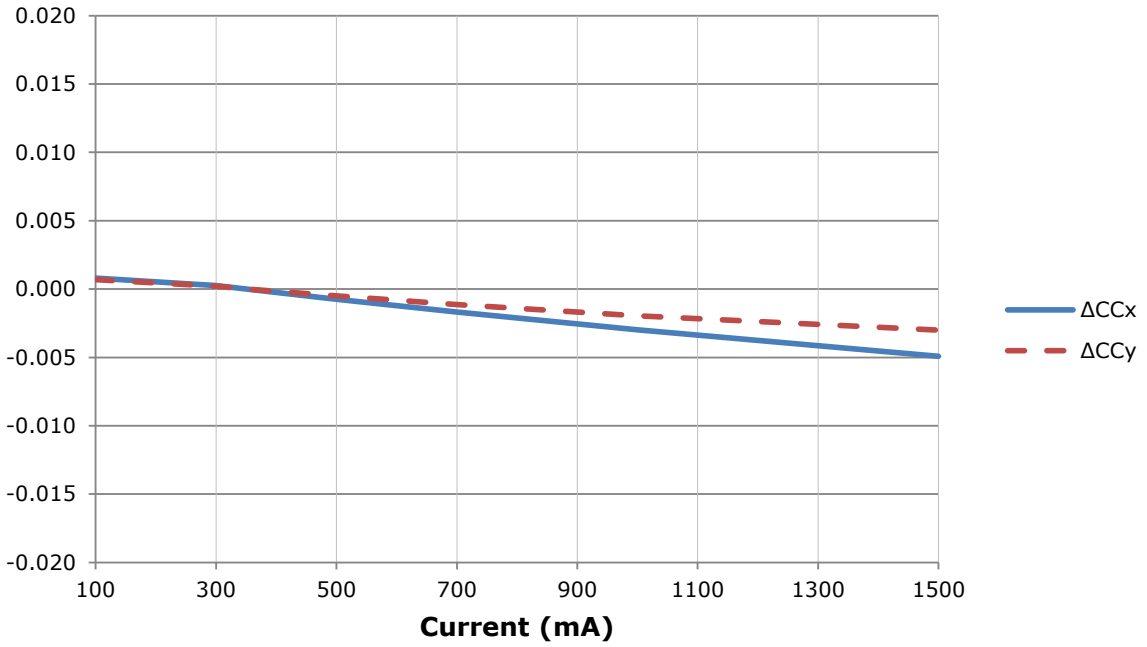

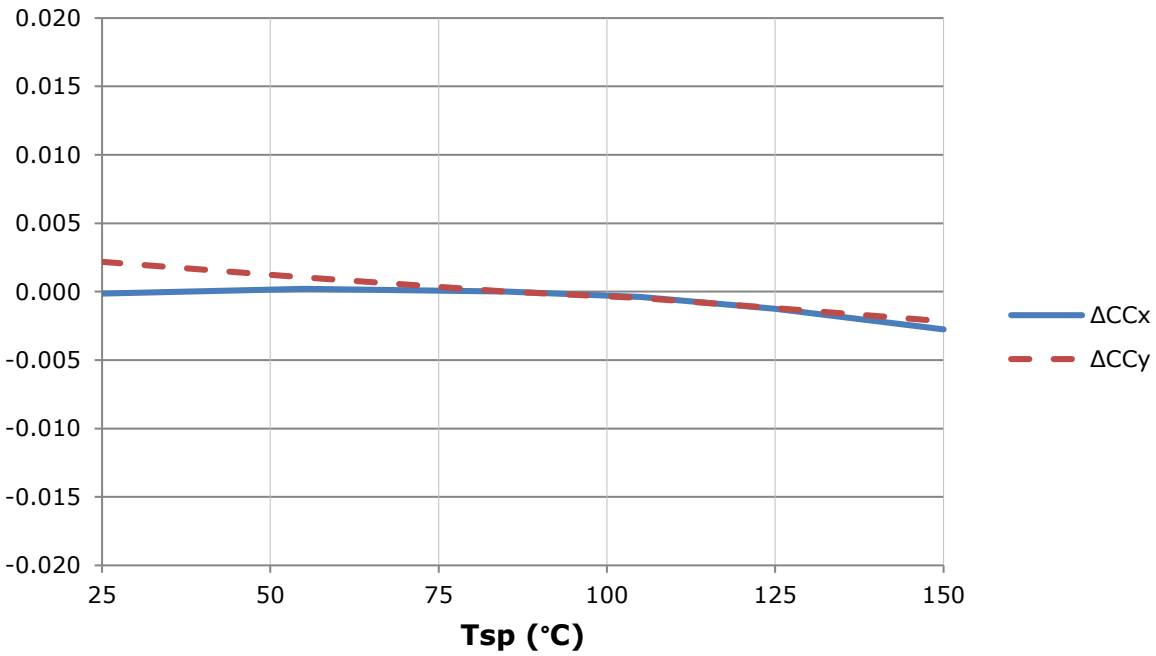

* Warm White XLamp XP-G2 LEDs have a typical CRI of 80.

Copyright © 2012-2013 Cree, Inc. All rights reserved. The information in this document is subject to change without notice. Cree®, the Cree logo and XLamp® are registered trademarks of Cree, Inc.

TYPICAL SPATIAL DISTRIBUTION

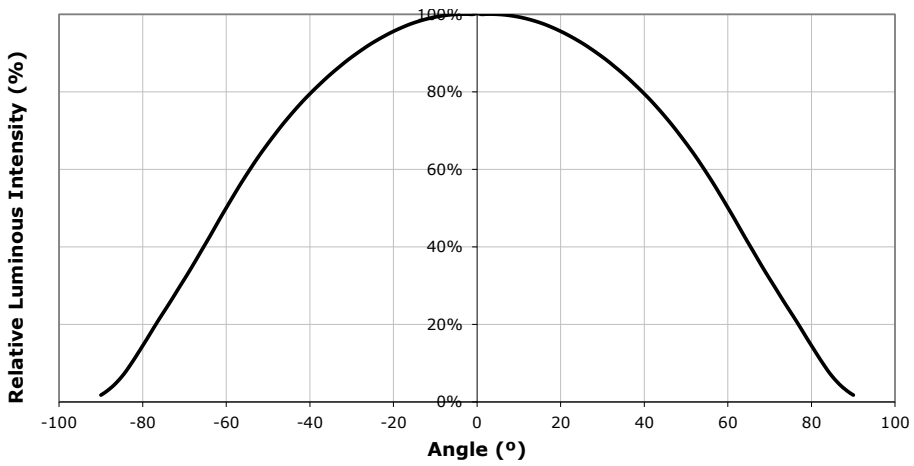

THERMAL DESIGN

The maximum forward current is determined by the thermal resistance between the LED junction and ambient. It is crucial for the end product to be designed in a manner that minimizes the thermal resistance from the solder point to ambient in order to optimize lamp life and optical characteristics.

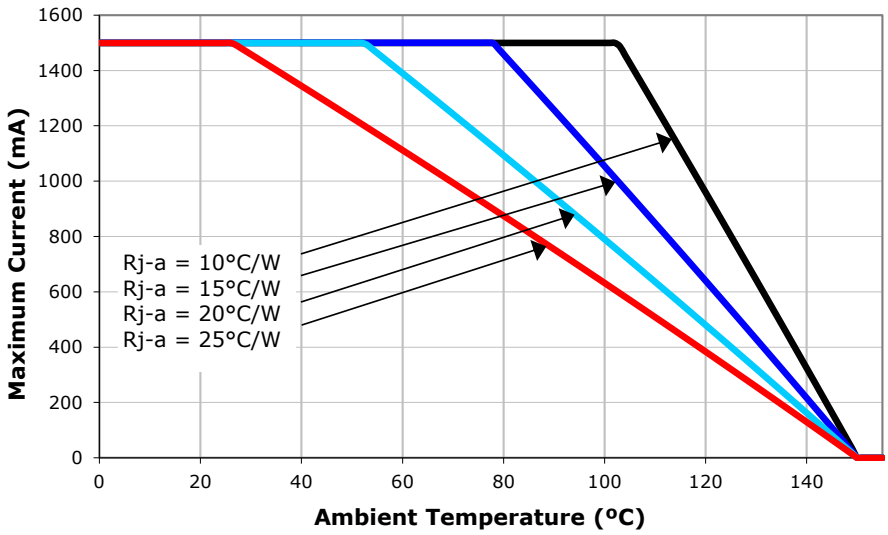

Copyright © 2012-2013 Cree, Inc. All rights reserved. The information in this document is subject to change without notice. Cree®, the Cree logo and XLamp® are registered trademarks of Cree, Inc.

REFLOW SOLDERING CHARACTERISTICS

In testing, Cree has found XLamp XP-G2 LEDs to be compatible with JEDEC J-STD-020C, using the parameters listed below. As a general guideline, Cree recommends that users follow the recommended soldering profile provided by the manufacturer of solder paste used.

Note that this general guideline may not apply to all PCB designs and configurations of reflow soldering equipment.

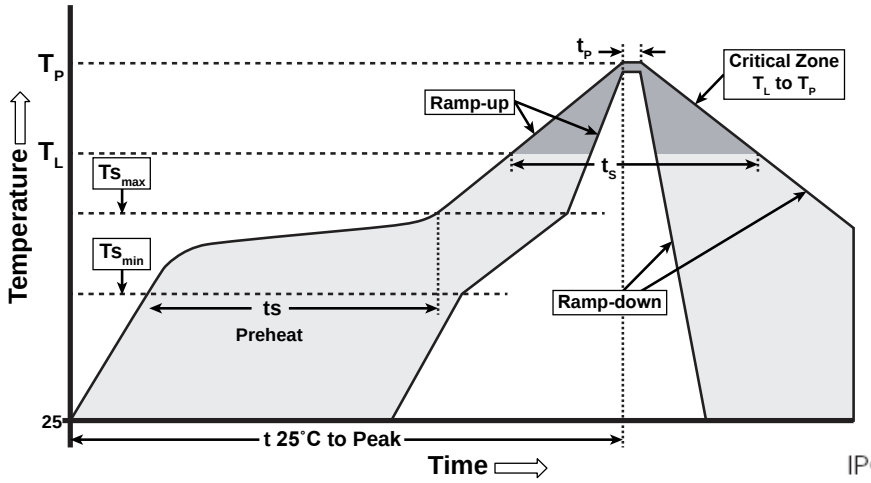

IPC/JEDEC J-STD-020C

Profile Feature	Lead-Based Solder	Lead-Free Solder
Average Ramp-Up Rate (Ts_{max} to Tp)	3 °C/second max.	3 °C/second max.
Preheat: Temperature Min (Ts_{min})	100 °C	150 °C
Preheat: Temperature Max (Ts_{max})	150 °C	200 °C
Preheat: Time (ts_{min} to ts_{max})	60-120 seconds	60-180 seconds
Time Maintained Above: Temperature (T_L)	183 °C	217 °C
Time Maintained Above: Time (t_L)	60-150 seconds	60-150 seconds
Peak/Classification Temperature (Tp)	215 °C	260 °C
Time Within 5 °C of Actual Peak Temperature (tp)	10-30 seconds	20-40 seconds
Ramp-Down Rate	6 °C/second max.	6 °C/second max.
Time 25 °C to Peak Temperature	6 minutes max.	8 minutes max.

Note: All temperatures refer to topside of the package, measured on the package body surface.

Copyright © 2012-2013 Cree, Inc. All rights reserved. The information in this document is subject to change without notice. Cree®, the Cree logo and XLamp® are registered trademarks of Cree, Inc.

NOTES

Lumen Maintenance Projections

Cree now uses standardized IES LM-80-08 and TM-21-11 methods for collecting long-term data and extrapolating LED lumen maintenance. For information on the specific LM-80 data sets available for this LED, refer to the public LM-80 results document at www.cree.com/xlamp_app_notes/LM80_results.

Please read the XLamp Long-Term Lumen Maintenance application note at www.cree.com/xlamp_app_notes/lumen_maintenance for more details on Cree's lumen maintenance testing and forecasting. Please read the XLamp Thermal Management application note at www.cree.com/xlamp_app_notes/thermal_management for details on how thermal design, ambient temperature, and drive current affect the LED junction temperature.

Moisture Sensitivity

In testing, Cree has found XLamp XP-G2 LEDs to have unlimited floor life in conditions ≤ 30 ºC/85% relative humidity (RH). Moisture testing included a 168-hour soak at 85 ºC/85% RH followed by 3 reflow cycles, with visual and electrical inspections at each stage.

Cree recommends keeping XLamp LEDs in their sealed moisture-barrier packaging until immediately prior to use. Cree also recommends returning any unused LEDs to the resealable moisture-barrier bag and closing the bag immediately after use.

RoHS Compliance

The levels of RoHS restricted materials in this product are below the maximum concentration values (also referred to as the threshold limits) permitted for such substances, or are used in an exempted application, in accordance with EU Directive 2011/65/EC (RoHS2), as implemented January 2, 2013. RoHS Declarations for this product can be obtained from your Cree representative or from the Product Documentation sections of www.cree.com.

REACh Compliance

REACh substances of high concern (SVHCs) information is available for this product. Since the European Chemical Agency (ECHA) has published notice of their intent to frequently revise the SVHC listing for the foreseeable future, please contact a Cree representative to insure you get the most up-to-date REACh Declaration. REACh banned substance information (REACh Article 67) is also available upon request.

UL Recognized Component

Level 4 enclosure consideration. The LED package or a portion thereof has been investigated as a fire and electrical enclosure per ANSI/UL 8750.

Vision Advisory Claim

WARNING: Do not look at exposed lamp in operation. Eye injury can result. See LED Eye Safety at www.cree.com/xlamp_app_notes/led_eye_safety.

Copyright © 2012-2013 Cree, Inc. All rights reserved. The information in this document is subject to change without notice. Cree®, the Cree logo and XLamp® are registered trademarks of Cree, Inc.

MECHANICAL DIMENSIONS (T_A = 25 °C)

All measurements are ±.13 mm unless otherwise indicated.

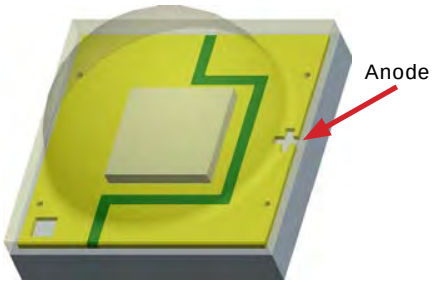

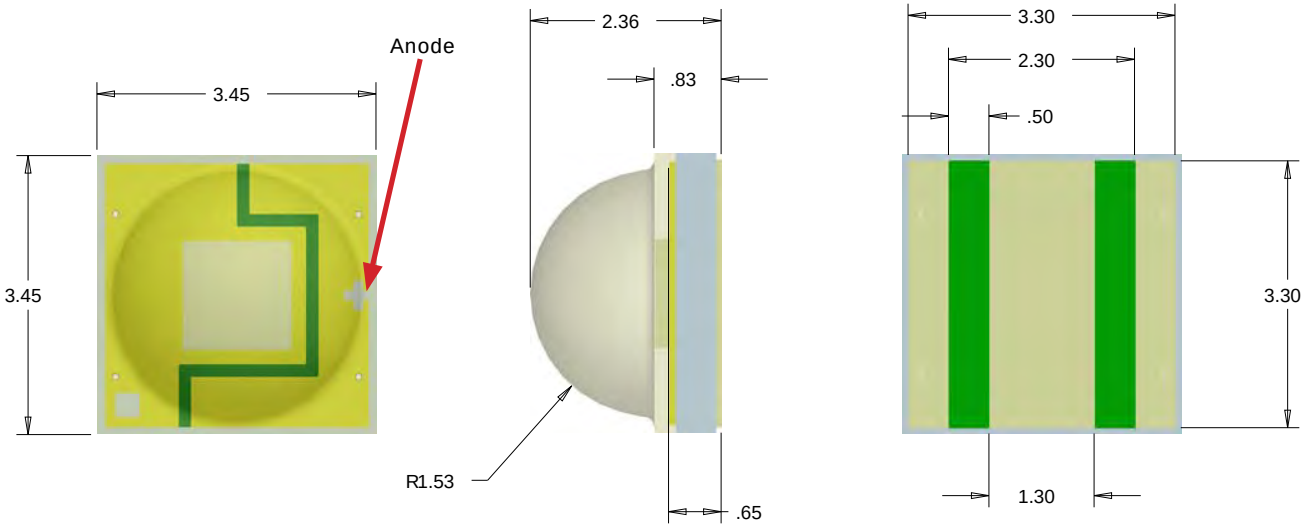

Top View **Side View** **Bottom View**

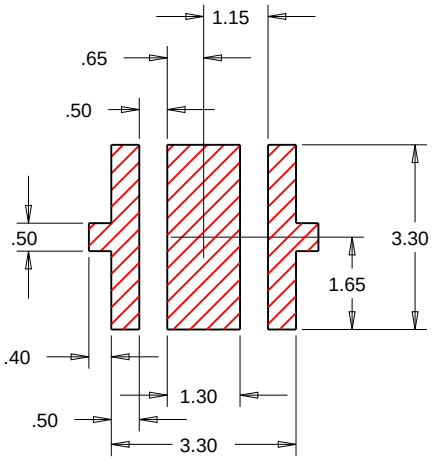

RECOMMENDED PCB SOLDER PAD

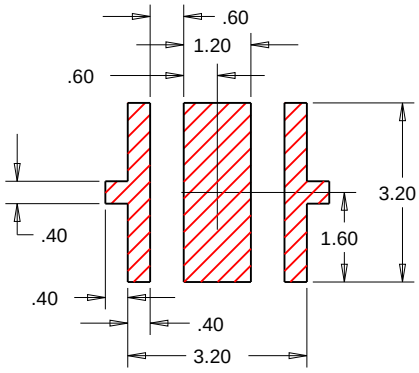

RECOMMENDED STENCIL PATTERN
(HATCHED AREA IS OPENING)

Copyright © 2012-2013 Cree, Inc. All rights reserved. The information in this document is subject to change without notice. Cree®, the Cree logo and XLamp® are registered trademarks of Cree, Inc.

TAPE AND REEL

All Cree carrier tapes conform to EIA-481D, Automated Component Handling Systems Standard.

All dimensions in mm.

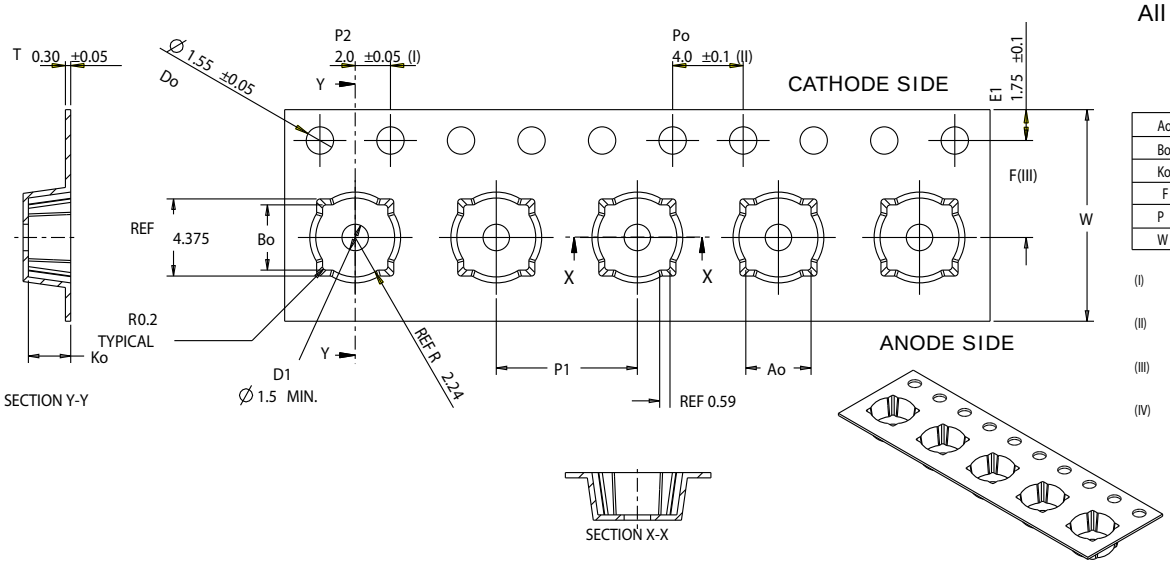

Ao	3.70	+/- 0.1
Bo	3.70	+/- 0.1
Ko	2.40	+0.0/-0.1
F	5.50	+/- 0.05
P 1	8.00	+/- 0.1
W	12.00	+0.3/-0.1

(I) Measured from centerline of sprocket hole to centerline of pocket.

(II) Cumulative tolerance of 10 sprocket holes is ± 0.20.

(III) Measured from centerline of sprocket hole to centerline of pocket.

(IV) Other material available.

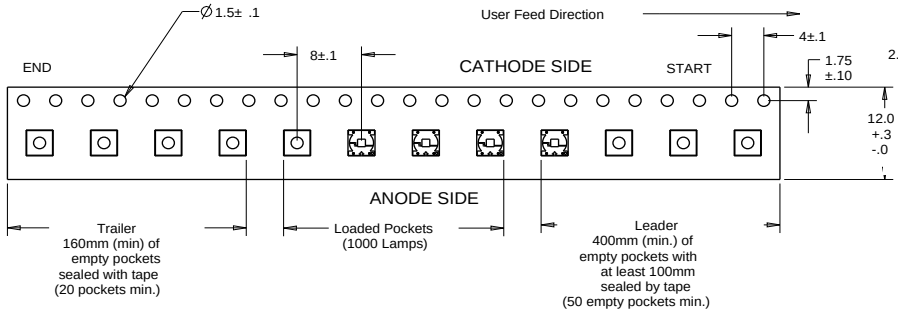

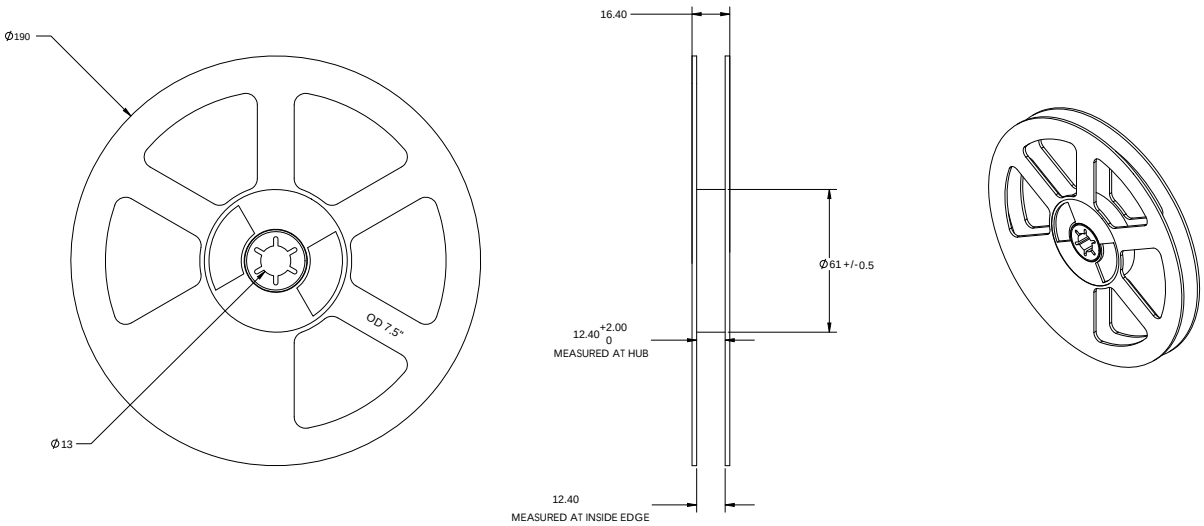

Copyright © 2012-2013 Cree, Inc. All rights reserved. The information in this document is subject to change without notice. Cree®, the Cree logo and XLamp® are registered trademarks of Cree, Inc.

PACKAGING

Unpackaged Reel

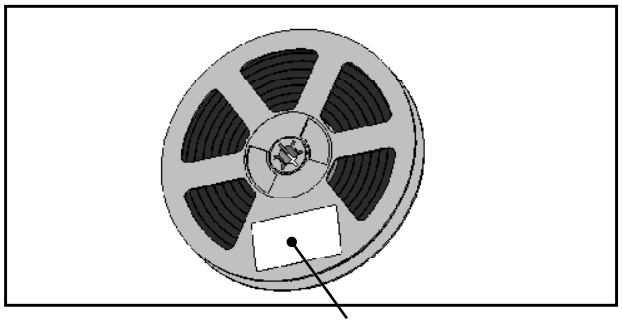

Label with Cree Bin Code, Qty, Reel ID

Packaged Reel

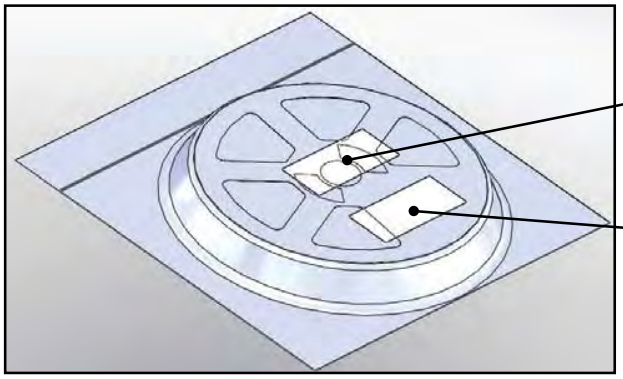

Label with Cree Order Code, Qty, Reel ID, PO #

Label with Cree Bin Code, Qty, Reel ID

Boxed Reel

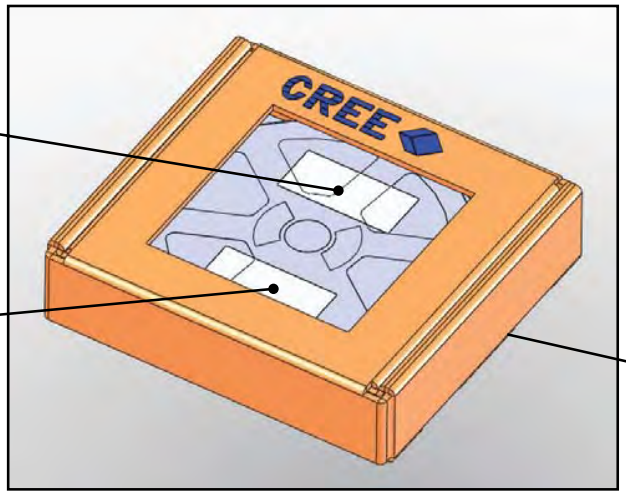

Label with Cree Order Code, Qty, Reel ID, PO #

Label with Cree Bin Code, Qty, Reel ID

Patent Label (on bottom of box)

Copyright © 2012-2013 Cree, Inc. All rights reserved. The information in this document is subject to change without notice. Cree®, the Cree logo and XLamp® are registered trademarks of Cree, Inc.

OSLON SSL
Ceramic package - 80° radiation pattern
Lead (Pb) Free Product - RoHS Compliant

LCW CQ7P.CC

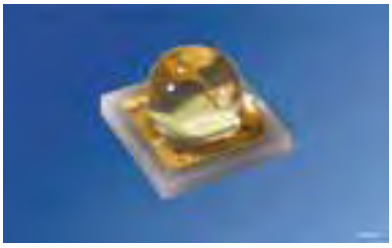

Released

Besondere Merkmale
- **Gehäusetyp:** SMT-Keramikgehäuse mit Silikonverguss und Linse
- **Typischer Lichtstrom:** 74 lm bei 350 mA und bis zu 127 lm bei 700 mA (4000 K)
- **Besonderheit des Bauteils:** Kompakte Lichtquelle für platzsparende Designs
- **Farbtemperatur:** 2700 K bis 4000 K
- **Farbwiedergabeindex:** 95 (typ.)
- **Abstrahlwinkel:** 80°
- **Typischer optischer Wirkungsgrad:** 66 lm/W bei 350 mA (4000 K)
- **Gruppierungsparameter:** Lichtstrom, Farbort, Durchlassspannung
- **Lötmethode:** Reflow-Löten
- **Vorbehandlung:** nach JEDEC Level 2
- **Gurtung:** 12-mm Gurt mit 600/Rolle, ø180 mm
- **ESD-Festigkeit:** ESD-sicher bis 8 kV nach JESD22-A114-D
- **Erweiterte Korrosionsfestigkeit:** Details siehe **Seite 15**
- **Testergebnis zur Lichtstromerhaltung nach IESNA-LM-80 verfügbar**

Features
- **package:** SMt ceramic package with silicon resin with lens
- **typical Luminous Flux:** 74 lm at 350 mA and up to 127 lm at 700 mA (4000 K)
- **feature of the device:** small size high-flux LED for slim designs
- **typ. color temperature:** 2700 K to 4000 K
- **color rendering index:** 95 (typ.)
- **viewing angle:** 80°
- **typical optical efficiency:** 66 lm/W at 350 mA (4000 K)
- **grouping parameter:** luminous flux, color coordinates, forward voltage
- **soldering methods:** reflow soldering
- **preconditioning:** acc. to JEDEC Level 2
- **taping:** 12-mm tape with 600/reel, ø180 mm
- **ESD-withstand voltage:** up to 8 kV acc. to JESD22-A114-D
- **Superior Corrosion Robustness:** details see **page 15**
- **Lumen maintanance test report according to IESNA LM-80 available**

Anwendungen
- Ladenbeleuchtung
- Lampen- und Leuchten-Retrofits
- Spot-Lichtquellen
- Museumsbeleuchtung
- Bühnenbeleuchtung

Applications
- Shop lighting
- Residential retrofits & fixtures
- Spot lights
- Museum lighting
- Stage lighting

OSRAM
Opto Semiconductors

Bestellinformation
Ordering Information

Typ **Type**	**Farb-temperatur** **color temperature**	**Lichtstrom** 1) Seite 22 **Luminous Flux**[1) page 22] I_F **= 350 mA** Φ_V**(lm)**	**Lichtstärke** 2) Seite 22 **Luminous Intensity**[2) page 22] I_F **= 350 mA** I_V **(cd)**	**Bestellnummer** **Ordering Code**
LCW CQ7P.CC-JUKQ-5U8X-1 LCW CQ7P.CC-JTKP-5U8X-1	2700 K	65.8 ... 82.0 61.0 ... 76.3	41.0 (typ.) 38.0 (typ.)	Q65111A1898 Q65111A1897
LCW CQ7P.CC-KPKR-5R8T-1 LCW CQ7P.CC-JUKQ-5R8T-1	3000 K	71.0 ... 89.2 65.8 ... 82.0	45.0 (typ.) 41.0 (typ.)	Q65111A1893 Q65111A1892
LCW CQ7P.CC-KQKS-5O8Q-1 LCW CQ7P.CC-KPKR-5O8Q-1	3500 K	76.3 ... 97.0 71.0 ... 89.2	48.5 (typ.) 45.0 (typ.)	Q65111A1891 Q65111A1890
LCW CQ7P.CC-KQKS-5L7N-1 LCW CQ7P.CC-KPKR-5L7N-1	4000 K	76.3 ... 97.0 71.0 ... 89.2	48.5 (typ.) 45.0 (typ.)	Q65111A1889 Q65111A1866

OSRAM
Opto Semiconductors

Anm.: *Die oben genannten Typbezeichnungen umfassen die bestellbaren Selektionen. Diese bestehen aus wenigen Helligkeitsgruppen (siehe **Seite 10** für nähere Informationen). Es wird nur eine einzige Helligkeitsgruppe pro Gurt geliefert. Z.B.: LCW CQ7P.CC-JUKQ-5U8X-1 bedeutet, dass auf dem Gurt nur eine der Helligkeitsgruppen JU, KP oder KQ enthalten ist.*
Um die Liefersicherheit zu gewährleisten, können einzelne Helligkeitsgruppen nicht bestellt werden.

*Gleiches gilt für die Farben, bei denen Farbortgruppen gemessen und gruppiert werden. Pro Gurt wird nur eine Farbortgruppe geliefert. Z.B.: LCW CQ7P.CC-JUKQ-5U8X-1 bedeutet, dass auf dem Gurt nur eine der Farbortgruppen -5U bis -8X enthalten ist (siehe **Seite 6** für nähere Information).*
Um die Liefersicherheit zu gewährleisten, können einzelne Farbortgruppen nicht bestellt werden.

*Gleiches gilt für die LEDs, bei denen die Durchlassspannungsgruppen gemessen und gruppiert werden. Pro Gurt wird nur eine Durchlassspannungsgruppe geliefert. Z.B.: LCW CQ7P.CC-JUKQ-5U8X-1 bedeutet, dass nach Durchlassspannung gruppiert wird. Auf einem Gurt ist nur eine der Durchlasspannungsgruppen 3, 4 oder 5 enthalten (siehe **Seite 10** für nähere Information).*
Um die Liefersicherheit zu gewährleisten, können einzelne Durchlassspannungsgruppen nicht direkt bestellt werden.

Note: *The above Type Numbers represent the order groups which include only a few brightness groups (see **page 10** for explanation). Only one group will be shipped on each reel (there will be no mixing of two groups on each reel). E.g.LCW CQ7P.CC-JUKQ-5U8X-1means that only one group JU, KP or KQ will be shippable for any one reel.*
In order to ensure availability, single brightness groups will not be orderable.

*In a similar manner for colors where chromaticity coordinate groups are measured and binned, single chromaticity coordinate groups will be shipped on any one reel. E.g. LCW CQ7P.CC-JUKQ-5U8X-1 means that only 1 chromaticity coordinate group -5U to -8X will be shippable (see **page 6** for explanation).*
In order to ensure availability, single chromaticity coordinate groups will not be orderable.

*In a similar manner for LED, where forward voltage groups are measured and binned, single forward voltage groups will be shipped on any one reel. E.g. LCW CQ7P.CC-JUKQ-5U8X-1 means that only 1 forward voltage group 3, 4 or 5 will be shippable. In order to ensure availability, single forward voltage groups will not be orderable(see **page 10** for explanation).*

Grenzwerte
Maximum Ratings

Bezeichnung **Parameter**	**Symbol** **Symbol**	**Wert** **Value**	**Einheit** **Unit**
Betriebstemperatur Operating temperature range	T_{op}	– 40 … + 120	°C
Lagertemperatur Storage temperature range	T_{stg}	– 40 … + 120	°C
Sperrschichttemperatur Junction temperature	T_j	135	°C
Durchlassstrom (min.) Forward current (max.) (T_S=25°C)	I_F I_F	100 800	mA mA
Stoßstrom Surge current $t \leq$ 50 ms, D = 0.016, T_S=25°C	I_{FM}	2000	mA
Reverse Current* Sperrstrom* (max.)	I_R	200	mA

* A minimum of 10 h of reverse operation is permissable in total.
Eine Gesamtbetriebszeit von wenigstens 10 h in Sperrrichtung ist gewährleistet.

OSRAM
Opto Semiconductors

Kennwerte
Characteristics
(T_S = 25 °C)

Bezeichnung **Parameter**		**Symbol** **Symbol**	**Wert** **Value**	**Einheit** **Unit**
Farbtemperatur [2) Seite 22)] Color temperature [2) page 22] I_F = 350 mA	(min.) (max.)	T T	2700 4000	K K
Abstrahlwinkel bei 50 % I_V (Vollwinkel) Viewing angle at 50 % I_V	(typ.)	2φ	80	Grad deg.
Durchlassspannung [4) Seite 22)] Forward voltage[4) page 22] I_F = 350 mA	(min.) (typ.) (max.)	V_F V_F V_F	2.75 3.2 3.5	V V V
Reverse Voltage[3) page 22)] Sperrspannung [3) Seite 23] I_R = 20 mA	(max.)	V_R	1.2	V
Wärmewiderstand Thermal resistance Sperrschicht/Lötpad Junction/solder point	 (typ.) (max.)	 $R_{th\ el\ JS}$ $R_{th\ el\ JS}$	 7 9.4*	 K/W K/W

*R_{th}(max) basiert auf statistischen Werten
R_{th}(max) is based on statistic values

OSRAM
Opto Semiconductors

Farbortgruppen[3) Seite 22]
Chromaticity Coordinate Groups[3) *page 22*]

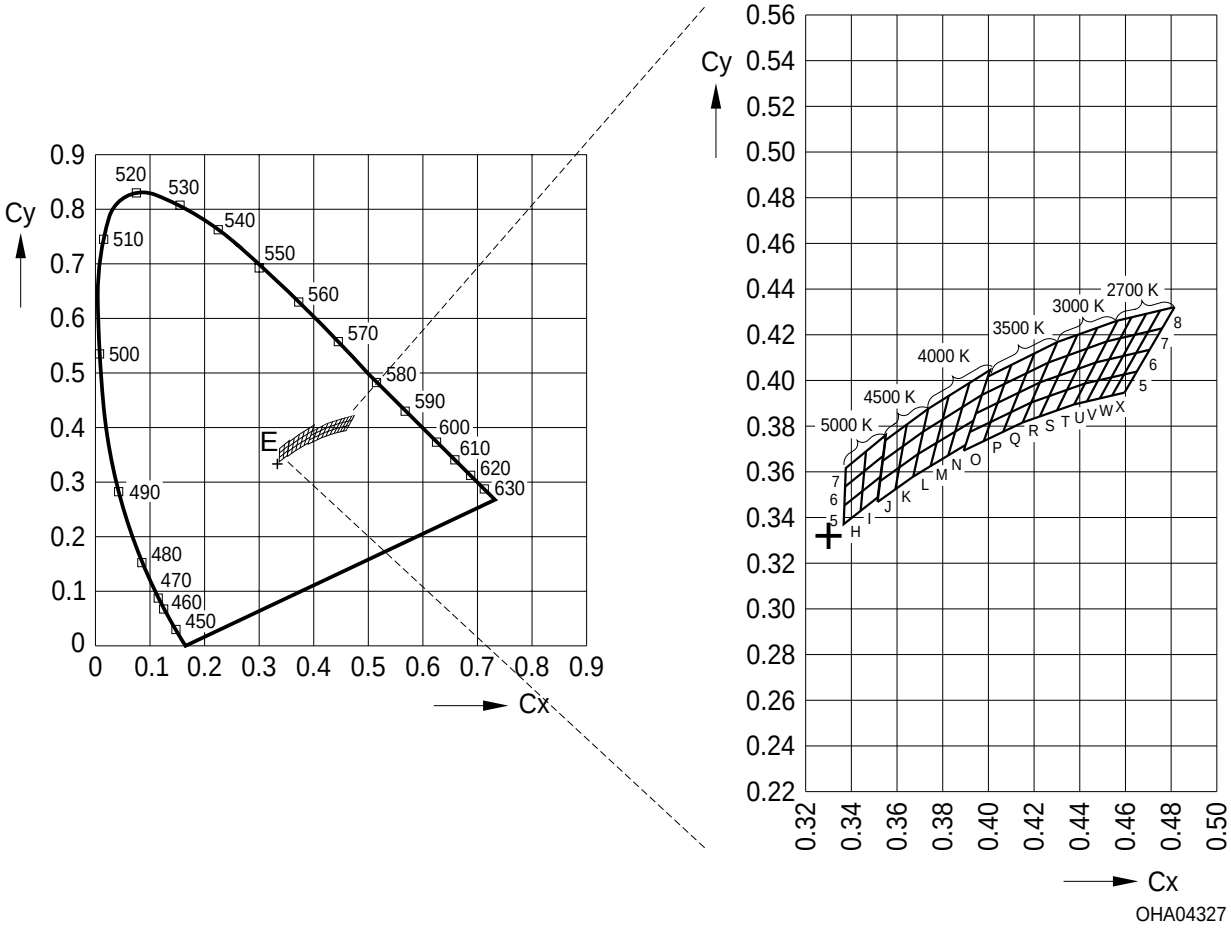

Color temperature 2700K
Farbtemperatur 2700 K

Gruppe Group	Cx	Cy
5U	0.437	0.389
	0.442	0.398
	0.448	0.400
	0.443	0.391
6U	0.442	0.398
	0.447	0.408
	0.453	0.409
	0.448	0.400
7U	0.447	0.408
	0.451	0.417
	0.458	0.418
	0.453	0.409
8U	0.451	0.417
	0.456	0.426
	0.462	0.427
	0.458	0.418
5V	0.443	0.391
	0.448	0.400
	0.453	0.401
	0.448	0.392
6V	0.448	0.400
	0.453	0.409
	0.459	0.410
	0.453	0.401

Gruppe Group	Cx	Cy
7V	0.453	0.409
	0.458	0.418
	0.464	0.420
	0.459	0.410
8V	0.458	0.418
	0.462	0.427
	0.469	0.429
	0.464	0.420
5W	0.448	0.392
	0.453	0.401
	0.459	0.402
	0.454	0.393
6W	0.453	0.401
	0.459	0.410
	0.464	0.412
	0.459	0.402
6W	0.453	0.401
	0.459	0.410
	0.464	0.412
	0.459	0.402
7W	0.459	0.410
	0.464	0.420
	0.470	0.421
	0.464	0.412

Gruppe Group	Cx	Cy
8W	0.464	0.420
	0.469	0.429
	0.475	0.430
	0.470	0.421
5X	0.454	0.393
	0.459	0.402
	0.465	0.404
	0.459	0.394
6X	0.459	0.402
	0.464	0.412
	0.470	0.413
	0.465	0.404
7X	0.464	0.412
	0.470	0.421
	0.476	0.423
	0.470	0.413
7X	0.464	0.412
	0.470	0.421
	0.476	0.423
	0.470	0.413
8X	0.4697	0.4211
	0.4750	0.4304
	0.4758	0.4225
	0.4697	0.4211

OSRAM Opto Semiconductors

Color temperature 3000 K
Farbtemperatur 3000 K

Gruppe Group	Cx	Cy
5R	0.415	0.381
	0.419	0.390
	0.426	0.393
	0.422	0.384
6R	0.419	0.390
	0.422	0.399
	0.430	0.402
	0.426	0.293
7R	0.422	0.399
	0.426	0.408
	0.435	0.411
	0.430	0.402
8R	0.426	0.408
	0.430	0.417
	0.439	0.420
	0.435	0.411

Gruppe Group	Cx	Cy
5S	0.422	0.384
	0.426	0.393
	0.434	0.396
	0.430	0.387
6S	0.426	0.393
	0.430	0.402
	0.439	0.405
	0.434	0.396
7S	0.430	0.402
	0.435	0.411
	0.443	0.414
	0.439	0.405
8S	0.435	0.411
	0.439	0.420
	0.447	0.423
	0.443	0.414

Gruppe Group	Cx	Cy
5T	0.430	0.387
	0.434	0.396
	0.442	0.398
	0.437	0.389
6T	0.434	0.396
	0.439	0.405
	0.447	0.408
	0.442	0.398
7T	0.439	0.405
	0.443	0.414
	0.451	0.417
	0.447	0.408
8T	0.443	0.414
	0.447	0.423
	0.456	0.426
	0.451	0.417

Color temperature 3500 K
Farbtemperatur 3500 K

Gruppe Group	Cx	Cy
5O	0.389	0.369
	0.392	0.377
	0.401	0.381
	0.398	0.373
6O	0.392	0.377
	0.394	0.385
	0.404	0.390
	0.401	0.381
7O	0.394	0.385
	0.397	0.393
	0.407	0.398
	0.404	0.390
8O	0.397	0.393
	0.400	0.401
	0.410	0.408
	0.407	0.398

Gruppe Group	Cx	Cy
5P	0.398	0.373
	0.401	0.381
	0.410	0.386
	0.406	0.377
6P	0.401	0.381
	0.404	0.390
	0.413	0.394
	0.410	0.386
7P	0.404	0.390
	0.407	0.398
	0.416	0.403
	0.413	0.394
8P	0.407	0.398
	0.410	0.406
	0.420	0.412
	0416	0.403

Gruppe Group	Cx	Cy
5Q	0.406	0.377
	0.410	0.386
	0.419	0.390
	0.415	0.381
6Q	0.410	0.386
	0.413	0.394
	0.422	0.399
	0.419	0.390
7Q	0.413	0.394
	0.416	0.403
	0.426	0.408
	0.422	0.399
8Q	0.416	0.403
	0.420	0.412
	0.430	0.417
	0.426	0.408

OSRAM Opto Semiconductors

Color temperature 4000 K
Farbtemperatur 4000 K

Gruppe Group	Cx	Cy
5L	0.367	0.358
	0.369	0.368
	0.377	0.373
	0.375	0.362
6L	0.369	0.368
	0.371	0.378
	0.380	0.383
	0.377	0.373
7L	0.371	0.378
	0.374	0.387
	0.383	0.393
	0.380	0.383

Gruppe Group	Cx	Cy
5M	0.375	0.362
	0.377	0.373
	0.385	0.378
	0.382	0.367
6M	0.377	0.373
	0.380	0.383
	0.388	0.388
	0.385	0.376
7M	0.380	0.383
	0.383	0.393
	0.392	0.399
	0.388	0.388

Gruppe Group	Cx	Cy
5N	0.382	0.367
	0.385	0.376
	0.393	0.383
	0.390	0.372
6N	0.385	0.378
	0.388	0.388
	0.397	0.393
	0.393	0.383
7N	0.388	0.388
	0.392	0.399
	0.401	0.404
	0.397	0.393

OSRAM Opto Semiconductors

Forward Voltage Groups[6) *page 22*]
Durchlassspannungsgruppen[6) Seite 22]

Group Gruppe	Forward voltage Durchlaßspannung		Unit Einheit
	min.	max.	
3	2.75	3.0	V
4	3.0	3.25	V
5	3.25	3.5	V

Helligkeits-Gruppierungsschema
Brightness Groups

Helligkeitsgruppe Brightness Group	Lichtstrom[1) Seite 22] Luminous Flux[1) page 22] Φ_V (lm)	Lichtstärke[2) Seite 22] Luminous Intensity[2) page 22] I_V (cd)
JT	61.0 ... 65.8	35.5 (typ.)
JU	65.8 ... 71.0	38.0 (typ.)
KP	71.0 ... 76.3	41.0 (typ.)
KQ	76.3 ... 82.0	44.0 (typ.)
KR	82.0 ... 89.2	48.0 (typ.)
KS	89.2 ... 97.0	52.0 (typ.)

Anm.: Die Standardlieferform von Serientypen beinhaltet eine Familiengruppe. Diese besteht aus nur wenigen Helligkeitsgruppen. Einzelne Helligkeitsgruppen sind nicht bestellbar.

Note: The standard shipping format for serial types includes a family group of only a few individual brightness groups. Individual brightness groups cannot be ordered.

Gruppenbezeichnung auf Etikett
Group Name on Label
Beispiel: JU-5U
Example: JU-5U

Helligkeitsgruppe Brightness Group	Farbortgruppe Chromaticity Coordinate Group
JU	5U

Anm.: In einer Verpackungseinheit / Gurt ist immer nur eine Helligkeitsgruppe enthalten.

Note: No packing unit / tape ever contains more than one brightness group.

OSRAM
Opto Semiconductors

Relative spektrale Emission[2) Seite 22]
Relative Spectral Emission[2) page 22]
V(λ) = spektrale Augenempfindlichkeit / Standard eye response curve
$\Phi_{rel} = f(\lambda)$; T_S = 25 °C; I_F = 350 mA

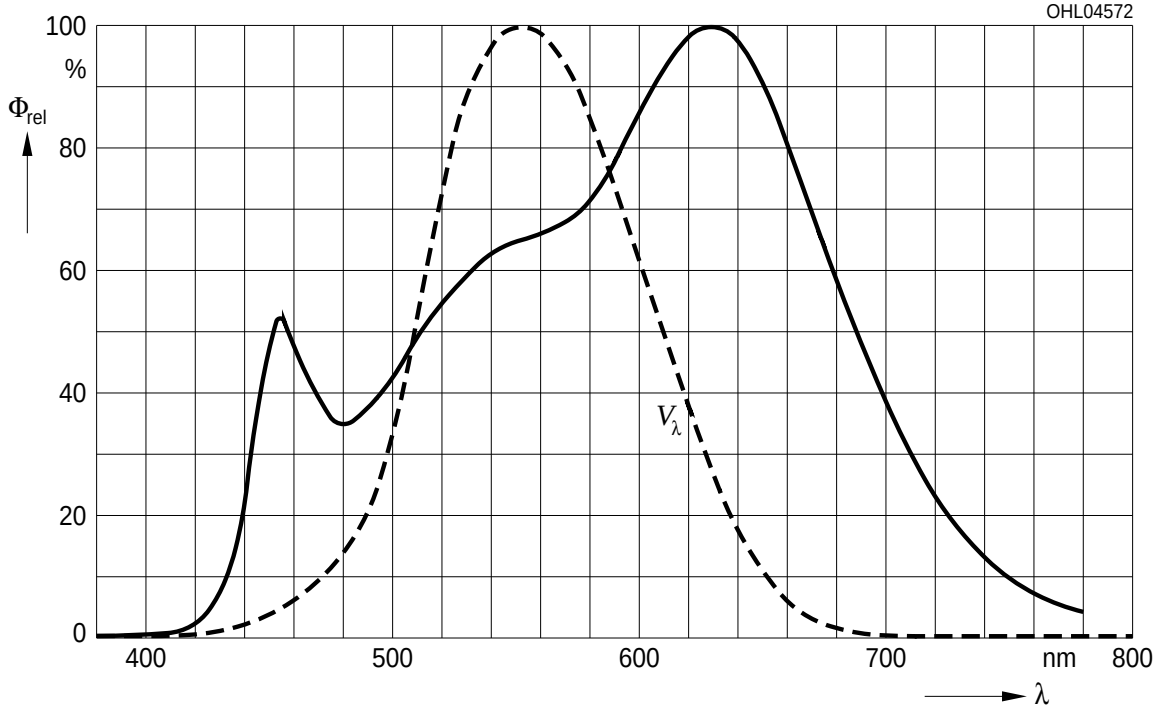

Abstrahlcharakteristik[2) Seite 22]
Radiation Characteristic[2) page 22]
$I_{rel} = f(\varphi)$; T_S = 25 °C

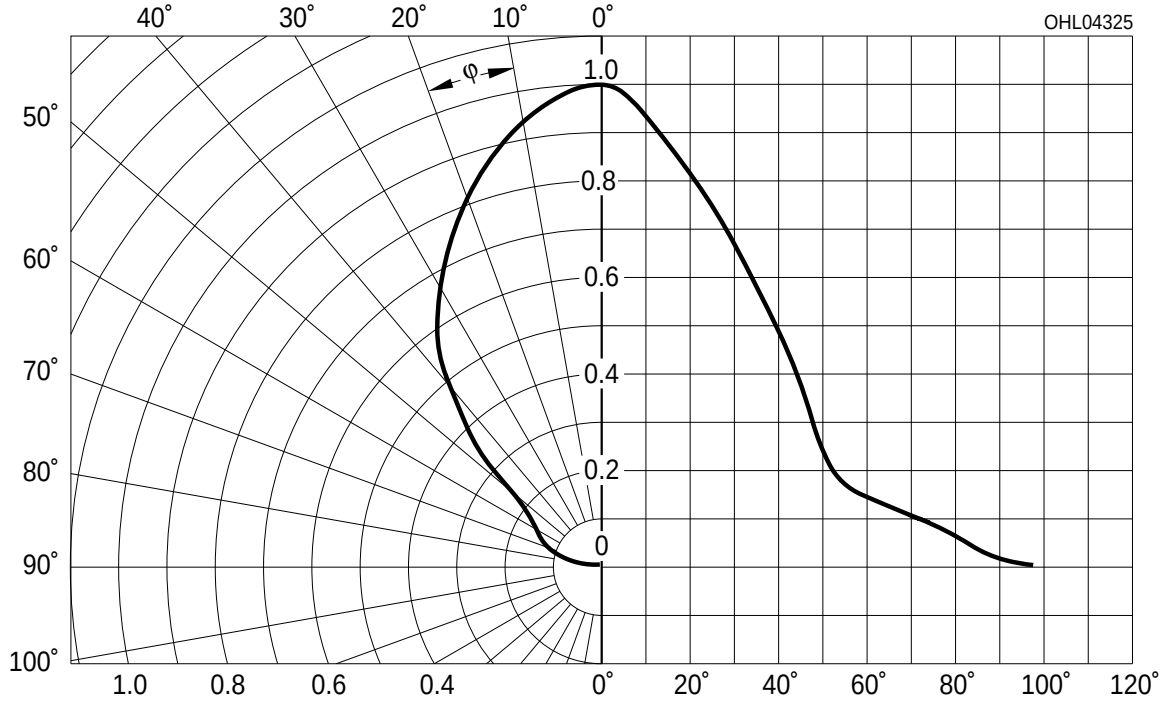

Durchlassstrom[2) Seite 22]
Forward Current[2) page 22]
$I_F = f(V_F)$; T_S = 25 °C

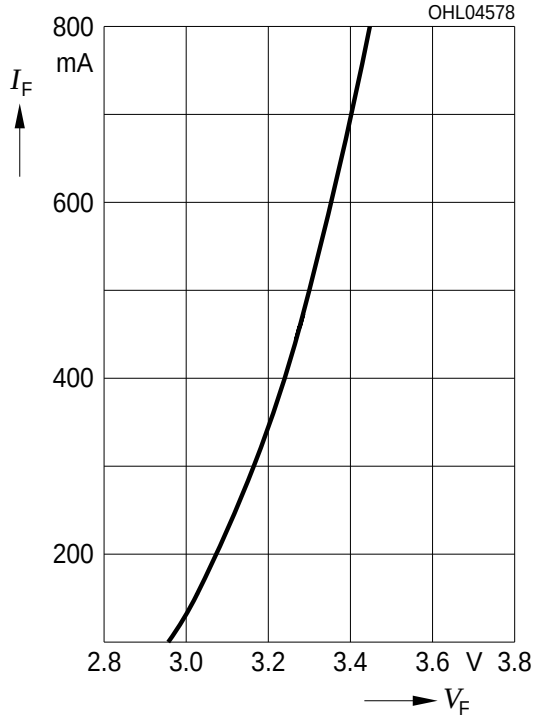

Relativer Lichtstrom[2) Seite 22]
Relative Luminous Flux[2) page 22]
$\Phi_V/\Phi_V(350\ mA) = f(I_F)$; T_S = 25 °C

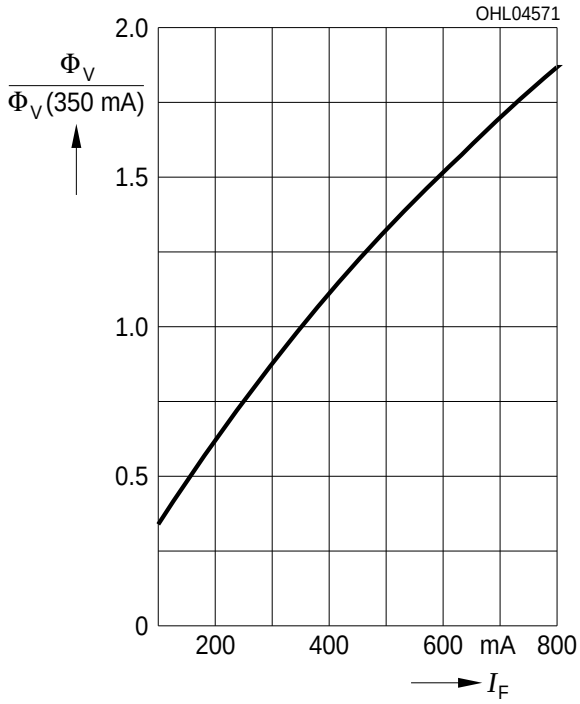

Farbortverschiebung[2) Seite 22]
Chromaticity Coordinate Shift[2) *page 22*]
x, y = $f(I_F)$; T_S = 25 °C

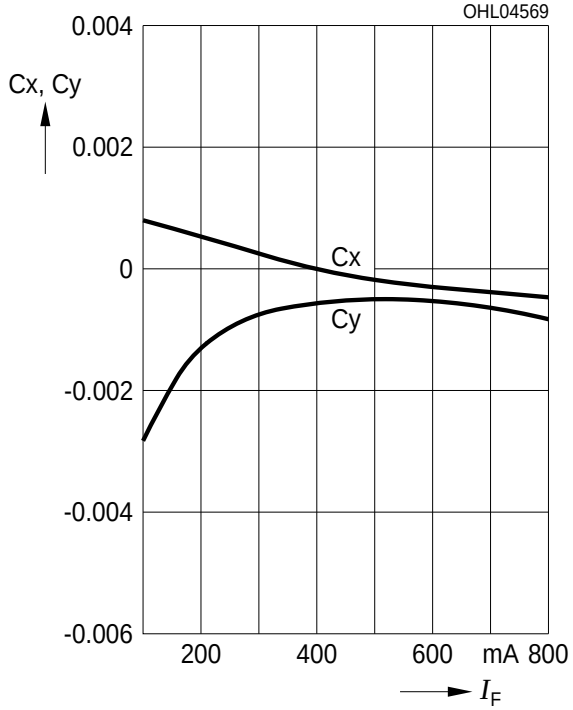

OSRAM
Opto Semiconductors

Relative Vorwärtsspannung[2) Seite 22]
Relative Forward Voltage[2) *page 22*]
$\Delta V_F = V_F - V_F(25\ °C) = f\,(T_j)$; I_F = 350 mA

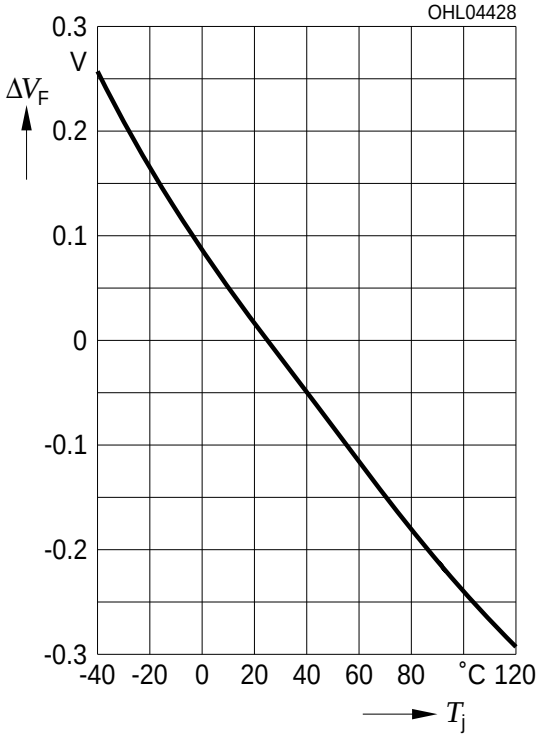

Relativer Lichtstrom[2) Seite 22]
Relative Luminous Flux[2) page 22]
$\Phi_V/\Phi_V(25\ °C) = f\,(T_j)$; I_F = 350 mA

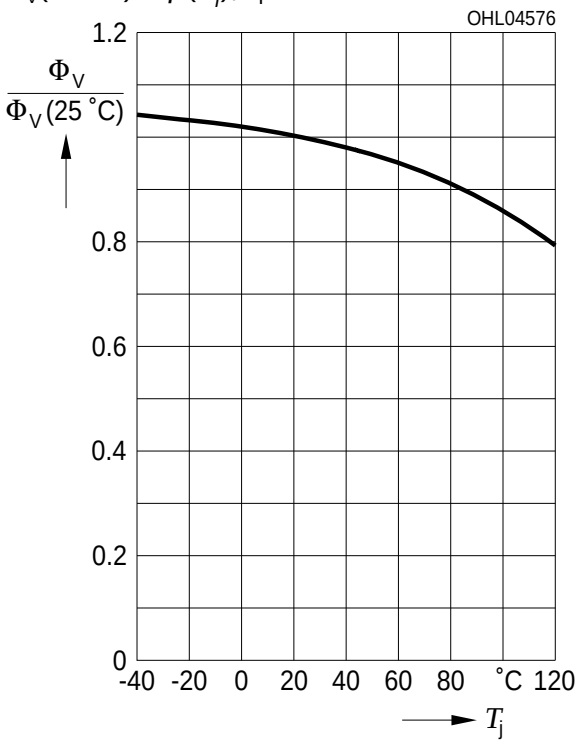

Farbortverschiebung[2) Seite 22]
Chromaticity Coordinate Shift[2) page 22]
x, y = $f\,(T_j)$; I_F = 350 mA

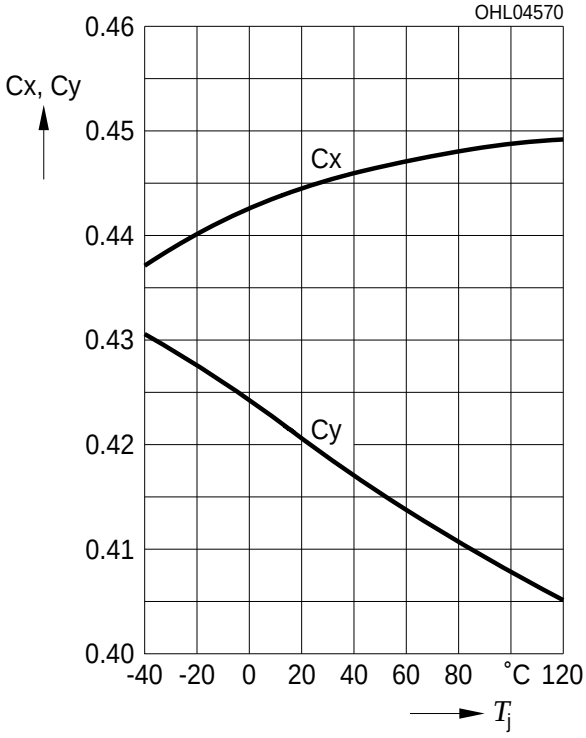

OSRAM
Opto Semiconductors

Maximal zulässiger Durchlassstrom
Max. Permissible Forward Current
$I_F = f(T_S)$

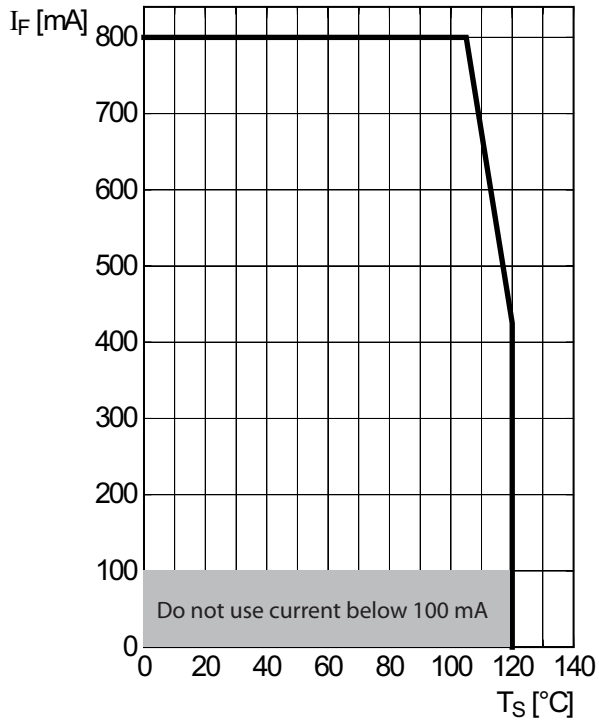

Zulässige Impulsbelastbarkeit $I_F = f(t_p)$
Permissible Pulse Handling Capacity
Duty cycle D = parameter, T_S = 25 °C

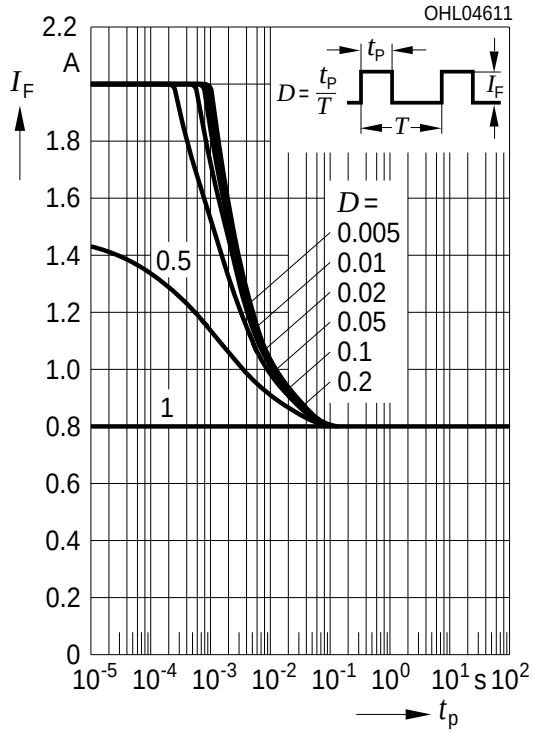

Zulässige Impulsbelastbarkeit $I_F = f(t_p)$
Permissible Pulse Handling Capacity
Duty cycle D = parameter, T_S = 85 °C

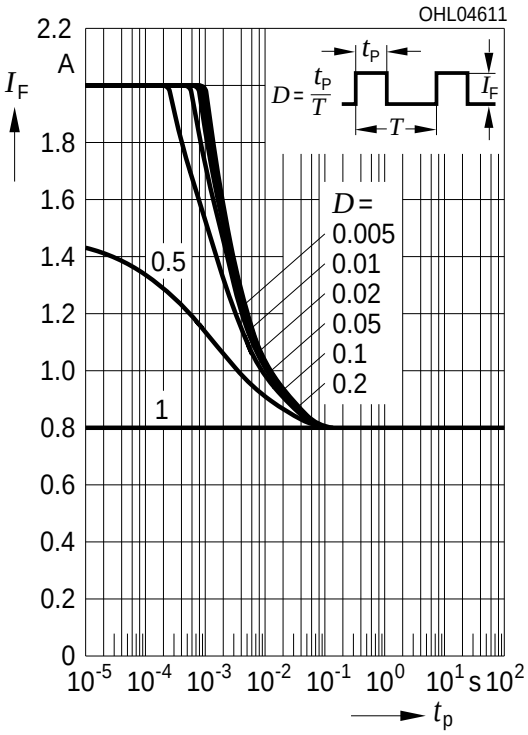

OSRAM
Opto Semiconductors

Maßzeichnung[5) Seite 22]
Package Outlines[5) page 22]

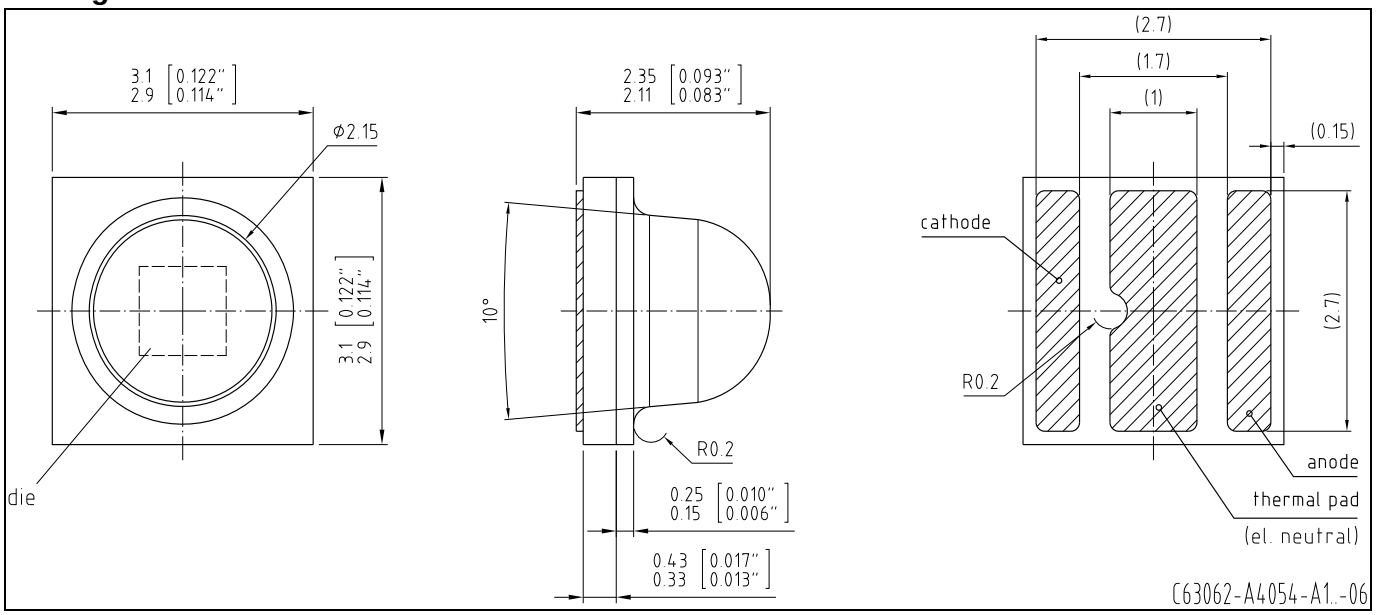

Anm.: Die LED enthält ein ESD-Bauteil, das parallel zum Chip geschalten ist.

Note: LED is protected by ESD device which is connected in parallel to LED-Chip.

Anm.: Das Gehäuse ist für Ultraschallreinigung nicht geeignet

Note: Package not suitable for ultra sonic cleaning

Kathodenkennung:	Markierung
Cathode mark:	mark
Gewicht / Approx. weight:	2.5 mg

Korrosionsfestigkeit besser als EN 60068-2-60 (method 4):
mit erweitertem Korrosionstest: 40°C / 90%rh / 15ppm H_2S / 336h
Corrosion robustness better than EN 60068-2-60 (method 4):
with enhanced corrosion test: 40°C / 90%rh / 15ppm H_2S / 336h

OSRAM Opto Semiconductors

Gurtung / Polarität und Lage[5)] ***Seite 22***

Method of Taping / Polarity and Orientation[5)] ***page 22***

Verpackungseinheit 600/Rolle, ø180 mm

Packing unit 600/reel, ø180 mm

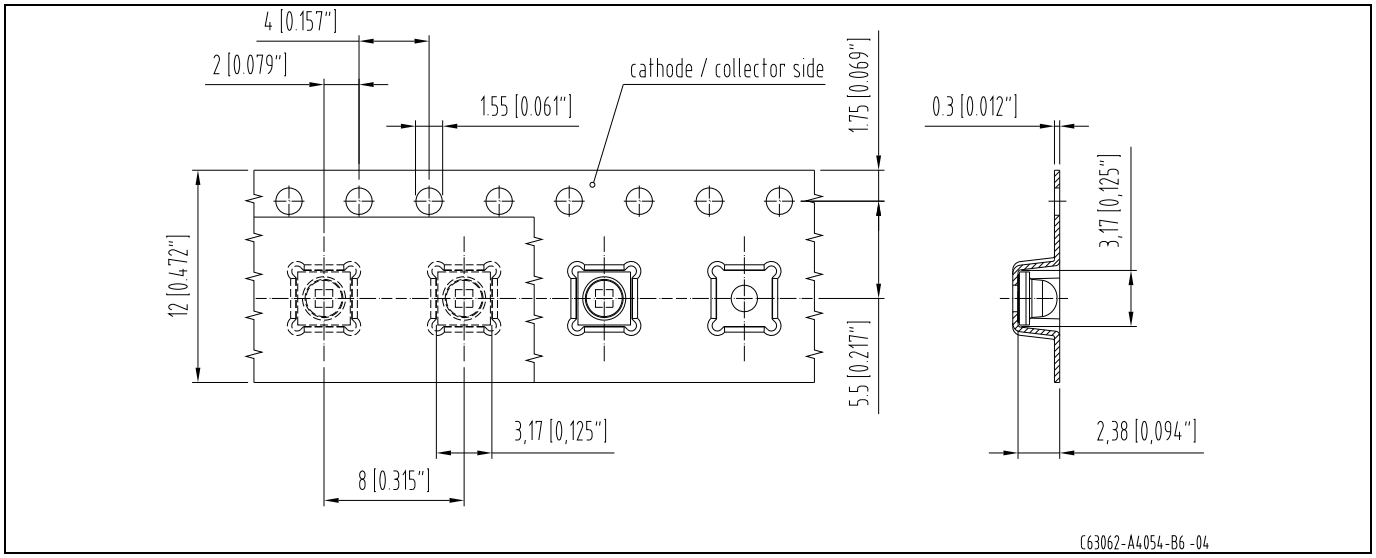

Empfohlenes Lötpaddesign[5)] Seite 22
Recommended Solder Pad[5)] page 22

Reflow Löten
Reflow Soldering

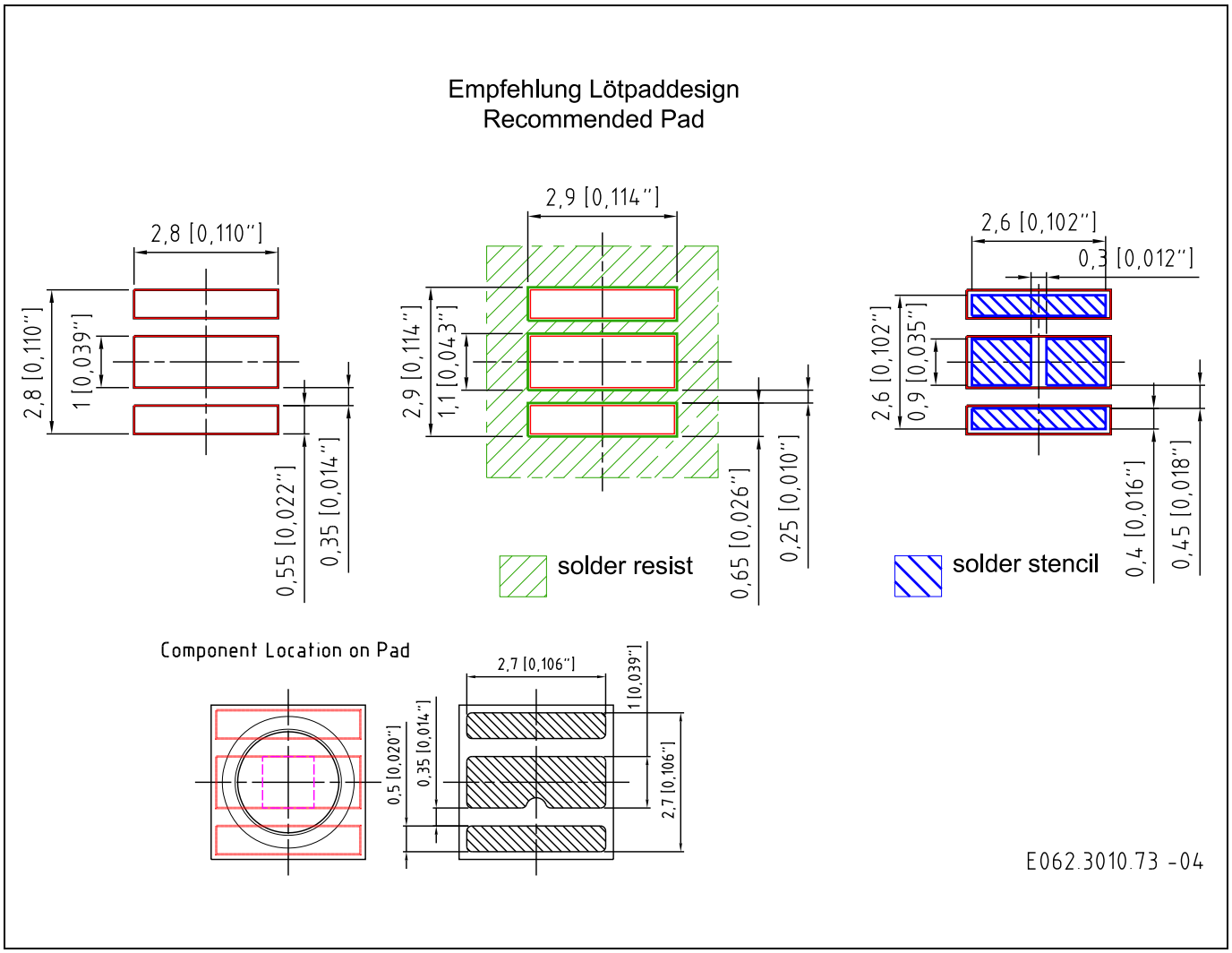

Anm.: Um eine verbesserte Lötstellenkontaktierung zu erreichen, empfehlen wir, unter Standard-stickstoffatmosphäre zu löten.
Weitere Informationen finden Sie in der Applikationsschrift „Handling and Processing Details for Ceramic LEDs“

Note: For superior solder joint connectivity results we recommend soldering under standard nitrogen atmosphere.
For further information please refer to our Application Note „Handling and Processing Details for Ceramic LEDs“

OSRAM Opto Semiconductors

Lötbedingungen
Soldering Conditions

Vorbehandlung nach JEDEC Level 2
Preconditioning acc. to JEDEC Level 2

Reflow Lötprofil für bleifreies Löten
Reflow Soldering Profile for lead free soldering

(nach J-STD-020D.01)
(acc. to J-STD-020D.01)

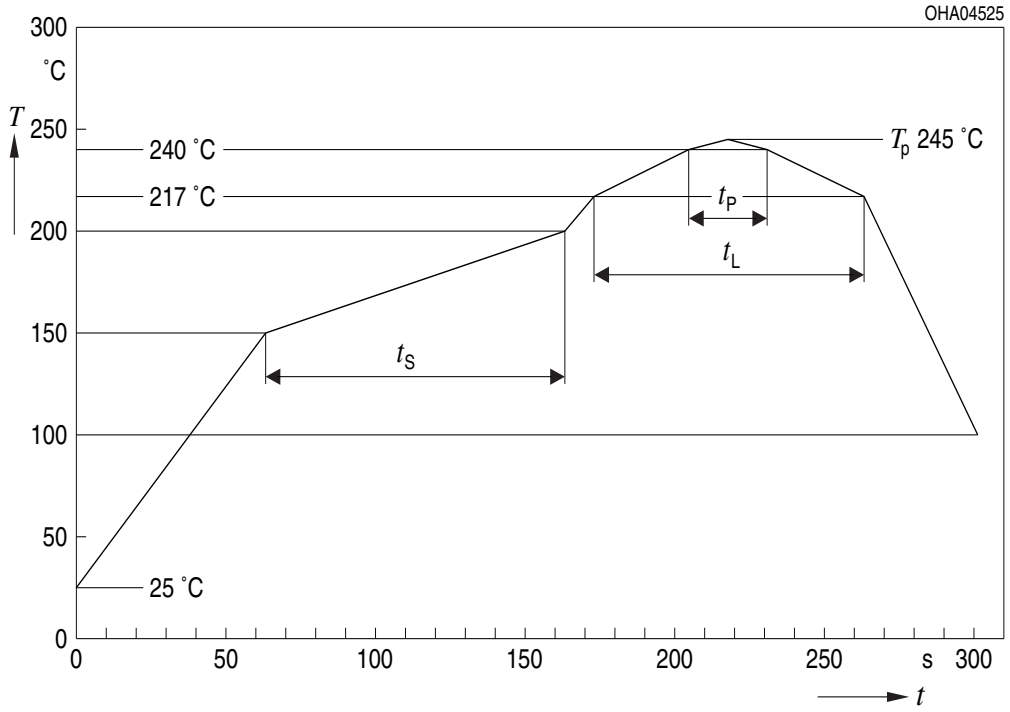

Profile Feature	Pb-Free (SnAgCu) Assembly	
	Recommendation	**Max. Ratings**
Ramp-up Rate to Preheat*) 25 °C to 150 °C	2 K /s	3 K / s
Time t_s from T_{Smin} to T_{Smax} (150 °C to 200 °C	100 s	min. 60 s max. 120 s
Ramp-up Rate to Peak*) 180 °C to T_P	2 K / s	3 K / s
Liquidus Temperture T_L	217 °C	
Time t_L above T_L	80 s	max. 100 s
Peak Temperature T_P	245 °C	max. 260 °C
Time t_P within 5 °C of the specified peak temperature T_P - 5 K	20 s	min. 10 s max. 30 s
Ramp-down Rate* T_P to 100 °C	3 K / s	6 K / s maximum
Time 25 °C to Peak temperature		max. 8 min.

All temperatures refer to the center of the package, measured on the top of the component
* slope calculation ΔT/Δt: Δt max. 5 sec; fulfillment for the whole T-range

OSRAM Opto Semiconductors

Barcode-Produkt-Etikett (BPL)
Barcode-Product-Label (BPL)

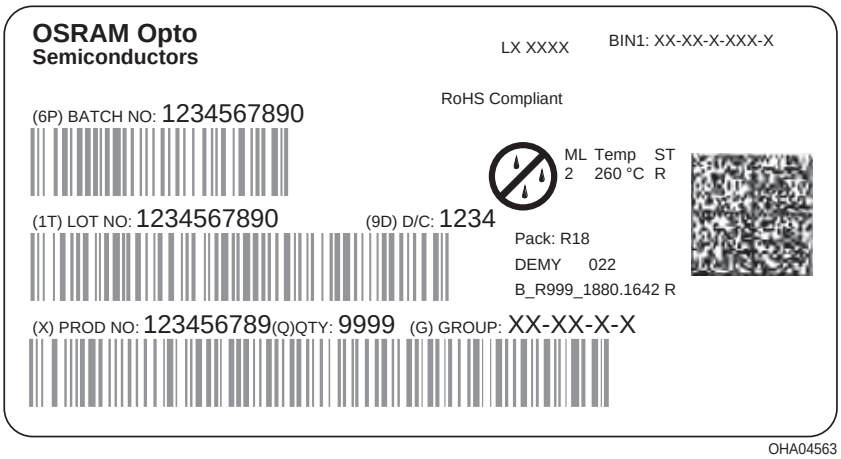

Gurtverpackung
Tape and Reel

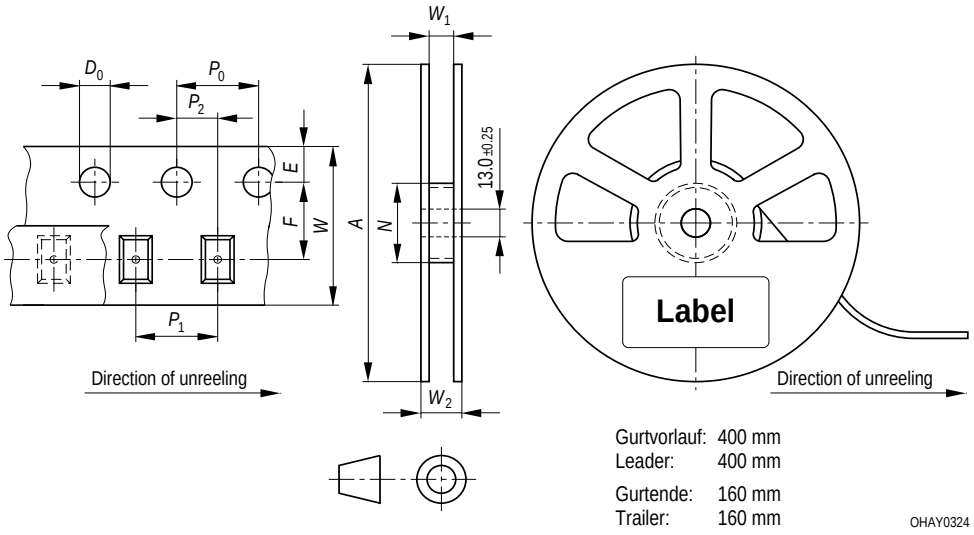

Tape dimensions in mm (inch)

W	P_0	P_1	P_2	D_0	E	F
$12^{+0.3}_{-0.1}$	4 ± 0.1 (0.157 ± 0.004)	8 ± 0.1 (0.315 ± 0.004)	2 ± 0.05 (0.079 ± 0.002)	1.5 + 0.1 (0.059 + 0.004)	1.75 ± 0.1 (0.069 ± 0.004)	5.5 ± 0.05 (0.217 ± 0.002)

Reel dimensions in mm (inch)

A	W	N_{min}	W_1	$W_{2\ max}$
180 (7)	12 (0.472)	60 (2.362)	12.4 + 2 (0.488 + 0.079)	18.4 (0.724)

Trockenverpackung und Materialien
Dry Packing Process and Materials

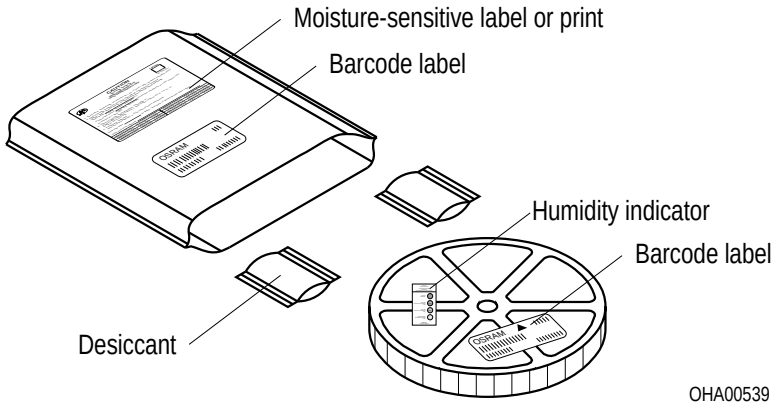

Anm.: Feuchteempfindliche Produkte sind verpackt in einem Trockenbeutel zusammen mit einem Trockenmittel und einer Feuchteindikatorkarte
Bezüglich Trockenverpackung finden Sie weitere Hinweise im Internet und in unserem Short Form Catalog im Kapitel "Gurtung und Verpackung" unter dem Punkt "Trockenverpackung". Hier sind Normenbezüge, unter anderem ein Auszug der JEDEC-Norm, enthalten.

Note: Moisture-sensitve product is packed in a dry bag containing desiccant and a humidity card.
Regarding dry pack you will find further information in the internet and in the Short Form Catalog in chapter "Tape and Reel" under the topic "Dry Pack". Here you will also find the normative references like JEDEC.

Kartonverpackung und Materialien
Transportation Packing and Materials

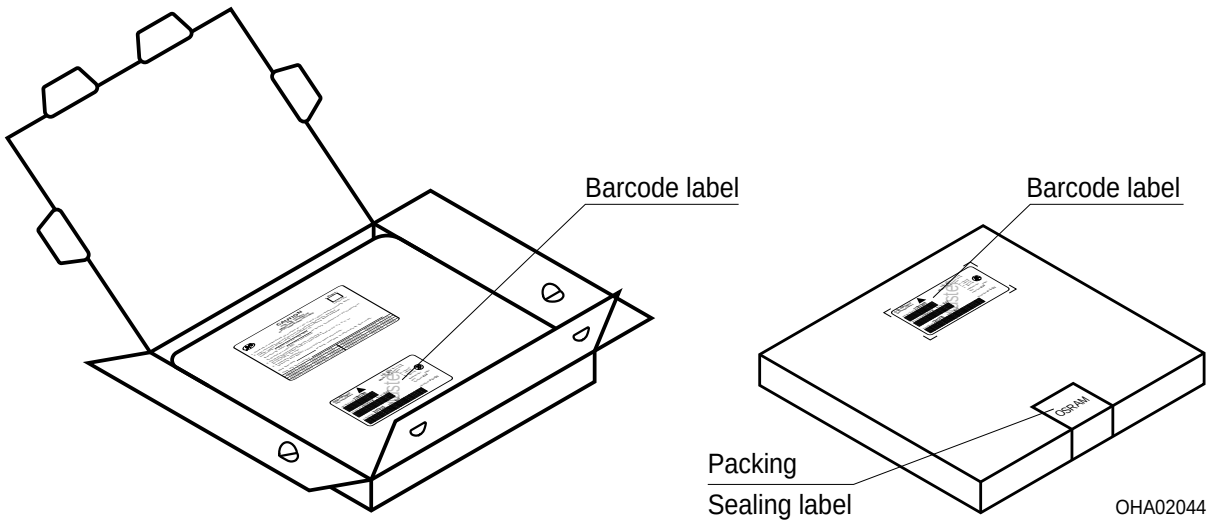

Dimensions of transportation box in mm (inch)

Breite / Width	*Länge / length*	*Höhe / height*
200 ±5 (7,874 ±0,1968)	200 ±5 (7,874 ±0,1968)	30 ±5 (1,1811 ±0,1968)

Revision History: **2011-12-23**
Previous Version: 2011-10-04

Page	Subjects (major changes since last revision)	Date of change
all	Preliminary data sheet created	2010-10-27
2	Ordering codes added	2011-01-17
all	Final datasheet created	2011-03-23
19	Reel dimensions corrected	2011-07-25
1, 2	OS-IN-2011-019	2011-09-01
all	OS-PCN-2011-015	2011-10-04
4,5	reverse specifications added	2011-12-23

Patent List

Patent No.
US 6 066 861 US 6 277 301 US 6 245 259

Wegen der Streichung der LED aus der IEC 60825 erfolgt die Bewertung der Augensicherheit nach dem Standard IEC 62471:2006 ("photobiological safety of lamps and lamp systems")
Im Risikogruppensystem dieser CIE- Norm erfüllen die in diesem Datenblatt angegebenen LED die "exempt"- Gruppe (die die sich im "sichtbaren" Spektralbereich auf eine Expositionsdauer von 10000 s bezieht). Unter realen Umständen (für Expositionsdauer, Augenpupille, Betrachtungsabstand) geht damit von diesen Bauelementen keinerlei Augengefährdung aus.
Grundsätzlich sollte jedoch erwähnt werden, dass intensive Lichtquellen durch ihre Blendwirkung ein hohes sekundäres Gefahrenpotenzial besitzen. Wie nach dem Blick in andere helle Lichtquellen (z.B. Autoscheinwerfer) auch, können temporär eingeschränktes Sehvermögen und Nachbilder je nach Situation zu Irritationen, Belästigungen, Beeinträchtigungen oder sogar Unfällen führen.

Due to the cancellation of the LED from IEC 60825, the evaluation of eye safety occurs according to the standard IEC 62471:2006 ("photobiological safety of lamps and lamp systems").
Within the risk grouping system of this CIE standard, the LEDs specified in this data sheet fall into the "exempt" group (relating to devices in the visible spectrum with an exposure time of 10000 s). Under real circumstances (for exposure time, eye pupils, observation distance), it is assumed that no endangerment to the eye exists from these devices.
As a matter of principle, however, it should be mentioned that intense light sources have a high secondary exposure potential due to their blinding effect. As is also true when viewing other bright light sources (e.g. headlights), temporary reduction in visual acuity and afterimages can occur, leading to irritation, annoyance, visual impairment, and even accidents, depending on the situation.

Attention please!
The information describes the type of component and shall not be considered as assured characteristics.
Terms of delivery and rights to change design reserved. Due to technical requirements components may contain dangerous substances. For information on the types in question please contact our Sales Organization.
If printed or downloaded, please find the latest version in the Internet.
Packing
Please use the recycling operators known to you. We can also help you – get in touch with your nearest sales office. By agreement we will take packing material back, if it is sorted. You must bear the costs of transport. For packing material that is returned to us unsorted or which we are not obliged to accept, we shall have to invoice you for any costs incurred.
Components used in life-support devices or systems must be expressly authorized for such purpose! Critical components[6) page 22] may only be used in life-support devices or systems[7) page 22] with the express written approval of OSRAM OS.

OSRAM
Opto Semiconductors

Fußnoten:

1) Helligkeitswerte werden während eines Strompulses einer typischen Dauer von 25 ms, mit einer internen Reproduzierbarkeit von +/- 8 % und einer erweiterten Messunsicherheit von +/- 11 % gemessen (gemäß GUM mit Erweiterungsfaktor k = 3).
2) Wegen der besonderen Prozessbedingungen bei der Herstellung von LED können typische oder abgeleitete technische Parameter nur aufgrund statistischer Werte wiedergegeben werden. Diese stimmen nicht notwendigerweise mit den Werten jedes einzelnen Produktes überein, dessen Werte sich von typischen und abgeleiteten Werten oder typischen Kennlinien unterscheiden können. Falls erforderlich, z.B. aufgrund technischer Verbesserungen, werden diese typischen Werte ohne weitere Ankündigung geändert.
3) Farbkoordinaten werden während eines Strompulses einer typischen Dauer von 25 ms, mit einer internen Reproduzierbarkeit von +/- 0,005 und einer erweiterten Messunsicherheit von +/- 0,01 gemessen (gemäß GUM mit Erweiterungsfaktor k = 3).
4) Vorwärtsspannungen werden während eines Strompulses einer typischen Dauer von 8 ms, mit einer internen Reproduzierbarkeit von +/- 0,05 V und einer erweiterten Messunsicherheit von +/- 0,1 V gemessen (gemäß GUM mit Erweiterungsfaktor k=3).
5) Maße werden wie folgt angegeben: mm (inch)
6) Ein kritisches Bauteil ist ein Bauteil, das in lebenserhaltenden Apparaten oder Systemen eingesetzt wird und dessen Defekt voraussichtlich zu einer Fehlfunktion dieses lebenserhaltenden Apparates oder Systems führen wird oder die Sicherheit oder Effektivität dieses Apparates oder Systems beeinträchtigt.
7) Lebenserhaltende Apparate oder Systeme sind für
(a) die Implantierung in den menschlichen Körper
oder
(b) für die Lebenserhaltung bestimmt.
Falls sie versagen, kann davon ausgegangen werden, dass die Gesundheit und das Leben des Patienten in Gefahr ist.

Remarks:

1) Brightness values are measured during a current pulse of typical 25 ms, with an internal reproducibility of +/- 8 % and an expanded uncertainty of +/- 11 % (acc. to GUM with a coverage factor of k = 3).
2) Due to the special conditions of the manufacturing processes of LED, the typical data or calculated correlations of technical parameters can only reflect statistical figures. These do not necessarily correspond to the actual parameters of each single product, which could differ from the typical data and calculated correlations or the typical characteristic line. If requested, e.g. because of technical improvements, these typ. data will be changed without any further notice.
3) Chromaticity coordinates are measured during a current pulse of typical 25 ms, with an internal reproducibility of +/- 0,005 and an expanded uncertainty of +/- 0,01 (acc. to GUM with a coverage factor of k = 3).
4) The forward voltage is measured during a current pulse of typical 8 ms, with an internal reproducibility of +/- 0,05 V and an expanded uncertainty of +/- 0,1 V (acc. to GUM with a coverage factor of k=3).
5) Dimensions are specified as follows: mm (inch).
6) A critical component is a component used in a life-support device or system whose failure can reasonably be expected to cause the failure of that life-support device or system, or to affect its safety or the effectiveness of that device or system.
7) Life support devices or systems are intended
(a) to be implanted in the human body,
or
(b) to support and/or maintain and sustain human life.
If they fail, it is reasonable to assume that the health and the life of the user may be endangered.

Published by
OSRAM Opto Semiconductors GmbH
Leibnizstrasse 4, D-93055 Regensburg
www.osram-os.com
© All Rights Reserved.

EU RoHS and China RoHS compliant product
此产品符合欧盟 RoHS 指令的要求，
按照中国的相关法规和标准，不含有毒有害物质或元素。

OSRAM
Opto Semiconductors

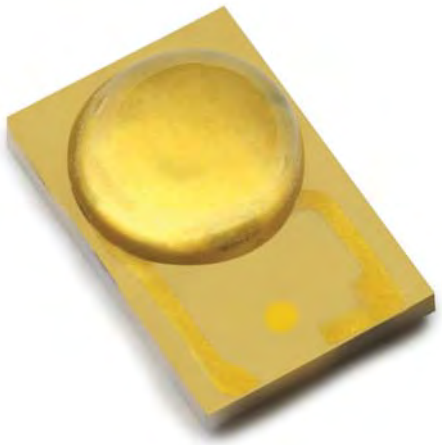

LUXEON Rebel PLUS

Freedom From Binning
Hot Tested
Superior Quality of Light

Technical Datasheet DS107

LUXEON® Rebel PLUS

Freedom From Binning

Introduction

LUXEON® Rebel PLUS LEDs from Philips Lumileds are a product family with a rich history of use in just about every possible illumination application. LUXEON Rebel PLUS LEDs are designed to offer single emitter, Illumination Grade LED light sources with the highest possible efficacy and light output. With hot testing and color binning, every LUXEON Rebel PLUS is tested and specified at real world operating conditions, Tj = 85°C. Our exceptional color control enables design simplicity for luminaire manufacturers and ensures that they can be confident in color consistency from LED to LED. The superior quality of light, light output, and real world efficacy enable leading performance and efficient solution development in a wide variety of indoor lighting segments including retrofit bulbs, office, hospitality, school, and home lighting. LUXEON Rebel PLUS comes in an industry standard 4530 package with a 2.55mm dome that is optimized for maximum light output.

- Superior efficacy, color consistency and high light output
- Hot tested at real world conditions at T_j = 85°C
- LM80 compliant
- Typical V_f of 2.76V at 350 mA, 85°C
- Optically compatible with LUXEON Rebel platform
- Available in 3-step and 5-step MacAdam Ellipse.

Table of Contents

General Product Information 3

Product Nomenclature 3

Lumen Maintenance 3

Environmental Compliance 3

Product Selection & Optical Characteristics 4

Product Selection Guide for LUXEON Rebel PLUS Emitters 4

Electrical Characteristics 5

Absolute Maximum Ratings 5

JEDEC Moisture Sensitivity 5

Reflow Soldering Characteristics 6

Mechanical Dimensions 7

Pad Configuration 8

Solder Pad Design 8

Typical Light Output Characteristics over Temperature 9

Typical Forward Current Characteristics 10

Typical Radiation Patterns 11

Emitter Pocket Tape Packaging 12

Emitter Reel Packaging 13

Product Binning and Labeling 14

Luminous Flux and Forward Voltage Bins 15

LUXEON Rebel PLUS 3-step and 5-step MacAdam Ellipse Color Definition 16

General Product Information

Product Nomenclature

LUXEON Rebel PLUS emitters are tested and binned "hot" under conditions comparable to those found in "real-world" lighting products. The test conditions for LUXEON Rebel PLUS are 350 mA D.C. with junction temperature at 85°C.

The part number designation for the LUXEON Rebel PLUS emitters is explained as follows:

L X 1 8 - P 1 X X - Y

Where:

8 — designates minimum CRI performance (value 8 = 80 minimum)
P — designates radiation pattern (value P for Lambertian)
1 — 80 CRI min designation
XX — designates nominal ANSI CCT (value 27 = 2700K, 30 = 3000K, 35 = 3500K, 40 = 4000K, and 50 = 5000K)
Y — 3 for 3-step and 5-step MacAdam Ellipse

Lumen Maintenance

LUXEON Rebel PLUS products are tested in compliance with LM-80. Please visit www.philipslumileds.com/support/documentation/lumen-maintenance or contact your local Philips Lumileds Technical Solutions Manager for TM-21 extrapolations or other support.

Environmental Compliance

Philips Lumileds is committed to providing environmentally friendly products to the solid-state lighting market. LUXEON Rebel PLUS is compliant to the European Union directives on the restriction of hazardous substances in electronic equipment, namely the RoHS and REACH directives. Philips Lumileds will not intentionally add the following restricted materials to the LUXEON Rebel PLUS: lead, mercury, cadmium, hexavalent chromium, polybrominated biphenyls (PBB) or polybrominated diphenyl ethers (PBDE).

Product Selection & Optical Characteristics

Product Selection Guide for LUXEON Rebel PLUS Emitters Junction Temperature = 85°C

Table 1.

Part Number	Nominal ANSI CCT	Performance @ 350 mA Test Current: CRI Min	Min Luminous Flux (lm)	Test Condition	Typ. Luminous Flux (lm) 350 mA	Typ. Luminous Flux (lm) 700 mA	Typ. Forward Voltage (V) 350 mA	Typ. Forward Voltage (V) 700 mA	Typ. Efficacy (lm/W) 350 mA	Typ. Efficacy (lm/W) 700 mA
LX18-P127-Y	2700K	80	80	Tj = 85°C	85	156	2.76	2.85	88	78
LX18-P130-Y	3000K	80	85	Tj = 85°C	95	166	2.76	2.85	98	83
LX18-P135-Y	3500K	80	90	Tj = 85°C	98	172	2.76	2.85	101	86
LX18-P140-Y	4000K	80	90	Tj = 85°C	103	180	2.76	2.85	107	90
LX18-P150-Y	5000K	80	95	Tj = 85°C	106	186	2.76	2.85	110	93

Notes for Table 1:

1. Minimum luminous flux performance within published operating conditions. Philips Lumileds maintains a tolerance of ± 6.5% on luminous flux measurements.
2. Philips Lumileds maintains a tolerance of ±0.06V on forward voltage measurements.

Optical Characteristics LUXEON Rebel PLUS at Test Current [1], Junction Temperature = 85°C

Table 2.

Nominal ANSI CCT	Part Number	Color Temperature CCT Typical	Typical Total Included Angle [2] (degrees) $\theta_{0.90V}$	Typical Viewing Angle [3] (degrees) 2θ 1/2
2700K	LX18-P127-Y	2725K	160	120
3000K	LX18-P130-Y	3045K	160	120
3500K	LX18-P135-Y	3465K	160	120
4000K	LX18-P140-Y	3985K	160	120
5000K	LX18-P150-Y	5028K	160	120

Notes for Table 2:

1. Test current is 350 mA D.C. for all LX18-P1xx emitters.
2. Total angle at which 90% of total luminous flux is captured.
3. Viewing angle is the off axis angle from lamp centerline where the luminous intensity is ½ of the peak value.

Electrical Characteristics

Electrical Characteristics at 350 mA for LUXEON Rebel PLUS Junction Temperature = 85°C

Table 3.

Nominal ANSI CCT	Forward Voltage V_f [1] (V) Min.	Max.	Typical Temperature Coefficient of Forward Voltage [2] (mV/°C) $\Delta V_F / \Delta T_J$	Typical Thermal Resistance Junction to Thermal Pad (°C/W) $R\theta_{J-C}$
2700K	2.5	3.00	-1.0 to -3.0	9
3000K	2.5	3.00	-1.0 to -3.0	9
3500K	2.5	3.00	-1.0 to -3.0	9
4000K	2.5	3.00	-1.0 to -3.0	9
5000K	2.5	3.00	-1.0 to -3.0	9

Notes for Table 3:

1. Philips Lumileds maintains a tolerance of ±0.06V on forward voltage measurements.
2. Measured between T_J = 25°C and T_J = 110°C at I_f = 350 mA.

Absolute Maximum Ratings

Table 4.

Parameter	LUXEON Rebel PLUS
DC Forward Current (mA)	1000 [2]
Peak Pulsed Forward Current (mA)	1000 [3]
ESD Sensitivity	< 8000V Human Body Model (HBM) Class 3A JESD22-A114-E
LED Junction Temperature [1]	150°C
Operating Case Temperature at 700 mA	-40°C - 135°C
Storage Temperature	-40°C - 135°C
Soldering Temperature	JEDEC 020c 260°C
Allowable Reflow Cycles	3
Reverse Voltage (Vr)	LUXEON Rebel PLUS LEDs are not designed to be driven in reverse bias

Notes for Table 4:

1. Proper current derating must be observed to maintain junction temperature below the maximum. For additional information on thermal measurement guidelines please refer to Application Brief AB33.
2. Residual periodic variations due to power conversion from alternating current (AC) to direct current (DC), also called "ripple', with frequencies ≥ 100 Hz and amplitude ≤ 300 mA are acceptable, assuming the average current throughout each cycle does not exceed 1000 mA.
3. Pulsed operation with a peak drive current of 1000 mA is acceptable if the pulse on-time is ≤ 5 ms per cycle and the duty cycle is ≤ 50%.

JEDEC Moisture Sensitivity

Table 5.

Level	Floor Life Time	Conditions	Soak Requirements Standard Time	Conditions
1	unlimited	≤ 30°C / 85% RH	168h + 5 / -0	85°C / 85% RH

Reflow Soldering Characteristics

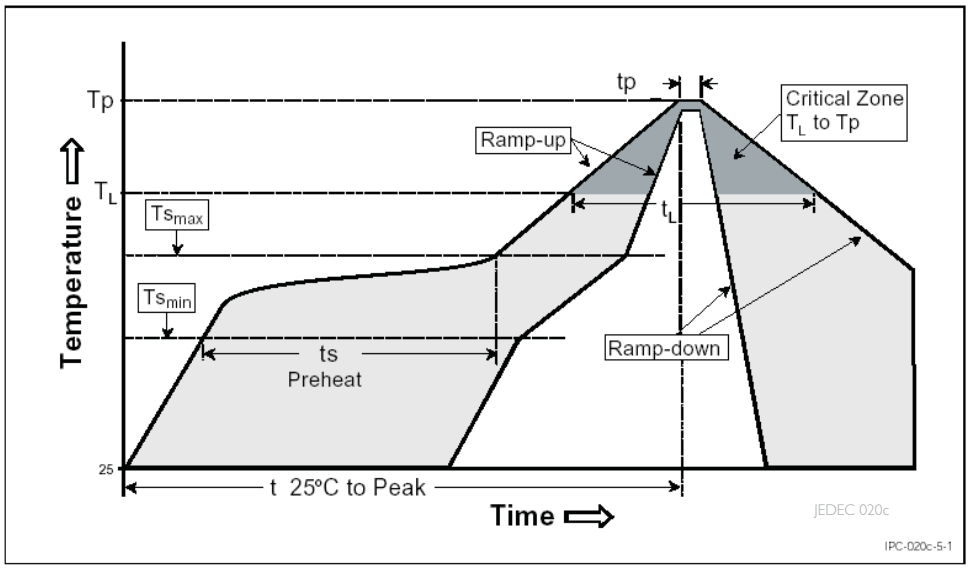

Temperature Profile for Table 6.

Table 6.

Profile Feature	Lead Free Assembly
Average Ramp-Up Rate (Ts_{max} to T_p)	3°C / second max
Preheat Temperature Min (Ts_{min})	150°C
Preheat Temperature Max (Ts_{max})	200°C
Preheat Time (ts_{min} to ts_{max})	60 - 180 seconds
Temperature (T_L)	217°C
Time Maintained Above Temperature (T_L)	60 - 150 seconds
Peak / Classification Temperature (T_p)	260°C
Time Within 5°C of Actual Peak Temperature (t_p)	20 - 40 seconds
Ramp - Down Rate	6°C / second max
Time 25°C to Peak Temperature	8 minutes max

Notes for Table 6:

- All temperatures refer to the application Printed Circuit Board (PCB), measured on the surface adjacent to the package body.

Mechanical Dimensions

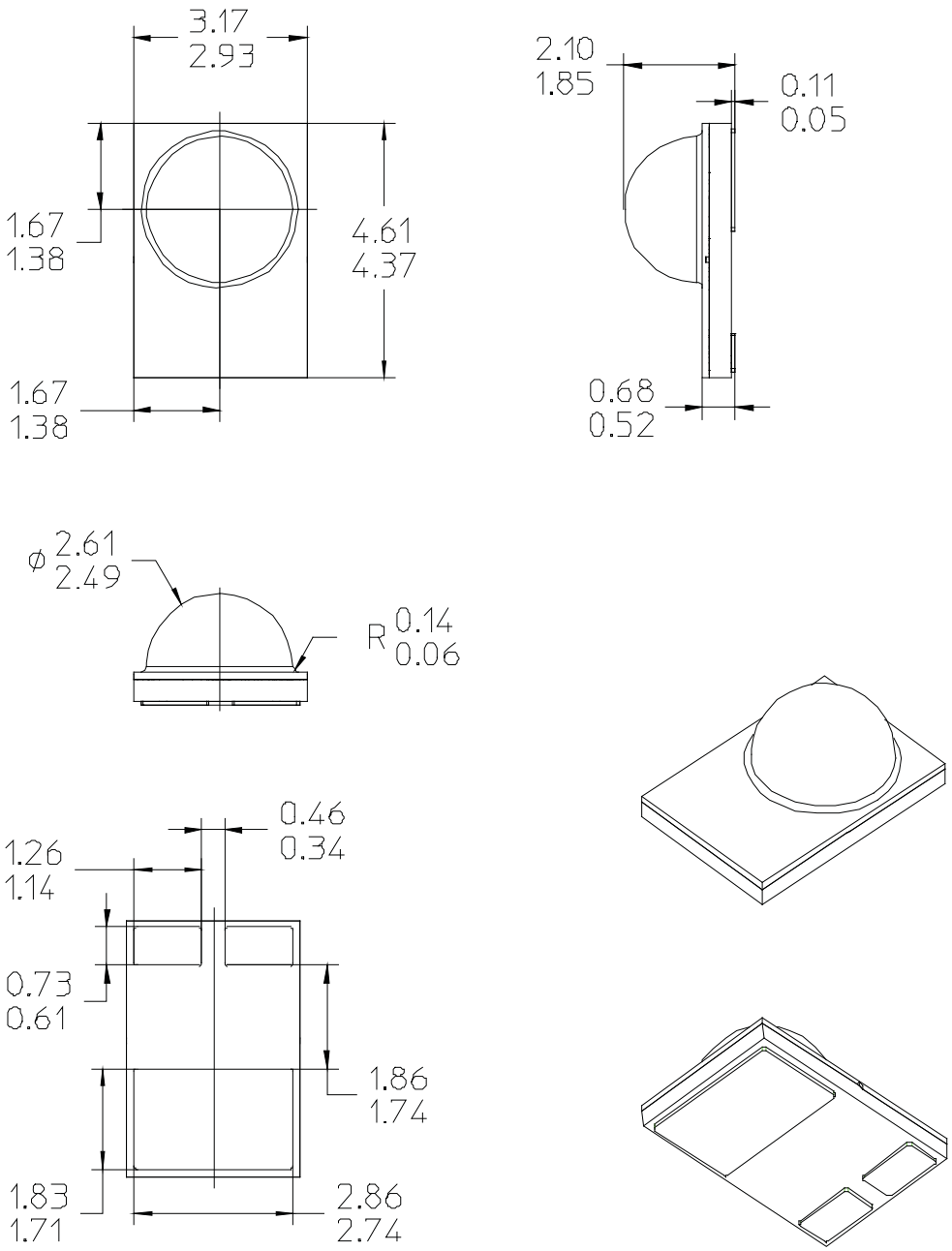

Figure 1. Package outline drawing.

Notes for Figure 1:

- Do not handle the device by the lens, as the lens or the interior of the device can be damaged by excessive force to the lens.
- Drawings not to scale. All dimensions are in millimeters.
- The thermal pad is electrically isolated from the anode and cathode contact pads.

Pad Configuration

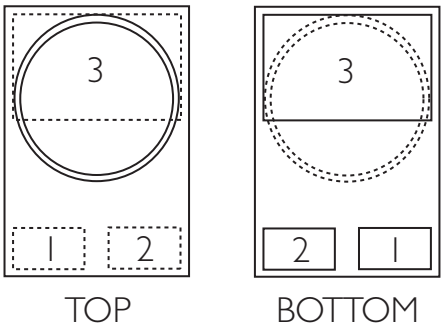

PAD	FUNCTION
1	CATHODE
2	ANODE
3	THERMAL

Figure 2. Pad configuration.

Note for Figure 2:

- The Thermal Pad is electrically isolated from the Anode and Cathode contact pads.

Solder Pad Design

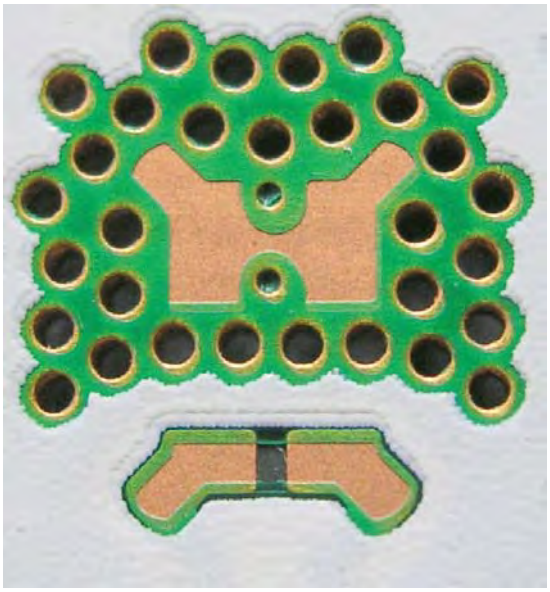

Figure 3. Solder pad layout.

Note for Figure 3:

- The photograph shows the recommended LUXEON Rebel PLUS layout on Printed Circuit Board (PCB). This design easily achieves a thermal resistance of 7K/W.
- Application Brief AB32 provides extensive details for this layout. Printed Circuit Board layout files (.dwg) are available at www.philipslumileds.com and www.philipslumileds.cn.com.

Typical Light Output Characteristics over Temperature

All LUXEON Rebel PLUS Emitters at Test Current, 350 mA

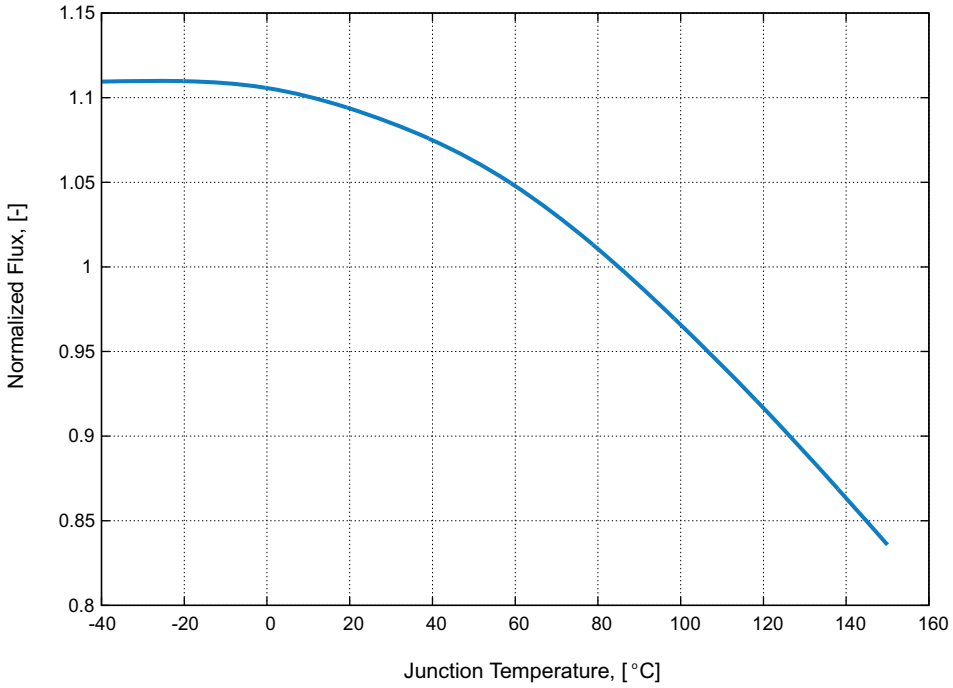

Figure 4. Relative light output vs. junction temperature.

Typical Forward Current Characteristics

All LUXEON Rebel PLUS Emitters, Junction Temperature = 85°C

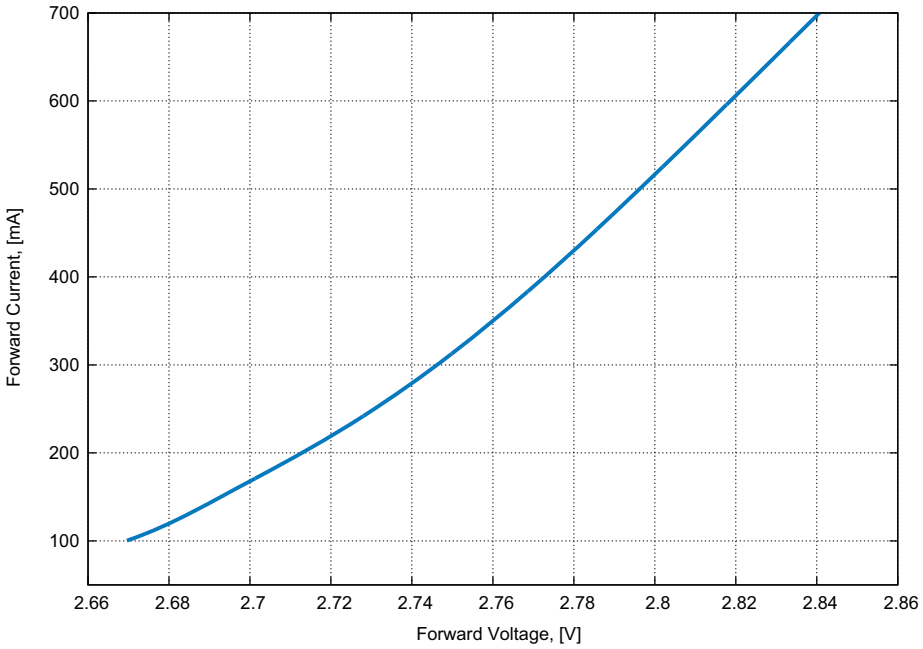

Figure 5. Forward current vs. forward voltage.

Typical Relative Luminous Flux vs. Forward Current for All LUXEON Rebel PLUS Emitters, Junction Temperature = 85°C

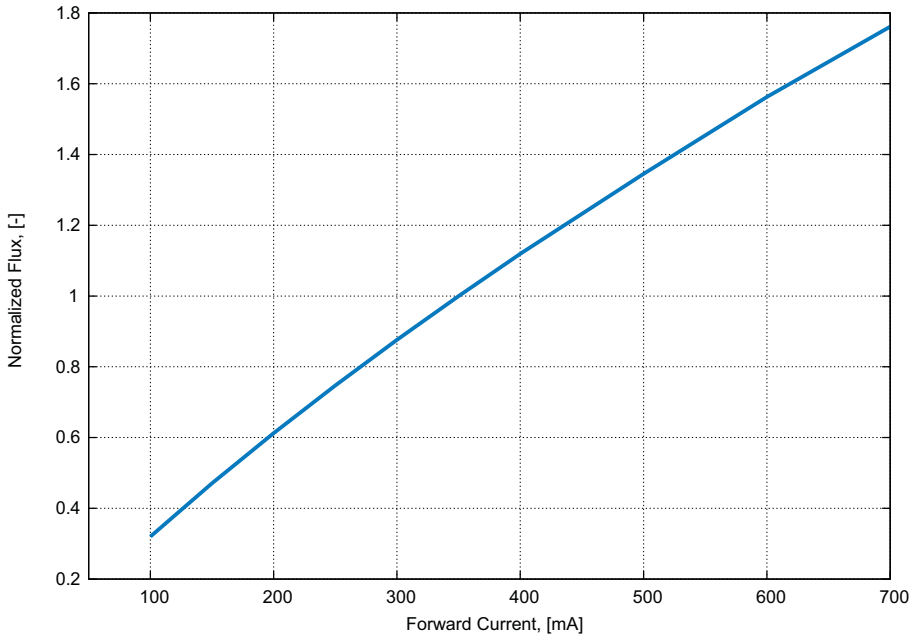

Figure 6. Typical relative luminous flux vs. forward current, junction temperature = 85°C.

Typical Radiation Patterns

Relative Spectral Distribution for LUXEON Rebel PLUS Emitters

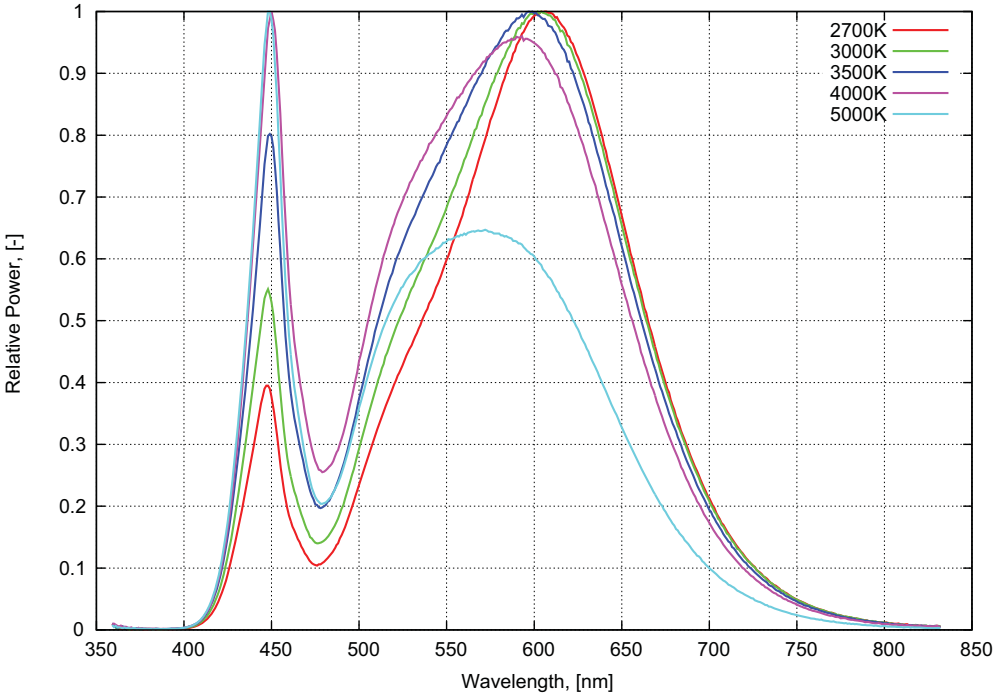

Figure 7. Cartesian plot of typical luminous intensity.

Typical Polar Radiation Pattern

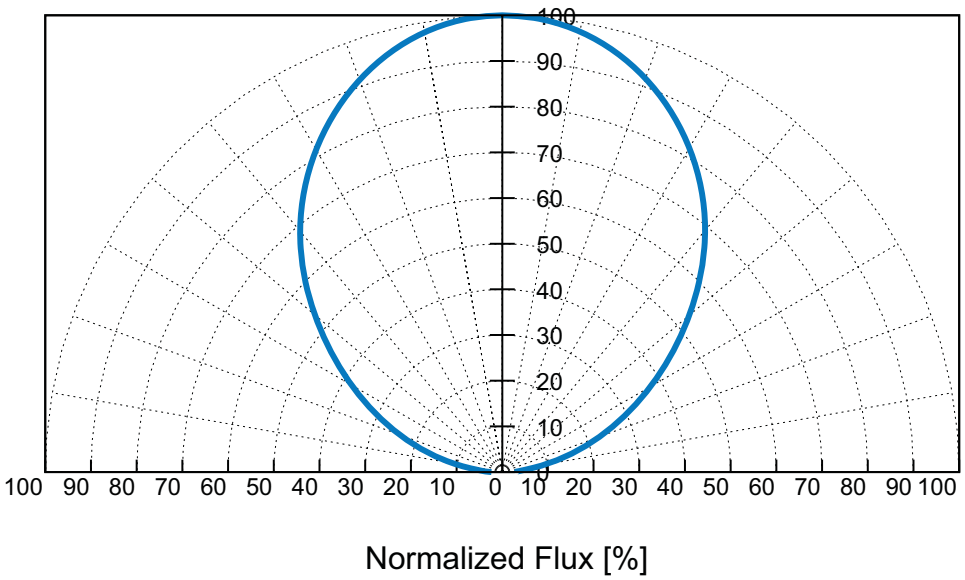

Figure 8. Typical polar radiation pattern.

Emitter Pocket Tape Packaging

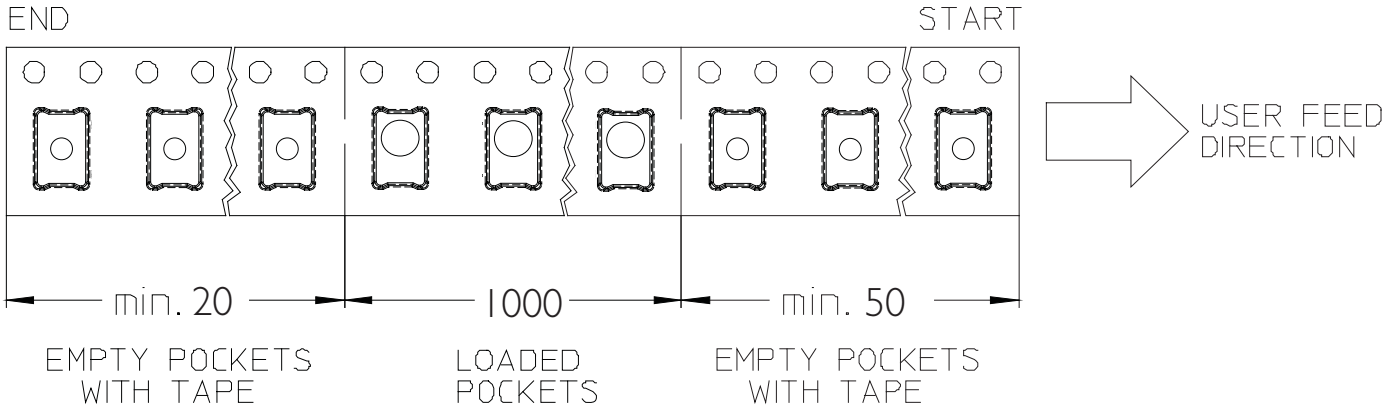

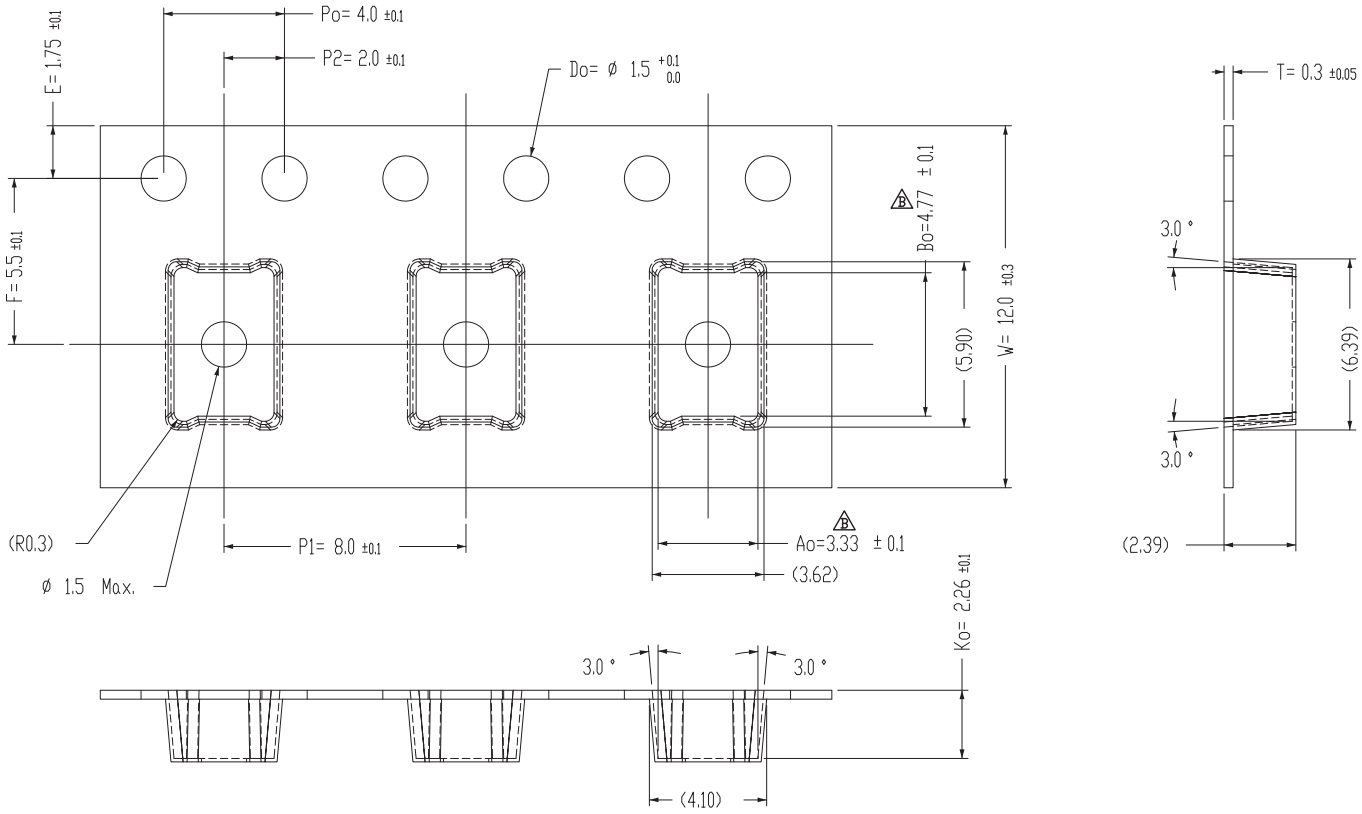

Emitter Reel Packaging

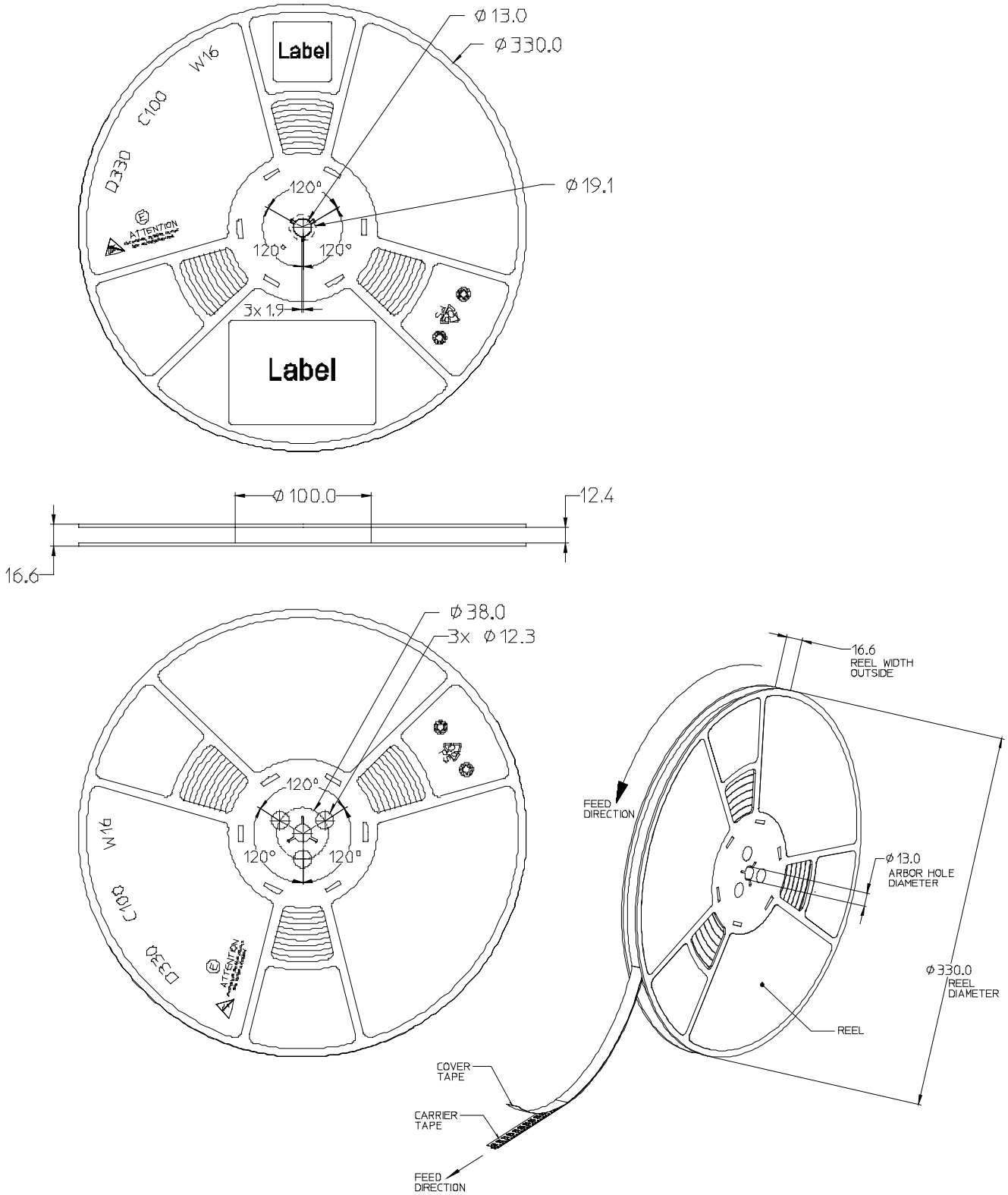

Product Binning and Labeling

Purpose of Product Binning

In the manufacturing of semiconductor products, there is a variation of performance around the average values given in the technical data sheets. For this reason, Philips Lumileds bins the LED components for luminous flux and forward voltage (V_f). Color is offered in a single 3-step or 5-step MacAdam ellipse color space centered on the ANSI CCT color bins. For additional information please review the MacAdam ellipse technical definition section.

Decoding Product Bin Labeling

LUXEON Rebel PLUS emitters are labeled using a two digit alphanumeric code (CAT code) depicting the bin values for emitters packaged on a single reel. All emitters packaged within a reel are of the same 2-variable bin combination. Using these codes, it is possible to determine optimum mixing and matching of products for consistency in a given application.

Reels of LUXEON Rebel PLUS emitters are labeled with a two digit alphanumeric CAT code following the format below.

XY

X = Flux bins (A, B, C, D, E, F)
Y = Y = Voltage Bins (1, 2)

Luminous Flux and Forward Voltage Bins

Table 7 lists the standard photometric luminous flux bins for LUXEON Rebel PLUS emitters (tested and binned at 350 mA D.C., Junction Temperature = 85°C. Minimum luminous flux performance within published operating conditions. Philips Lumileds maintains a tolerance of ± 6.5% on luminous flux measurements.

Although several bins are outlined, product availability in a particular bin varies by production run and by product performance.
Not all bins are available in all CCT's.

Table 7.

Flux Bins		
Bin Code	Minimum Photometric Flux (lm)	Maximum Photometric Flux (lm)
A [2]	75	85
B	85	95
C	95	105
D	105	115
E	115	125
F	125	135

Note for Table 7:

1. Minimum luminous flux performance within published operating conditions. Philips Lumileds maintains a tolerance of ± 6.5% on luminous flux measurements.
2. For LX18-P127 minimum flux is 80 lm.
   - A is the cat code for 80-85 lm for the above emitters.
3. For LX18-P135 and LX18-P140 minimum flux is 90 lm.
   - B is the cat code for 90-95 lm for the above emitters.

Table 8 lists minimum and maximum V_f bin values per emitter (tested and binned at 350 mA). Although several bins are outlined, product availability in a particular bin varies by production run and by product performance.

Table 8.

V_f Bins		
Bin Code	Minimum Forward Voltage (V)	Maximum Forward Voltage (V)
1	2.50	2.75
2	2.75	3.00

LUXEON Rebel PLUS 3-step and 5-step MacAdam Ellipse Color Definition

Tested at 350 mA D.C. & Junction Temperature = 85°C

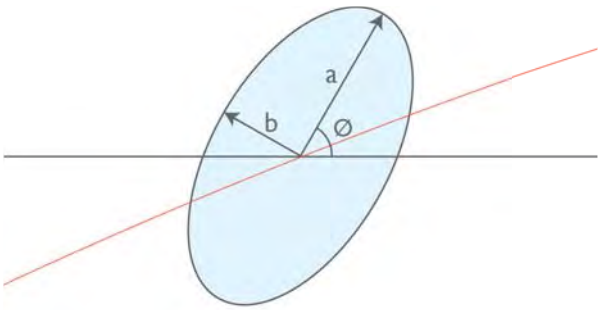

Table 9. LUXEON Rebel PLUS Product Characteristics for 3-step MacAdam Ellipse

Part Number	Nominal ANSI CCT	Color Space	Center Point (cx, cy)	Major Axis, a	Minor Axis, b	Ellipse Rotation Angle
LX18-P127-3	2700K	Single 3-step MacAdam ellipse	(0.4578, 0.4101)	0.00810	0.00420	53.7
LX18-P130-3	3000K	Single 3-step MacAdam ellipse	(0.4338, 0.4030)	0.00834	0.00408	53.2
LX18-P135-3	3500K	Single 3-step MacAdam ellipse	(0.4073, 0.3917)	0.00927	0.00414	54.0
LX18-P140-3	4000K	Single 3-step MacAdam ellipse	(0.3818, 0.3797)	0.00939	0.00402	53.7
LX18-P150-3	5000K	Single 3-step MacAdam ellipse	(0.3447, 0.3553)	0.00822	0.00354	59.6

Table 10. LUXEON Rebel PLUS Product Characteristics for 5-step MacAdam Ellipse

Part Number	Nominal ANSI CCT	Color Space	Center Point (cx, cy)	Major Axis, a	Minor Axis, b	Ellipse Rotation Angle
LX18-P127-5	2700K	Single 5-step MacAdam ellipse	(0.4578, 0.4101)	0.01350	0.00700	53.7
LX18-P130-5	3000K	Single 5-step MacAdam ellipse	(0.4338, 0.4030)	0.01390	0.00680	53.2
LX18-P135-5	3500K	Single 5-step MacAdam ellipse	(0.4073, 0.3917)	0.01545	0.00690	54.0
LX18-P140-5	4000K	Single 5-step MacAdam ellipse	(0.3818, 0.3797)	0.01565	0.00670	53.7
LX18-P150-5	5000K	Single 5-step MacAdam ellipse	(0.3447, 0.3553)	0.01370	0.00590	59.6

Note for Tables 9 & 10:

- Philips Lumileds maintains a tester tolerance of ± 0.005 on x, y color coordinates.

Company Information

Philips Lumileds is a leading provider of LEDs for everyday lighting applications. The company's records for light output, efficacy and thermal management are direct results of the ongoing commitment to advancing solid-state lighting technology and enabling lighting solutions that are more environmentally friendly, help reduce CO_2 emissions and reduce the need for power plant expansion. Philips Lumileds LUXEON® LEDs are enabling never before possible applications in outdoor lighting, shop lighting, home lighting, consumer electronics, and automotive lighting.

Philips Lumileds is a fully integrated supplier, producing core LED material in all three base colors, (Red, Green, Blue) and white. Philips Lumileds has R&D centers in San Jose, California and in the Netherlands, and production capabilities in San Jose, Singapore and Penang, Malaysia. Founded in 1999, Philips Lumileds is the high flux LED technology leader and is dedicated to bridging the gap between solid-state technology and the lighting world. More information about the company's LUXEON LED products and solid-state lighting technologies can be found at www.philipslumileds.com.

©2013 Philips Lumileds Lighting Company. All rights reserved.
Product specifications are subject to change without notice.

PHILIPS
LUMILEDS

www.philipslumileds.com
www.philipslumileds.cn.com

Technical Data Sheet

SEOUL SEMICONDUCTOR

X42180

X42180

Z-Power series is designed for high current operation and high flux output applications.

Z-Power LED's thermal management perform exceeds other power LED solutions.
It incorporates state of the art SMD design and Thermal emission material.
Z Power LED is ideal light sources for general illumination applications, custom designed solutions, automotive large LCD backlights

Features

- Super high flux output and high luminance
- Designed for high current operation
- Low thermal resistance
- SMT solderability
- Lead free product
- RoHS compliant

Applications

- Mobile phone flash
- Automotive interior / Exterior lighting
- Automotive signal lighting
- Automotive forward lighting
- Torch
- Architectural lighting
- LCD TV / Monitor backlight
- Projector light source
- Traffic signals
- Task lighting
- Decorative / Pathway lighting
- Remote / Solar powered lighting
- Household appliances

*The appearance and specifications of the product may be changed for improvement without notice.

Rev. 10
February. 2011
www.acriche.com
Document No. : SSC-QP-7-07-24 (Rev.00)

Full Code of Z-Power LED Series

Full code form : $X_1 X_2 X_3 X_4 X_5 X_6 X_7 – X_8 X_9 – X_{10} X_{11} X_{12} X_{13} X_{14}$

1. Part Number

- X_1 : Color
- X_2 : Z-Power LED series number
- X_3 : LENS type
- X_4 : Chip quantity (or Power Dissipation)
- X_5 : Package outline size
- X_6 : Type of PCB
- X_7 : Grade of characteristic code

2. Internal Number

- X_8, X_9 : Revision No.

3. Code Labeling

- X_{10} : Luminous flux (or Radiant flux for royal blue)
- $X_{11} X_{12} X_{13}$: Dominant wavelength (or x,y coordinates rank code)
- X_{14} : Forward voltage

4. Sticker Diagram on Reel & Aluminum Vinyl Bag

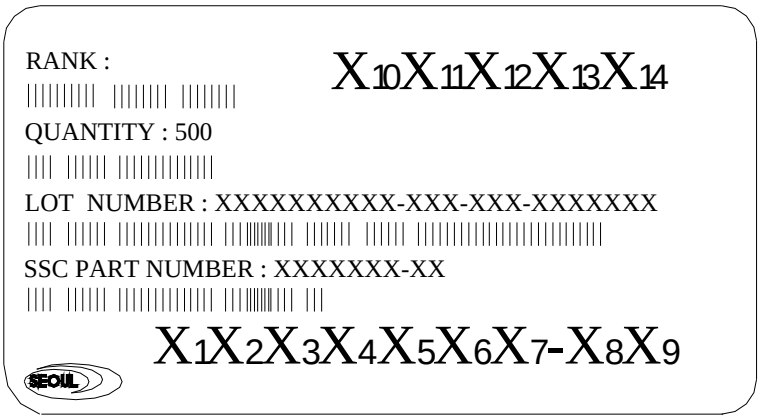

For more information about binning and labeling, refer to the Application Note -1

Outline Dimension

1. Dome Type

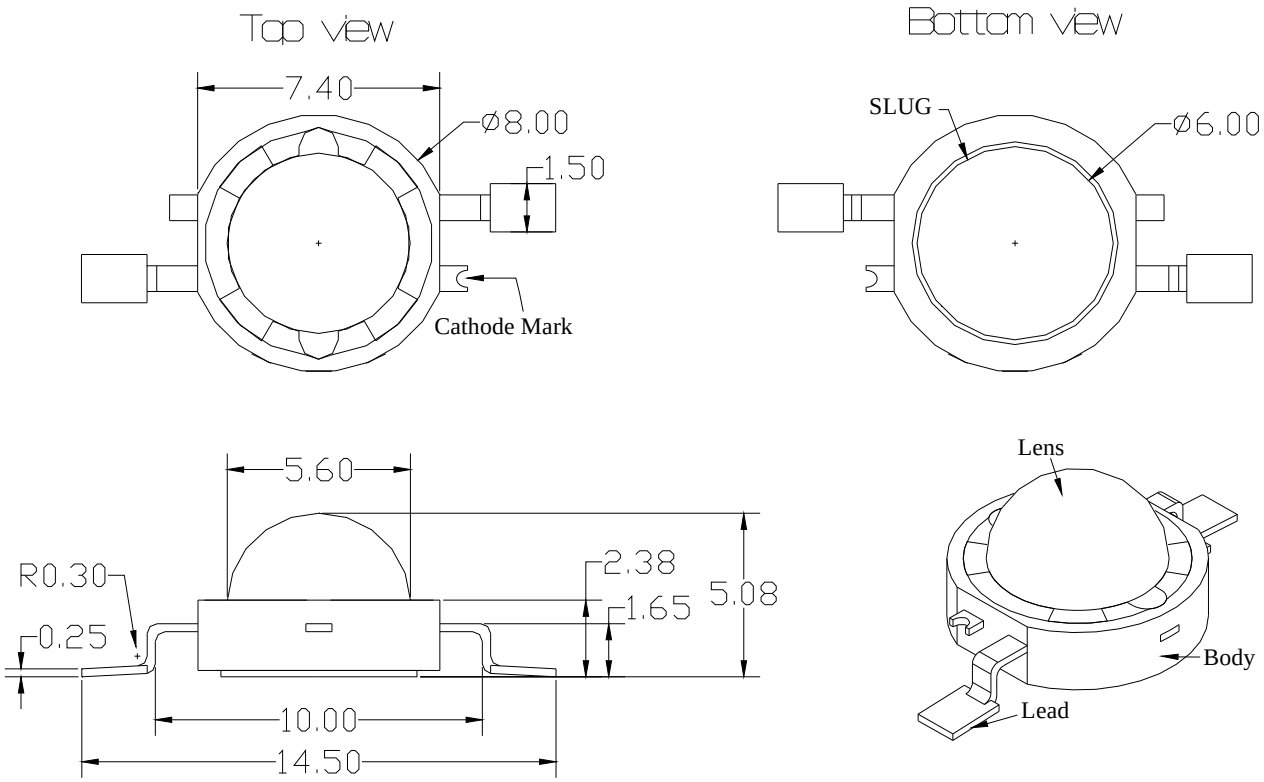

Notes :

1. All dimensions are in millimeters. (tolerance : ±0.2)
2. Scale : none
3. Slug of package is connected to anode.

*The appearance and specifications of the product may be changed for improvement without notice.

Characteristics for Z-Power LED

1. Pure White (W42180)

1-1 Electro-Optical characteristics at I_F=350mA, T_A=25°C

Parameter		Symbol	Value			Unit
			Min	Typ	Max	
Luminous Flux [1]	T rank	Φ_V [2]	70	80	91	lm
	U rank	Φ_V [2]	91	105	-	lm
Correlated Color Temperature [3]		CCT	-	6300	-	K
CRI		R_a	-	75	-	-
Forward Voltage [4]		V_F	3.0	3.25	4	V
View Angle		2Θ ½	127			deg.
Thermal resistance [5]		$R\theta_{J-B}$	8.8			°C /W
Thermal resistance [6]		$R\theta_{J-C}$	7.2			°C /W

1-2 Absolute Maximum Ratings

Parameter	Symbol	Value	Unit
Forward Current	I_F	1000 (@ Tj = 90 °C) [7]	mA
		1800 (@ 1KHz, 1/10 duty)	
Power Dissipation	P_d	4	W
Junction Temperature	T_j	145(@ $I_F \leq 700mA$)	°C
Operating Temperature	T_{opr}	-40 ~ +85	°C
Storage Temperature	T_{stg}	-40 ~ +100	°C
ESD Sensitivity [8]	-	±10,000V HBM	-

*Notes :

[1] SSC maintains a tolerance of ±10% on flux and power measurements.

[2] Φ_V is the total luminous flux output as measured with an integrated sphere.

[3] Correlated Color Temperature is derived from the CIE 1931 Chromaticity diagram. CCT ±5% tester tolerance.

[4] A tolerance of ±0.06V on forward voltage measurements

[5], [6] $R\theta_{J-B}$ is measured with a SSC metal core pcb.(25 °C ≤T_J ≤ 110 °C)
$R\theta_{J-C}$ is measured with only emitter. (25 °C ≤T_J ≤ 110 °C)
Break voltage of Metal PCB is 6.5kVAC.

[7] I_F Max is guaranteed under the T_J ≤90 °C.

[8] It is included the zener chip to protect the product from ESD.

----------Caution----------

1. Please do not drive at rated current more than 5 sec. without proper heat sink.

Characteristics for Z-Power LED

2. Warm White (N42180)

2-1 Electro-Optical characteristics at I_F=350mA, T_A=25°C

Parameter	Symbol	Value			Unit
		Min	Typ	Max	
Luminous Flux [1]	Φ_V [2]	-	72	-	lm
Correlated Color Temperature [3]	CCT	-	3000	-	K
CRI	R_a	-	93	-	-
Forward Voltage [4]	V_F	3.0	3.25	4	V
View Angle	2Θ 1/2	124			deg.
Thermal resistance [5]	$R\theta_{J-B}$	8.8			°C /W
Thermal resistance [6]	$R\theta_{J-C}$	7.2			°C /W

2-2 Absolute Maximum Ratings

Parameter	Symbol	Value	Unit
Forward Current	I_F	800	mA
Power Dissipation	P_d	3.2	W
Junction Temperature	T_j	145	°C
Operating Temperature	T_{opr}	-40 ~ +85	°C
Storage Temperature	T_{stg}	-40 ~ +100	°C
ESD Sensitivity [7]	-	±10,000V HBM	-

*Notes :

[1] SSC maintains a tolerance of ±10% on flux and power measurements.

[2] Φ_V is the total luminous flux output as measured with an integrated sphere.

[3] Correlated Color Temperature is derived from the CIE 1931 Chromaticity diagram.
CCT ±5% tester tolerance

[4] A tolerance of ±0.06V on forward voltage measurements

[5], [6] $R\theta_{J-B}$ is measured with a SSC metal core pcb.(25 °C ≤T_J ≤ 110 °C)
$R\theta_{J-C}$ is measured with only emitter. .(25 °C ≤T_J ≤ 110 °C)
Break voltage of Metal PCB is 6.5kVAC

[7] It is included the zener chip to protect the product from ESD.

----------Caution----------

1. Please do not drive at rated current more than 5 sec. without proper heat sink

Characteristics for Z-Power LED

3. Warm White (N42180H)

3-1 Electro-Optical characteristics at I_F=350mA, T_A=25°C

Parameter	Symbol	Value			Unit
		Min	Typ	Max	
Luminous Flux [1]	Φ_V [2]	-	86	-	lm
Correlated Color Temperature [3]	CCT	-	3000	-	K
CRI	R_a	-	80	-	-
Forward Voltage [4]	V_F	3.0	3.25	4	V
View Angle	2Θ 1/2	124			deg.
Thermal resistance [5]	$R\theta_{J-B}$	8.8			°C /W
Thermal resistance [6]	$R\theta_{J-C}$	7.2			°C /W

3-2 Absolute Maximum Ratings

Parameter	Symbol	Value	Unit
Forward Current	I_F	800	mA
Power Dissipation	P_d	3.2	W
Junction Temperature	T_j	145	°C
Operating Temperature	T_{opr}	-40 ~ +85	°C
Storage Temperature	T_{stg}	-40 ~ +100	°C
ESD Sensitivity [7]	-	±10,000V HBM	-

*Notes :

[1] SSC maintains a tolerance of ±10% on flux and power measurements.

[2] Φ_V is the total luminous flux output as measured with an integrated sphere.

[3] Correlated Color Temperature is derived from the CIE 1931 Chromaticity diagram.
CCT ±5% tester tolerance

[4] A tolerance of ±0.06V on forward voltage measurements

[5], [6] $R\theta_{J-B}$ is measured with a SSC metal core pcb.(25 °C ≤T_J ≤ 110 °C)
$R\theta_{J-C}$ is measured with only emitter. .(25 °C ≤T_J ≤ 110 °C)
Break voltage of Metal PCB is 6.5kVAC

[7] It is included the zener chip to protect the product from ESD.

----------Caution----------

1. Please do not drive at rated current more than 5 sec. without proper heat sink

Characteristics for Z-Power LED

4. Natural White (S42180)

4-1 Electro-Optical characteristics at I_F=350mA, T_A=25ºC

Parameter	Symbol	Value			Unit
		Min	Typ	Max	
Luminous Flux [1]	Φ_V [2]	-	76	-	lm
Correlated Color Temperature [3]	CCT	-	4000	-	K
CRI	R_a	-	93	-	-
Forward Voltage [4]	V_F	3.0	3.25	4	V
View Angle	2Θ 1/2	124			deg.
Thermal resistance [5]	$R\theta_{J-B}$	8.8			ºC /W
Thermal resistance [6]	$R\theta_{J-C}$	7.2			ºC /W

4-2 Absolute Maximum Ratings

Parameter	Symbol	Value	Unit
Forward Current	I_F	800	mA
Power Dissipation	P_d	3.2	W
Junction Temperature	T_j	145	ºC
Operating Temperature	T_{opr}	-40 ~ +85	ºC
Storage Temperature	T_{stg}	-40 ~ +100	ºC
ESD Sensitivity [8]	-	±10,000V HBM	-

*Notes :

[1] SSC maintains a tolerance of ±10% on flux and power measurements.

[2] Φ_V is the total luminous flux output as measured with an integrated sphere.

[3] Correlated Color Temperature is derived from the CIE 1931 Chromaticity diagram. CCT ±5% tester tolerance.

[4] A tolerance of ±0.06V on forward voltage measurements

[5], [6] $R\theta_{J-B}$ is measured with a SSC metal core pcb.(25 ºC ≤T_J ≤ 110 ºC)
$R\theta_{J-C}$ is measured with only emitter. (25 ºC ≤T_J ≤ 110 ºC)
Break voltage of Metal PCB is 6.5kVAC.

[7] It is included the zener chip to protect the product from ESD.

----------Caution----------

1. Please do not drive at rated current more than 5 sec. without proper heat sink

Characteristics for Z-Power LED

5. Natural White (S42180H)

5-1 Electro-Optical characteristics at I_F=350mA, T_A=25ºC

Parameter	Symbol	Value			Unit
		Min	Typ	Max	
Luminous Flux [1]	Φ_V [2]	-	94	-	lm
Correlated Color Temperature [3]	CCT	-	4000	-	K
CRI	R_a	-	80	-	-
Forward Voltage [4]	V_F	3.0	3.25	4	V
View Angle	2Θ 1/2	124			deg.
Thermal resistance [5]	$R\theta_{J-B}$	8.8			ºC /W
Thermal resistance [6]	$R\theta_{J-C}$	7.2			ºC /W

5-2 Absolute Maximum Ratings

Parameter	Symbol	Value	Unit
Forward Current	I_F	800	mA
Power Dissipation	P_d	3.2	W
Junction Temperature	T_j	145	ºC
Operating Temperature	T_{opr}	-40 ~ +85	ºC
Storage Temperature	T_{stg}	-40 ~ +100	ºC
ESD Sensitivity [8]	-	±10,000V HBM	-

*Notes :

[1] SSC maintains a tolerance of ±10% on flux and power measurements.

[2] Φ_V is the total luminous flux output as measured with an integrated sphere.

[3] Correlated Color Temperature is derived from the CIE 1931 Chromaticity diagram. CCT ±5% tester tolerance.

[4] A tolerance of ±0.06V on forward voltage measurements

[5], [6] $R\theta_{J-B}$ is measured with a SSC metal core pcb.(25 ºC ≤T_J ≤ 110 ºC)
$R\theta_{J-C}$ is measured with only emitter. (25 ºC ≤T_J ≤ 110 ºC)
Break voltage of Metal PCB is 6.5kVAC.

[7] It is included the zener chip to protect the product from ESD.

----------Caution----------

1. Please do not drive at rated current more than 5 sec. without proper heat sink

Characteristics for Z-Power LED

6. Blue (B42180)

6-1 Electro-Optical characteristics at I_F=350mA, T_A=25°C

Parameter	Symbol	Value			Unit
		Min	Typ	Max	
Luminous Flux [1]	Φ_V [2]	-	22	-	lm
Dominant Wavelength[3]	λ_D	455	465	475	nm
Forward Voltage [4]	V_F	3.0	3.25	4	V
View Angle	2Θ 1/2		130		deg.
Thermal resistance [5]	$R\theta_{J-B}$		8.8		°C /W
Thermal resistance [6]	$R\theta_{J-C}$		7.2		°C /W

6-2 Absolute Maximum Ratings

Parameter	Symbol	Value	Unit
Forward Current	I_F	1000	mA
Power Dissipation	P_d	4	W
Junction Temperature	T_j	145	°C
Operating Temperature	T_{opr}	-40 ~ +85	°C
Storage Temperature	T_{stg}	-40 ~ +100	°C
ESD Sensitivity [7]	-	±10,000V HBM	-

*Notes :

[1] SSC maintains a tolerance of ±10% on flux and power measurements.

[2] Φ_V is the total luminous flux output as measured with an integrated sphere.

[3] Dominant wavelength is derived from the CIE 1931 Chromaticity diagram.
A tolerance of ±0.5nm for dominant wavelength

[4] A tolerance of ±0.06V on forward voltage measurements

[5], [6] $R\theta_{J-B}$ is measured with a SSC metal core pcb.(25 °C ≤T_J ≤ 110 °C)
$R\theta_{J-C}$ is measured with only emitter. .(25 °C ≤T_J ≤ 110 °C)
Break voltage of Metal PCB is 6.5kVAC

[7] It is included the zener chip to protect the product from ESD.

----------Caution----------

1. Please do not drive at rated current more than 5 sec. without proper heat sink

2. Blue power light sources represented here are IEC825 Class 2 for eye safety

Characteristics for Z-Power LED

7. Royal Blue (D42180)

7-1 Electro-Optical characteristics at I_F=350mA, T_A=25°C

Parameter	Symbol	Value			Unit
		Min	Typ	Max	
Radiant Power [1]	Φ_V [2]	-	468	-	mW
Dominant Wavelength [3]	λ_D	455	457	460	nm
Forward Voltage [4]	V_F	3.0	3.25	3.8	V
View Angle	2Θ 1/2		130		deg.
Thermal resistance [5]	$R\theta_{J-B}$		8.8		°C /W
Thermal resistance [6]	$R\theta_{J-C}$		7.2		°C /W

7-2 Absolute Maximum Ratings

Parameter	Symbol	Value	Unit
Forward Current	I_F	1000	mA
Power Dissipation	P_d	4	W
Junction Temperature	T_j	145	°C
Operating Temperature	T_{opr}	-40 ~ +85	°C
Storage Temperature	T_{stg}	-40 ~ +100	°C
ESD Sensitivity [7]	-	±10,000V HBM	-

*Notes :

[1] SSC maintains a tolerance of ±10% on flux and power measurements.

[2] Φ_V is the total luminous flux output as measured with an integrated sphere.

[3] Correlated Color Temperature is derived from the CIE 1931 Chromaticity diagram.
CCT ±5% tester tolerance

[4] A tolerance of ±0.06V on forward voltage measurements

[5], [6] $R\theta_{J-B}$ is measured with a SSC metal core pcb.(25 °C ≤T_J ≤ 110 °C)
$R\theta_{J-C}$ is measured with only emitter. .(25 °C ≤T_J ≤ 110 °C)
Break voltage of Metal PCB is 6.5kVAC

[7] It is included the zener chip to protect the product from ESD.

----------Caution----------

1. Please do not drive at rated current more than 5 sec. without proper heat sink

2. Blue power light sources represented here are IEC825 Class 2 for eye safety

Characteristics for Z-Power LED

8. Green (G42180)

8-1 Electro-Optical characteristics at I_F=350mA, T_A=25ºC

Parameter	Symbol	Value			Unit
		Min	Typ	Max	
Luminous Flux [1]	Φ_V [2]	-	70	-	lm
Dominant Wavelength[3]	λ_D	520	525	535	nm
Forward Voltage [4]	V_F	3.0	3.25	4.1	V
View Angle	2Θ 1/2		130		deg.
Thermal resistance [5]	$R\theta_{J-B}$		9.5		ºC /W
Thermal resistance [6]	$R\theta_{J-C}$		8.0		ºC /W

8-2 Absolute Maximum Ratings

Parameter	Symbol	Value	Unit
Forward Current	I_F	1000	mA
Power Dissipation	P_d	4	W
Junction Temperature	T_j	145	ºC
Operating Temperature	T_{opr}	-40 ~ +85	ºC
Storage Temperature	T_{stg}	-40 ~ +100	ºC
ESD Sensitivity [7]	-	±10,000V HBM	-

*Notes :

[1] SSC maintains a tolerance of ±10% on flux and power measurements.

[2] Φ_V is the total luminous flux output as measured with an integrated sphere.

[3] Dominant wavelength is derived from the CIE 1931 Chromaticity diagram.
A tolerance of ±0.5nm for dominant wavelength

[4] A tolerance of ±0.06V on forward voltage measurements

[5], [6] $R\theta_{J-B}$ is measured with a SSC metal core pcb.(25 ºC ≤T_J ≤ 110 ºC)
$R\theta_{J-C}$ is measured with only emitter. .(25 ºC ≤T_J ≤ 110 ºC)
Break voltage of Metal PCB is 6.5kVAC

[7] It is included the zener chip to protect the product from ESD.

----------Caution----------

1. Please do not drive at rated current more than 5 sec. without proper heat sin

Characteristics for Z-Power LED

9. Red (R42180)

9-1 Electro-Optical characteristics at I_F=350mA, T_A=25ºC

Parameter	Symbol	Value			Unit
		Min	Typ	Max	
Luminous Flux [1]	Φ_V [2]	-	48	-	lm
Dominant Wavelength[3]	λ_D	618	625	630	nm
Forward Voltage [4]	V_F	2.0	2.3	3.0	V
View Angle	2Θ 1/2		130		deg.
Thermal resistance [5]	$R\theta_{J-B}$		9		ºC /W
Thermal resistance [6]	$R\theta_{J-C}$		7.8		ºC /W

9-2 Absolute Maximum Ratings

Parameter	Symbol	Value	Unit
Forward Current	I_F	800	mA
Power Dissipation	P_d	2.4	W
Junction Temperature	T_j	145	ºC
Operating Temperature	T_{opr}	-40 ~ +85	ºC
Storage Temperature	T_{stg}	-40 ~ +100	ºC
ESD Sensitivity [7]	-	±10,000V HBM	-

*Notes :

[1] SSC maintains a tolerance of ±10% on flux and power measurements.

[2] Φ_V is the total luminous flux output as measured with an integrated sphere.

[3] Dominant wavelength is derived from the CIE 1931 Chromaticity diagram.
A tolerance of ±0.5nm for dominant wavelength

[4] A tolerance of ±0.06V on forward voltage measurements

[5], [6] $R\theta_{J-B}$ is measured with a SSC metal core pcb.(25 ºC ≤T_J ≤ 110 ºC)
$R\theta_{J-C}$ is measured with only emitter. .(25 ºC ≤T_J ≤ 110 ºC)
Break voltage of Metal PCB is 6.5kVAC

[7] It is included the zener chip to protect the product from ESD.

----------Caution----------

1. Please do not drive at rated current more than 5 sec. without proper heat sink

Characteristics for Z-Power LED

10. Amber (A42180)

10-1 Electro-Optical characteristics at I_F=350mA, T_A=25°C

Parameter	Symbol	Value			Unit
		Min	Typ	Max	
Luminous Flux [1]	Φ_V [2]	-	48	-	lm
Dominant Wavelength[3]	λ_D	585	590	595	nm
Forward Voltage [4]	V_F	2.0	2.3	3.0	V
View Angle	2Θ 1/2		130		deg.
Thermal resistance [5]	$R\theta_{J-B}$		9		°C /W
Thermal resistance [6]	$R\theta_{J-C}$		7.8		°C /W

10-2 Absolute Maximum Ratings

Parameter	Symbol	Value	Unit
Forward Current	I_F	800	mA
Power Dissipation	P_d	2.4	W
Junction Temperature	T_j	145	°C
Operating Temperature	T_{opr}	-40 ~ +85	°C
Storage Temperature	T_{stg}	-40 ~ +100	°C
ESD Sensitivity [7]	-	±10,000V HBM	-

*Notes :

[1] SSC maintains a tolerance of ±10% on flux and power measurements.

[2] Φ_V is the total luminous flux output as measured with an integrated sphere.

[3] Dominant wavelength is derived from the CIE 1931 Chromaticity diagram.
A tolerance of ±0.5nm for dominant wavelength

[4] A tolerance of ±0.06V on forward voltage measurements

[5], [6] $R\theta_{J-B}$ is measured with a SSC metal core pcb.(25 °C ≤T_J ≤ 110 °C)
$R\theta_{J-C}$ is measured with only emitter. .(25 °C ≤T_J ≤ 110 °C)
Break voltage of Metal PCB is 6.5kVAC

[7] It is included the zener chip to protect the product from ESD.

----------Caution----------

1. Please do not drive at rated current more than 5 sec. without proper heat sink

Color Spectrum, T_A=25°C

1. Pure White

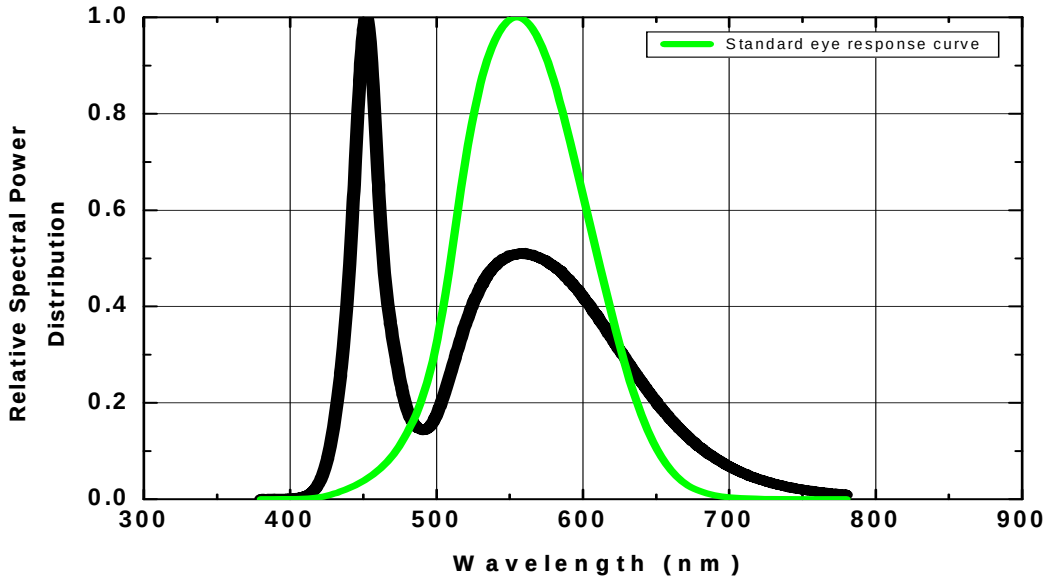

2. Warm White (N42180)

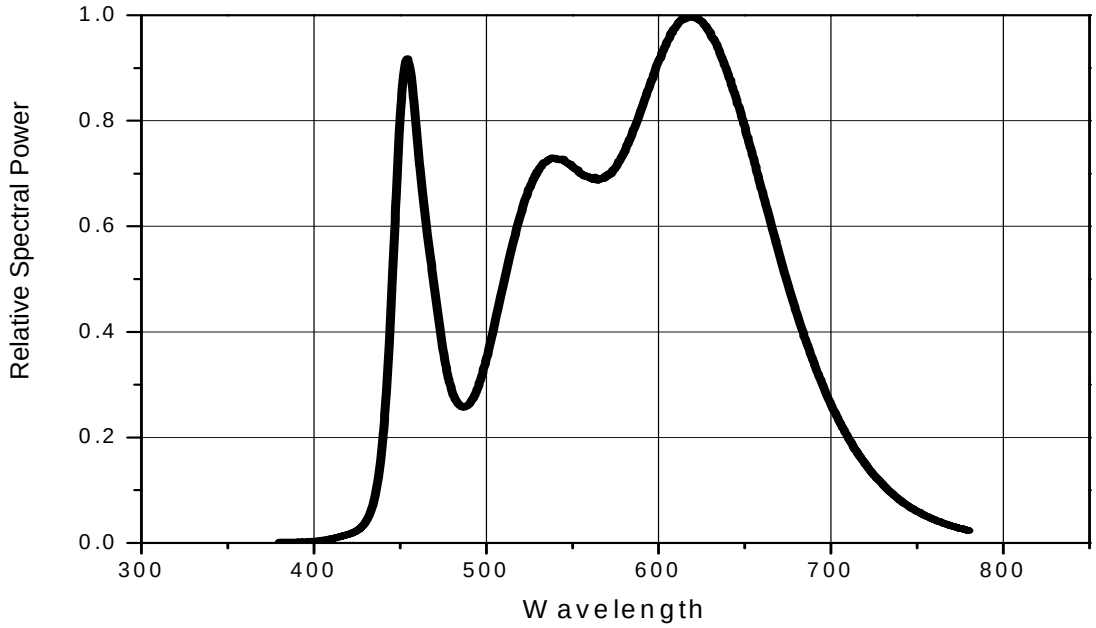

Color Spectrum, T_A=25°C

3. Warm White (N42180H)

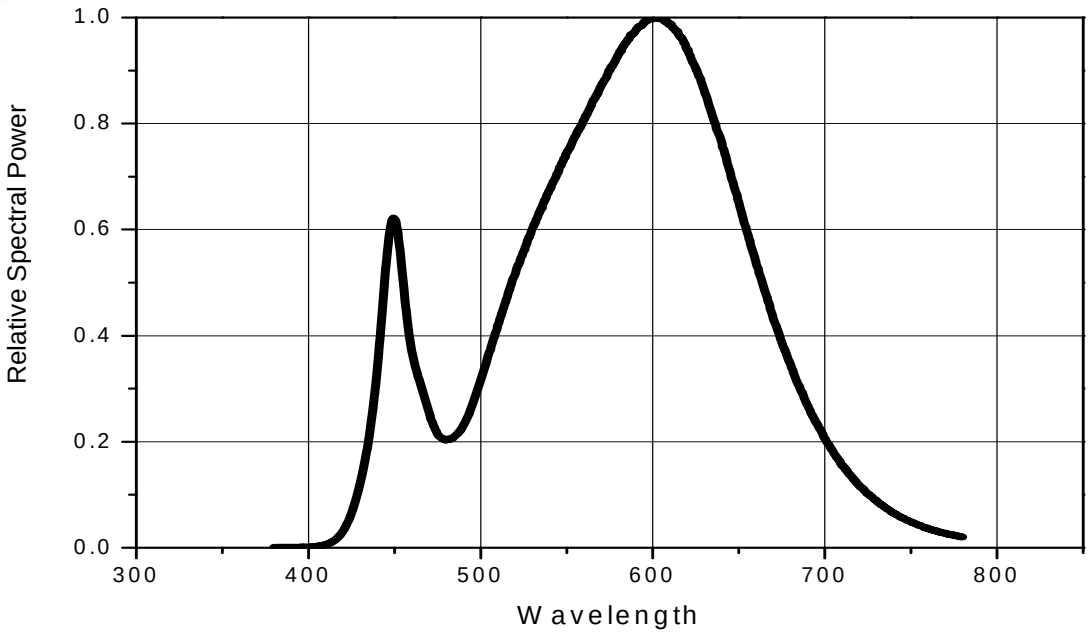

4. Natural White (S42180)

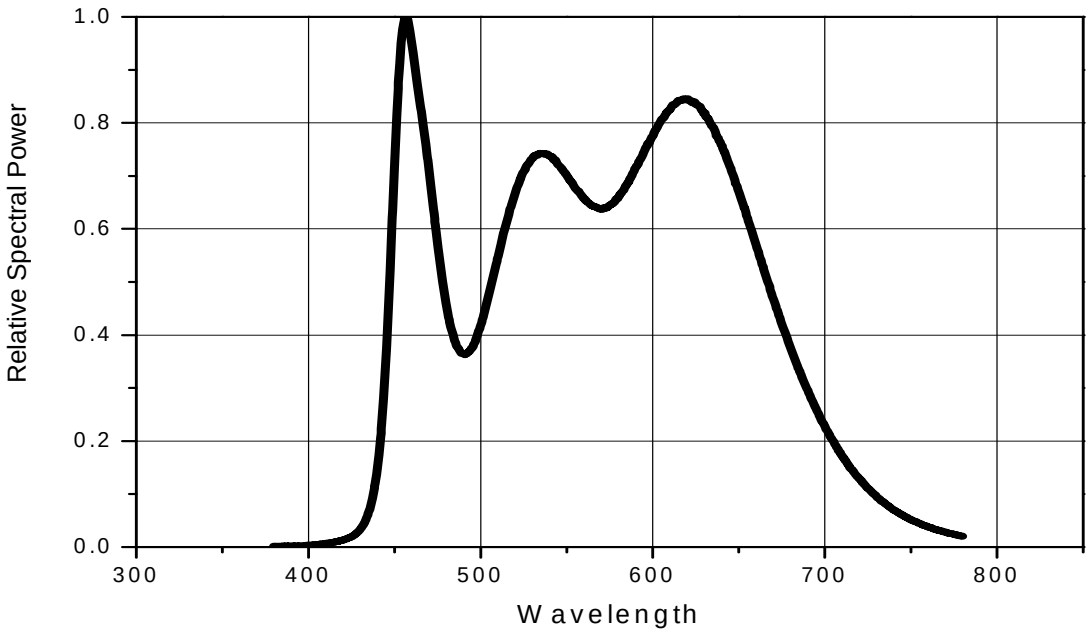

Color Spectrum, T_A=25°C

5. Natural White (S42180H)

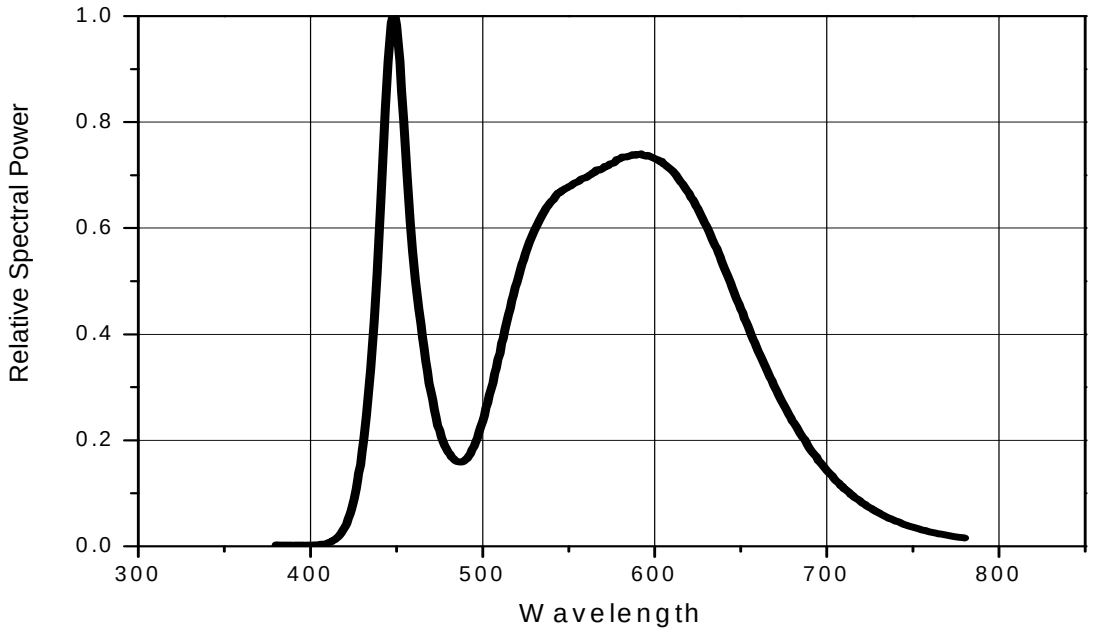

6. Red, Amber, Green, Blue(Royal Blue)

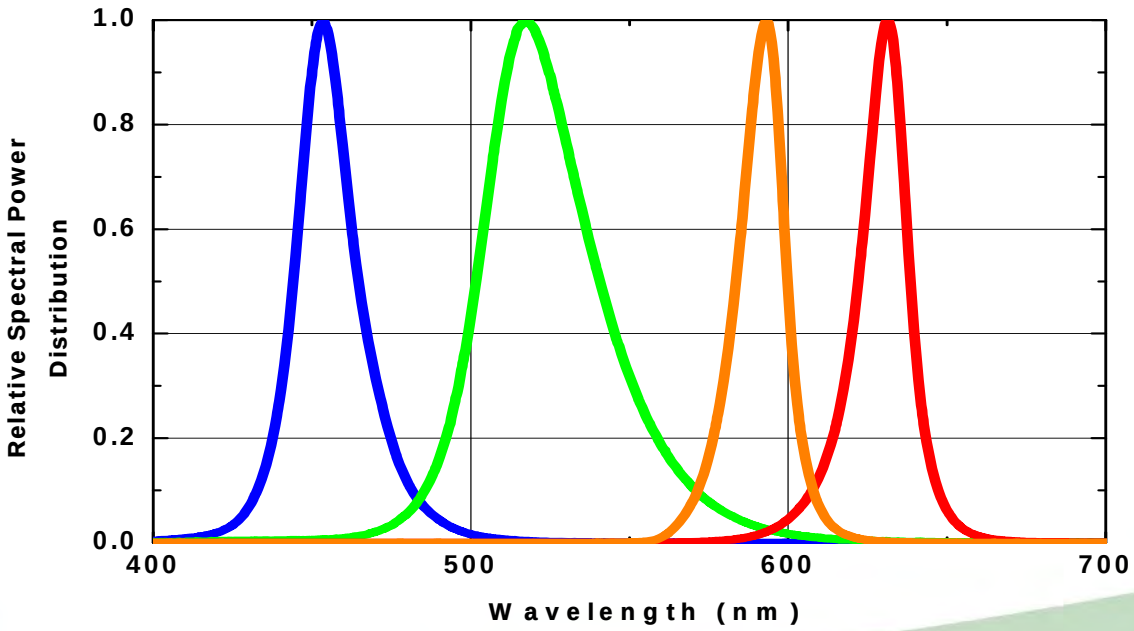

Junction Temperature Characteristics

1. Relative Light Output vs. Junction Temperature at I_F=350mA

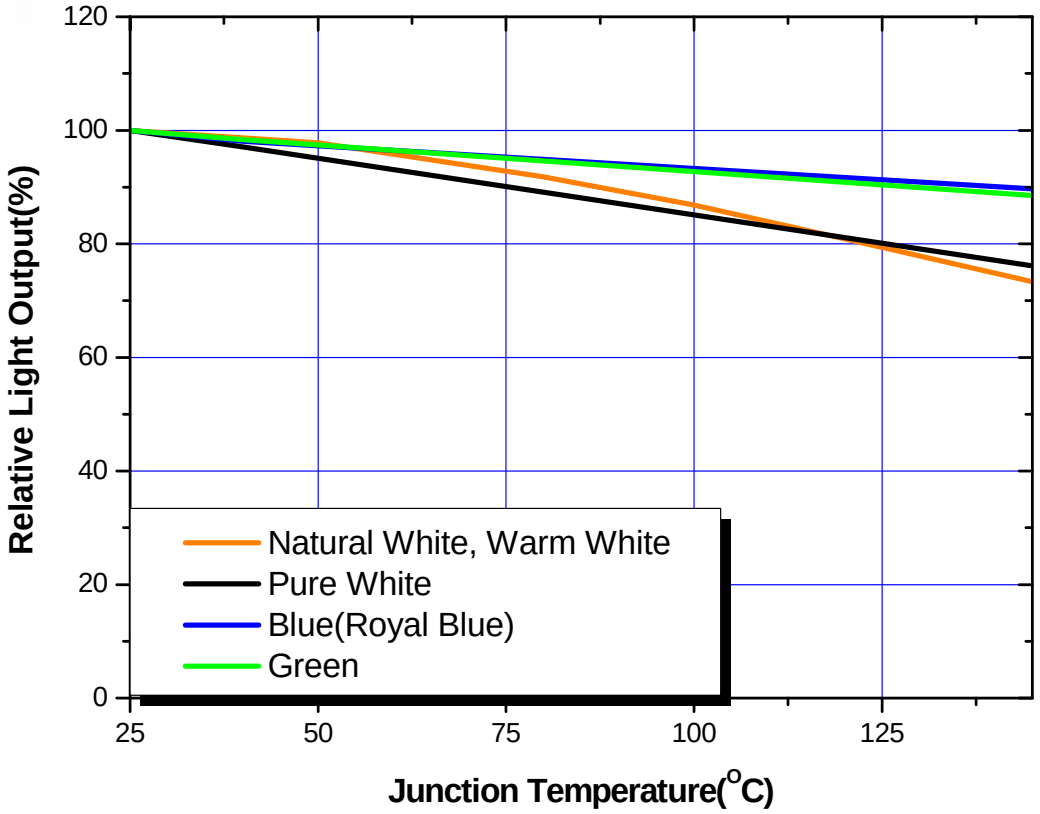

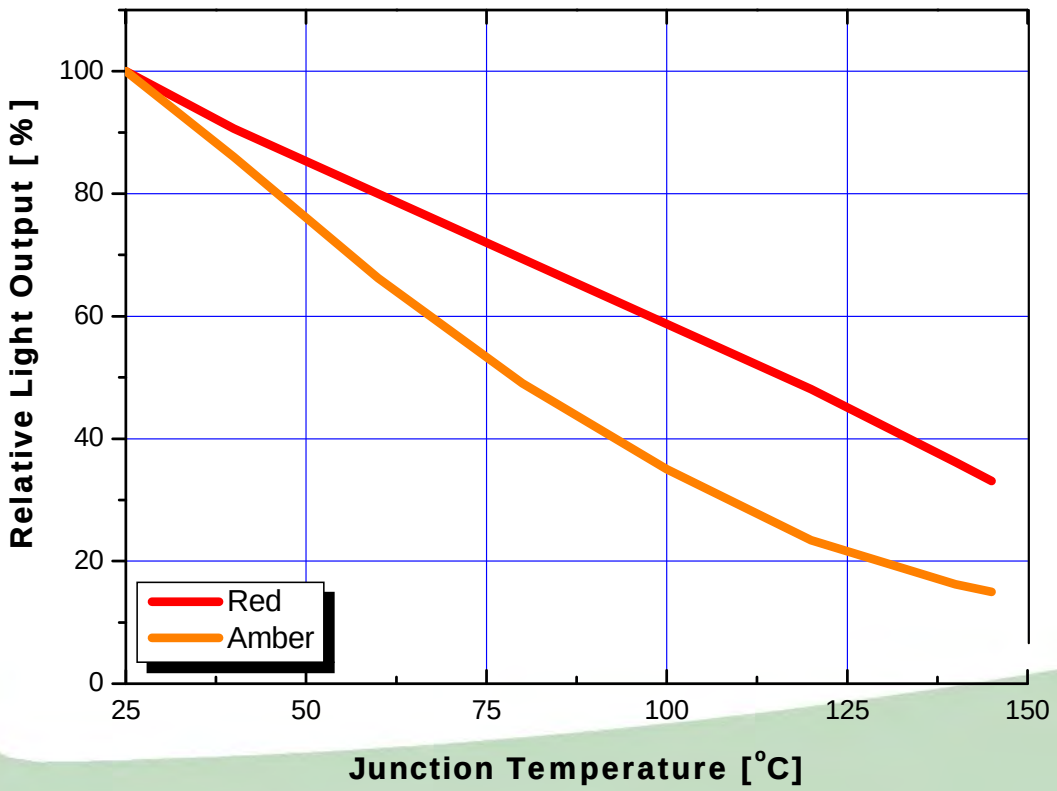

Junction Temperature Characteristics

2. Forward Voltage Shift vs. Junction Temperature at I_F=350mA

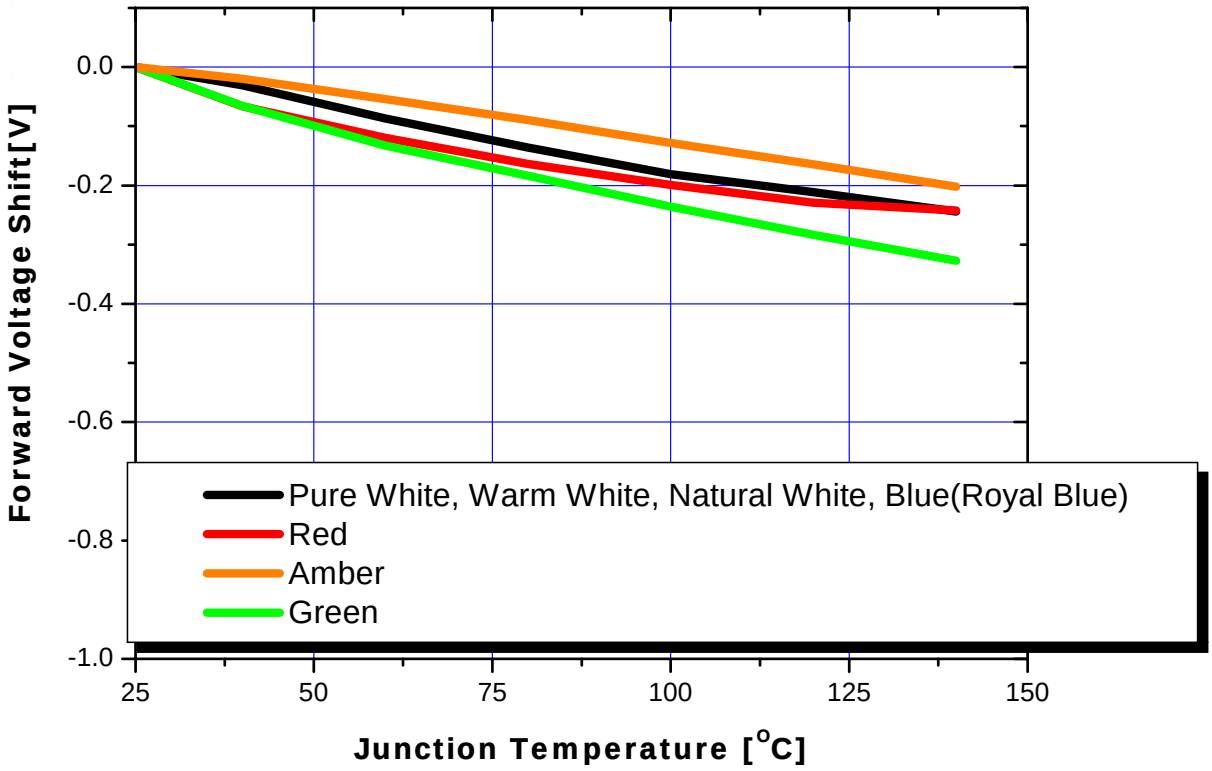

3. Wavelength Shift vs Junction Temperature at I_F=350mA

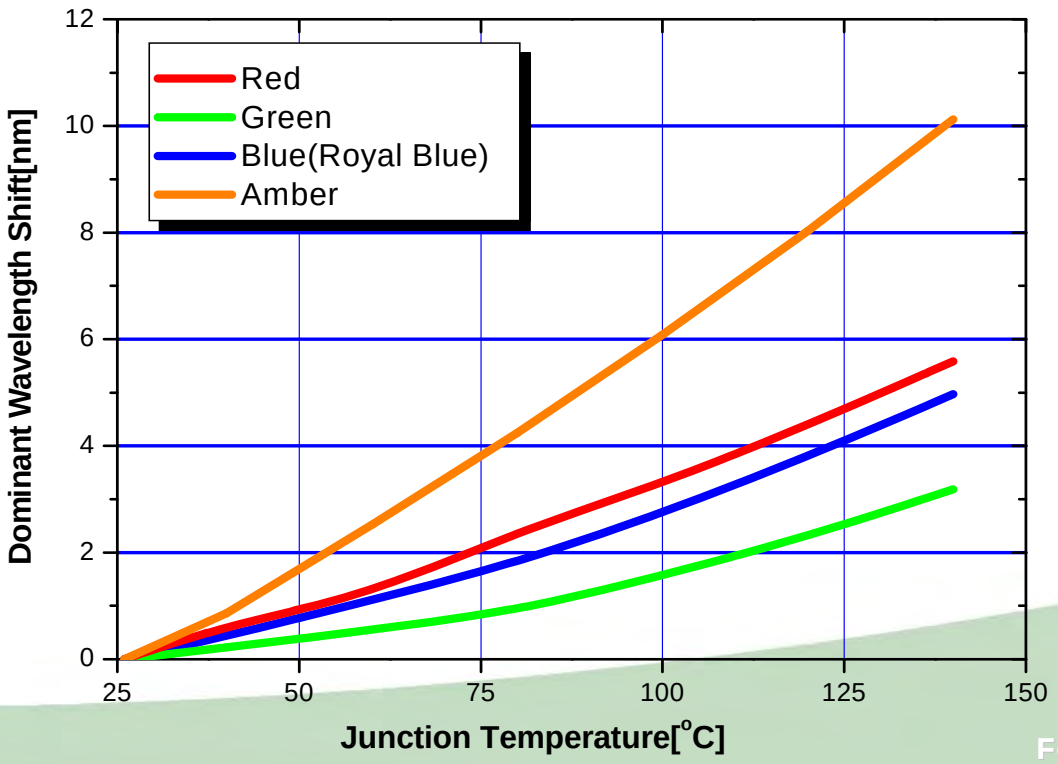

Forward Current Characteristics

1. Forward Voltage vs. Forward Current , T_A=25 °c

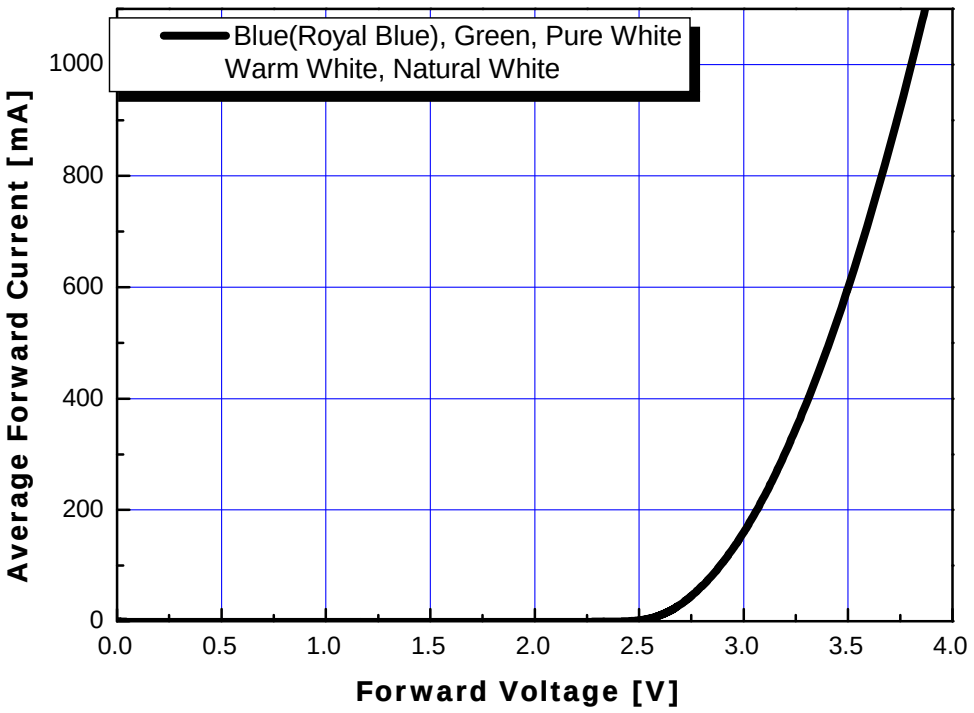

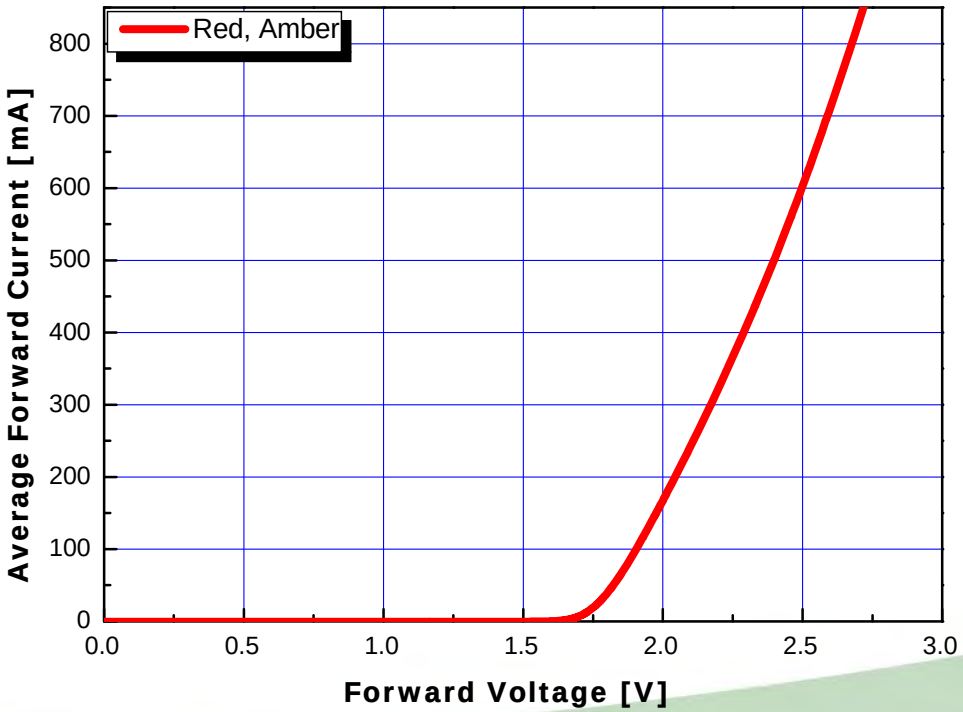

Forward Current Characteristics

2. Forward Current vs. Normalized Relative Luminous Flux, T_A=25 °c

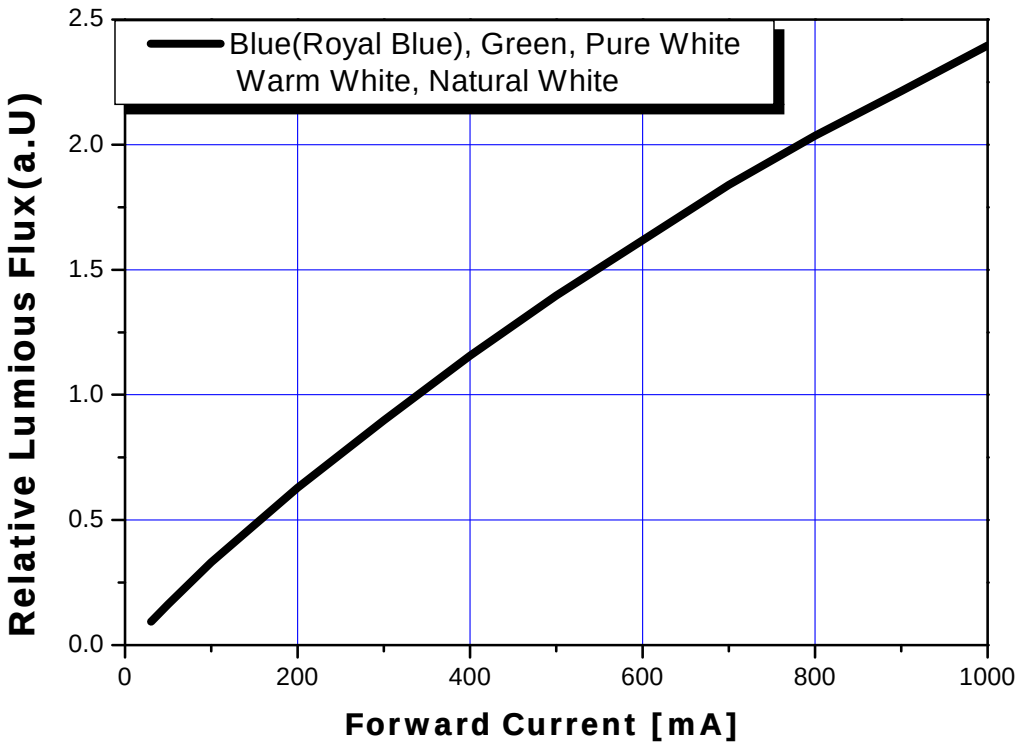

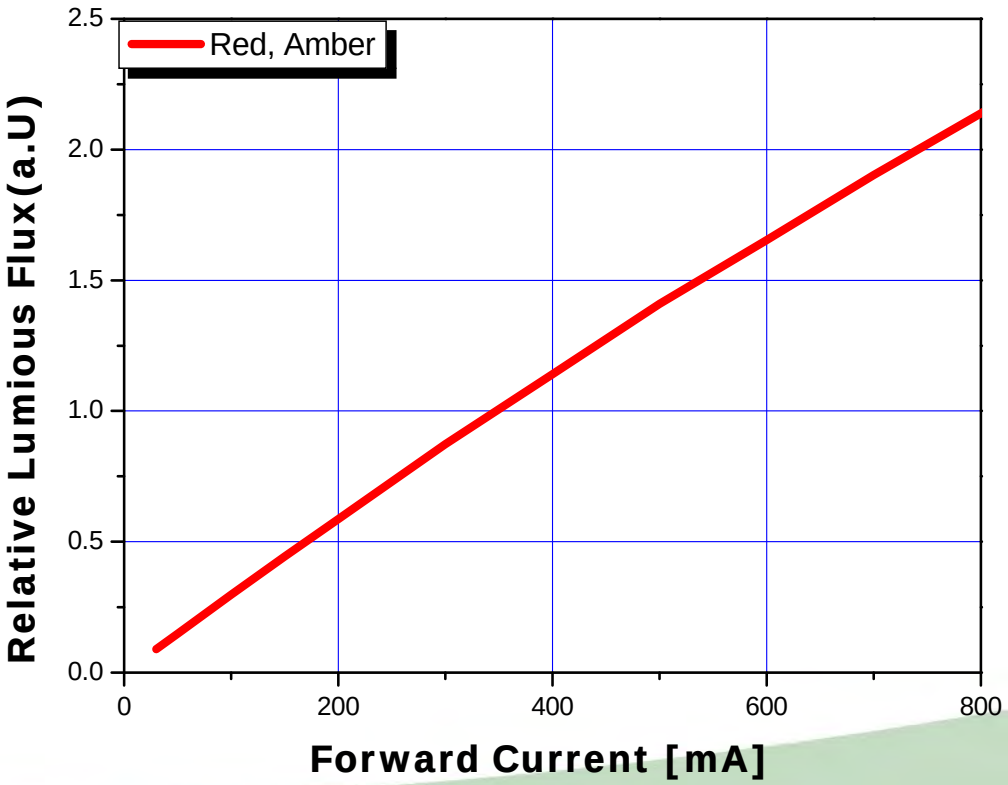

Forward Current Characteristics

3. Forward Current vs Wavelength Shift, T_A=25 °c

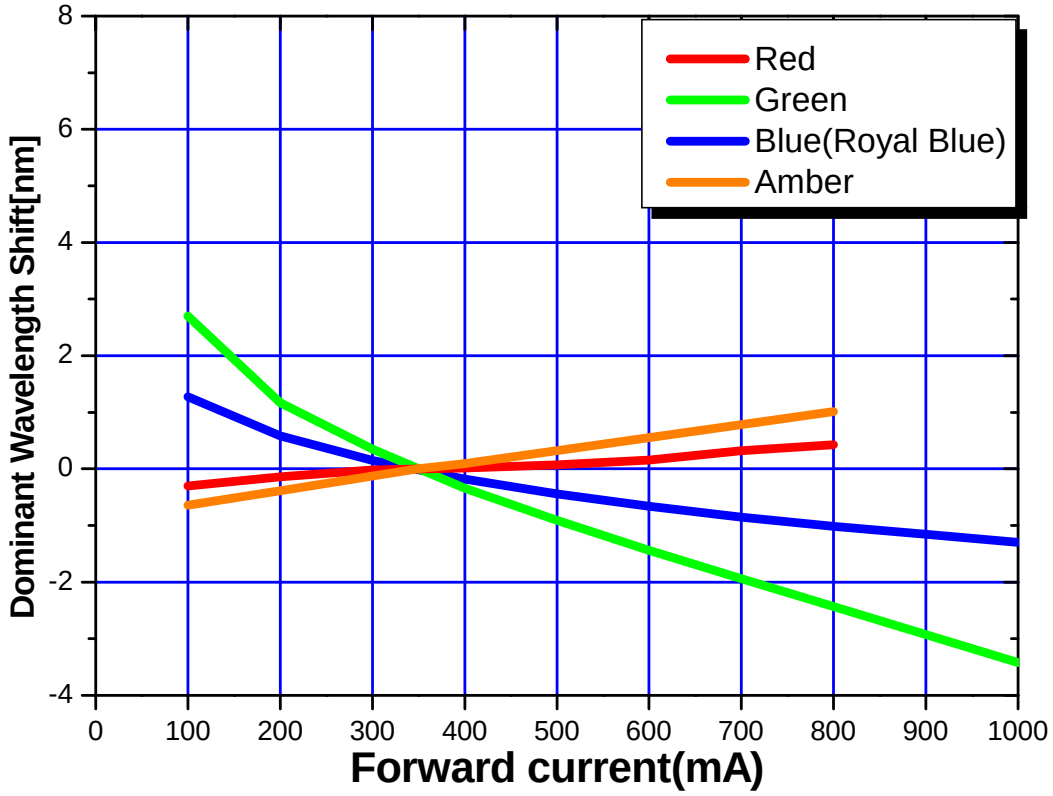

Ambient Temperature vs Allowable Forward Current

1-1. Pure White, Warm White, Natural White, Green, Blue(Royal Blue) (T_{JMAX} = 145 ◦C, @350mA)

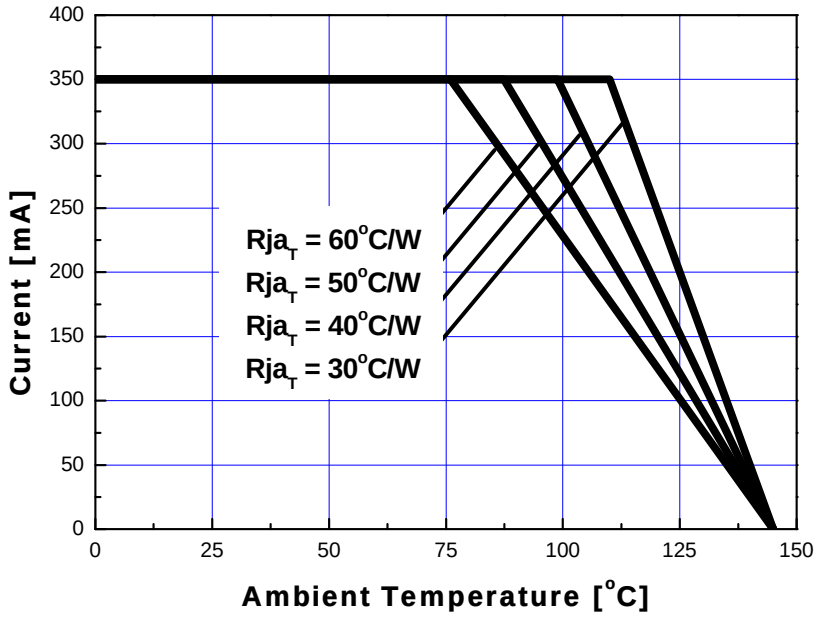

1-2. Pure White, Warm White, Natural White, Green, Blue(Royal Blue) (T_{JMAX} = 145 ◦C, @700mA)

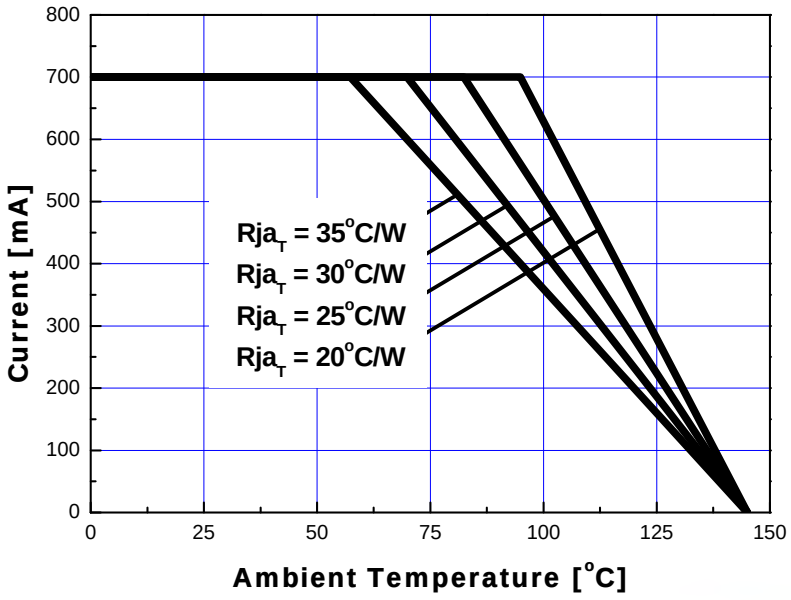

Ambient Temperature vs Allowable Forward Current

1-3. Pure White, Green, Blue(Royal Blue) (T_{JMAX} = 90 °C, at 1000mA)

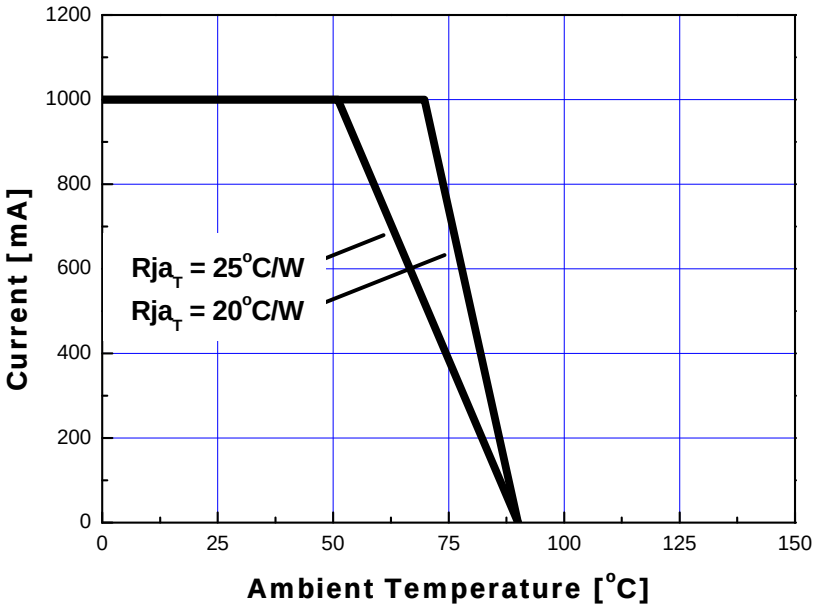

Ambient Temperature vs Allowable Forward Current

1-4. Red, Amber (T_{JMAX} = 145 °C, at 350mA)

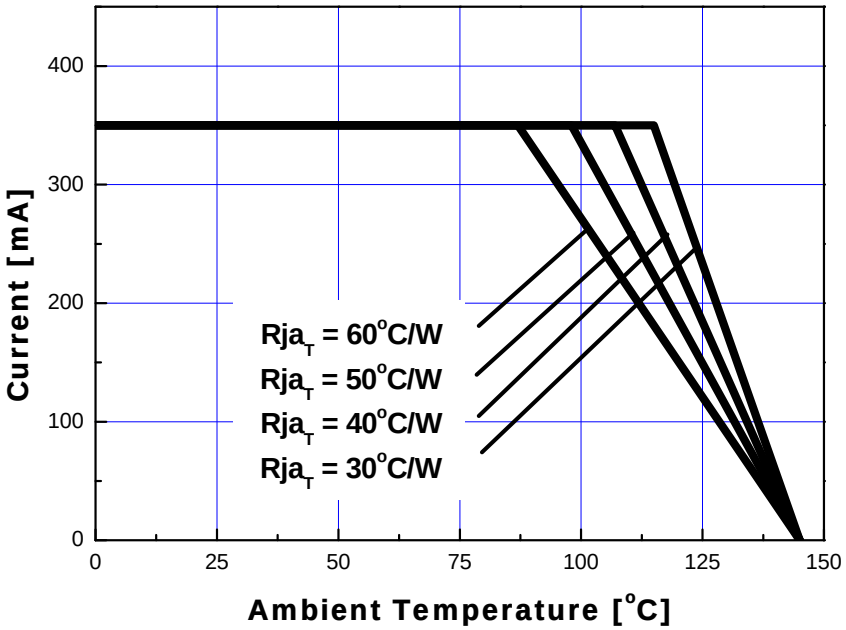

1-5. Red, Amber (T_{JMAX} = 145 °C, @700mA)

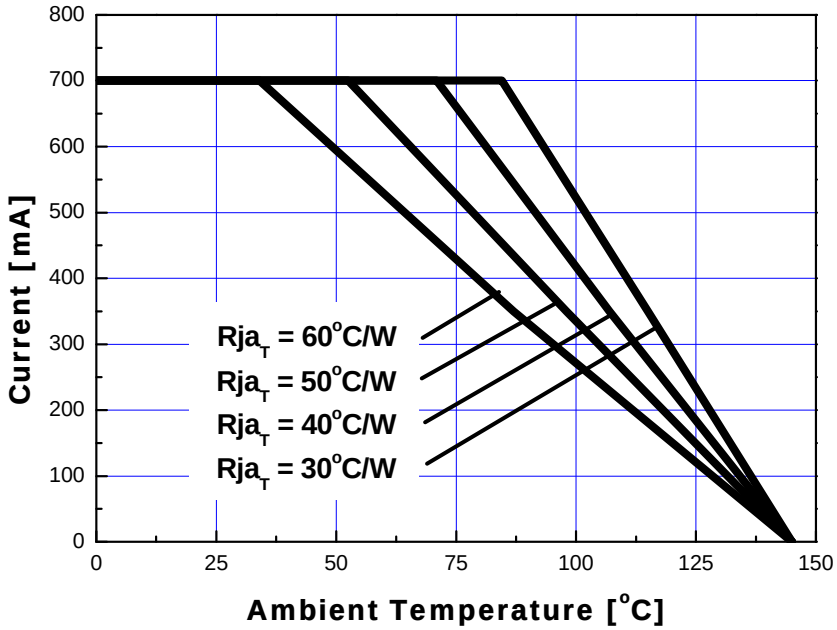

Typical Dome Type Radiation pattern

1. Pure White

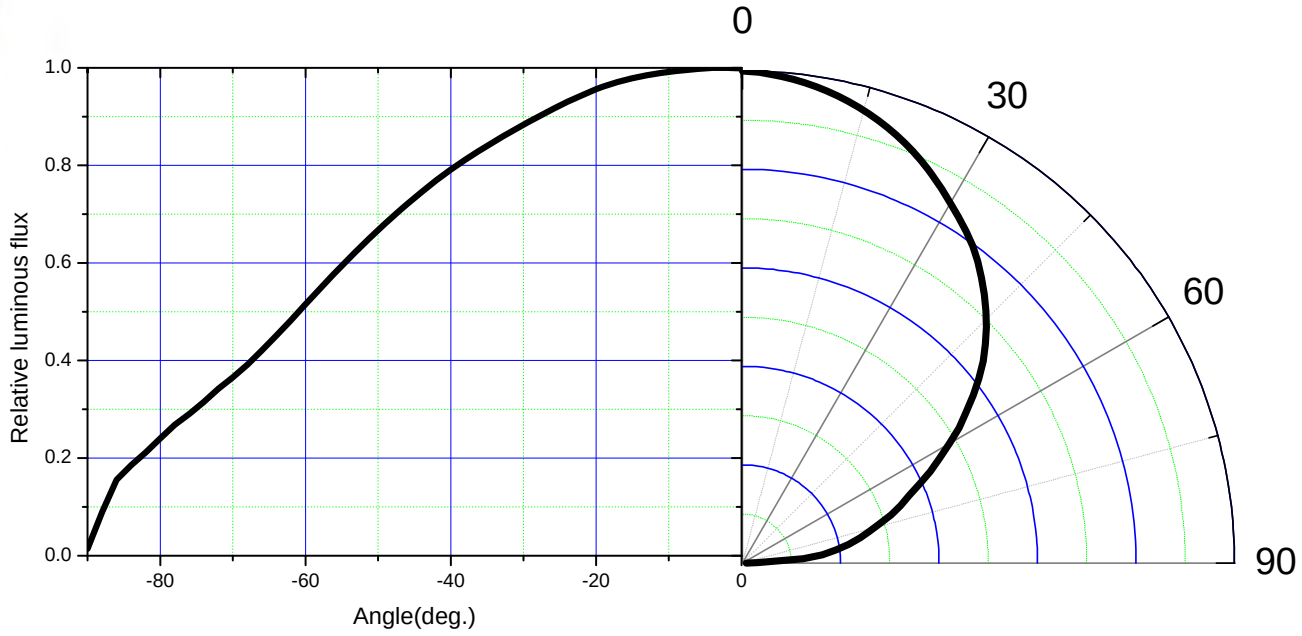

2. Warm White, Natural White

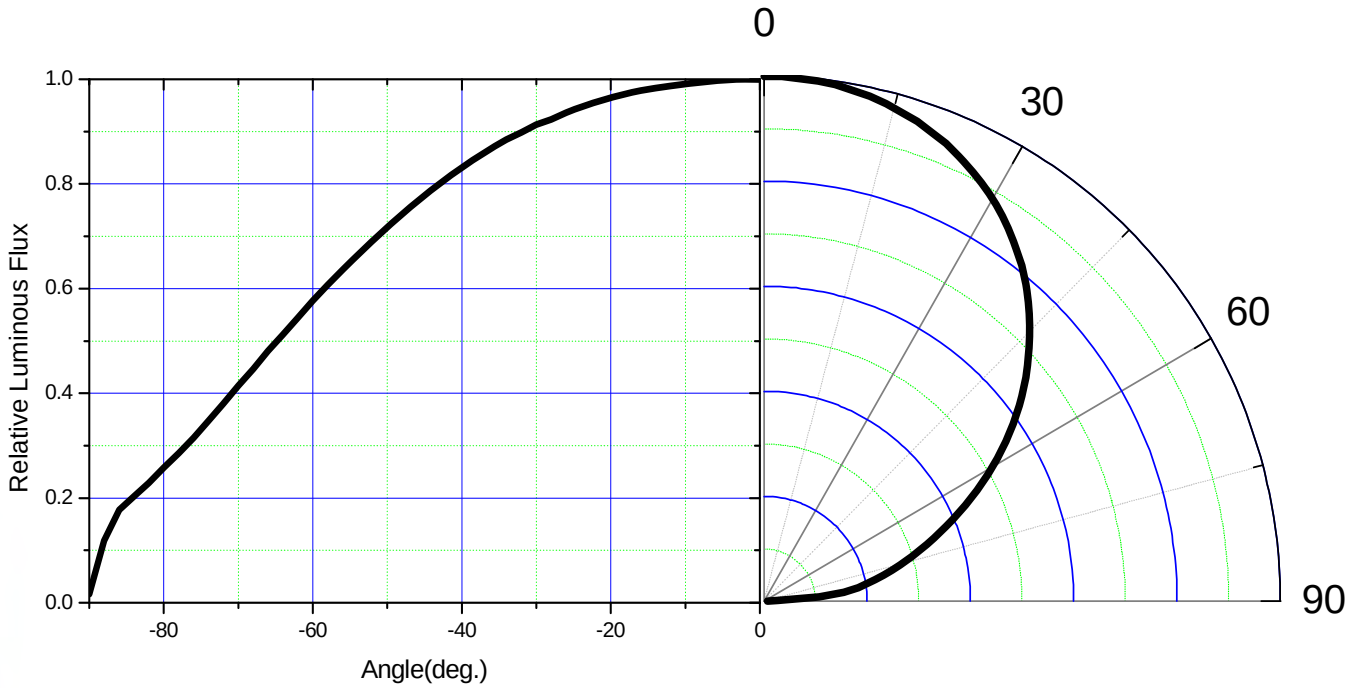

Typical Dome Type Radiation pattern

3. Blue(Royal Blue), Green

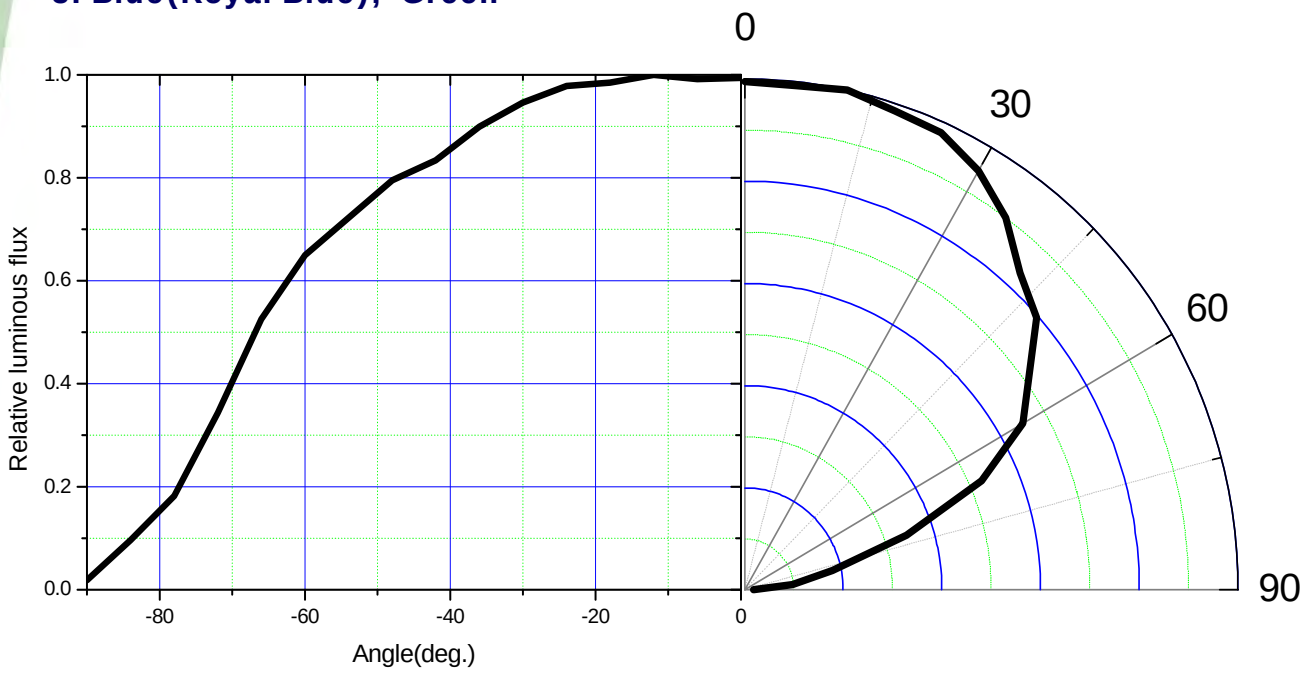

4. Red, Amber

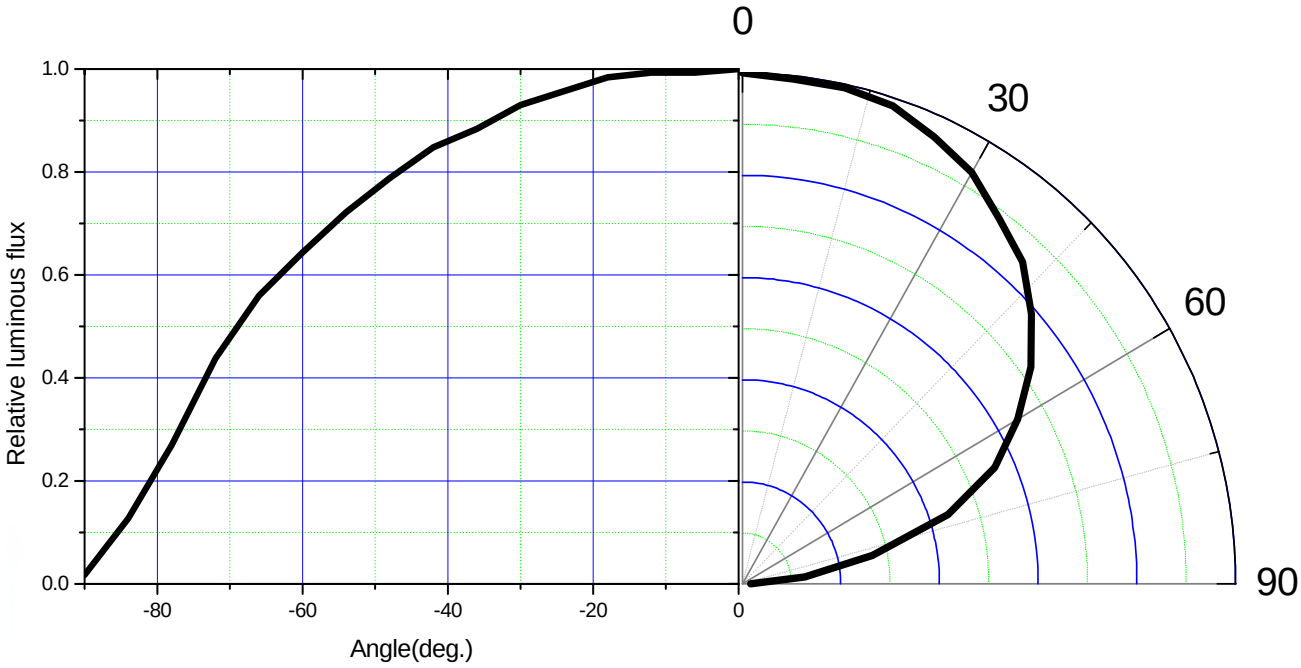

Recommended Solder pad

1. Solder pad

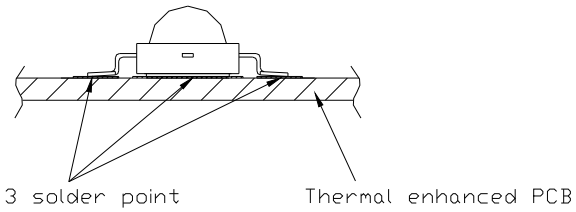

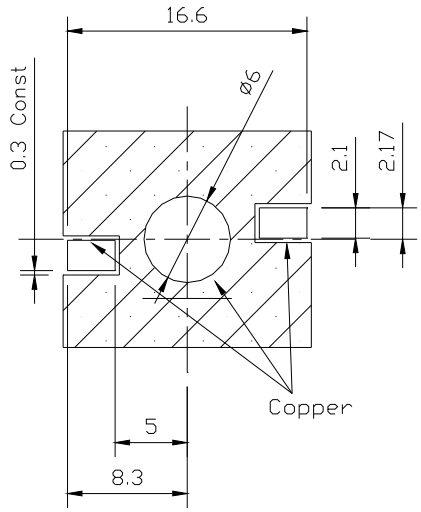

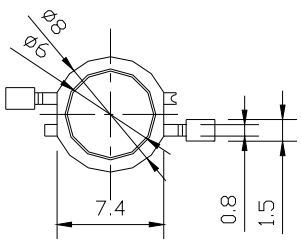

<Rear view>

2. Solder paste pattern

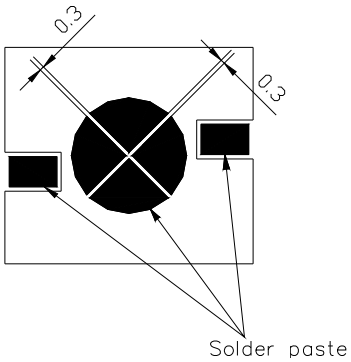

Note :

1. All dimensions are in millimeters (tolerance : ±0.2)
2. Scale none

*The appearance and specifications of the product may be changed for improvement without notice.

3. Reflow Soldering Conditions / Profile

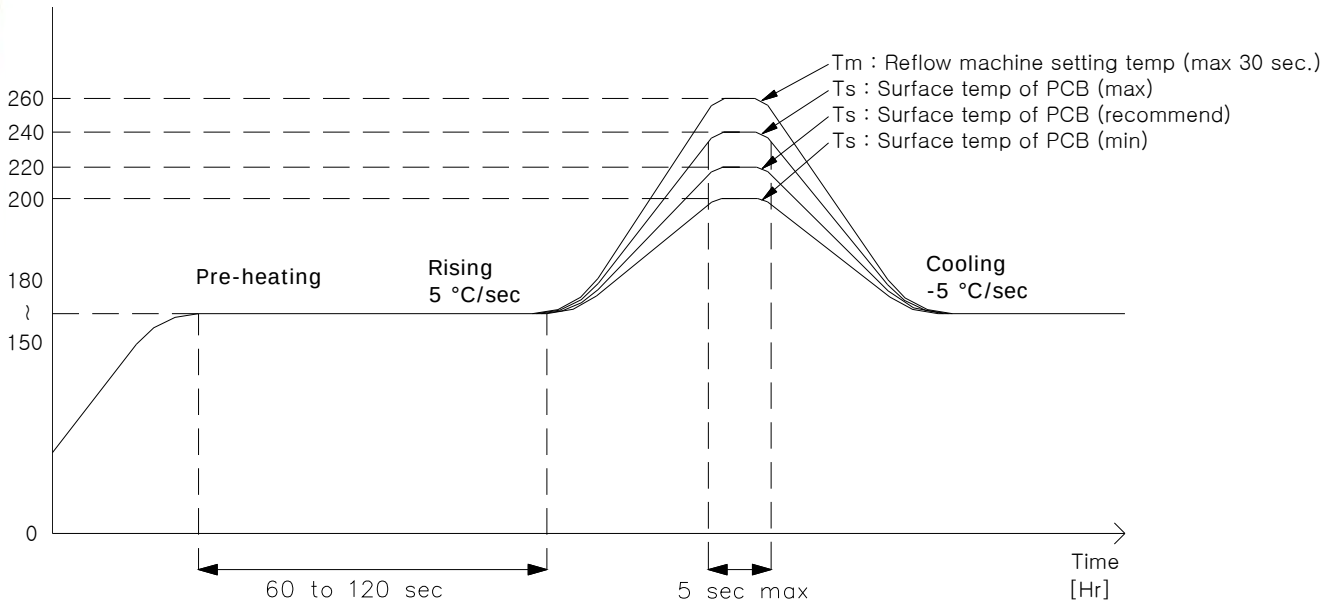

4. Hand Soldering conditions

Lead : Not more than 3 seconds @MAX280℃

Slug : Use a thermal-adhesives

*** Caution**

1. **Reflow soldering should not be done more than one time.**
2. **Repairing should not be done after the LEDs have been soldered. When repairing is unavoidable, suitable tools have to be used.**
3. **Die slug is to be soldered.**
4. **When soldering, do not put stress on the LEDs during heating.**
5. **After soldering, do not warp the circuit board.**
6. **Recommend to use a convection type reflow machine with 7 ~ 8 zones.**

SEOUL SEMICONDUCTOR

Emitter Type Reel Packaging

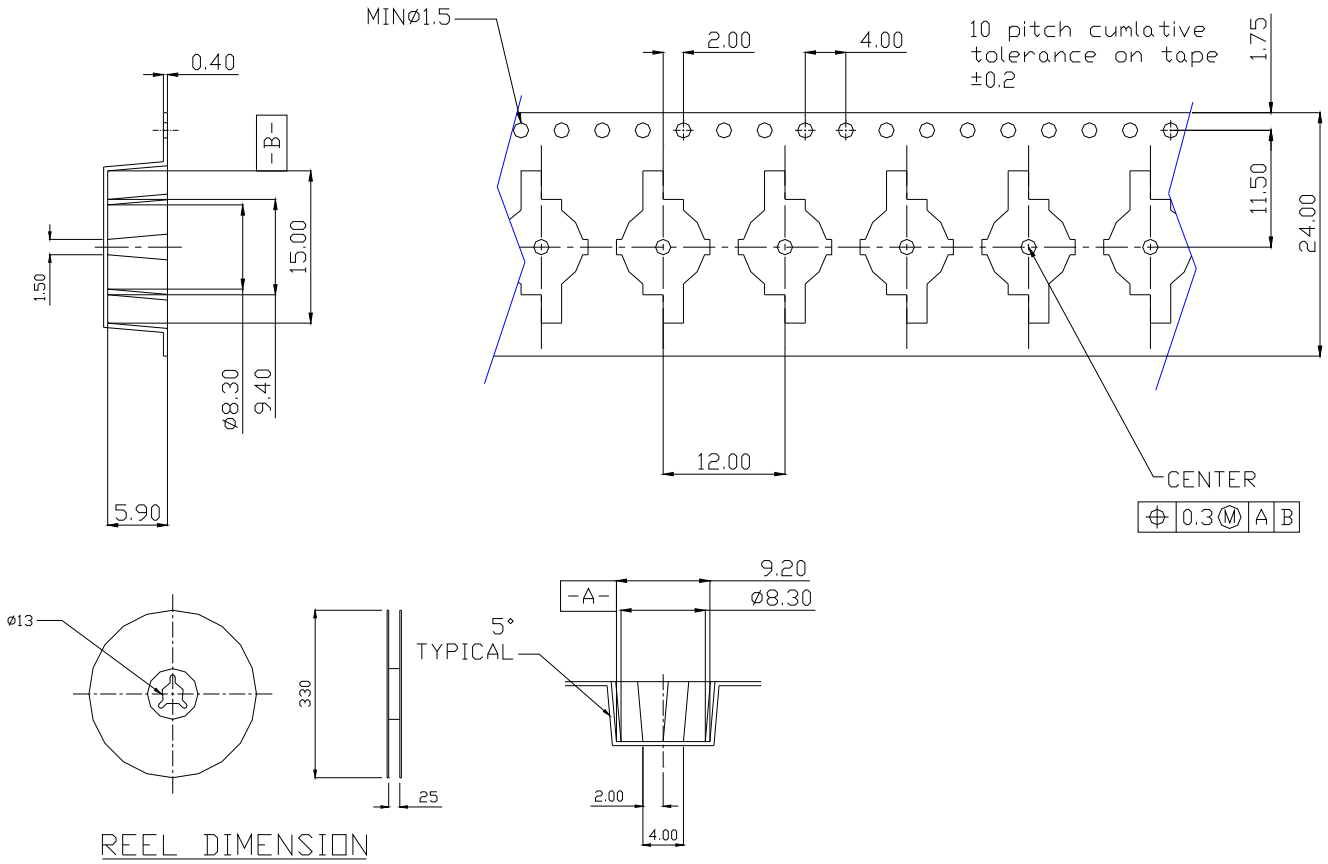

Note :

1. The number of loaded products in the reel is 500ea
2. All dimensions are in millimeters (tolerance : ±0.2)
3. Scale none

*The appearance and specifications of the product may be changed for improvement without notice.

Packaging Structure

Aluminum Vinyl Bag

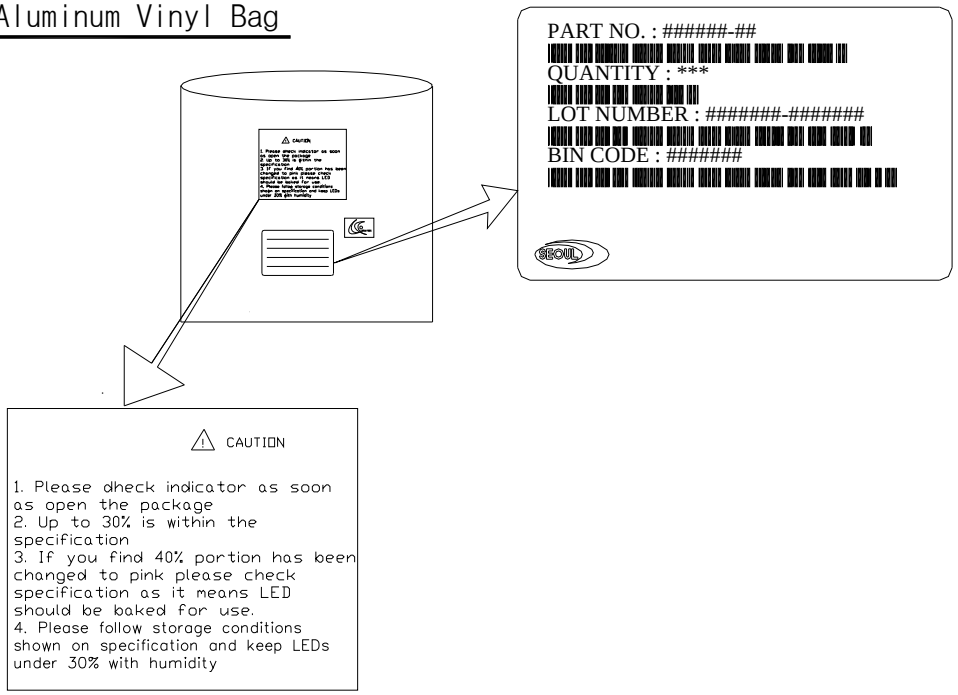

Outer Box

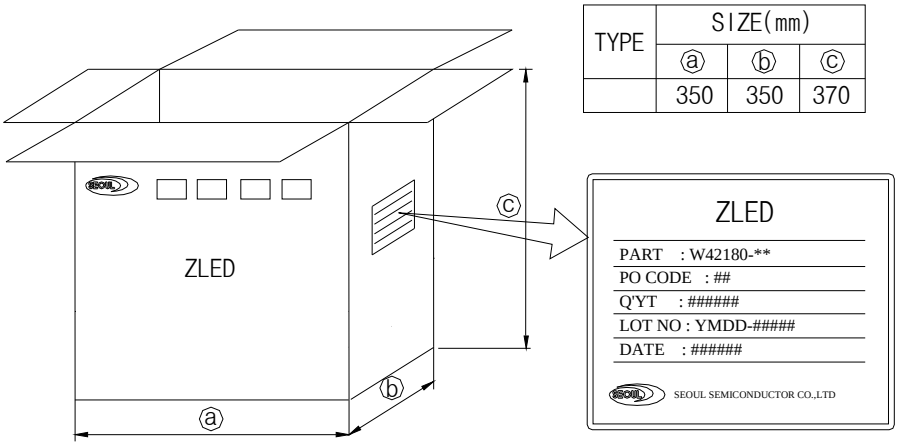

TYPE	SIZE(mm)		
	ⓐ	ⓑ	ⓒ
	350	350	370

Note :

1. 6~10 reels are loaded in box
2. Scale none
3. For more information about binning and labeling, refer to the Application Note - 1

precaution for use

- Storage

  To avoid the moisture penetration, we recommend storing Z Power LEDs in a dry box (or desiccator) with a desiccant . The recommended storage conditions are Temperature 5 to 30 degrees Centigrade. Humidity 50% maximum.
- Precaution after opening packaging

  However LED is correspond SMD, when LED be soldered dip, interfacial separation may affect the light transmission efficiency, causing the light intensity to drop.

  Attention in followed.

  a. Soldering should be done right after opening the package(within 24Hrs).

  b. Keeping of a fraction

  - Sealing
  - Temperature : 5 ~ 40℃ Humidity : less than 30%

  c. If the package has been opened more than 1week or the color of desiccant changes, components should be dried for 10-12hr at 60±5℃
- Any mechanical force or any excess vibration shall not be accepted to apply during cooling process to normal temp. after soldering.
- Please avoid rapid cooling after soldering.
- Components should not be mounted on warped direction of PCB.
- Anti radioactive ray design is not considered for the products listed here in.
- Gallium arsenide is used in some of the products listed in this publication. These products are dangerous if they are burned or shredded in the process of disposal. It is also dangerous to drink the liquid or inhale the gas generated by such products when chemically disposed.
- This device should not be used in any type of fluid such as water, oil, organic solvent and etc. When washing is required, IPA(Isopropyl Alcohol) should be used.
- When the LEDs are illuminating, operating current should be decided after considering the package maximum temperature.
- LEDs must be stored to maintain a clean atmosphere. If the LEDs are stored for 3 months or more after being shipped from SSC, a sealed container with a nitrogen atmosphere should be used for storage.
- The appearance and specifications of the product may be modified for improvement without notice.
- Long time exposure of sunlight or occasional UV exposure will cause lens discoloration.
- The slug is connected to the anode. Therefore, we recommend to isolate the heat sink.
- Attaching LEDs, don't use adhesives to generate organic vapor.

Handling of Silicone resin LEDs

Z-Power LED is encapsulated by silicone resin for the highest flux efficiency.
Notes for handling of Silicone resin Z-Power LEDs

- Avoid touching silicone resin parts especially by sharp tools such as Pincette(Tweezers)
- Avoid leaving fingerprints on silicone resin parts.
- Dust sensitivity silicone resin need containers having cover for storage.
- When populating boards in SMT production, there are basically no restrictions regarding the form of the pick and place nozzle, except that mechanical pressure on the surface of the resin must be prevent.
- Please do not force over 2000 gf impact or pressure diagonally on the silicon lens. It will cause fatal damage of this product
- Please do not recommend to cover the silicone resin of the LEDs with other resin (epoxy, urethane, etc)

Identifying and Evaluating Aging Signatures in Light Emitting Diode Lighting Systems

Résumé

Dans ce travail, les dégradations des diodes électroluminescentes (DEL) ont été étudiées en identifiant et en évaluant leurs signatures électriques et photométriques en vieillissement accéléré sous stress thermique et électrique. Un prototype de banc de test expérimental a été développé et construit spécifiquement pour cette étude ce qui nous a permis de tester 128 échantillons en appliquant différentes conditions de stress thermiques et électriques. Quatre types différents de DEL ont été étudié avec des caractéristiques techniques similaires (température de couleur, courant nominal, mono-puce,…) mais avec des technologies différentes couvrant les principaux acteurs du marché (Cree, Osram, Philips et Seoul Semiconductor). Les échantillons ont d'abord été caractérisés à leur état initial, puis soumis à des conditions de stress électrique (à 350mA ou 1050mA) et thermique (fixé à 50°C).

Les mécanismes de défaillance ont été analysés en étudiant l'évolution des signatures électriques et photométriques. Ces caractérisations ont permis d'évaluer et de déterminer l'origine des dégradations à différents niveaux : puce semi-conductrice, interconnexions, phosphore ou encapsulation du dispositif. Les caractérisations électriques nous ont permis d'identifier les mécanismes de dégradation de la puce semi-conductrice et de déterminer la nature des dégradations au niveau du contact ohmique du dispositif (sous fort courant injecté). Les caractérisations photométriques complètent cette étude en évaluant les dégradations associées à l'optique (encapsulation et packaging).

Mots Clefs : diodes électroluminescentes, DEL, vieillissement, stress thermiques et électriques, caractérisations électriques et photométriques

Abstract

In this work, the degradation of light emitting diodes (LEDs) is studied by identifying and evaluating their aging signature during the stress time. The custom-made experimental test bench is built for realization of the test measurement. Through this experimental test bench, it allows to test a large amount of LED samples and enable to select different temperature condition and different current stress level. There are four different types of LED with similar characteristic in term of their color temperature, I_F, V_F, power (1W) and as monochip, but different technology coming from Cree, Osram, Philips and Seoul Semiconductor. The devices are firstly characterized their electrical and photometrical characteristic at their initial state, then they are submitted to different current stress condition at low current stress (350mA) and high current stress (1000mA) while the thermal stress is fixed at one temperature (50°C).

The study of these devices failure mechanism is archived by using the primary method based on the electrical and photometrical characterization of the devices that allows to evaluate their degradation at different locations of the device components such as semiconductor chip, interconnection and device's package. The electrical characteristic of the device's I-V curve: at low injected current level and reverse bias allow us to identify the degradation characteristic of device's ***semiconductor chip***, at high injected current level allows us to determine the degradation of device's ***ohmic contact*** and photometric characteristic allows us to evaluate the degradation of device's package system.

Keywords: light emitting diodes, LED, aging, thermal stress and electrical stress, electrical and photometric characterizations